VESSEL STABILITY IN THE EDINBURGH MODEL OF RETINOPATHY OF PREMATURITY: INVESTIGATION OF MURAL CELL COVERAGE & GROWTH FACTOR EXPRESSION

ZEENAT YAQOOB
BSc (Hons)

Thesis for the Degree of Doctor of Philosophy

The University of Edinburgh
2003

This thesis is dedicated to Ubbo and Umma,

'I want you to know how much I admire and respect you, and how lucky I feel to have such good and caring parent,'

and to my sister, Saeema,

'thank-you for your continued encouragement and support over the years.'

DECLARATION

The work presented in this thesis was conducted under the supervision of Professor Neil McIntosh and Dr. Kofi Sedowofia, Child Life and Health, Reproductive and Developmental Sciences, University of Edinburgh.

In accordance with the requirements of the University of Edinburgh, I hereby declare that the contents contained herein are my own and that any assistance and advice has been duly acknowledged.

This work has not been submitted for any other degree or professional qualification.

Child Life and Health
Reproductive and Developmental Sciences
University of Edinburgh
20 Sylvan Place
Edinburgh
EH9 1UW

January 2004

ACKNOWLEDGEMENTS

I would like to thank Professor Neil McIntosh and Dr. Kofi Sedowofia for their supervision, encouragement and constructive advice throughout the period of this study.

My thanks also to Dr. Jan McColm for helping me to initiate this project. Particular acknowledgment goes to Jean Wade who provided invaluable guidance and encouragement in the laboratory, and to Linda Sharp for her much appreciated assistance with the confocal microscope. My sincere gratitude to Helen Wilson and Steve Mitchell who conducted the radiolabelled *in situ* hybridisation and electron microscopy, respectively.

A big thank-you goes to the staff of the Medical Faculty Animal Facility and to the remaining research team who at one point or another have provided a much appreciated helping hand.

ABSTRACT

Retinal blood vessels consist of endothelial tubules surrounded by a single layer of smooth muscle cells or pericytes, collectively called the mural cells. Coverage of the vessel with mural cells is suggested to signal their stability, and requires the actions of several locally secreted growth factors including: platelet-derived growth factor, which promotes mural cell migration and proliferation; transforming growth factor-β, that induces the differentiation of precursors cells into pericytes and smooth muscle cells; and the angiopoietins, for maintaining the interactions between endothelial cells and pericytes.

Stability of blood vessels is believed to be compromised in retinopathy of prematurity (ROP), a potentially binding eye disease characterised by the invasion of the vitreous by proliferating retinal blood vessels. In the past the use of high oxygen levels for the treatment of extremely premature infants was associated with the incidence of this condition. However, it was recently suggested that rather than absolute oxygen levels, the variability of the transcutaneous (blood) oxygen levels within clinically 'safe' limits during the first two weeks of life may be more important in ROP. Thus, a clinically relevant animal model of ROP was developed (Edinburgh model). The first 14 days of the transcutaneous oxygen profile of an infant who developed severe ROP was selected and converted into percentage inspired oxygen levels to produce the equivalent arterial oxygen in a rat. The aims of this thesis were to investigate mural cell coverage and the expression of the factors suggested to participate in vessel stabilisation during normal retinal development and in the Edinburgh model.

Rat pups were raised in room air or exposed to the oxygen regime of the Edinburgh model from birth to postnatal days 2, 7 and 14. The pups were then killed, the eyes enucleated and analysed for mural cell coverage and expression of platelet-derived growth factor-B, transforming growth factor-β_1 and angiopoietin-2 using

immunohistochemical, Western blotting, electron microscopy and *in situ* hybridisation techniques.

In comparison to room air raised pups, the retinal vasculature of the pups raised in the variable oxygen regime had reduced mural cell coverage; smooth muscle cell coverage was only slightly reduced, however there was a marked and significant reduction in pericyte coverage. The protein expression of both platelet-derived growth factor-B and transforming growth factor-β_1 were also reduced. Unfortunately, the analysis of angiopoietin-2 mRNA expression was inconclusive due to insensitive detection methods.

In conclusion, the reduction in mural cell coverage and in the expression of platelet-derived growth factor and transforming growth factor-β_1 suggest that blood vessel stability is compromised in the Edinburgh model of retinopathy of prematurity.

ABBREVIATIONS

α-SMA	alpha-smooth muscle actin
Ang-1	angiopoietin-1
Ang-2	angiopoietin-2
ch	choriod
°C	degrees Celcius (temperature)
DNA	dioxiribonucleic acid
E	embryonic day
GCL	ganglion cell layer
INL	inner nuclear layer
IPL	inner plexiform layer
kDa	kilodaltons (molecular weight)
kPa	kilopascals
mRNA	messenger ribonucleic acid
µg	micrograms
µl	microlitres
µm	micrometres
mg	milligrams
mls	millilitres
mmHg	millimetres mercury
mM	millimolar (concentration)
mins	minutes
M	molar (concentration)
ng	nanograms
nm	nanometers (wavelength)
NBL	neuroblast layer
NFL	nerve fibre layer
OD_{562}	optical density at 562nm
ONL	outer nuclear layer
OPL	outer pexiform layer

O_2	oxygen
PBS	phosphate-buffered saline
PDGF-B	platelet-derived growth factor chain B
PDGF receptor-β	platelet-derived growth factor receptor-beta
P	postnatal day
RPE	retinal pigmented epithelium
ROP	retinopathy of prematurity
secs	seconds
TcO_2	transcutaneous oxygen
TGF-β	transforming growth factor-beta
TGF receptor-β	transforming growth factor receptor-beta
Tie-1	tyrosine kinase with immunoglobulin and epidermal growth factor homology domains-1
Tie-2	tyrosine kinase with immunoglobulin and epidermal growth factor homology domains-2
VEGF	vascular endothelial growth factor

CONTENTS

DETAILED CONTENTS

CHAPTER TWO: MURAL CELLS OF THE RETINAL VESSELS

CHAPTER THREE: EXPRESSION OF PLATELET-DERIVED GROWTH FACTOR IN THE EDINBURGH MODEL OF ROP **Page**

CHAPTER SIX: TESTING THE EDINBURGH MODEL OF ROP

CHAPTER SEVEN: DISCUSSION

LIST OF TABLES

LIST OF FIGURES

Figure **Page**

CHAPTER FIVE: THE ANGIOPOIETINS IN THE DEVELOPING RAT RETINA

CHAPTER SIX: TESTING THE EDINBURGH ROP MODEL

CHAPTER ONE

INTRODUCTION

1.1 THE FORMATION OF BLOOD VESSELS

Blood vessel development is a very complicated and delicate process which occurs by vasculogenesis and angiogenesis [reviewed in Risau, 1997]. In vasculogenesis, endothelial cells spontaneously co-assemble into tubules to form a homogenous primary vascular plexus which is later remodelled and encapsulated by support cells, called mural cells. Angiogenesis, on the other hand, is the formation of new vessels from existing ones. It is currently assumed that vasculogenesis is limited to early embryogenesis, while angiogenesis occurs both during development and in postnatal life.

1.1.1 Vasculogenesis

Vasculogenesis begins with the generation of angioblasts from mesoderm cells of the embryo [reviewed in Risau, 1997], which appears to require the action of the fibroblast growth factor family [reviewed in Flame and Risau, 1992]. The

angioblasts then differentiate into endothelial cells that proliferate and form *de novo* vessels [reviewed in Risau, 1997]. Vascular endothelial growth factor (VEGF) is essential for inducing and maintaining the angioblast to endothelial cell differentiation [Carmeliet et al., 1996], and for promoting the proliferation of endothelial cells [Ferrara and Henzel, 1989].

During the later stages of vasculogenesis, the primitive vasculature is rapidly remodelled into large and small vessels to become a mature network, and excess endothelial cells generated during vasculogenesis regress due to the down-regulation of VEGF [reviewed in Risau, 1997]. As the vasculature is remodelled, the endothelial tubules that remain are surrounded by a basement membrane [Croker, Murad and Geer, 1970] and by mural cells, called pericytes and smooth muscle cells [Rhodin, 1968]. The coverage of the vessels with mural cells has been suggested to signal their stability [Patz, 1968; Speiser, Gittelsohn and Patz, 1968]. Several growth factors are thought to be involved in regulating vessel stabilisation, including the platelet-derived growth factors [Lindahl et al., 1997], transforming growth factor-β [Antonelli-Orlidge et al., 1989], and the angiopoietins [Suri et al., 1996]. These growth factors will be discussed in detail in subsequent chapters.

1.1.2 Angiogenesis

Angiogenesis is a process where new blood vessels develop by either sprouting directly from a pre-existing vessel (sprouting angiogenesis) or by splitting from their vessel of origin (non-sprouting angiogenesis or intussusception) [reviewed in Risau, 1997].

In the adult, the proliferation rate of endothelial cells is very low and the vasculature essentially remains quiescent. The exceptions to this, during normal physiological situations, are wound healing and menstruation where angiogenesis is tightly regulated. Briefly, during the early stages of wound repair and tissue regeneration, additional vessels (neovascularisation) develop at the edge of the wound to achieve

rapid closure of the injury site. Once the skin has developed over the wound, the wound edges contract and the microvessels regress [Wong et al., 1997]. In females, the ovaries and uterus are under hormonal control and are subjected to the formation and breakdown of vessels on a regular basis. The vasculature of the uterus and placenta undergo angiogenesis during pregnancy, but the new vessels regress after the birth of the child [reviewed in Reynolds, Killilea and Redmer, 1992].

Occasionally, unregulated angiogenesis can cause pathologic conditions, including tumours and ophthalmic diseases. Tumour growth is often a multi-step process that begins with the rapid division of cancerous cells, in most cases forming a small avascular mass. With time, this mass may grow further and make contact with a nearby vessel or it may induce the formation of blood vessels into it. Once the avascular mass establishes a blood supply, it then has the potential to invade the surrounding tissue [Folkman, 1971]. Ocular disorders resulting from uncontrolled angiogenesis include diabetic retinopathy and retinopathy of prematurity. These conditions are characterised by the profuse growth of retinal vessels and can result in blindness if left untreated [Patz, 1980a].

1.1.3 Investigating Blood Vessel Development

The above is a general overview of vessel formation; the exact process differs slightly from species to species and from organ to organ. One organ which has been widely used to study vessel formation is the mammalian retina. For several reasons it provides a good model:

- it is relatively small and vessels form rapidly over a short period of time
- the whole vascular bed can be easily investigated
- it utilises both vasculogenesis and angiogenesis in a temporally and spatially segregated sequence
- the vascularisation in many species occurs either late in gestation or postnatally, hence the vasculature can be investigated at almost any developmental timepoint

- new vessel growth can be induced readily by manipulating environmental conditions, such as oxygen exposure, to allow the investigation of abnormal or pathologic vessels
- during development the vascular and avascular regions of the retina are well separated, thus factors that promote or suppress vessel growth can be investigated.

1.2 THE RETINA

Human retinal development is similar to that of other mammals including rodents, cats and dogs; it proceeds from the optic disc at the back of the eye towards the ora serrata at the periphery, in two major gradients, vertical and horizontal [Carlson, 1999]. For example, in humans at six weeks gestation the inner and outer walls of the optic cup give rise to the neural and pigmented retina, respectively [Larsen, 1997; Carlson, 1999]. The neural retina undergoes extensive differentiation, and by about 32 weeks gestation forms several vertically aligned cell layers. The horizontal spread of blood vessels, from the centre of the retina to the periphery, is initiated around the 16th week of gestation [Ashton, Ward and Serpell, 1954; Ashton, 1966]. The vessels of the retina reach the ora serrata nasally by approximately 36 weeks, and temporally by full term. While the retinal vessels are forming, a temporary network of blood vessels supplies the front of the eye via the hyaloid artery [reviewed in Avery and Glass, 1998]. However, this system gives off no retinal branches and normally disappears by 34 weeks gestation.

The embryonic vascular system in general arises from mesenchymal tissue. Since the avascular retina lacks mesenchymal elements, the vessels develop from undifferentiated spindle cells that enter the retina via the optic nerve [Ashton, 1966; Henkind and de Oliveria, 1967]. It is believed that these spindle cells differentiate into angioblasts [Ashton, 1966] which undergo further differentiation to become the endothelial cells. The endothelial cells then coalesce to form the solid vascular cords which in turn give rise to patent vessels [reviewed in Risau, 1997].

1.2.1 Retinal Layers

Initially, the neural retina is divided into three layers: the nerve fibre layer, the inner neuroblast layer, and the outer neuroblast layer [Larsen, 1997]. As the retina matures, the cells of both neuroblast layers differentiate, producing a retina that

consists of six layers (Figure 1.1, page 7) [McDonnel, 1994; Larsen, 1997; Carlson, 1999].

The inner neuroblast layer gives rise to the ganglion cell layer (GCL), the inner nuclear layer (INL) and the outer nuclear layer (ONL) [McDonnel, 1994; Larsen, 1997; Carlson, 1999]. Ganglion cells make direct contact with bipolar cells of the INL, which also contains amacrine and horizontal cells. The dendrites from both horizontal and bipolar cells interact with the cell bodies of photoreceptors in the ONL.

As cells within the outer neuroblast layer send out processes, the inner and outer plexiform layers (IPL and OPL, respectively) become better defined [McDonnel, 1994; Larsen, 1997; Carlson, 1999]. The IPL contains the dendrites of ganglion cells and their synapses with amacrine and bipolar axons, whereas in the OPL bipolar and horizontal cell processes make contact with the axons of the photoreceptors. The eventual differentiation of the photoreceptor cells completes the horizontal development of the retina.

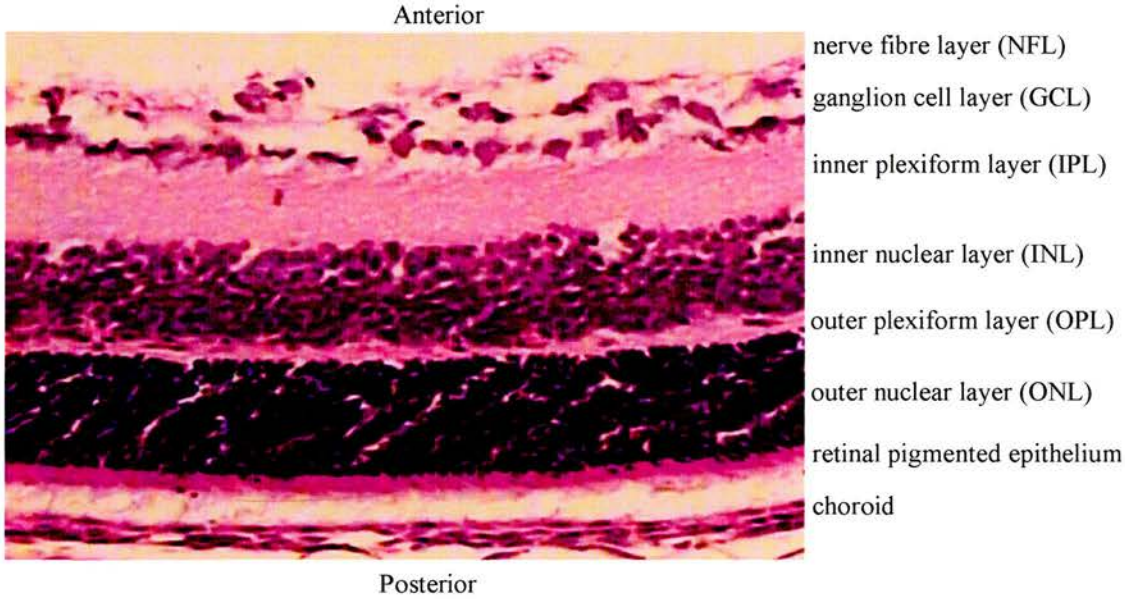

Figure 1.1 Layers of the rat retina.
10μm frozen section of the rat retina stained with hematoxylin and eosin. The retinal morphology is similar in most animals; species differences are confined to the depth of the layers.
Magnification: x20.

1.2.2 Retinal Vessel Formation

Retinal vessel formation proceeds in a centrifugal fashion along a superficial layer (within the GCL) and a deep layer (within the INL), and is essentially controlled by oxygen and, as mentioned above, VEGF.

Control of vessel formation

Oxygen

During early development, the retina is completely avascular and the entire retina receives its oxygen supply from the choroidal vessels located on the outer aspect of the retinal pigmented epithelium. As the retinal layers form and the thickness of the retina increases, this oxygen supply becomes insufficient. As a result the superficial vascular layer forms first followed by the deep vascular layer. These two layers meet the oxygen demands of the inner layers of the retina. The ONL and the OPL remain avascular and continue to consume most of the oxygen delivered by the choroid [reviewed by Provis, 2001].

The importance of oxygen in blood vessel formation was first demonstrated by Ashton and colleagues [Ashton, Ward and Serpell, 1954]. In order to investigate a retinal disorder called retrolental fibroplasia that affects ventilated preterm infants, the researchers raised kittens in various oxygen environments and reported that hyperoxia has an inhibitory effect on the growth of the kitten's retinal vasculature, whereas hypoxia promotes faster spread of vessels into the avascular retina than normoxia.

Almost thirty years later, it came to light that hypoxia is required for the controlled growth of vessels during normal development [Weiter, Zuckerman and Schepens, 1982]. Chan-Ling and colleagues then suggested that normal retinal vessel formation depends on a transient period of hypoxia that is localised, induces the division of retinal endothelial cells, and occurs at the edge of the spreading vasculature [Chan-Ling, Halasz and Stone, 1990]. Once the newly formed vessels open, the oxygen carried in the blood relieves local tissue hypoxia and the

proliferation rate of the endothelial cells is reduced. This hypoxia is termed 'physiological hypoxia' [Chan-Ling and Stone, 1993] because it occurs during the normal process of development, and is well tolerated by the tissue. It now emerges that oxygen is vital during blood vessel formation because it regulates the expression of many growth factors essential to the process.

VEGF

The concept that the retina produces a 'chemical' or 'X factor' to control the formation of its vessels was suggested by Michaelson [Michaelson, 1948]. He went on to suggest that the production of this angiogenic factor is driven by the local metabolic needs of the retina, that it is essential in the development of the vasculature, and that the same factor is involved in neovascular retinal diseases. A series of studies were initiated to identify this all important chemical factor. Fibroblast growth factor was the first retinal growth factor to be discovered [Arruti and Courtois, 1978] and was immediately linked to Michaelson's 'X factor'. However, since this growth factor is not induced by hypoxia [Brogi et al., 1993], it is no longer believed to control vessel development. Later, another growth factor, VEGF, was found to induce endothelial cell proliferation and migration [Ferrera and Henzel, 1989; Millauer et al., 1993] by interacting with VEGF receptor-1 and VEGF receptor-2 [Barleon et al., 1994].

Further evidence for a role of VEGF in vessel formation came from studies on transgenic mice. The studies reported that in comparison to normal embryos, which have a dense plexus of small vessels and larger connecting vessels, mouse embryos lacking the VEGF gene [Carmeliet et al., 1996], or the gene for either of the two VEGF receptors [Fong et al., 1995; Shalaby et al., 1995] display either an irregular plexus of small vessels and lack of larger connecting vessels or fail to develop functional blood vessels. Consequently, all three transgenic mice die at mid-gestation, demonstrating that VEGF is crucial for early vascular development.

However, what allows researcher to label VEGF as Michaelson's 'X factor' is the finding that VEGF is up-regulated by hypoxia. VEGF mRNA levels are dramatically increased within a few hours of exposing different cell cultures to hypoxia [Shweiki et al., 1992; Aiello et al., 1995; Stein et al., 1995]. Its expression eventually returns to background levels when a normal oxygen supply is resumed [Shweiki et al., 1992], but is down-regulated in response to hyperoxia [Stone et al., 1995, 1996]. Therefore, VEGF is the vaso-formative growth factor that acts in both normal and abnormal retinal vessel formation.

The vascular layers

Superficial plexus

The optic disc is the first region of the retina to experience 'physiological hypoxia' [Chan-Ling and Stone, 1993]. Astrocytes, which act as oxygen sensors, migrate from the optic nerve head into the retina [Ling and Stone, 1988; Watanabe and Raff, 1998] and arrange themselves into an array to form a template for the initial retinal vessels [Stone et al., 1995]. Detecting the hypoxia of the avascular retina, astrocytes increase their expression of VEGF [Stone et al., 1995] which promotes the migration and growth of endothelial cells, to form a network of vessels [Ferrara and Henzel, 1989]. Once the area is vascularised and the vessels carry oxygenated blood, the hypoxia is relieved and astrocytes reduce their production of VEGF, limiting vessel growth [Chan-Ling and Stone, 1993; Stone et al., 1995]. Astrocytes then continue to form an array just peripheral to the edge of the growing vasculature [Ling and Stone, 1988], where 'physiological hypoxia' is presumably maximal [Chan-Ling and Stone, 1993]. This entire process of astrocytes invading the avascular areas, secreting VEGF, and then decreasing VEGF production continues until the vessels reach the peripheral edge. Once the astrocytes have fulfilled their role in vessel formation, by providing a scaffold for the endothelial cells, they then function to maintain the blood-retinal barrier by contributing to the formation of the glial limitans [Provis et al., 1995].

The capillary network is then remodelled to again meet the metabolic demands of the tissue, and spaces (called capillary-free zones) develop by the retraction or atrophy of some immature capillaries that are no longer required [Ashton, 1966; Henkind and de Oliveria, 1967]. These spaces are larger on the arterial side and diminish towards the venous side of the capillary circulation [Ashton, 1966]. The vessels that remain are then encapsulated by mural cells [Rhodin, 1968] which may contribute to the stabilisation of the vasculature [Patz, 1968; Speiser, Gillelsohn and Patz, 1968].

The deep plexus

At a later stage, a second vascular layer develops by the blood vessels of the superficial plexus within the GCL extending downwards into the INL of the retina [Chan-Ling, Halasz and Stone, 1990]. This layer is referred to as the deep plexus and in many ways develops in a similar manner as the upper layer. Instead of astrocytes, Müller cells (another class of glial cells) act as a template for new vessels [Flower et al., 1985]. The Müller cells, like astrocytes, detect hypoxia, up-regulate their expression of VEGF and recruit endothelial cells [Stone et al., 1995]. However, the Müller cells do not migrate as the blood vessels form; the vessels grow in a strict radial pattern, following the radial processes of the Müller cells [Flower et al., 1985]. The oxygen brought by these vessels later down-regulates VEGF expression, limiting the growth of the plexus [Stone et al., 1995].

Like the superficial layer, the vasculature of the deep layer first forms centrally and then peripherally; vessels of the superficial plexus at the centre first form the deeper plexus and then the vessels of the superficial layer further out extend into the deep layer and so on until the deep layer finally reaches the periphery. Unlike the superficial layer, however, the vessels of the deep layer seem to form more precisely to the retina's need; there is little evidence of overproduction and retraction among these vessels [Stone and Maslim, 1997].

1.3 RETINOPATHY OF PREMATURITY

Retinopathy of prematurity (ROP) is an eye disease that principally affects ventilated preterm infants. In threshold ROP, normal vasculogenesis of the retina is interrupted and abnormal vessels invade the vitreous. If the disease progresses, retinal scarring can develop followed by retinal detachment, resulting in the loss of vision [Flynn, 1987].

1.3.1 History

The disease was first described by Terry in 1942 who found a greyish-white opaque membrane behind each lens of a six-month old infant that was born at around 32 week gestation. This disease was named retrolental fibroplasia [Terry, 1942] and was soon associated with the supplemental oxygen treatment that premature babies received to increase their chance of survival [Campbell, 1951].

To find out whether high or low concentrations of supplemental oxygen induced retrolental fibroplasia, Campbell compared the clinical set-up of three nurseries with different therapeutic oxygen regimes [Campbell, 1951]. She found that the disease usually developed in premature babies and that high oxygen treated infants developed the disorder more often than those who received low oxygen treatment. These results were confirmed by Patz and colleagues [Patz, Hoeck and Cruz, 1952]. Consequently, oxygen therapy was restricted to 40% or less in the late 1950s and early 1960s, resulting in a significant decrease in the incidence of retrolental fibroplasia [Crosse and Evans, 1952; Ryan, 1952; Guy, Lanman and Dancis, 1956]. Unfortunately, this restrictive use of oxygen also caused an increase in neurological mortality and morbidity as well as respiratory mortality [Avery and Oppenheimer, 1960]. Thus, in the 1970s and early 1980s, the use of oxygen was again liberalised with the reappearance of the disease [reviewed in Weakley and Spencer, 1992; and in Ziavras and Javitt, 1995].

The term 'retinopathy of prematurity' replaced retrolental fibroplasia in the 1980s to stress the importance of neonatal immaturity in causing the disease [Flynn, 1987]. The current disease differs from the original disease because, unlike in the 1950s-1970s, infants are no longer exposed to continuing high oxygen concentrations; instead their blood oxygen levels are monitored and controlled within clinically 'safe' limits [Cunningham et al., 1992, 1995].

1.3.2 Risk Factors

In humans, the retina is not completely vascularised until approximately 40 weeks gestation [reviewed in Avery and Glass, 1988]; hence, all preterm babies are born with some degree of retinal avascularity. The size of the peripheral avascular zone at birth is directly related to the degree of prematurity; the more premature an infant, the larger the retinal avascular area at birth. Although the central retinal area of preterm babies is vascularised, it consists of many delicate capillaries that are still growing and lack the support of more mature vessels. Consequently, these vessels are susceptible to injury. Thus, neonatal immaturity is the single most determining risk factor for ROP [Palmer et al., 1991].

In the 1950s, the survival rate of infants with a birthweight of 1000g or less was very low, but by the late 1980s (with the development of modern intensive care, ventilators and other technology) smaller, more premature infants were surviving. It is now reported that a preterm baby born at or beyond 25 weeks gestation, or with a birthweight of 700g or more, has a 50% chance of survival [Hack and Fanaroff, 1989]. Multicenter clinical trials report that 65% of infants born weighing less than 1251g develop some degree of ROP [Cryotherapy for Retinopathy of Prematurity Cooperative Group, 1990]. The incidence rises to over 80% and 90% in those preterms weighing less than 1000g and 750g, respectively. Hence, ROP is associated with birthweight and is very rarely seen to affect infants with a birthweight greater than 1500g.

As mentioned above, high oxygen levels have a toxic effect on the premature retina. In the 1950s, ROP was not seen to affect those infants who received limited oxygen treatment (concentrations of less than 40%) [Crosse and Evans, 1952; Ryan, 1952; Guy, Lanman and Dancis, 1956]. In addition, the longer a premature infant was kept in an oxygen-enriched environment, the greater was its chance of developing ROP [Kinsey, 1956]. Therefore, next to immaturity, prolonged treatment with high oxygen levels is an important factor.

The incidence of ROP rose in the late 1980s due to the survival of more premature infants; however supplemental oxygen therapy was not considered to play a significant role because continuous transcutaneous oxygen monitoring and blood gas analysis allowed better control of oxygen delivery. So, if infants are no longer exposed to excess oxygen, why do some still develop this disease? A recent study suggests that small fluctuations in oxygen levels within clinically 'safe' limits can cause severe ROP [Cunningham et al., 1995]. It is possible that in these infants hyperoxic episodes or absolute oxygen levels are not the determining factors, but the frequent switching between relatively high and low oxygen levels within clinical limits is more important. As a consequence, there has been a renewed interest in the role of oxygen in the pathology and management of ROP.

A small proportion of infants develop ROP despite never receiving oxygen treatment. Conversely, many infants who receive oxygen therapy never develop the condition. Thus, it is believed that ROP is a multifactorial disease and although numerous risk factors have been implicated, including hypercarbia, hypocarbia, vitamin E deficiency, and metabolic acidosis [reviewed in Avery and Glass, 1988; and in McColm and Fleck, 2001], their role in inducing or promoting the disease are still debated. Only early gestational age, low birthweight and excess oxygen therapy have been consistently associated with the disease. Hence, extremely premature babies of low birthweight that receive supplemental oxygen therapy have the highest incidence as well as the greatest severity of ROP [Campbell, 1951; Patz, Hoeck and

Cruz, 1952; Cryotherapy for Retinopathy of Prematurity Cooperative group, 1988, 1990].

1.3.3 Pathogenesis

The first clinical and animal studies to provide an insight into the pathogenesis of ROP were conducted by Patz [Patz, Hoeck and Cruz, 1952] and by Ashton [Ashton, Ward and Serpell, 1954], respectively. They demonstrated that the disease consists of two clinical phases. During the first phase, called vaso-obliteration, supplemental oxygen therapy interrupts normal vasculogenesis and causes the occlusion and obliteration of existing blood vessels. Once the infant is returned to normal oxygen levels, the disease either regresses naturally, or progresses to the vaso-proliferative phase which involves the formation of new pathologic blood vessels into the vitreous.

Effects

The initial response of the vasculature to elevated oxygen levels is suppression of new vessel formation [Patz, Hoeck and Cruz, 1952; Ashton, Ward and Serpell, 1954; Chan-Ling et al., 1992], and constriction of the most immature vessels, those near the peripheral vanguard of the advancing vasculature [Ashton, Ward and Serpell, 1954]. This is followed by narrowing of the arterioles and venules (causing a decrease in retinal blood flow) and obliteration of the vessels, starting with the capillaries [Ashton, Ward and Serpell, 1954; Chan-Ling et al., 1992]. If the insult continues, the arterioles and venules close and the retina appears avascular [Ashton, Ward and Serpell, 1954].

When an infant or an animal is returned to room air after excess oxygen exposure, the obliteration is reversible in a majority of the affected vessels, and normal vascularisation may resume from the centre of the retina to the peripheral avascular retina [Ashton, Ward and Serpell, 1954]. The likelihood of this depends on the extent of damage, which is determined by the concentration and duration of oxygen

exposure. If, however, the retinal vessels have been extensively obliterated, they are prevented from reopening adequately [Ashton, Ward and Serpell, 1954]. Vasculogenesis is initiated, but the abnormal proliferation of the cells causes a large number of vessels to bud either from the disc or from pre-existing vessels into the retina and then burst into the vitreous [Ashton, Ward and Serpell, 1954]. This profuse growth of new vessels is termed neovascularisation and is the critical step in the chain of events that can cause retinal detachment and blindness in the months or years that follow.

Mechanism

The high oxygen environment of ventilated premature babies makes the avascular portion of the retina hyperoxic (which during normal development is hypoxic). Astrocytes, which usually move into the avascular area and produce VEGF, instead decrease their production of VEGF in response to the increased oxygen levels [Stone et al., 1995]. As a result, spindle cells fail to enter the avascular area and differentiate into the endothelial cells that form the tubules, and the process of vasculogenesis is halted. Normally, once the vasculature is formed, VEGF continues to be expressed in small quantities in order to prevent vessel regression [Stone and Maslim, 1997]. However in ROP, VEGF production is decreased to the extent that many existing vessels undergo regression.

As a result of the oxygen induced vaso-obliteration, on transfer to air the retina suffers an acute lack of oxygen which causes astrocytes, that are present on the retinal surface, to degenerate; but it promotes the migration of new astrocytes into the retina [Stone et al., 1995]. In response to the relative hypoxia the astrocytes produce vast amounts of VEGF and this overproduction of VEGF causes excessive growth of blood vessels [Stone et al., 1995; Pierce et al., 1995a]. In cases where the retina experiences severe hypoxia, astrocytes can degenerate [Chan-Ling and Stone, 1993; Stone et al., 1996], and VEGF is instead expressed by the neurones of the GCL [Stone and Maslim, 1997]. Without astrocytes to serve as a template, the vessels

break through the inner limiting membrane of the retina into the vitreous humour, forming pre-retinal vessels [Zhang and Stone, 1997].

These early animal studies were in line with the clinical practise at the time. High levels of oxygen were used during the first days and weeks of life, followed by return to room air. This produced a vaso-obliterative followed by vaso-proliferative form of retinopathy. Whilst these are adequate to describe the pathogenesis of the old disease, the pathogenesis of the disease seen today cannot be understood by these studies.

1.3.4 Classification

In 1984, a new and precise classification system for ROP was introduced which defines five stages of the disease and fully describes the active retinal changes that occur. Furthermore, it takes into account the location of the disease in the retina and the extent of the vasculature involved [The Committee for the Classification of Retinopathy of Prematurity, 1984].

Location

The retina is divided into 3 circular zones, each centred on the optic disc. Zone I is the most posterior zone and has a radius of twice the distance from the disc to the centre of the macula. Zone II extends from the peripheral edge of Zone I to the ora serrata nasally and to an area near the temporal equator. If the nasal retina is fully vascularised, the limit of vascularisation temporally is considered to be in Zone III. Because Zone III is the last zone to be vascularised, it is most frequently involved in ROP.

Extent

The extent of the disease is specified as clock hours with each hour representing a 30° area of the retina. The greater the number of affected clock hours, the more severe the disease.

Staging

Stage 1, the first of the acute phases of retinopathy, is characterised by a distinct demarcation line separating the avascular retina anteriorly from the vascular retina posteriorly. During stage 2, the line of stage 1 develops into a ridge and has height, width, volume and extends out of the plane of the retina. In most cases of stage 1 and 2 disease, the retinal lesions spontaneously regress, leaving no residual scars. In stage 3 new vessels (or neovascularisation) project upwards from the ridge into the vitreous. This stage is, therefore, characterised by extraretinal fibrovascular proliferation. During stage 4, the fibrous proliferating blood vessels contract causing tractional retinal detachment which may or may not involve the detachment of the macula. The final stage is stage 5, formerly referred to as retrolental fibroplasia, where total retinal detachment occurs.

Progressive vascular incompetence is characterised by increasing dilation and tortuosity of the central retinal vessels, as well as iris vascular engorgement with pupillary rigidity. These vascular changes can occur at any time and when they do, a 'plus' is added to the ROP stage number.

1.3.5 Treatment

In a high number of infants affected by acute ROP (stages 1 and 2), the disease spontaneously regresses and the retina appears normal. If, however, the disease progresses to stage 3, ophthalmologic treatment is necessary. If the retina is still attached then retinal cryotherapy, and more recently diode laser photoablation therapy is used [reviewed in Phelps, 1993]. These therapies make use of lasers focused through the pupil, or supercold probes applied to the outside of the eye, to destroy the avascular peripheral retina that is ischaemic. It is believed that the destruction of the ischaemic tissue prevents the continued production of growth factors and therefore continued vessel growth, while preserving the retina already vascularised. By producing extensive chorioretinal scars, cryotherapy is expected to reduce or halt fibrovascular proliferation. While this therapy is often successful, it

none-the-less destroys the peripheral retina irrevocably and can limit the vision of the child. If the retina detaches from the sclera, then a scleral buckle procedure is used in combination with cryotherapy. The aim is to bring the sclera close to the retina and then to 'weld' the retina to the underlying choroid with cryotherapy or laser burns [reviewed in Phelps, 1993].

1.4 MODELS OF OXYGEN-INDUCED RETINOPATHY

Several animal models of ROP have been generated which have provided invaluable insights to the pathogenesis of the disease. These models depend on extreme levels of oxygen to induce retinal vascular changes in neonatal animals, and are therefore more representative of the old disease, retrolental fibroplasia. Although many models parallel the early stages of the human disease, the exact disease has never been reproduced in animals. Conversely, some models develop abnormal features that are not described in human ROP.

1.4.1 Dog

Flower and Blake exposed two day old puppies to 95-100% oxygen for three days and reported a significant constriction of the retinal blood vessels [Flower and Blake, 1981]. These results were later confirmed by McLeod et al. who maintained newborn puppies in 100% oxygen for four days [McLeod, Brownstein and Lutty, 1996; McLeod, Crone and Lutty, 1996]. In this model, the progressive constriction of the developing retinal vasculature resulted in vaso-obliteration, and upon return to room air, the abnormal proliferation of the blood vessels progressed into the vitreous.

Advantages / disadvantages

Retinal vessels of both the newborn dog and the premature infant exposed to hyperoxia share many morphological features: vaso-obliteration [McLeod, Crone and Lutty, 1996]; dilation and tortuosity of the posterior pole vessel, known as plus disease in infants [McLeod, D'Anna and Lutty, 1998]; severe overgrowth of the capillaries, producing an elevated ridge of vessels at the border of the vascular retina [McLeod, D'Anna and Lutty, 1998]; and neovascular lesions [McLeod, D'Anna and Lutty, 1998]. However, the optic nerve head neovascularisation and posterior vascular tufts that are somewhat common in hyperoxic dogs are not usually associated with human ROP [McLeod, D'Anna and Lutty, 1998].

1.4.2 Kitten

Ashton and colleagues were the first to mimic ROP in an animal by exposing kittens to 70-80% oxygen and reported the effects of various oxygen concentrations (25% up to 80%) and duration of exposure (three to 26 days) on the development of the feline retina at different ages [Ashton, Ward and Serpell, 1954]. They found that constant hyperoxia caused vaso-constriction of the growing vessels followed by vaso-obliteration. The capillary bed slowly disappeared and soon the retina appeared avascular, but if the insult was severe enough the vasculature could be completely destroyed. When the kittens were returned to room air, vaso-proliferation was observed at the optic disc of the retina and in the vitreous [Ernest and Goldstick, 1984; Chan-Ling et al., 1992]. After relief of this relative hypoxic phase, the retina revascularised from the optic disc outwards [Ashton, Ward and Serpell, 1954]. This final stage was called normalisation [Chan-Ling et al., 1992].

Advantages / disadvantages

Retinal vascularisation in a newborn kitten is similar to a 25-30 week human fetus [Patz, 1968], and is completed by postnatal day eight (P8) [Ernest and Goldstick, 1984]. Similarities between the cat and human forms of ROP are: the growth of proliferative intraretinal vessels; leakiness of both the pre-retinal and peripheral intra-retinal vessels; and normalisation of the proliferative vasculature, termed regression in humans [Chan-Ling et al., 1992]. The closure and obliteration of the retinal vessels during hyperoxia are not well described in premature infants, but it is assumed that this is due to the cloudiness of the optics of the eye. The features have, however, been reported in post-mortem human retina [Ashton, 1966]. Therefore, the cat provides a relatively accurate model of human ROP.

1.4.3 Rat

In one of the earliest animal experiments investigating oxygen-induced retinopathy rats (age not stated) were exposed to 40-50% oxygen which resulted in vaso-constriction of the retinal vessels [Patz et al., 1953]. However, when rats were raised

in 70-80% oxygen, complete obliteration of the vessels was observed within four days and by 12-15 days, capillary tufts (abnormal neovascularisation) were noted on the surface of the retina.

Ashton and Blach exposed rats at various ages, from birth to P11, to high oxygen levels (concentrations not stated) and found that hyperoxia alone caused partial obliteration of the retinal vessels [Ashton and Blach, 1961]. When the rats were returned to room air much of the retina remained permanently obliterated and no abnormal vaso-proliferation occurred.

Rat models of ROP have been widely used by Penn and colleagues [Penn, Tolman and Lowery, 1993; Penn, Tolman and Henry, 1994; Penn, Henry and Tolman, 1994; Penn et al., 1995]. Their first study involved exposing newborn rats to a constant oxygen concentration of 80% for up to 14 days. This regime produced the first stage (vaso-attenuation) of the disease, but failed to produce the subsequent phases of abnormal proliferation and pre-retinal neovascularisation [Penn, Tolman and Lowery, 1993]. Instead, newborn rats exposed to alternating 40% and 80% oxygen followed by relative hypoxia (by placing them in room air) developed pre-retinal neovascularisation [Penn, Tolman and Lowery, 1993]. The group then investigated the retinal changes induced by various oxygen cycling regimes, and determined that alternating between 50% and 10% inspired oxygen every 24 hours for 14 days followed by a four day period in room air produced the highest incidence (100%) and the greatest severity of neovascularisation [Penn, Henry and Tolman, 1994].

Advantages / disadvantages

The rat retina at birth is avascular and normally vascularisation is completed by day 14 [Penn, Tolman and Lowery, 1993; Holmes, Duffner and Kappil, 1994]. Thus, formation of the retinal vessels in rats can be observed at various time points. Although there are some developmental differences, the rat oxygen-induced retinopathy model closely resembles the vascular changes seen in the human disease. In addition, this model is reproducible and well established in the literature.

1.4.4 Mouse

The most widely used mouse model of oxygen-induced retinopathy was developed by Smith and colleagues. From day seven (when the hyaloid vessels had regressed and the retina resembled that of the premature infant) to day 12 (at which point normal vascularisation was near completion) mice were exposed to 75% oxygen. The mice were then returned to room air and sacrificed between P17 and P21. The initial response of the mice to high oxygen was central vaso-constriction followed by non-perfusion. The larger vessels became tortuous and engorged, and between P17 and P21 maximum neovascularisation was observed. With a longer recovery period in room air, the neovascularisation regressed and the vascular pattern normalised [Smith et al., 1994].

Newborn mice raised in 90-95% oxygen for five days, followed by room air recovery also developed retinopathy [Browning, Wylie and Gole, 1997]. This regime produced reliable and consistent results and the extent of neovascularisation could be quantified. By day 20, the rate of vessel growth was similar to control animals, however a peripheral avascular area still remained.

Advantages / disadvantages

Like rats, the vascular development of newborn mice occurs postnatally and resembles that of the infant. The mouse models are reproducible, inexpensive and reflect the retinal neovascularisation and the proliferative neovascular phase of ROP. The drawback to the model developed by Smith et al. is that the vascular changes occurred only centrally and the peripheral vasculature is spared from any damage [Smith et al., 1994]. Although Browning's model produces quantifiable neovascularisation and an increase in peripheral capillary density, adult mice are very vulnerable to extreme levels of oxygen, and the mortality rate of the mothers in these experiments is high [Browning, Wylie and Gole, 1997]. Nevertheless, because the mouse retina responds rapidly to hyperoxia, it is an excellent model for the study of angiogenesis and inhibition of vessel growth [Browning, Wylie and Gole, 1997].

1.5 A CLINICALLY-RELEVANT MODEL OF ROP

1.5.1 Basis for a New Model

The current animal models of oxygen-induced retinopathy use large swings in oxygen concentration to produce the retinal vascular changes observed in human ROP. One criticism is that these models are characteristic of the disease seen in the 1950s and 1960s, when supplemental oxygen therapy was neither monitored nor controlled, and therefore, are not reflective of the oxygen environment experienced by present-day premature babies.

Ventilated neonates in the Simpson's Maternity Pavilion, Edinburgh have their transcutaneous oxygen (TcO_2) levels recorded every second by a cotside monitor and stored as an average each minute [Cunningham et al., 1992]. Over a period of almost three years, the recorded data of preterm infants from birth to 21 days of age was analysed; 69 babies were included of which 38 had no, stage 1 or 2 ROP and 31 had stage 3 or greater ROP. The study found that although there was no difference in the average blood oxygen levels between the two groups, preterm infants who developed severe ROP experienced a greater number of small fluctuations in blood oxygen levels within clinically 'safe' limits than those with no or acute ROP [Cunningham et al., 1995]. The study also showed that greater variability in TcO_2 during the first two weeks of life was particularly significant in inducing the disease.

Taking this cohort study into consideration, a computer controlled oxygen delivery system was developed that produced minute-by-minute changes in oxygen concentration within an animal chamber, by injections of oxygen or nitrogen gas, mimicking the changing oxygen environment of this cohort of ventilated preterm infants [McColm and Cunningham, 2000].

1.5.2 The Edinburgh Model

A 14-day profile of the oxygen data from a preterm infant who developed stage 4 ROP was translated into percentage inspired oxygen levels for the rat (diagram below) since the relationship between blood oxygen level and inspired oxygen is linear [Penn et al., 1995]. Rats exposed to this clinically relevant oxygen profile, that had a mean oxygen concentration of 21.3%, developed features of ROP; the retinas had a significantly reduced vascular area and capillary density compared to the controls (details of measuring avascularity and capillary density are given in Chapter 6) [Cunningham et al., 2000]. The retinal vasculature of the experimental pups was also unremodelled and immature in appearance.

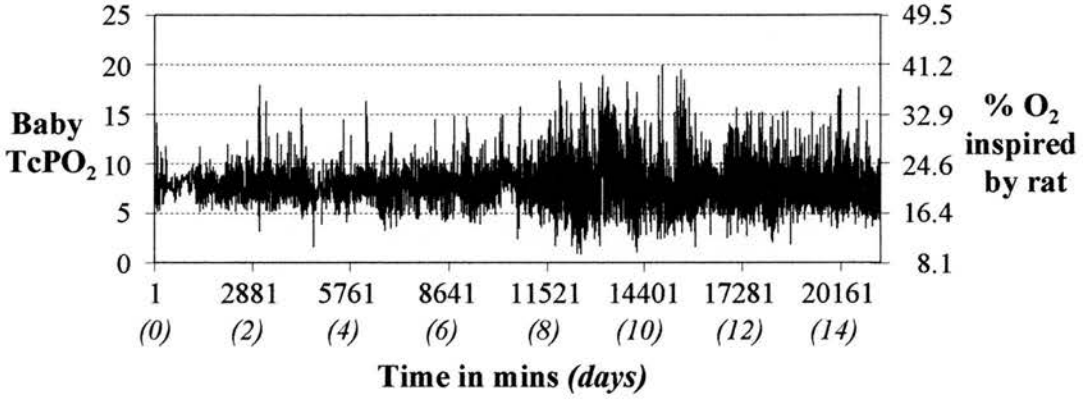

Figure 1.2[1] The 14-day minute variable oxygen profile.
The oxygen profile of a preterm infant translated into equivalent oxygen levels for the rat.

In summary, by exposing rat pups to small frequent fluctuations, rather than large swings in oxygen levels every 12 or 24 hours, this model induced the early stages of ROP. Thus, the Edinburgh model is more comparable to the retinal disorder that can occur in present-day ventilated extremely premature infants.

Clinically the lower and upper TcO_2 limits for infants are set to 6kPa and 10kPa, respectively [Cunningham et al., 1995], therefore neonatal staff attempt to maintain the babies at a mean of 8kPa. In the original animal study, the oxygen profile also

[1] Taken, with permission, from McColm and Cunningham, 2000.

had a mean of 8kPa, termed normoxia [Cunningham et al., 2000]. Next the relative contribution of hypoxia (6kPa) and hyperoxia (10kPa) with fluctuating oxygen on the rat retina was investigated [McColm et al., 2004]. The data was again translated into inspired oxygen levels for the rat with a mean of 6kPa (17.9% O_2) and 10kPa (24.7% O_2). This study showed that pups raised in the 10kPa regime, where they spent 90% of their time above 21% inspired oxygen, had a larger avascular peripheral area and a higher capillary density than those raised in the 8kPa regime, where only 50% of their time was spent above 21% oxygen. In contrast, retinas of rats exposed to the 6kPa profile, spending 90% of their time below 21% oxygen, appeared relatively normal. Thus, pups exposed to the hyperoxic variable regime developed the most severe disease.

Although no neovascularisation was observed, abnormal dilated terminal vessels were noted at the vascular/avascular interface in 21% and 43% of the normoxic and hyperoxic retinas, respectively [Cunningham et al., 2000; McColm et al., 2004]. These abnormal vessels could be precursors of pre-retinal vessels. In other models of oxygen-induced retinopathy, a period of room air recovery is needed to induce neovascularisation [Penn, Tolman and Lowery, 1993; Penn, Tolman and Henry, 1994; Penn, Henry and Tolman, 1994; Smith et al., 1994] and this model might also have done, however, the research group did not allow rats this period in room air because in the clinical setup preterm infants do not experience a switch from a high oxygen to a relatively low oxygen environment; the infants progress to threshold ROP whilst they are receiving supplemental oxygen therapy and are gradually reintroduced to room air.

1.5.3 The Species of Choice

The rat was the species of choice in developing this model for several reasons. Compared to the kitten and dog, the rat model has low cost, low animal maintenance, large litter sizes, and short gestation. More importantly, the rat retina takes 14 days to completely vascularise, allowing the investigation of vessel growth at any stage of

development. Although, the mouse is an excellent model for the general study of angiogenesis, and has the added advantage of investigating the effects of oxygen on various transgenics, the mouse retina proliferates only centrally after hypoxic exposure [Smith et al., 1994], making it less valuable for studying the pathogenesis of ROP.

1.6 AIMS AND HYPOTHESIS

A vast body of literature is available on the processes and mechanisms of early vasculogenesis, including endothelial cell production, migration and proliferation. In comparison, less attention has been directed towards the later stages of vasculogenesis, especially maturation and stabilisation of the vasculature by investment of mural cells and production of basement membrane. In an infant born at 24 weeks gestation, only about half the retina is vascularised [Phelps, 1992], and without the support of basement membrane, pericytes and smooth muscle cells of the more mature vessels, the capillaries are particularly susceptible to injury from hyperoxia [Patz, 1968].

The purpose of the work described in this thesis was first to investigate the stabilisation of retinal blood vessels in normal development by studying:

- the cell-to-cell interactions between endothelial cells, pericytes and smooth muscle cells
- the expression patterns of the principle regulators of vessel stabilisation, which include platelet-derived growth factor, transforming growth factor-β and the angiopoietin/Tie-2 system;

and second, to determine if the expression of these stabilising factors were altered in a clinically relevant model of ROP (Edinburgh model).

As discussed above retinal blood vessels are particularly vulnerable to changes in inspired oxygen levels. Thus, it is proposed that the cell-to-cell contacts in the retinas of the Edinburgh model would be compromised. It is also expected that the expression of growth factors that promote and maintain retinal blood vessel stability would be altered by the oxygen regime, since other growth factors, such as VEGF, have been shown to be directly regulated by oxygen [Shweiki et al., 1992; Aiello et al., 1995; Stein et al., 1995; Stone et al., 1995, 1996].

CHAPTER TWO

MURAL CELLS OF THE RETINAL VESSELS

2.1 INTRODUCTION

2.1.1 The Vascular Network of the Retina

The vasculature is composed of two distinct cell types: endothelial cells which assemble into a network of blood vessels; and mural cells which encapsulate the vessels [reviewed in Risau, 1997]. There are two types of mural cells; smooth muscle cells which densely cover larger vessels [Bloom and Fawcett, 1968], and pericytes that form a non-continuous layer around smaller vessels [Rhodin, 1968]. In comparison to endothelial cells, relatively little is know about the mural cells. There are several hypothesises regarding mural cell origin, their functions, mechanisms of action and recruitment during blood vessel development. These hypothesises will be discussed in this chapter, followed by a detailed account of mural cell coverage of the rat retinal vasculature.

The vessel system feeding the retina begins with the central retinal artery within the optic nerve that resembles other small arteries of the circulatory system [Wise, Dollery and Henkind, 1971]. When the artery enters the retina, it divides into several intraretinal branches (arterioles), where the endothelial cells are orientated parallel to the vessel axis and are surrounded by smooth muscle cells. The central vein also divides into intraretinal branches (venules) that are larger than the arterioles, but have a much thinner wall. The capillary network connecting the arterioles and venules are classified into pre-capillaries, true-capillaries and post-capillaries [Zimmermann, 1923[1]]. As retinal arterioles split into pre-capillaries, the smooth muscle cell coverage is decreased and the microvessels begin to develop a pericyte coating that extends onto the venules.

Although both types of mural cells will be examined in my studies, more attention will be directed towards pericytes for two reasons. Firstly, the main vessels of the retina resemble other small arterioles and venules in the circulatory system, therefore smooth muscle cell coverage is expected to be limited to these larger vessels. Secondly, in animal models mimicking retrolental fibroplasia, hyperoxia causes the retinal arterioles to contract resulting in the regression of the capillary network [Ashton, Ward and Serpell, 1954]. It is possible that in these animals, vessel regression is due to delayed or loss of pericyte coverage.

2.1.2 Identification of Mural Cells

Microvascular mural cells were first identified in 1873 and described by Rouget as 'non-pigmented adventitial cells' present in the vasculature of many species[2]. Since their discovery, these cells have been called Rouget cells [Clark and Clark, 1925; de Oliveria, 1966], pericapillary cells [Battig and Low, 1961], undifferentiated cells, perivascular cells, and intramural pericytes [Ashton and de Oliveria, 1966; de

[1] The original paper was written in German and a translation was not available. This is taken from the review by Darland and D'Amore, 2001b.

[2] The original paper was written in French and a translation was not available. This is taken from the review by Ashton and Oliveria, 1966.

Oliveria, 1966]. However, the most widely used term today is pericyte ('peri' meaning around and 'cyte' meaning cell), as suggested by Zimmermann[3].

Mural cells can be distinguished from other cells of the vasculature, such as endothelial cells and fibroblasts, by their location within the vascular network, by their morphology, and more recently by their expression of certain protein markers. However, differentiating pericytes from smooth muscle cells is more difficult, firstly because some mural cells of smaller vessels lack the typical structure of either a pericyte or a smooth muscle cell, and secondly, because studies investigating the expression of protein markers by pericytes and smooth muscle cells have produced conflicting results.

Morphology

Using electron microscopy, the complete structure of blood vessels was gradually revealed. It was found that the relative frequency and distribution of mural cells varies among species and within different organs, and that coverage differs depending on the type and location of the vessel [Tilton et al., 1985].

Smooth muscle cells are elongated, spindle shaped cells with fine tapered ends and a wider central region which contains the elongated or ovoid nucleus. The length of these cells depends on the location, from about 20μm in diameter in smaller arteries to 500μm in larger vessels [Weiss, 1988]. Smooth muscle cells can be found arranged in small bundles surrounding large arteries, or as sheets of circumferentially orientated individual cells around arterioles. Veins also have a smooth muscle cell covering, but it is considerably reduced in comparison to arteries. All smooth muscle cells are arranged offset with respect to one another so that the nuclear region of one is adjacent to the tapered ends of its neighbours [Bloom and Fawcett, 1968; Leeson and Leeson, 1976].

---

[3] Reviewed in Sims, 1986.

In 1923, Zimmermann[4] investigated pericytes in many vertebrates, including fish, amphibians, reptiles, birds and mammals, and reported that the cell bodies of pericytes are often elongated with multiple, long and slender cytoplasmic processes that run parallel to the axis of capillaries or encircle the capillary wall. The pre-capillary pericyte processes are mainly wrapped around the vessel, with a few lying along the axis [Zimmermann, 1923[4]; Fujiwara & Uehara, 1984]. True capillaries are encircled by few widely scattered pericytes with many primary and secondary branches [Rhodin, 1968] that are arranged longitudinally and circumferentially, respectively [Zimmermann, 1923[4]; Fujiwara & Uehara, 1984]. Post-capillaries have the greatest number of pericytes [Rhodin, 1968]. The cells are more branched with shorter processes [Zimmermann, 1923[4]], and appear not to be confined to a particular orientation [Fujiwara & Uehara, 1984]. In addition, Zimmermann[5] found that pericytes of pre- and post-capillaries display a gradual transition to smooth muscle cells and termed them 'transitional' pericytes, and called the cells of the mid-capillaries 'true' pericytes.

Whereas smooth muscle cells are separated from endothelial cells by a thick layer of extracellular matrix, pericytes and endothelial cells of capillaries are separated by a thin layer of basement membrane [Steinberg, 1963]. So, in comparison to smooth muscle cells, pericytes lie in close proximity to endothelial cells with occasional points of direct contact [Rhodin, 1968; Fujiwara and Uehara, 1984], but the processes of one pericyte rarely contact those of a neighbouring pericyte [Rhodin, 1968].

Protein markers

α-smooth muscle actin (α-SMA)

Actin is a major cytoskeletal protein expressed in mammals as six isoforms, four of which are markers of muscle tissue [Owens and Thompson, 1986]. The expression of α-SMA (muscle-specific actin) by pericytes has been reported by several

[4] Reviewed in Sims, 1986.
[5] Reviewed in Nehls and Drenkhahn, 1993; Darland and D'Amore, 2001b.

researchers [Skalli et al., 1989; Mitchell et al., 1990; Newcomb and Herman, 1993; Nicosia and Villaschi, 1995]. Herman and D'Amore, for example, found from *in situ* and *in vitro* labelling of endothelial cells, pericytes and smooth muscle cells, that α-SMA stained both pericytes and smooth muscle cells whereas β-SMA (non-muscle specific actin) positively stained pericytes and endothelial cells, but not smooth muscle cells [Herman and D'Amore, 1985]. Some researchers, however, argue that pericytes do not express α-SMA. Nehls and Drenckhahn found that capillaries of the retina and mid-capillaries of the mesentery artery were devoid of α-SMA [Nehls and Drenckhahn, 1991]. The pre-capillary and post-capillary pericytes of the mesentery artery, however, stained positively for α-SMA. They suggested that the α-SMA positive mural cells that covered vessels were in fact smooth muscle cells. This, to some extent, agrees with Zimmermann[6] who stated that pre-capillary and post-capillary pericytes display a gradual transition to smooth muscle and that only the mid-capillary pericytes are 'true' pericytes.

Myosin

Myosin, like smooth muscle actin, consists of several isoforms, and is an essential component of the contractile system present in muscle and non-muscle cells. Studies of cultured pericytes and tissue sections demonstrated that pericytes expressed both the α and β isoforms of myosin [Joyce, Haire and Palade, 1985; Ehler et al., 1995], though β-myosin was more predominant in small capillaries [Joyce, Haire and Palade, 1985]. Myosin was also expressed by endothelial cells [Joyce, Haire and Palade, 1985; Ehler et al., 1995], but not by vascular smooth muscle cells [Mitchell et al., 1990].

Desmin

Desmin is one of the two principal intermediate filament proteins present in muscle and muscle-like cells [Debus, Weber and Osborn, 1983]. Many researchers agree that smooth muscle cells express desmin [Mitchell et al., 1990; Nehls, Denzer and Drenckhahn, 1992; Nicosia and Villaschi, 1995] however, their opinion regarding

[6] Reviewed in Darland and D'Amore, 2001b.

the expression of desmin by pericytes differ. In one study the desmin antibody stained fine processes running along the mid-capillaries; the authors suggested that these processes belonged to the youngest pericytes in the vasculature [Nehls, Denzer and Drenckhahn, 1992]. By that account, it is possible that desmin was the first marker to be expressed by pericytes. In contrast, another study reported that during the early stages of angiogenesis, pericytes cultured from rat aorta were desmin negative and became weakly positive later in development [Nicosia and Villaschi, 1995].

Other markers

Vimentin is another intermediate filament protein expressed by muscle cells. As well as staining endothelial cells, vimentin also stained pericytes of various tissues [Mitchell et al., 1990; Ehler et al., 1995]. Observations showed that as the mesenchyme cells matured, their expression of vimentin also increased, but the expression was down-regulated as the cells differentiated towards the smooth muscle lineage [Ehler et al., 1995].

3G5 (a ganglioside-like antigen) labelling was continuous and limited to the external margins of retinal capillary walls [Nayak et al., 1988]. Unlike the markers mentioned above, 3G5 only stained pericytes and not other vascular cells, such as endothelial cells or smooth muscle cells [Nayak et al., 1988; Schlingemann et al., 1990], thus the 3G5 antibody may be the most specific marker for pericytes within the microvasculature.

NG-2 is a high molecular weight melanoma-associated antigen [Schlingemann et al., 1990; Grako and Stallcup, 1995] which has been suggested to be a specific marker for activated pericytes during angiogenesis [Schlingemann et al., 1990]. Yet, NG-2 may not be a suitable marker for *in situ* detection of pericytes because it has also been reported to stain immature smooth muscle cells [Burg et al., 1999] and proliferating endothelial cells [Pagan-Mercado et al., 2002].

In summary, a marker specific to any one of the two mural cells is currently unavailable, since much of the published data is contradictory. Be that as it may, there are several reasons for the discrepancies between the reports. Firstly, the anatomy of the capillary system differs from tissue to tissue and no two studies have investigated the exact same vasculature from the same species. Secondly, in studies involving cell cultures the pericytes were obtained from different sources and instead of being from true capillaries, they may be of vascular smooth muscle origin. Thirdly, it is possible that the expression of the markers differs depending on the stage of pericyte differentiation or on the maturity of the pericyte.

2.1.3 Origin and Recruitment of Pericytes

One of the biggest controversies surrounding mural cells is their embryonic origin. There are three hypothesises, and it has been suggested that all three are correct and all contribute to pericyte differentiation.

Kuwabara and Cogan thought that pericytes stemmed from a layer of undifferentiated cells called the mesenchyme [Kuwabara and Cogan, 1963]. Their theory was soon backed by Shakib and de Oliveria [Shakib and de Oliveria, 1966]. Furthermore, Hirschi and colleagues grew 10T1/2 cells (presumptive mesenchymal cells or mural cell precursors) on their own and as co-cultures with endothelial cells and found that in the presence of endothelial cells, the 10T1/2 cells underwent dramatic shape change from polygonal to spindle-shaped (typical structure of mural cells) [Hirschi, Rohovsky and D'Amore, 1998]. In addition, when endothelial cells and 10T1/2 cells were grown in three-dimensional co-cultures, the cells were organised and orientated similar to vessels *in vivo*; the endothelial cells became tightly associated in cord like structures and the 10T1/2 cells either stretched along or wrapped around the endothelial cells [Darland and D'Amore, 2001a].

In 1873, Rouget[7] described pericytes as less differentiated smooth muscle cells, which implies that pericytes and smooth muscle cells are somehow related. Since Rouget's statement, a body of evidence has gathered confirming that pericytes and smooth muscle cells are indeed related:

- pericytes react with both muscle and non-muscle isoactin
- in culture the morphology of pericytes is very similar to smooth muscle cells
- both cells are similar in their location (external margin of the endothelium).

Over a century later this theory was developed further and it was suggested that pericytes might be derived from nearby vascular smooth muscle cells that 'dedifferentiate', proliferate and then associate with new sprouts [Nicosia and Villaschi, 1995; Lindahl et al., 1997; Hellström et al., 1999].

The third hypothesis is that pericytes are at least partly differentiated from stromal fibroblasts. Nehls and colleagues reported that desmin positive pericytes were fibroblast-like in morphology and found that once endothelial cells and fibroblasts established a contact, the fibroblasts differentiated into periendothelial cells and began to express desmin. The pericytes of the small capillaries then acquired smooth muscle-like features [Nehls, Denzer and Drenckhahn, 1992].

The method by which pericytes and smooth muscle cells cover the vasculature is unclear. It is proposed that the cells migrate systematically from the root to the tip of microvessels using pre-existing parent vessels as a guide and as a surface for attachment [Crocker, Murad and Geer, 1970]. However, Benjamin and colleagues observed that mural cell coating (identified using α-SMA) lagged significantly behind the formation of the blood vessels [Benjamin, Hemo and Keshet, 1998], and suggest that although retinal vessel formation proceeds radially from the optic disc outwards [Stone et al., 1995], vessel coverage proceeds in the arteriole to venule

[7] Reviewed in Darland and D'Amore, 2001b.

direction. Another mechanism may involve the *in situ* differentiation of mural precursor cells similar to differentiation of angioblasts into endothelial cells during vasculogenesis [Carmeliet and Collen, 1998]. It is also suggested that in the adult vasculature pericytes may sprout from a pre-existing parent vessel at sites of angiogenesis [Nehls and Drenckhahn, 1993].

2.1.4 Roles of Pericytes

A number of functions have been ascribed to pericytes, and since smooth muscle cells and pericytes are so closely related, the most obvious pericyte function is contraction, which was first suggested by Rouget[8]. This has been supported by studies showing that pericytes express many contractile proteins, including α-SMA [Herman and D'Amore, 1985; Herman et al., 1987; Skalli et al., 1989], myosin [Joyce, Haire and Palade, 1985; Ehler et al., 1995] and desmin [Mitchell et al., 1990; Nehls, Denzer and Drenckhahn, 1992]. Yet, this role is greatly debated since there is no direct evidence for pericyte contractility in the retina [Friedman et al., 1949].

Other general attributes of the pericytes are phagocytosis during inflammatory response [Majno and Palade, 1961] and maintenance of a selective permeability barrier for plasma constituents [Hirschi and D'Amore, 1996]. The latter function is supported by the varied pericyte distribution according to the needs of different tissues [Frank, Dutta and Mancini, 1987; Shepro and Morel, 1993].

Regarding blood vessel formation, the main role of pericytes is suggested to be stabilisation of the vessel wall and, therefore, maintenance of vascular integrity [Kuwabara and Cogen, 1963; Orlidge and D'Amore, 1987; Suri et al., 1996]. It is believed that the pericytes stabilise the vasculature by providing support for the endothelial tubules, by transforming a 'plastic' tubule into a 'static' structure and possibly by protecting the tubules from damage:

---

[8] Reviewed in Diaz-Flores et al., 1991, and in Nehls and Drenkhahn, 1993.

- endothelial tubules which lack a coating of mural cells are leaky and prone to rupture [Suri et al., 1996]
- loss of retinal capillary pericytes in diabetic retinopathy may be linked to the occurrence of microaneurysms reported in the disease [Kuwabara and Cogen, 1963]
- vessels with the slowest endothelial cell turnover have the highest extent of pericyte coverage [Tilton et al., 1985]
- in cell cultures, when endothelial cells and pericytes come into contact, endothelial cell proliferation is inhibited [Orlidge and D'Amore, 1987].

The exact mechanism by which pericytes promote vessel stability is unclear. There are, however, a number of factors involved: firstly, endothelial cells and pericytes must interact with each other by at least coming into close proximity; secondly, the production and secretion of basement membrane proteins by the pericytes; and thirdly, the release of vascular growth factors by both cells. These factors are described in further detail below.

2.1.5 Regulation of Pericyte Growth and Differentiation

Like all cell types, pericytes are affected by changes in the surrounding environment, for example, the increased or decreased expression of growth factors. During vessel development, the actions of pericytes are dependant on three main growth factors secreted by the pericytes themselves or by other cells in close proximity.

Platelet-derived growth factor-B, secreted by endothelial cells [Collins et al., 1985], binds to its receptor expressed on the cell surface of undifferentiated mesenchymal cells [Bernstein, Antoniades and Zetter, 1982]. PDGF-B is reported to induce the migration of undifferentiated mesenchymal cells towards endothelial cells [Hirschi, Rohovsky and D'Amore, 1998].

As discussed earlier, one of the functions of pericytes is to inhibit endothelial cell proliferation [Orlidge and D'Amore, 1987]. It is believed that this effect is mediated through transforming growth factor-β, which is activated when endothelial cells and pericytes make contact (or came into close proximity) [Antonelli and Orlidge, 1989; Sato and Rifkin, 1989]. Although this growth factor suppresses endothelial growth, it promotes the differentiation of mesenchymal cells into pericytes [Hirschi, Rohovsky and D'Amore, 1998] and promotes the proliferation of the pericytes [Hellström et al., 1999].

Transgenic mice lacking either the gene for angiopoietin-1 [Suri et al., 1996] or the gene for its receptor (Tie-2) [Dumont et al., 1992] share many phenotypic abnormalities including the lack of endothelial cell encapsulation by mural cells. Consequently, the vessels of these mice are fragile and prone to rupture and leakage. In addition, the angiopoietin-1/Tie-2 system also inhibits endothelial cell apoptosis [Kwak et al., 1999; Papapetropoulos et al., 1999].

It has been suggested that pericytes and smooth muscle cells are capable of producing basement membrane [Shakib and de Oliveria, 1966] and extracellular matrix components [reviewed in Owens, 1995], respectively, which in turn have profound effects on cell behaviour including migration, proliferation and differentiation. The basement membrane covering endothelial cells is mainly composed of collagen and has several functions, the most important of which is support; acting as a framework for the endothelial cells and pericytes and as an anchor for the vessel to the surrounding tissue.

Thus, the current theory with regard to how a mesh of unremodelled vessels becomes a mature network can be described in the following way. Once the endothelial tubules are formed and before smooth muscle cell or pericyte coverage begins, there is a time interval (or window of plasticity) during which the vasculature remodels and adjusts to the physiological needs of the tissue [Benjamin, Hemo and Keshet, 1998]. The endothelial cells then secrete platelet-derived growth

factor-B, which binds to the receptor on undifferentiated mesenchymal cells, and promotes their migration towards the endothelial cells [Hirschi, Rohovsky and D'Amore, 1998]. As these mesenchymal cells come into close contact with endothelial cells, both cells begin to release transforming growth factor-β promoting the differentiation of mesenchymal cells into mural cells [Antonelli-Orlidge et al., 1989; Sato and Rifkin, 1989], and suppressing vascular growth by inhibiting endothelial cell proliferation [Orlidge and D'Amore, 1987]. Pericytes then synthesise and secrete new basement membrane [Diaz-Flores et al., 1994], while smooth muscle cells produce extracellular matrix components [reviewed in Owens, 1995; and in Hungerford and Little, 1999], at which point the proliferative phase comes to an end. Vessel regression is inhibited by the interaction of angiopoietin-1 with the tie-2 receptor; however, the exact role of angiopoietin-1 in this process is yet to be fully elucidated.

2.1.6 Pericytes in Postnatal Life

The adult vasculature, although mature, still undergoes changes in physiological situations such as wound repair and menstruation. Thus, it is hypothesised that pericytes are involved in sprouting angiogenesis [Nehls, Denzer and Drenckhahn, 1992; Hirschi and D'Amore, 1997]. Briefly, pericytes are activated by a number of angiogenic stimuli and the basement membrane is degraded [Diaz-Flores et al., 1994]. As a result, the contact between the pericytes and endothelial cells is thought to be loosened, but the pericytes guide the migrating endothelial cells and continue to regulate their proliferation [Hirschi and D'Amore, 1997]. The endothelial cells form a connection between new sprouts [Nehls, Denzer and Drenckhahn, 1992] at which point angiogenesis comes to an end and the pericytes reoccupy their position, synthesise new basement membrane and stabilise the vasculature again. To date, however, there is little evidence for pericytes or smooth muscle cells directly regulating angiogenesis, although one report found desmin-positive pericytes at and in front of the advancing tips of endothelial sprouts, and suggested that pericytes

participate in angiogenesis from the earliest stages of capillary sprouting [Nehls, Denzer and Drenckhahn, 1992].

Pericyes are also thought to play a significant role in vascular diseases. For example, an increase in pericyte number has been reported in hypertension; vessels of the spontaneously hypertensive rat contained four times as many α-SMA positive pericytes than normal rats [Herman and Jacobson, 1988]. Pericytes are suggested to have a contractile function and are implicated in controlling vessel diameter [Rouget, 1873[9]; Kuwabara and Cogan, 1963]. Thus, a microvessel with increased pericyte coverage may have the potential to contract more than a microvessel with normal coverage, and thereby contribute to hypertension.

In contrast, Spieser and colleagues determined the ratio of endothelial cells to pericytes in non-diabetic and diabetic patients, and reported that prior to retinal neovascularisation, there was a selective loss of pericytes on the retinal capillaries (termed pericyte drop-off) [Spieser, Gittelsohn and Patz, 1968]. The reduction in pericyte number may cause a loss of support and stability of the capillaries, and may therefore underlie the formation of microaneurysms often seen in this condition. The exact mechanism which underlies the degeneration of the pericytes has not been established.

[9] Reviewed in Diaz-Flores et al., 1991, and in Nehls and Drenkhahn, 1993.

2.2 AIMS AND HYPOTHESIS

As discussed earlier, studies investigating the expression of biochemical markers by pericytes and smooth muscle cells have produced conflicting results with regard to localisation and marker expression during development. Therefore, the purpose of the work in this chapter was:

- to compare the distribution of two mural cell markers in the rat retina
- to determine the extent of mural cell coverage during development of the rat retina using the protein markers
- to determine if the retinal vessel coverage by mural cells was affected by the fluctuating oxygen regime of the Edinburgh model of retinopathy of prematurity (ROP).

The extent of mural cell coverage is of course expected to increase as the vasculature forms, however it is expected that both smooth muscle cell and pericyte coverage will only extend to the remodelled vasculature, thus the central vessels are expected to establish a mural cell coating before the peripheral vessels.

Literature on mural cell coverage in animal models of ROP is very limited, however, it is thought that there may be a loss of pericytes in this disease, as many growing vessels of the incompletely vascularised retina lack mural cell coverage [Hirschi and D'Amore, 1997]. Because the Edinburgh model results in reduced vascular remodelling, it is proposed that there shall be a reduction in the extent of pericyte and/or smooth muscle cell coverage.

2.3 METHODS

2.3.1 Experiments

Animal groups

Approval for these studies was given by the UK Home Office and all animals were cared for in accordance with UK Home Office legislation.

Sprague-Dawley rats were supplied by Bantan and Kingman, UK and mated in the Medical Faculty Animal Facility. Two groups of animals were studies, room-air controls and oxygen treated, and three litters were analysed per group. It has been previously shown that an increase in litter size induces a greater incidence and severity of disease due to postnatal growth retardation [Holmes and Duffner, 1996]. Therefore, litters with a minimum of 12 pups were used in order to induce a significant change in the retinal development of the oxygen treated pups. Pups from litters born on the same day were used to supplement any litters of fewer than 12 pups. Within four hours of the final pup of each experimental litter being delivered, the pups and their mother were transferred into an oxygen chamber and raised in the oxygen profile. The rats were exposed to a 12-hour light:12-hour dark cycle. The chambers were cleaned every seven days at which point the profile was paused and restarted about ten minutes later. The build-up of carbon dioxide was prevented through the flow of injected gases and by placing soda lime chips (Medisorb) in a corner of the animal chamber.

Control litters were raised in room air and sacrificed on postnatal day 2 (P2), P7, P14 and P21. Experimental litters were exposed to the minute-to-minute variable oxygen profile set at 10kPa (described in Chapter One and in McColm et al., 2004). Pups were anaesthetised and killed immediately upon removal from the oxygen profile on P2, P7 and P14.

Termination of experiment

The rat pups were weighed and anaesthetised by intraperitoneal injection of ketamine (2.5mg/kg bodyweight) and xylazine (1mg/kg bodyweight). The chest cavity was then opened and, depending on the weight of the pup, 1.5 - 2.5mls of 1M phosphate buffered saline (PBS) was injected slowly into the left ventricle followed by 1.5 - 2.5mls 0.5% paraformaldehyde. The animals were then euthanised by intracardiac injection of 0.5mls pentobarbitone. Both eyes were enucleated; the right eye was taken for immunohistochemistry and the left for Western blotting.

2.3.2 Immunohistochemistry

Fixation

Without taking any factors, such as pup weight, into consideration, the right eyes were randomly divided into two groups; one group was stained for lectin and α-SMA, the other for lectin and desmin. Eyes for α-SMA staining were fixed whole in 2% paraformaldehyde for 2 hours before being washed in 1M PBS. Eyes for desmin staining were first pierced by a needle and then fixed whole in 75% acetone in 1M PBS for approximately 30mins. To directly compare the expression of the two mural cell markers, some day 14 control retinas were double-labelled with α-SMA and desmin. These retinas were fixed in 75% acetone.

Retinal wholemounts

Under a dissecting microscope a scalpel incision was made in the cornea just above the ora serrata. Scissors were then used to cut round the junction between the cornea and sclera until the cornea could be completely removed after which the iris and lens were removed easily. For the eyes fixed in paraformaldehyde (α-SMA staining), the retina was gently eased from the sclera using fine forceps, taking care to leave the ora serrata intact as it defined the edge of the retina. The retinal cup was then transferred onto a glass slide. For the eyes fixed in acetone (desmin staining), the retina and sclera were so strongly attached that separating the two was very difficult, and so the retina was mounted onto a slide with the sclera still attached. Four

incisions perpendicular to the outer edge of the retina were made, which divided the retina into four equally sized quadrants. At this stage the retina was flattened onto the slide and as much vitreous as possible was removed by gently plucking the retinal surface using forceps.

Double staining: α-SMA/desmin and lectin

The flattened retinal wholemounts fixed in paraformaldehyde were further fixed in cold 70% ethanol (-20°C) for 20mins. All retinal wholemounts were then permeabilised in 1M PBS/1% Triton X-100 for 30mins and blocked using 5% normal rabbit serum (Diagnostic Scotland) diluted in 1M PBS/Triton X-100 for 20mins. The retinas were incubated overnight at 4°C in primary antibody prepared in the serum solution: α-SMA (Sigma) at 1:400; and desmin (Dako) at 1:50. The following day, the tissues were washed in 1M PBS/1% Triton X-100 (each wash stage in the protocol consisted of three 10mins incubation with this solution), and then incubated (with gentle shaking) for 2 hours at room temperature in biotinylated rabbit anti-mouse secondary antibody (Dako) diluted to 1:200 in 1M PBS/1% Triton X-100. The retinas were washed and Texas red streptavidin (1:100, Vector Laboratories) was applied for 2 hours at room temperature with gentle shaking. After washing, the retinas were blocked using avidin and biotin for 20mins each (Vector Laboratories) before incubating with biotinylated *G. simplicifolia* (Bandeiraea) isolectin B4 (1:50, Vector Laboratories) overnight at 4°C. The following day the washes were repeated and the retinas incubated in fluorescein streptavidin (1:100, Vector Laboratories) for 2 hours with gentle shaking at room temperature. The wholemounts were washed for the final time and mounted in PBS:glycerol (1:1) and the coverslip sealed with nail varnish.

Double staining: α-SMA and desmin

Once the day 14 control eyes were fixed in acetone and dissected, the retinas were stained using a protocol similar to that described above. Briefly, the wholemounts were permeabilised in 1M PBS/1% Triton X-100 for 30mins and blocked in 5% rabbit serum (Diagnostic Scotland) for 20mins. The retinas were first incubated in

desmin antibody (1:50) overnight at 4°C. The retinas were then washed and incubated for 2 hours in biotinylated secondary antibody (anti-mouse, 1:200). The washes were repeated and Texas red streptavidin (1:100) was applied to the tissues for another 2 hours. The retinas were then washed again and blocked using avidin, biotin and 5% rabbit serum for 20mins each, after which α-SMA antibody (1:400) was applied overnight at 4°C. The following day, the washes were repeated and the wholemounts were incubated in secondary antibody (anti-mouse 1:200) for 2 hours, followed by 2 hours in flourescein streptavidin (1:100). The wholemounts were then washed for the final time and mounted.

Triple staining: α-SMA, lectin and TO-PRO-3

A few eyes were fixed in 2% paraformaldehyde, the retinas dissected and stained for α-SMA and lectin as described above. The cell nuclei were then labelled using a nuclear marker, TO-PRO-3 iodide (Molecular Probes); TO-PRO-3 was prepared in 1M PBS at a concentration of 1:500 and applied to the wholemounts for 10mins. The wholemounts were briefly rinsed in 1M PBS and mounted.

Negative controls

For the α-SMA and desmin negative controls, fixed retinal wholemounts were first incubated in 5% serum solution overnight at 4°C and then in rabbit anti-mouse secondary antibody (1:200) for 2 hours. Texas red streptavidin (1:100) was then applied for a further 2 hours. For the lectin negative controls, the retinas were incubated in 1M PBS/1% Triton X-100 overnight at 4°C followed by flourescein streptavidin (1:200) for 2 hours.

Analysis

The retinal flatmounts were viewed using a Leica TCSNT confocal system with a mixed gas argon/krypton laser (Leica Microsystems, Germany). Cells stained using fluorescein were labelled green and excited at 488nm (filter BP 525/50), and cells stained with Texas red were labelled red and excited at 568nm (filter LP 590). TO-PRO-3 stained cell nuclei blue and was excited at 647nm. Representative

images at x5, x10, x20, x40 and x63-oil magnification were taken and digitally stored for later analysis. To eliminate cross-talk between the flurochromes which can give rise to false results, the retinas were scanned by sequential scanning; first the retinas were scanned for fluorescein, followed by Texas red, and where applicable for TO-PRO-3. The images were then overlaid.

2.3.3 Western Blot Analysis

Protein extraction and assays

Retinas from each control and experimental litter were dissected fresh in 1M PBS, pooled and stored at -70°C. At a later stage, the proteins were extracted from the retinas using the following method. The retinas were first homogenised in extraction buffer containing 50mM Tris-HCl, 4mM EDTA, 0.1% Tween and a mammalian cell and tissue proteinase inhibitor cocktail (Sigma). The samples were then centrifuged at 14,000g for 10mins after which the supernatant was removed and spun for a further 30mins. The supernatant was then transferred into eppendorf tubes and stored at -70°C.

The protein content of the samples was measured using the BCA protein assay method (Perbio) according to the manufacturer's instructions. Briefly, 5µl of each sample was added to the extraction buffer, followed by 95µl BCA protein assay reagent. All samples were incubated at 37°C for 30mins after which the OD_{562} of each sample was measured. Bovine serum albumin was used as standard.

Protein separation and transfer

75µg of total retinal protein for each control and experimental timepoint were loaded onto a 12% acrylamide gel along with a biotinylated molecular weight marker (Biorad). The proteins were then separated by SDS-PAGE electrophoresis for around 2 hours and transferred onto PVDF membranes (Bio-Rad Laboratories) using the semi-dry transfer cell (Bio-Rad Laboratories) according to the manufacturer's instructions.

Blotting

The membranes were washed twice (1M PBS/0.1% Tween) for 5mins while shaking gently and blocked overnight at 4°C in 5% non-fat dry milk prepared in the wash solution. The next morning, the membranes were washed twice with gentle shaking for 5mins each, and incubated in primary antibody (α-SMA at 1:1000 (Sigma) or desmin at 1:500, 1:200 and 1:100 (Santa Cruz and Dako)) prepared in the blocking solution for 1 hour at room temperature with gentle shaking. The membranes were then washed three times for 5mins followed by two 15mins washes, and incubated in horseradish peroxidase conjugated secondary antibody (for α-SMA, rabbit anti-mouse (Dako) and for desmin, rabbit anti-goat (Dako), both at 1:5000) prepared in the blocking solution. Additional horseradish peroxidase (Amersham Bioscience) at 1:2000 was added to the secondary antibody solution for detection of the molecular weight marker. The membranes were again washed several times and incubated for 5mins in ECL-Plus Western blotting developer (Amersham Bioscience). The membranes were then exposed to X-ray film for around 2mins.

To ensure that any difference in expression between control and experimental litters was not due to loading errors, each membrane was stripped and reprobed for actin. Briefly, the membranes were first stripped for 15mins at 37°C using Restore Western Blot Stripping Buffer (Pierce), washed and blocked in 5% non-fat milk overnight. The following morning, the membranes were incubated in actin primary antibody (1:100, Santa Cruz) and then in anti-goat secondary antibody containing horseradish peroxidase. After the washing stage, developer solution was applied to the membranes which were then exposed to X-ray film.

Analysis

An image of the X-ray film was captured using software called 'Quantity One' (Bio-Rad Laboratories). Individual bands that had developed on the X-ray film were manually selected and the software calculated the quantity of α-SMA protein expression in each sample by taking its area and intensity into consideration.

2.3.4 Threshold Analysis for Desmin Expression

Desmin labelling of the retinal vasculature was measured in the retinas of pups raised in room-air and the 10kPa regime of the Edinburgh model by threshold analysis. Images of the central and peripheral retina from each quadrant were taken using the confocal microscope, the offset and gain of which were adjusted to eliminate background signalling. Images for lectin staining and desmin staining were stored separately. Later, using data analysis software called 'Image Tool' (designed by The University of Texas, Health Sciences Centre, San Antonio), the threshold for each lectin and desmin image was manually set, and the software calculated the number of black and white pixels. The extent of desmin coverage was then expressed as a percentage of the lectin staining.

2.3.5 Transmission Electron Microscopy

Only two P14 control and two P14 experimental retinas were processed for electron microscopic analysis to establish whether pericytes made direct contact with endothelial cells. In addition, the electron microscopic analysis allowed me to determine if the association between the two cell types was compromised as a result of oxygen exposure.

Fixation

The retinas were dissected fresh in 1M PBS, but the sclera was not removed as it provided support for the retina when it was cut into quadrants. Once the retina was flattened onto a slide, they were fixed using 3% glutaraldehyde in 0.1M sodium cacodylate buffer for around 2 hours.

Sectioning and staining

The tissue processing, sectioning and staining were carried out by Steve Mitchell in the electron microscope suite within the Royal Dick Vet School.

All processing was carried out with a constant rotation of the tissues. The tissues were washed in 0.1M sodium cacodylate buffer for an hour followed by post-fixation in 1% osmium tetroxide for 45-60mins. The wash was repeated and the tissues were dehydrated through a graded series of acetone solutions (50%, 70%, 90% and 100%). The tissues were infiltrated in a 50:50 mix of araldite and acetone for 30mins at room temperature and then at 60°C overnight. The next morning the tissues were infiltrated further in araldite/acetone mix for 3 hours, with a solution change every hour. The tissues were then infiltrated in araldite/acetone mix with Acclerator for 2 hours and embedded in the araldite/acetone mix with Acclerator for 48 hours at 60°C.

60-80nm serial sections of the retinal quadrants were obtained using an ultra-microtome and the sections mounted onto formvar-coated copper slots grides. Once the sections were dried, they were stained by an LKB ultrostainer using uranyl acetate and lead cirtrate.

Analysis

The retinal sections were viewed using the Philips CM12 transmission electron microscope and high-power images were obtained.

2.4 RESULTS

2.4.1 Spread of the Superficial Vasculature

The spread of the retinal vessels during normal development was briefly studied (Figure 2.1) before investigating their coverage by mural cells. On P2, the endothelial tubules had spread from the optic nerve area to around a third of the retinal surface, but the vasculature was only a dense immature mesh which had undergone very little remodelling. By P7, about two-thirds to three-quarters of the retinal surface was vascularised and many of the small vessels seen on P2 had withdrawn around the arterioles to produce capillary-free zones; the leading edge of the vasculature was still developing, thus was immature in appearance. Formation of the retinal vascular bed was complete by P14; the endothelial tubules had reached the ora serrata and the vasculature had undergone considerable remodelling. Between P14 and P21 there was no appreciable difference in the appearance of the vasculature.

2.4.2 Effects of Variable Oxygen Exposure on Endothelial Tubule Formation

The oxygen regime of the Edinburgh model caused abnormalities in the formation of the endothelial tubules that resembled the early stages of ROP in that retinal vascular development was delayed (called vaso-obliteration). As mentioned above, pups raised in room-air, had a fully formed superficial retinal vasculature by P14. In comparison, retinas of pups exposed to the 10kPa oxygen profile from birth to P14 had a less remodelled and mature vasculature (indicated by an increase in the number of capillary branches) and a significant peripheral avascular area (Figure 2.2). A more detailed report can be found in McColm et al. [2004].

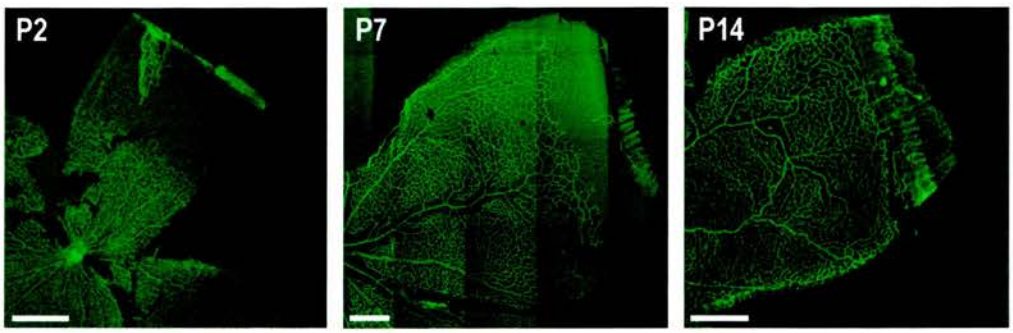

Figure 2.1: Formation of the retinal vasculature.
The endothelial cells were labelled using lectin followed by fluorescein streptavidin.
P - postnatal day.
Scale bar: (P2) 400μm; (P7) 500μm; (P14) 400μm.

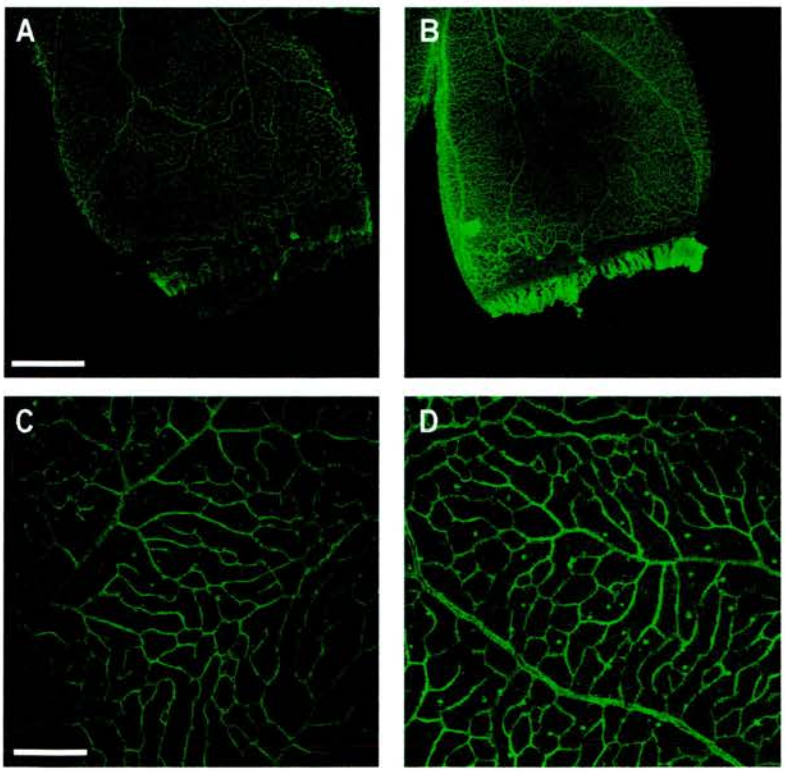

Figure 2.2: Rat pup retinas after exposure to the Edinburgh model of ROP.
Retinas were stained using lectin and fluorescein streptavidin. (A) Retinal quadrant of P14 control pup. (B) Retinal quadrant of P14 oxygen treated pup. (C) Retinal capillary density of control pup. (D) Retinal capillary density of oxygen treated pup.
Scale bar: (A) 400μm; (B) as A; (C) 200μm; (D) as C.

2.4.3 Defining α-SMA and Desmin Staining

To begin the investigation of mural cell coverage, the labelling of both markers was first determined.

α-SMA labelled a single layer of closely packed spindle-shaped cells with tapered ends and a wider central region which contained the nucleus (Figure 2.3 A, page 54). The cells were arranged perpendicular to the axis of the vessel and in a manner so that the nuclear region of one cell lay next to, and possibly in contact with, the tapered ends of the adjacent cells. The cells were located on the external surface of the vessel and covered the entire circumference of the arteriole (Figure 2.3 B).

Desmin stained very fine, elongated cells along the arteriole and its branches (Figure 2.3 C). Like α-SMA, desmin positive cells were located on the external surface of the lectin stained endothelial cells and were wrapped around the arteriole; but unlike α-SMA, the coverage of desmin stained cells was non-continuous. The extent of labelling was markedly greater with desmin than α-SMA, as shown in Figure 2.4 (page 55). α-SMA labelling was confined to the arteriole, its branches and, to a lesser degree, the venule; no staining was observed within the deep capillary bed nor on the branches of the venule. In comparison, desmin coverage was seen across the whole vasculature, although it appeared to be most predominant around the venule.

At a higher magnification the structure and distribution of cells positive for α-SMA and/or desmin could be further established. As mentioned above, α-SMA and desmin predominantly stained the arterioles and venules, respectively. Although desmin staining was sparse on the arteriole, it followed the same pattern as α-SMA; the few fine processes of the cells were wrapped around the vessel. As illustrated in Figure 2.5, some cells stained positively for both markers. These cells either had the typical structure of smooth muscle cells (elongated spindle shaped cells with tapered ends, arrow b) and expressed very little desmin, or were strongly positive for desmin (arrow a), but lacked the typical shape of a pericyte or smooth muscle cell.

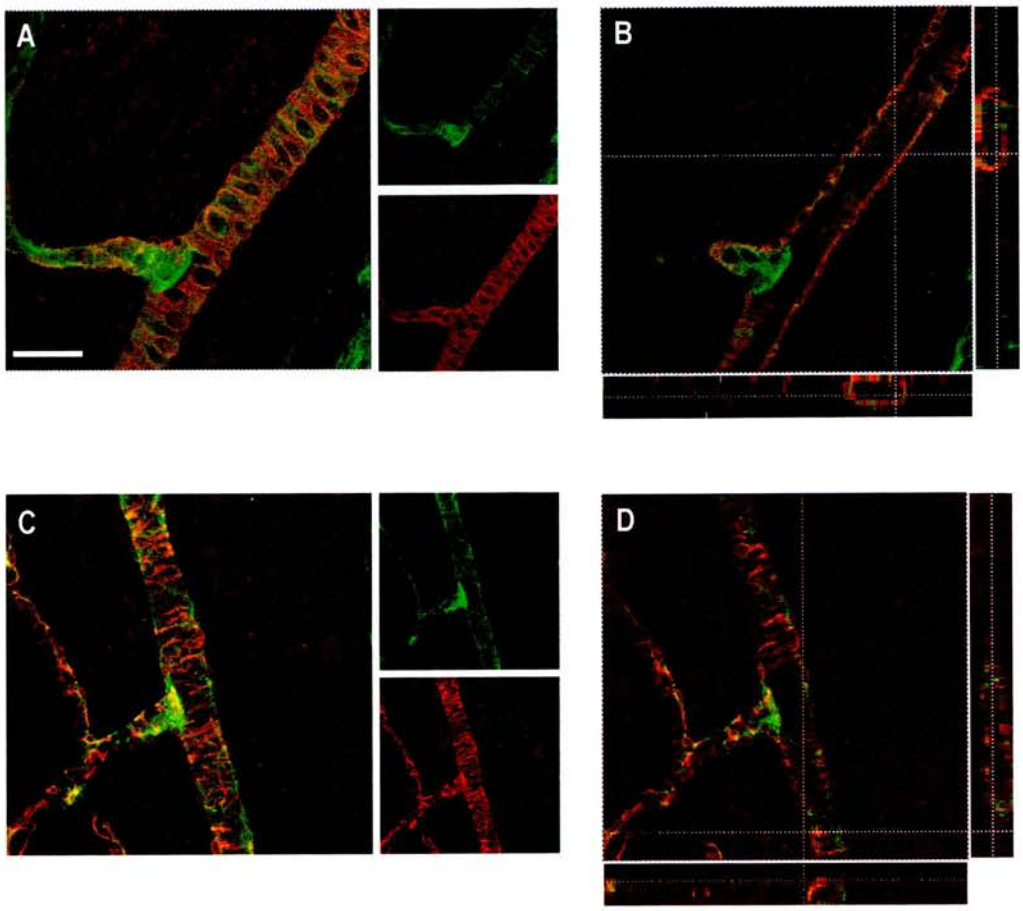

Figure 2.3: Arterioles of P14 control retinas double-labelled with lectin and α-SMA or desmin

(A) Double-stained using lectin (green) and α-SMA (red). Projected focus stack of 5 optical sections at 0.85μm. (B) Cross-section of image A. The side panels are orthogonal slides through the Z-stack. (C) Double-stained using lectin (green) and desmin (red). Projected focus stack of 9 optical sections at 1.06μm. (D) Cross-section of image C. The side panels are orthogonal slides through the Z-stack.
Scale bar: 32μm.

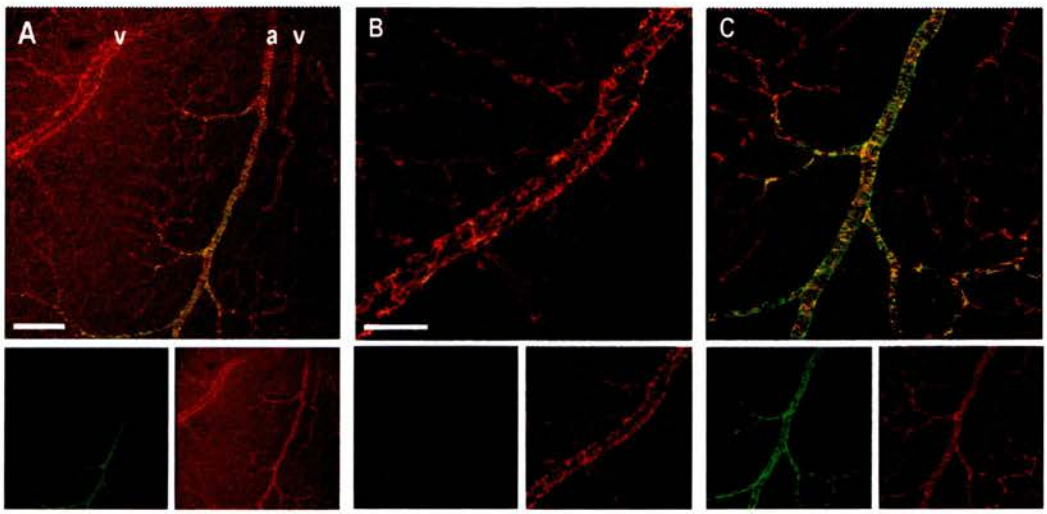

Figure 2.4: Comparison of α-SMA and desmin staining of P14 control retina.
Retinal flatmount double-labelled with α-SMA (green) and desmin (red). (A) The central area containing an arteriole (a) and venules (v). (B) Enlargement of the venule in image A. (C) Enlargement of the arteriole in image A.
Scale bar: (A) 200μm; (B) 100μm; (C) as B.

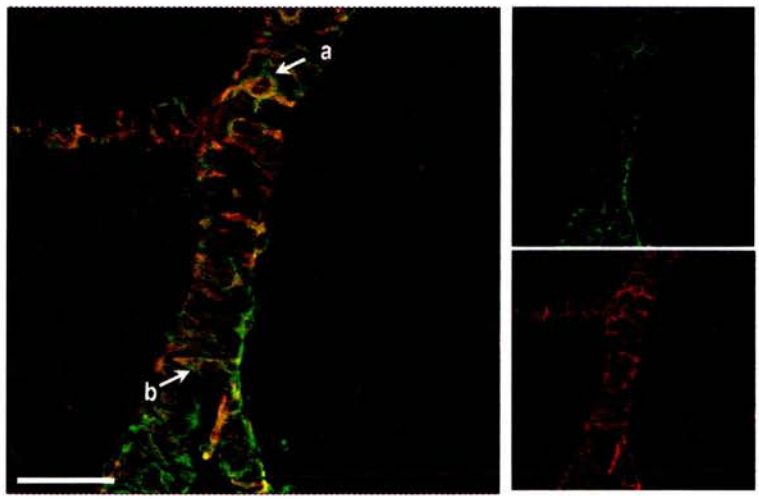

Figure 2.5: Comparison of α-SMA and desmin staining of an arteriole.
Some cells stained for both markers, a few were predominantly stained with desmin (red, arrow a), and others were predomiantly stained with α-SMA (green, arrow b). Projected focus stack of 7 optical sections at 0.98μm.
Scale bar: 32μm.

2.4.4 Retinal Expression of α-SMA in Normal and Oxygen Exposed Pups

Postnatal day 2 (Figure 2.6, page 59)

The vasculature of the P2 retina was very immature in appearance, although capillary-free zones were beginning to form centrally. α-SMA labelling was present only on the arteriole, however this coverage lagged behind the outgrowth of the vessels; labelling was strong near the optic nerve, but progressively decreased towards the advancing peripheral edge of the vasculature. At a higher magnification the labelling appeared as a sheath over the lectin stained endothelial cells; the marker did not appear to label cells that had the structure typical of smooth muscle cells.

The retinas of pups exposed to the variable oxygen regime had around the same extent of α-SMA labelling as the control retinas; coverage was only present on the arteriole, but had not progressed very far. In comparison to the image of the control retina (Figure 2.6 E), the image of the experimental retina (Figure 2.6 F) was taken closer to the optic disc. As mentioned above α-SMA staining of the arteriole was strongest at the optic disc region and weakest at the periphery. This could explain the greater extent of staining observed on the arteriole of the experimental retina.

Postnatal day 7 (Figures 2.7 and 2.8, pages 60 and 61)

By P7 capillary-free zones had formed in the central area, but the capillary network had undergone limited remodelling. α-SMA coverage of the arterioles was now more obvious and had progressed further peripherally than on P2. Further analysis (Figure 2.8) showed that the staining of the arteriole was weakest at the periphery (almost background levels) and strongest towards the centre of the retina, where the primary arteriole branches were also beginning to express α-SMA. The coverage, however, ended very abruptly, at the point where the capillary network had so far been remodelled. In comparison to P2, when α-SMA-positive cells appeared flattened, at P7 the cells were adopting the typical structure of smooth muscle cells.

The retinas of pups exposed to the variable oxygen profile had also established considerable α-SMA coverage. However, the coverage had not progressed as far as it had done in the control retina and appeared more as a flattened sheath rather than a layer of tapered cells; in comparison to the control retinas, the number of cells with a smooth muscle cell appearance was reduced. Surprisingly, α-SMA staining was observed on the venules in the central area; this labelling was significantly greater than the background labelling observed on the venules of the controls.

Postnatal day 14 (Figures 2.9 and 2.10, pages 62 and 63)

By this stage of normal development, the arterioles, in the central area, were encapsulated by a closely packed layer of cells that resembled smooth muscle cells. Acquisition of the α-SMA coating within the central area had taken place on the primary arteriole branches and had advanced onto the secondary branches, but as in P7 retinas, the coverage ended abruptly and the cells of the branches were not fully differentiated. Coverage of the arterioles peripherally and the venule however, was still very limited; only background levels of labelling were observed. Thus, the staining pattern of α-SMA on the arterioles seemed to differ along its length. This was investigated by taking several high-power images of an arteriole from the centre to the periphery (Figure 2.10). Centrally, the arteriole and all its primary branches were encapsulated by a dense layer of smooth muscle cells. At a mid-point between the optic nerve and the peripheral edge of the vasculature, the arteriole was still strongly positive for α-SMA, the cells were arranged around the circumference of the arteriole, but the number of cells resembling smooth muscle cells had greatly reduced. At this point coverage continued on to the primary branches, but did not progress to the very edge. Further towards the periphery, the staining levels of α-SMA had markedly reduced; levels slightly above background were observed, and the cells had no distinct structure.

As illustrated in Figure 2.9, α-SMA labelling of the experimental retinas was observed on the arterioles, its primary branches and on the venules. On the arterioles of the central area, the cells had differentiated into smooth muscle cells

and were arranged in a similar manner to those of the control retinas. As previously mentioned, the vasculature of these retinas was not fully formed, which may explain the lack of α-SMA labelling on the secondary branches. Another difference between the control and experimental retinas was that in the former, labelling of the peripheral arteriole and of the venule was very weak, however in the latter, moderate labelling was noted on both vessels, though the structure of the cells that stained could not be determined.

Postnatal day 21 (Figure 2.11, page 64)

Although there was not much difference in the lectin staining of P14 and P21 retinas, α-SMA expression had increased; centrally, the primary and secondary arteriole branches were completely labelled, and peripherally the staining was intense. In addition, labelling was also present on the central venules. As on P14, α-SMA positive cells of the peripheral arteriole did not have any distinct shape. Likewise, the venules were positive for α-SMA, however the staining was weak and appeared as a thin layer of flat undifferentiated cells.

Western analysis

The immunohistochemical staining of the flatmounts showed that retinas of pups exposed to the Edinburgh model expressed less α-SMA than those of room-air raised pups. To establish if this was indeed the case, the retinal proteins from both groups were extracted and Western analysis performed. As illustrated in Figure 2.12 (page 65), in normal development no α-SMA protein was detected on day 2. Slight expression was observed on day 7, which increased markedly by day 14. The expression was still strong at day 21. In the oxygen-treated tissues, the expression on both day 7 and day 14 was slightly reduced in comparison to the controls. This was further confirmed by quantitative analysis.

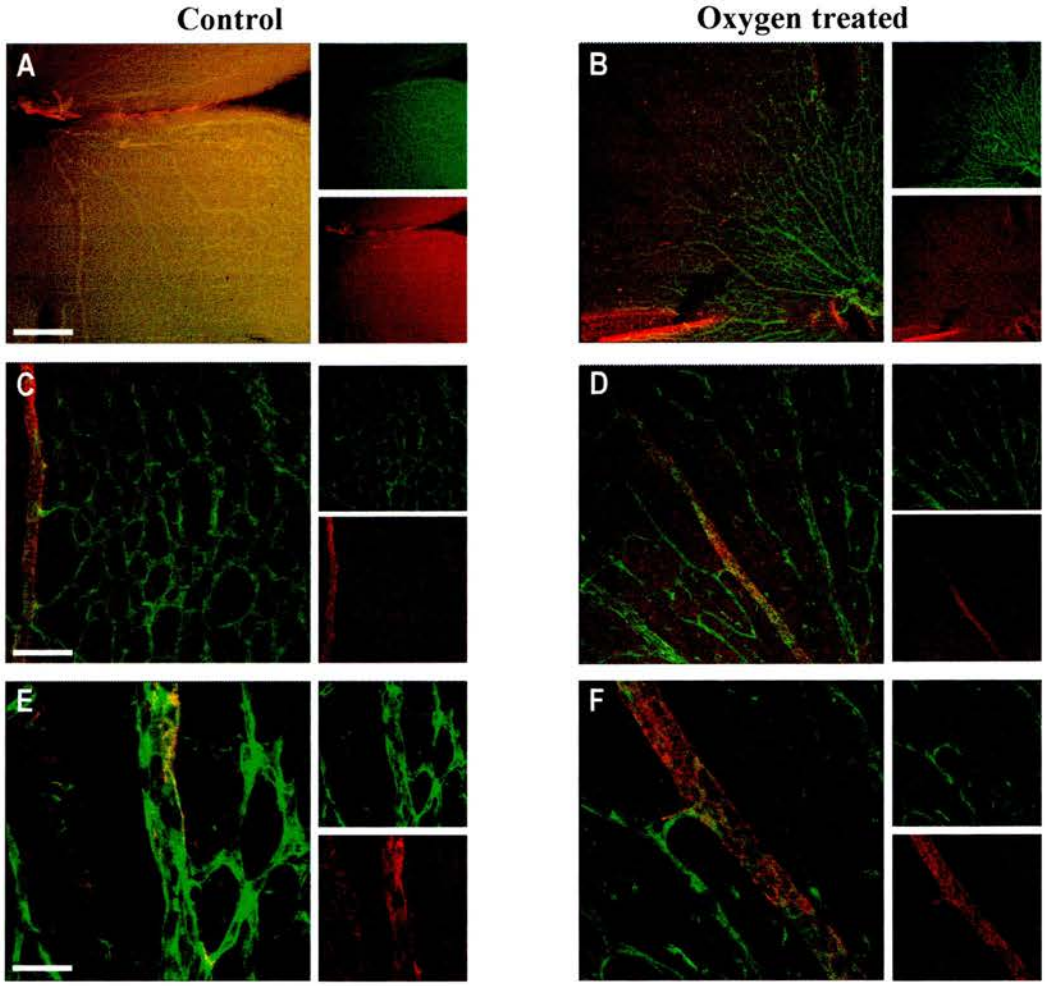

Figure 2.6: α-SMA labelling of P2 control and oxygen treated retinas.
Labelled with lectin (green) and α-SMA (red). (A) Overview of the central retina in a control pup. (B) Oxygen treated equivalent of image A. (C) The arteriole and capillary bed in a control pup. (D) Oxygen treated equivalent of image C. (E) Enlarged image of arteriole in image C. (F) Enlarged image of arteriole in image D.
Scale bar: (A) 400μm; (B) as A; (C) 100μm; (D) as C; (E) 32μm; (F) as E.

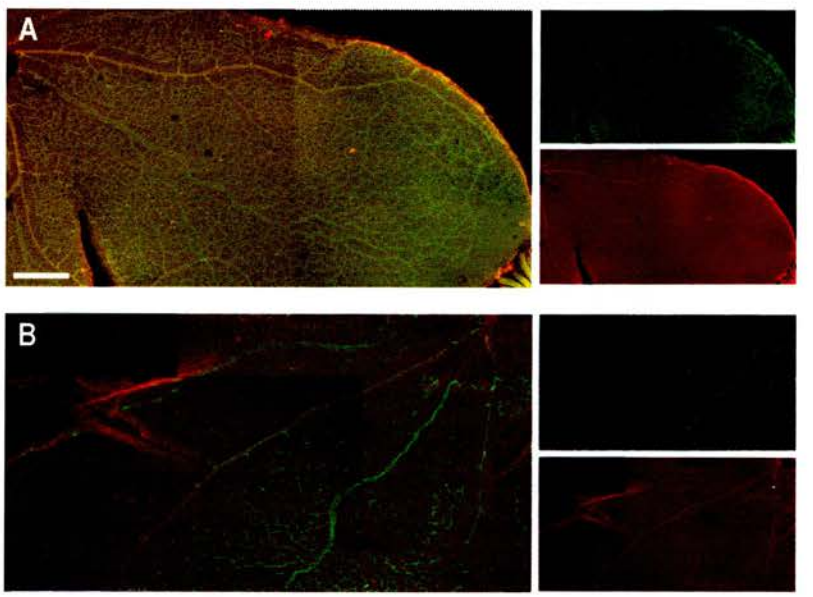

Figure 2.7: Overview of α-SMA labelling at P7.
Flatmounted retinas stained with lectin (green) and α-SMA (red). (A) Control retina. (B) Experimental retina.
Scale bar: 400μm.

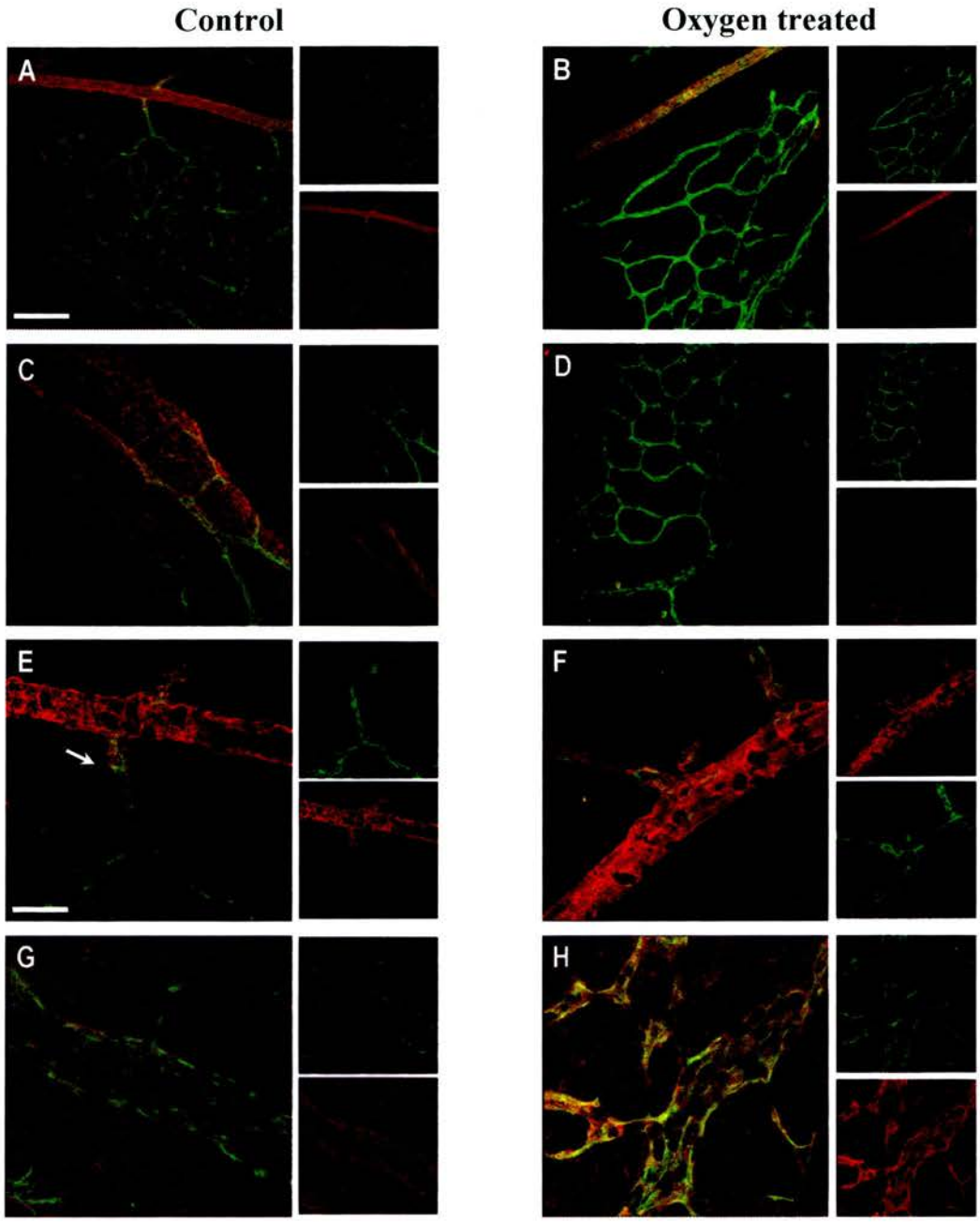

Figure 2.8: α-SMA labelling of P7 control and oxygen treated retinas.
Labelled with lectin (green) and α-SMA (red). (A) The central vasculature, containing an arteriole and venule of a control retina. (B) Oxygen treated retina comparable to image A. (C) The arteriole close to the peripheral edge of the control retina. (D) Oxygen treated retina comparable to image C. (E) Projected focus stack of 10 optical sections at 0.44µm of the same arteriole as in image A where the α-SMA staining ends abruptly on the branch (arrow). (F) Enlarged image of an arteriole in the oxygen treated retina. (G) Enlarged image of venule in image A. (H) Enlarged image of the venule in image B.
Scale bar: (A) 100µm; (B), (C) and (D) as A; (E) 32µm; (F), (G) and (H) as E.

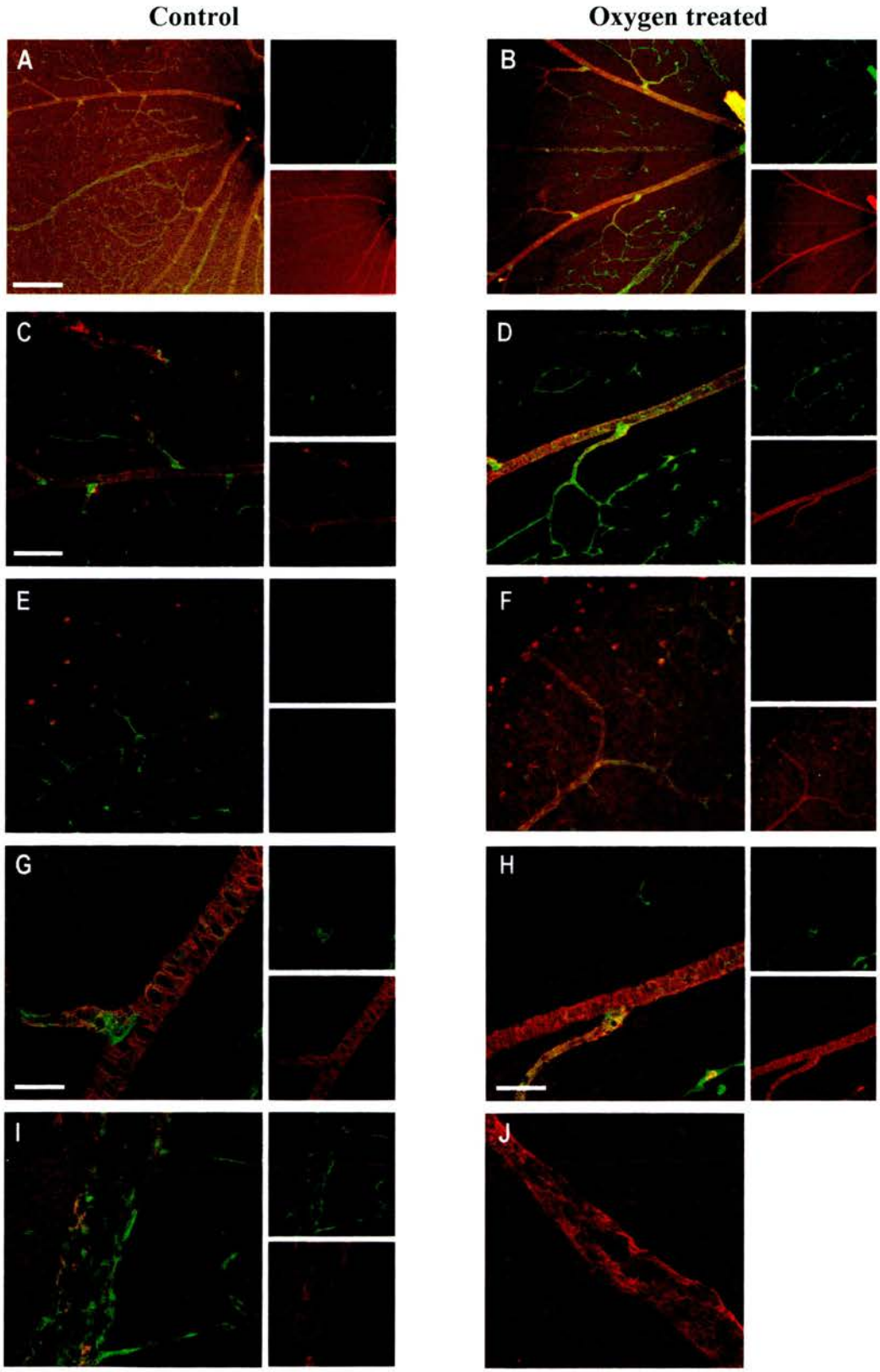
Control
Oxygen treated
A
B
C
D
E
F
G
H
I
J

Figure 2.9: α-SMA labelling of P14 control and oxygen treated retinas.
Labelled using lectin (green) and α-SMA (red). (A) The central network of the blood vessels in a control retina. (B) Oxygen treated retina equivalent image A. (C) The central arteriole in control. (D) Oxygen treated retina equivalent to image C. (E) The peripheral arteriole in control. (F) Oxygen treated retina equivalent to image E. (G) Enlarged image of a control arteriole; projected focus stack of 7 optical sections at 0.94μm. (H) Oxygen treated retina equivalent to image G. (I) Enlarged image of a control venule. (J). Single labelled oxygen treated retina equivalent to image G.
Scale bar: (A) 200μm; (B) as A; (C) 100μm; (D), (E) and (F) as C; (G) 32μm; (H) 50μm; (I) and (J) as G.

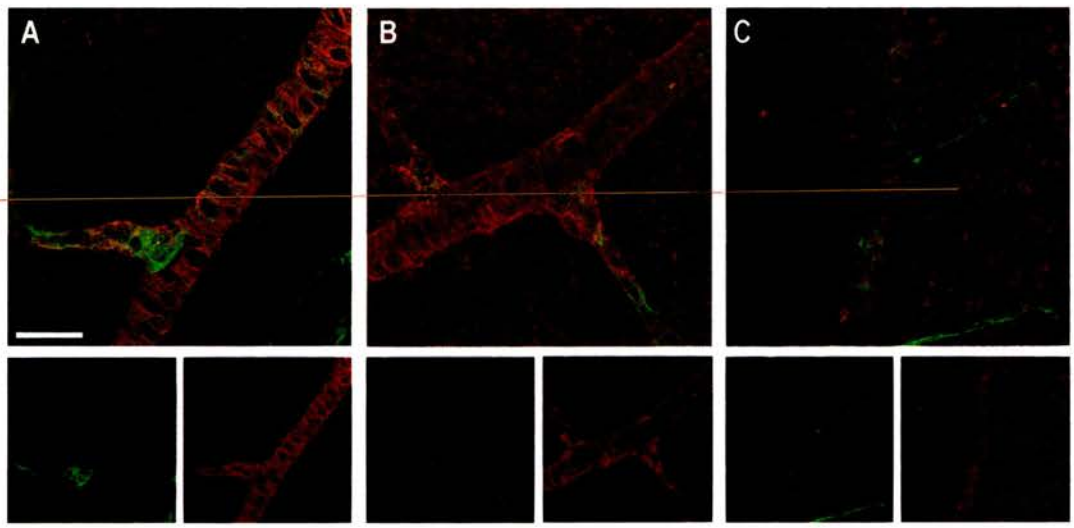

Figure 2.10: Arteriole of a P14 flatmounted control retina labelled with α-SMA.
Double-labelled with lectin (green) and α-SMA (red). (A) Central image of a projected focus stack of 7 optical sections at 0.93μm. (B) Midperipheral image of a projected focus stack of 8 optical sections at 0.90μm. (C) Peripheral image.
Scale bar: 32μm.

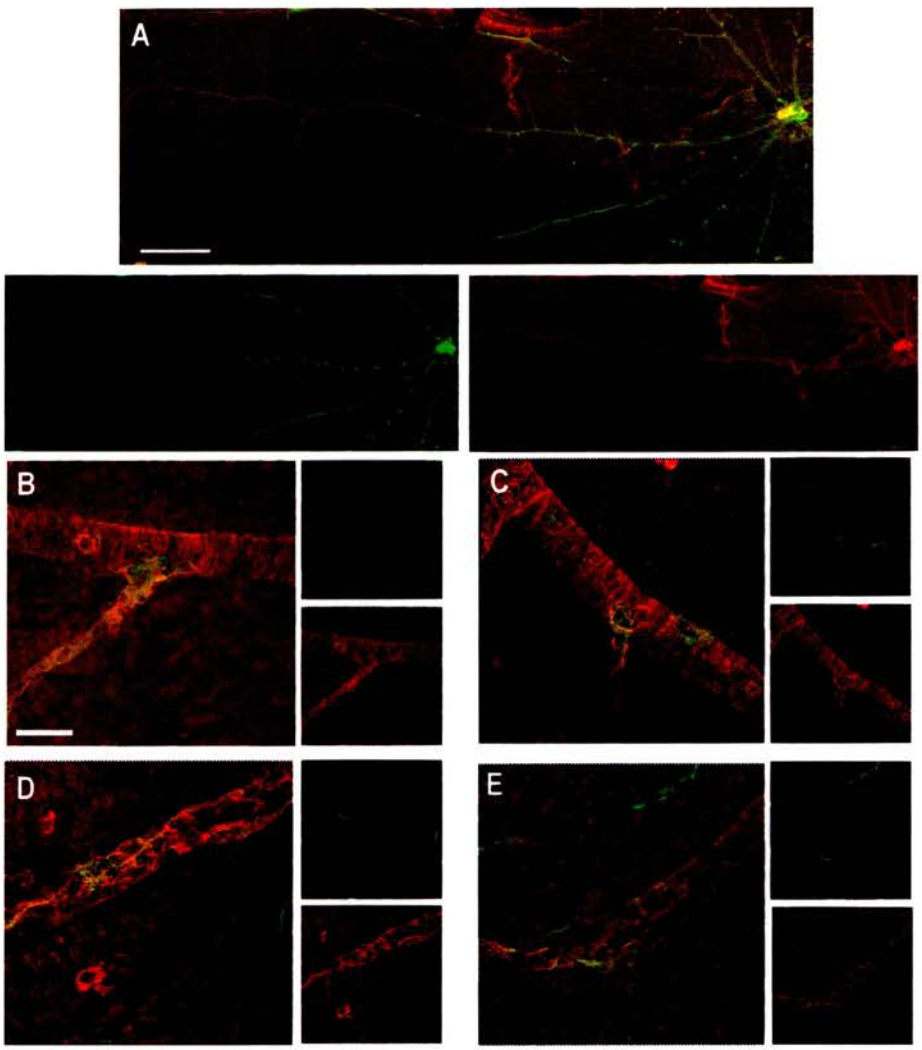

Figure 2.11: α-SMA labelling of P21 control retina.
Flatmounts double-labelled with lectin (green) and α-SMA (red). (A) Overview of the vasculature. (B) The arteriole, centrally; projected focus stack of 15 optical sections at 0.49μm. (C) The arteriole, peripherally. (D) The venule, centrally; projected focus stack of 7 optical sections at 1.10μm. (E) The venule, peripherally;.projected focus stack of 7 optical sections at 0.93μm.
Scale bar: (A) 400μm; (B) 32μm; (C), (D) and (E) as B.

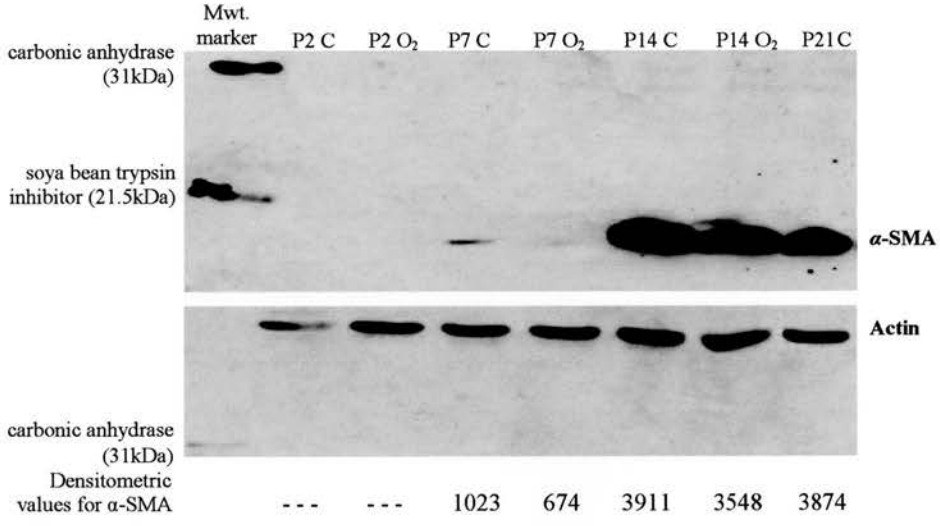

Figure 2.12: Western blot of retinal *α*-SMA expression in control and oxygen treated rat pups.
The lower blot shows actin (43kDa) expression as a loading control. The densitometric values were obtained using a computer software called 'Quantity-One'.
C - control litter; O_2 - oxygen treated litter; P - postnatal day.

2.4.5 Retinal Expression of Desmin in Normal and Oxygen Exposed Pups

Postnatal day 2 (Figure 2.13, page 69)

In the normally developing retina, desmin positive labelling occurred across the entire vasculature that had so far formed, however peripherally the labelling was much stronger. On arterioles, most of the stained cells were long, fine and wrapped around the vessel, but did not resemble pericytes or smooth muscle cells. On all capillaries, the cells lay across the axis of the endothelial tubules and were long, thin, and thread-like. In comparison, the cells of the venules had multiple processes and appeared as typical pericytes, but were not arranged in any particular orientation.

Cells present on many of the capillaries seemed very loosely attached; for example on the arterial branches (Figure 2.13 E) and at the advancing peripheral edge of the vasculature (Figure 2.13 I). Some retinal capillaries were negative for desmin expression. These capillaries may have been very immature and, therefore, had not yet been invested by support cells. Alternatively, these capillaries lacked a pericyte coverage because they were destined to regress.

With variable oxygen exposure, the desmin staining was reduced; desmin positive cells were visible at the peripheral edge, thus the extent of desmin was not affected, rather the number of cells stained in the vasculature seemed to have decreased. The cells present on the surface of the arterioles and capillaries were very similar to those of the control with respect to structure and orientation, but those of the venule were markedly different; the cells did not have the typical appearance of pericytes, but were long, lacked processes, and were lying longitudinal to the venule.

Postnatal day 7 (Figures 2.14 and 2.15, pages 70 and 71)

With further development it became apparent that the venules had considerably more coverage of desmin than the arterioles. The capillary network had also developed a significant amount of desmin coverage compared to P2, but the mid-

capillaries did not express desmin. The structure of the cells differed considerably from the arteriole to the venule (Figure 2.15). Centrally, the arteriole and pre-capillaries consisted of cells with several fine and short processes whereas those of the venule had longer processes. Regarding their orientation, the cells of the venule did not follow a distinct pattern, they lay in several directions, but those of the post-capillaries were arranged along the length of the vessels. Towards the peripheral vasculature the cells of all major vessels were similar; single long strands that lay longitudinal to the vessels.

As in the controls, desmin was observed through the entire vasculature of the oxygen treated retinas with more intense labelling of the venule than arteriole. However, the overall coverage appeared reduced in comparison to the controls. On the venules, the cells appeared to lack the typical pericyte shape; the cells were single strand-like structures that lay along the axis of the vessels. The arteriole, in contrast, was very similar to that of the control. A noticeable difference in these retinas was that the desmin positive cells were finer than those of the control retina.

Postnatal day 14 (Figure 2.16, page 72)

On day 14 in the room-air raised retinas, the entire vasculature, from the centre to the periphery, had established a coating of desmin staining. In Figure 2.16 A, it appeared that now the arteriole had stronger expression for desmin than the venule, however this could be due to poor focusing. Desmin labelling of the central retinal vasculature was similar to P7; the desmin positive cells were wrapped around the arteriole and its branches. Peripherally, cells on the arteriole were also beginning to appear as those in the centre. The cells on the venules had now formed multiple processes and were arranged in all directions, although those of the post-capillaries were lying along the axis of the vessels. All cells now appeared to be in close proximity to the endothelial cells; no cells were loosely attached as in early retinal development.

In the retinas of the oxygen raised pups, the desmin staining was present to the very edge of the peripheral vasculature. As was the case at other timepoints, the coverage of the venule continued to be stronger than the arteriole. Centrally the coverage of the arteriole was barely detected, and peripherally the cells were long, thin and lying along the axis, similar to those of the peripheral venules in controls. Although cells on the central venule were very similar to those of the control, peripherally the cells were finer (barely visible), longer and less branched than those in the control. Overall, the coverage was again qualitatively reduced in comparison to the controls.

Postnatal day 21 (Figure 2.17, page 73)

By day 21, most desmin stained cells had established their shape and were now fully developed. The coverage of the arteriole and its primary branches near the central area was distinct; the elongated cells had few branches all of which were wrapped around the circumference of the vessel surface. Coverage was not increased at the branching points, a feature observed with α-SMA. Further from the centre, the number of cells on the arterioles was reduced and the pattern of the cells was very similar to that of the centre, but on the primary branches the cells were arranged in several directions, not just circumferentially. Towards the periphery the number of desmin stained cells was further reduced and the cells now had several processes although most were still encircling the vessel. Moving onto the venule, near the central point, the processes of the cells were short and wrapped mostly around the vessels. Peripherally the processes were longer and although they were not lying longitudinally they were also not encircling the vessel.

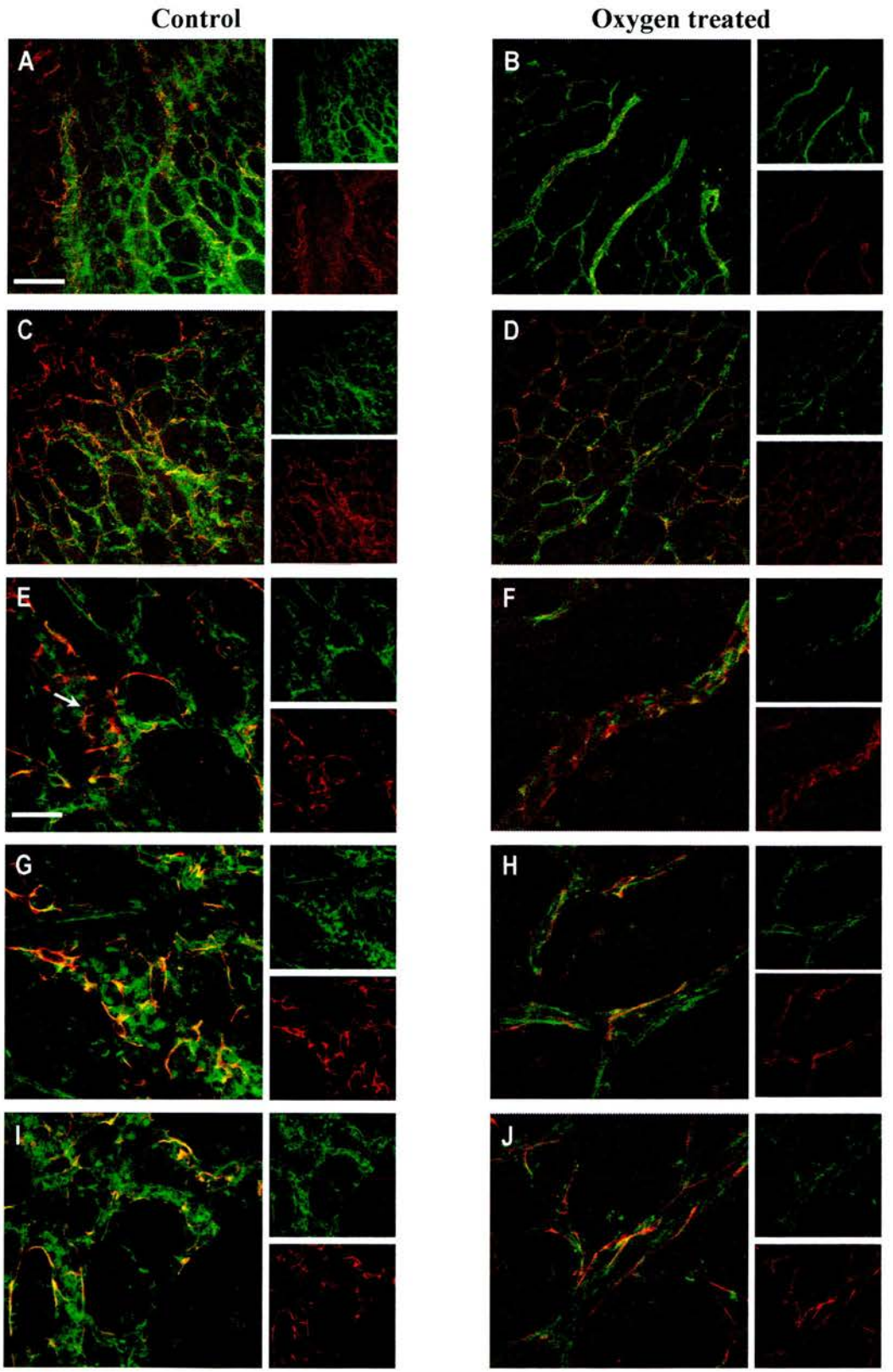
Control
Oxygen treated
A
B
C
D
E
F
G
H
I
J

Figure 2.13: Desmin staining of P2 control and oxygen exposed retinas.
Flatmounts double-labelled with lectin (green) and desmin (red). (A) Central retinal vasculature of control pup. (B) Experimental retina comparable to image A. (C) Peripheral retinal vasculature of control pup. (D) Experimental retina comparable to image C. (E) Enlarged image of an arteriole, central area of control retina. Some cells had the typical structure of pericytes (arrow). (F) Experimental retina comparable to image E. (G) Enlarged image of a venule, central area of control retina. (H) Experimental retina comparable to image G. (I) Enlarged image of an arteriole, peripheral area of control retina. (J) Experimental retina comparable to image I.
Scale bar: (A) 100μm; (B), (C) and (D) as A; (E) 32μm; (F), (G), (H), (I) and (J) as E.

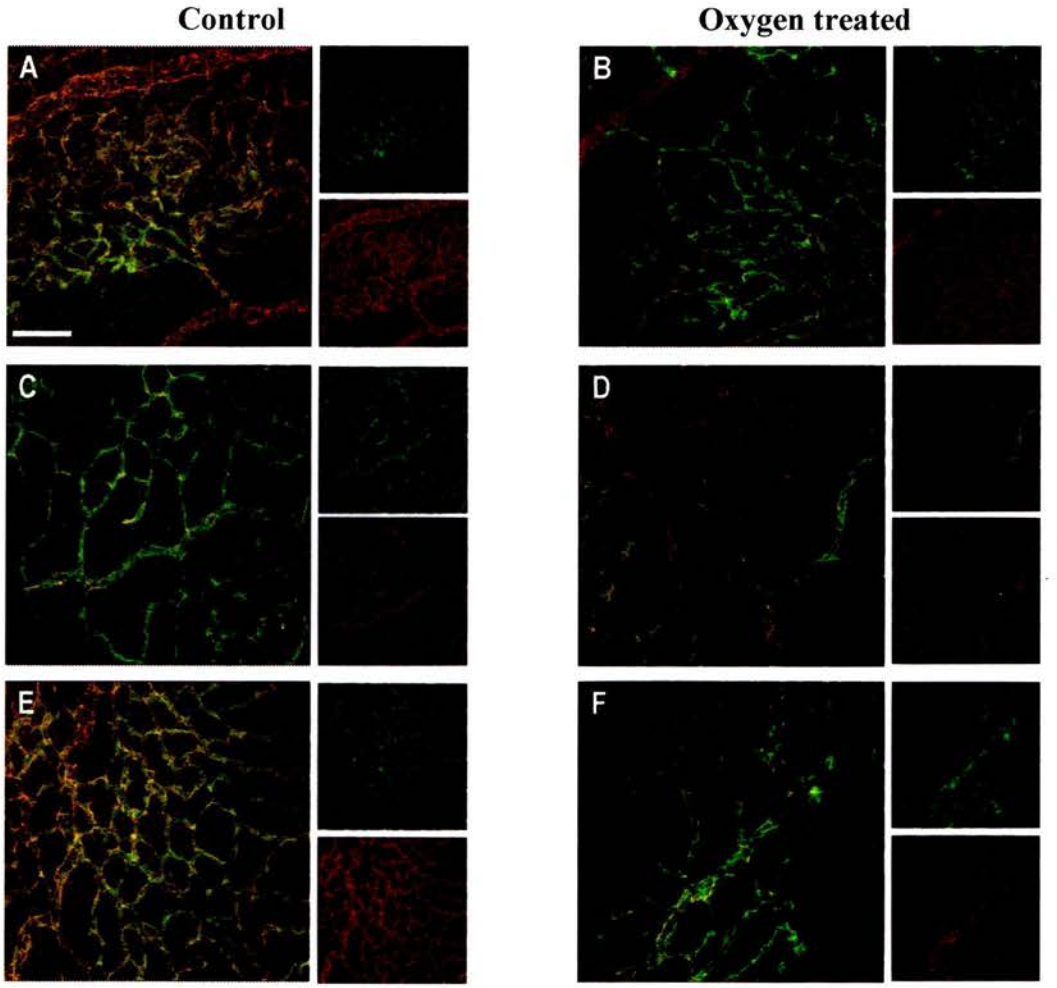

Figure 2.14: Desmin staining of P7 control and oxygen exposed retinas.
Flatmounts double-labelled with lectin (green) and desmin (red). (A) Central retinal vasculature of control pup. (B) Experimental equivalent to image A. (C) Arteriole of the peripheral retinal vasculature of control pup. (D) Experimental equivalent to image C. (E) Venule of the peripheral retinal vasculature of control pup. (F) Experimental equivalent to image E.
Scale bar: 100μm.

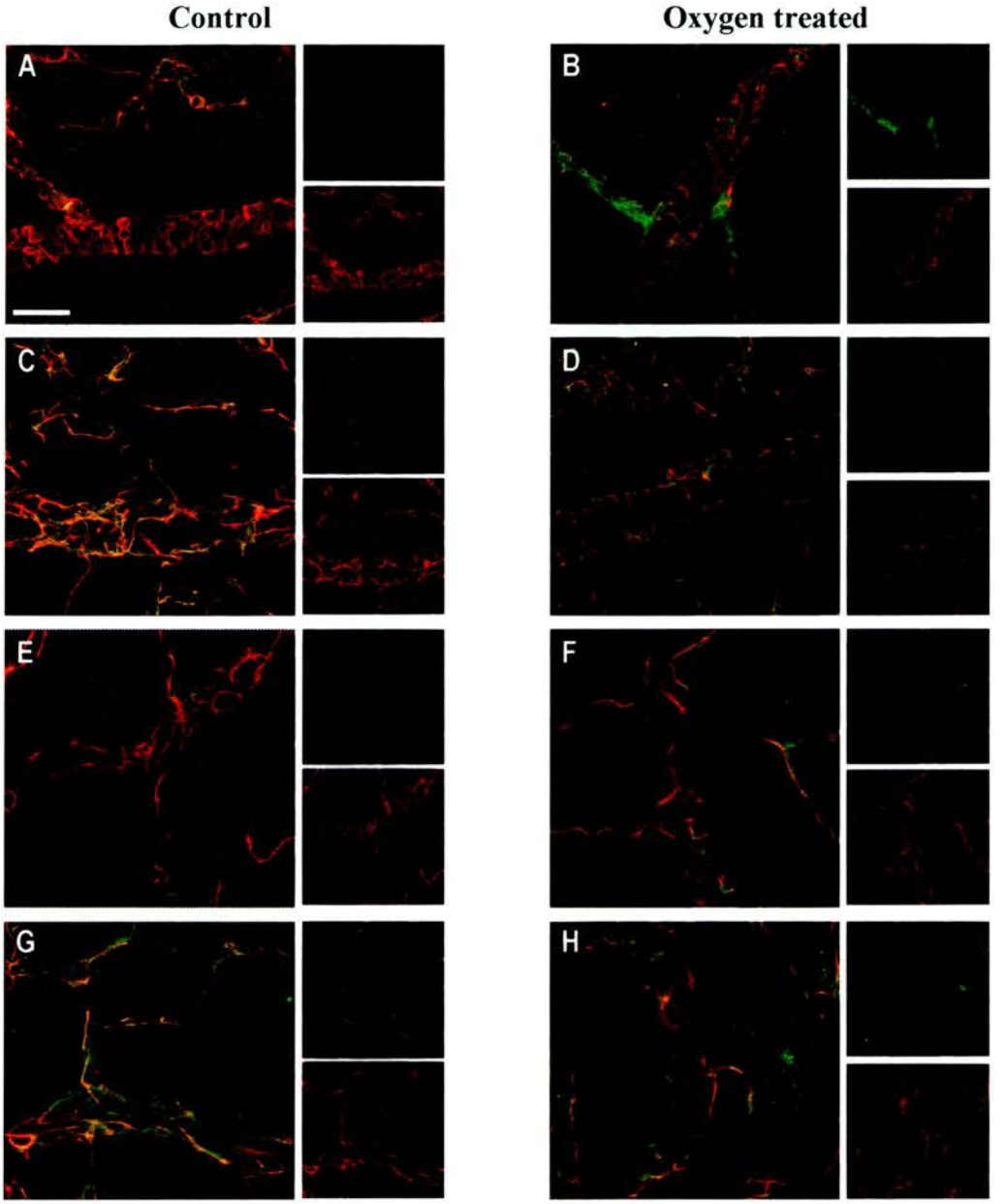

Figure 2.15: Desmin staining of P7 control and oxygen exposed retinas at higher magnification.
Flatmounts double-labelled with lectin (green) and desmin (red). (A) Arteriole of central vasculature of control pup; projected focus stack of 8 optical sections at 0.49μm. (B) Experimental retina comparable to image A. (C) Venule of central retinal vasculature of control pup; projected focus stack of 15 optical sections at 0.49μm. (D) Experimental retina comparable to image C; projected focus stack of 5 optical sections at 1.35μm. (E) Arteriole of peripheral vasculature of control pup; projected focus stack of 5 optical sections at 0.89μm. (F) Experimental retina comparable to image E. (G) Venule of peripheral vasculature of control pup; projected focus stack of 10 optical sections at 0.45μm. (H) Experimental retina comparable image G.
Scale bar: 32μm.

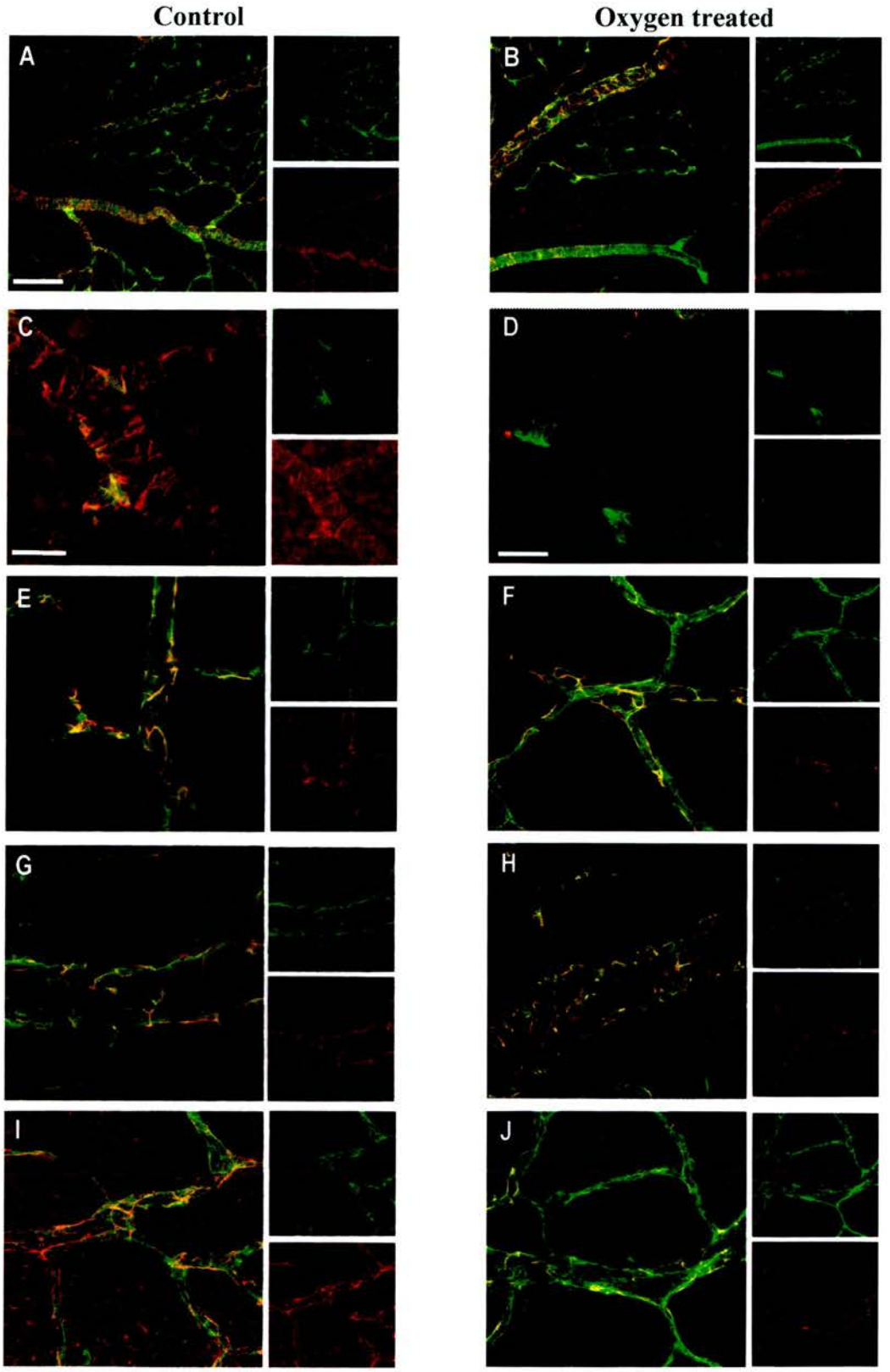
Control
Oxygen treated
A
B
C
D
E
F
G
H
I
J

Figure 2.16: Desmin staining of P14 control and oxygen exposed retinas.
Flatmounts double-labelled with lectin (green) and desmin (red). (A) Central vasculature of control pup. (B) Experimental retina comparable to image A. (C) Arteriole of central retinal vasculature of control pup; projected focus stack of 19 optical sections at 0.45μm (D) Experimental retina comparable to image C; projected focus stack of 8 optical sections at 1.34μm. (E) Arteriole of peripheral vasculature of control pup. (F) Experimental retina comparable to image E; projected focus stack of 6 optical sections at 0.5μm. (G) Venule of central vasculature of control pup. (H) Experimental retina comparable to image G; projected focus stack of 6 optical sections at 1.69μm. (I) Venule of peripheral vasculature of control pup; projected focus stack of 5 optical sections at 0.94μm. (J) Experimental retina comparable to image I; projected focus stack of 6 optical sections at 1.69μm.
Scale bar: (A) 100um; (B) as A; (C) 16μm; (D) 32μm; (E), (F), (G), (H), (I) and (J) as D.

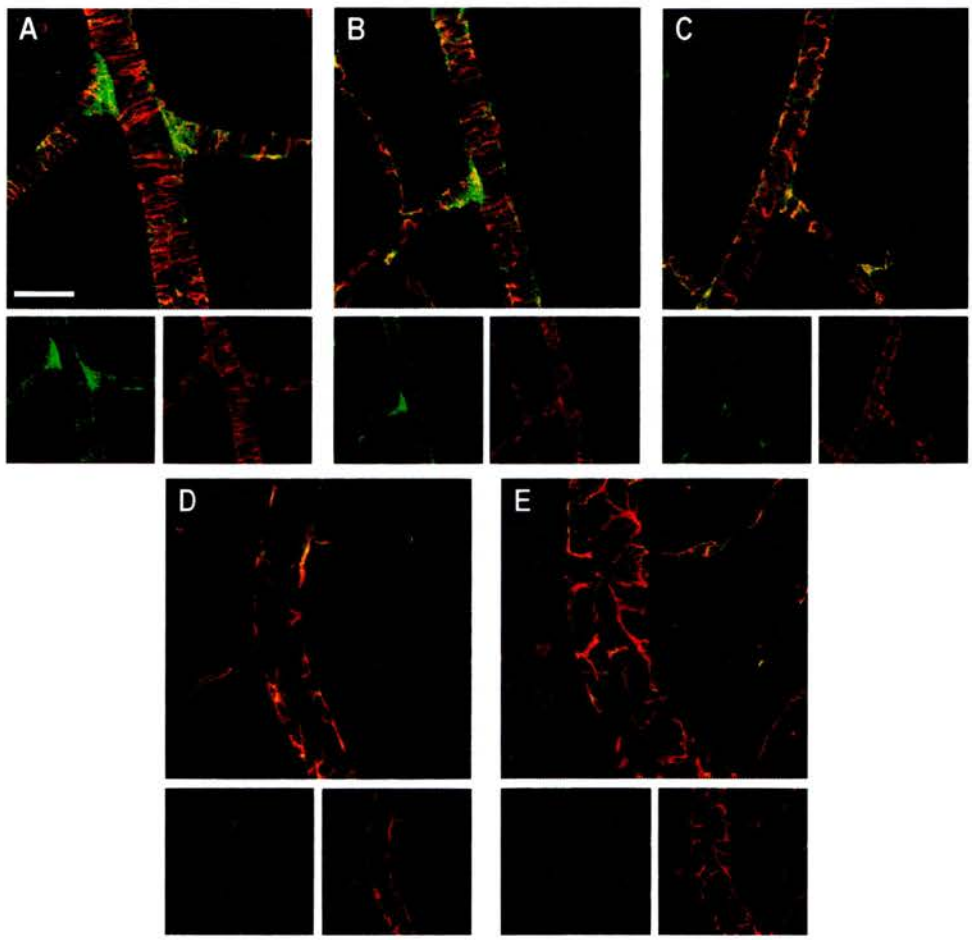

Figure 2.17: Desmin staining of P21 control retina.
Flatmount double-labelled with lectin (green) and desmin (red). (A) Central image of an arteriole; projected focus stack of 9 optical sections at 0.94μm. (B) Midperipheral image of an arteriole; projected focus stack of 10 optical sections at 0.94μm. (C) Peripheral image of an arteriole; projected focus stack of 7 optical sections at 0.89μm. (D) Central image of a venule. (E) Peripheral image of a venule projected focus stack of 16 optical sections at 0.50μm.
Scale bar: 32μm.

Western analysis

As with α-SMA, it appeared that the expression of desmin on the retinas of the oxygen treated pups was reduced in comparison to controls. Thus, Western analysis was conducted. Two different antibodies to desmin, were used at various concentrations (1:500, 1:200 and 1:100), but no positive labelling was observed on the blots. Despite increasing the concentration of the secondary antibody and lengthening the incubation times, positive results for the expression of desmin protein were not achieved. An alternative method for calculating and comparing the expression of desmin in control and oxygen treated retinas had to be used.

Extent of desmin coverage of the vasculature

Using the flatmounted retinas stained for endothelial cells (lectin) and pericytes (desmin), the extent of pericyte coverage of the vasculature was measured by taking images of the central and peripheral retina at P14. The amount of lectin and desmin staining was calculated by applying a threshold to the images and counting the black and white pixels. The desmin coverage of the vasculature was then expressed as a percentage:

		Endothelial cells	Pericytes	% coverage
Control	Retina 1	1754922	612521	34.90
	Retina 2	1437603	503121	35.00
	Retina 3	1369544	478906	34.97
	Retina 4	650095	236981	36.45
	Retina 5	652096	244198	37.45
	Mean			35.75
O_2 treated	Retina 1	1503427	359282	23.90
	Retina 2	1402541	321220	22.90
	Retina 3	1759933	370425	21.05
	Retina 4	646473	141983	21.96
	Retina 5	1085005	275143	25.36
	Mean			23.03 *

Table 2.1: Extent of pericyte coverage in retinas of P14 control and experimental rat pups.
* - p value was calculated as <0.000 using the unpaired t-test.

In controls it was calculated that around 35% of the vasculature was covered by desmin positive cells, whereas in the oxygen treated retinas, the extent of coverage had decreased significantly, to around 23%.

2.4.6 Electron Microscopy

Finally, using transmission electron microscopy, the relationship between endothelial cells and pericytes was briefly investigated to establish whether the two cell types made direct contact with each other or if they were just in close proximity to one another.

As illustrated in Figure 2.18 (page 77), an electron micrograph showing a retinal capillary of a normal rat at P14, pericytes have larger and lighter nuclei than endothelial cells, and lie within the basement membrane. This retinal capillary was relatively well invested with pericytes and appeared to have a 1:1 endothelial cell:pericyte ratio as previously suggested by others [Shepro and Morel, 1993]. The endothelial cell:pericyte ratio of the arterioles and venules was also 1:1 (Figure 2.19, page 77). The pericytes of all three types of vessels were either lying very close to the endothelial cells, or parts of their processes were in contact with the endothelium.

The micrographs of the retinal vessels of oxygen exposed pups (Figure 2.20, page 78 and 2.21, page 79) were difficult to interpret because some retinal vessels appeared relatively normal while some presented with quite marked degenerative features. The most common defect of the oxygen exposed retinas was the degradation of the basement membrane; in all electron microscope images of these retinal blood vessels, the basement membrane had lost the characteristic structure associated with the extracellular matrix proteins and, therefore, was very difficult to identify. Another difference was that the nuclei of the pericytes of the experimental retinas were much darker than the control retinas. The structure of some pericytes and endothelial cells were also altered, for example, in Figure 2.20 B, the pericyte had no processes, the endothelial cell cytoplasm was degraded and the two cell types no

longer appeared to lie within close proximity. In some cases the capillaries had collapsed, although pericytes were still in direct contact with the endothelium (Figure 2.21, A).

Thus, the loss of pericyte and endothelial cell association and the incomplete or degraded extracellular matrix in retinal capillaries of the experimental pups suggests that the oxygen exposure resulted in abnormal interactions between the endothelial cells and pericytes.

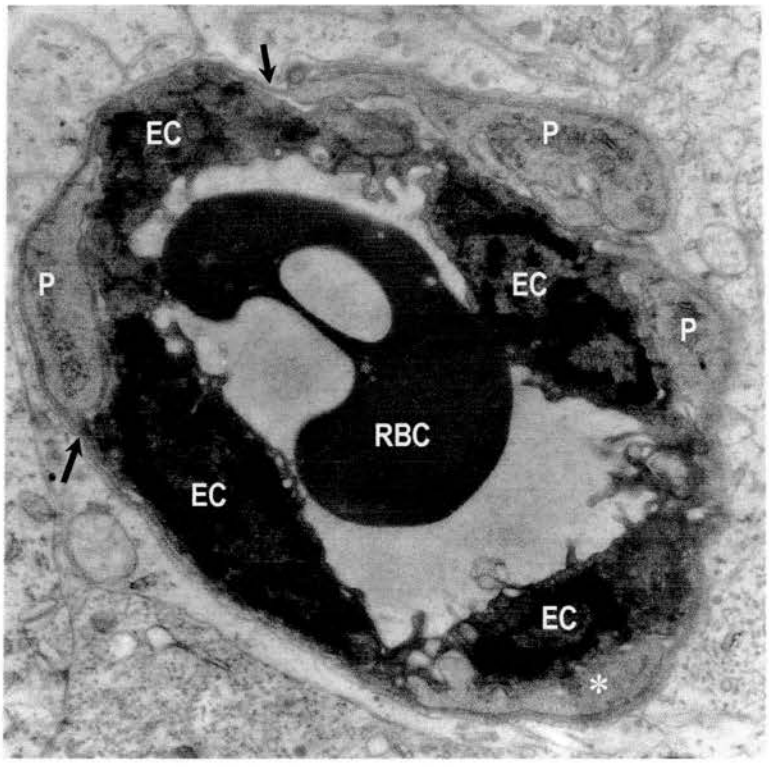

Figure 2.18: Electron micrograph of a P14 control retinal capillary.
EC - endothelial cell; P - pericyte; RBC - red blood cell; asterisk - possibly a pericyte process; arrows - indicate the basement membrane.
Magnification: x8,000.

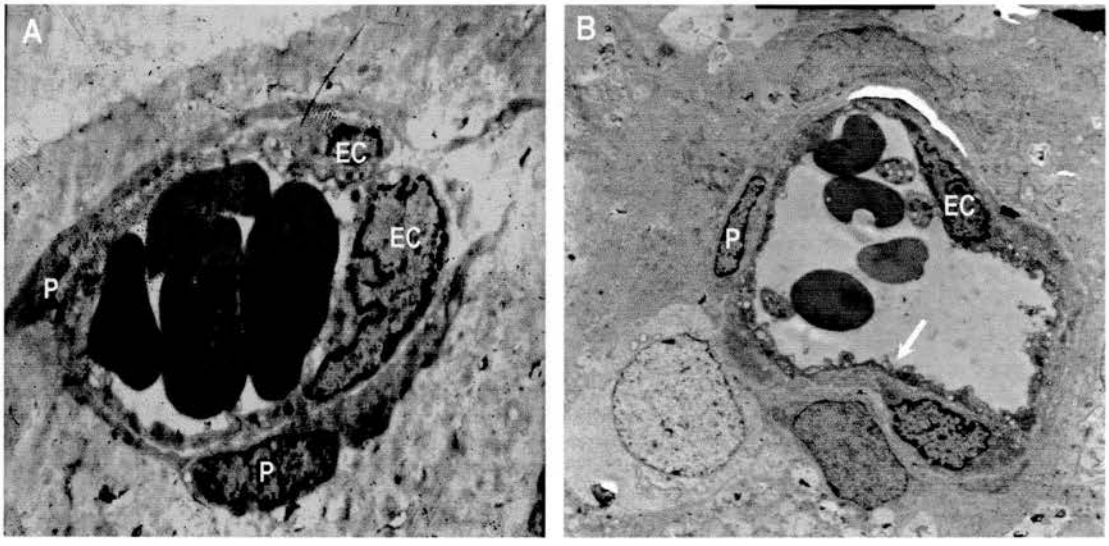

Figure 2.19: Electron micrographs of P14 control retinal vessels.
(A) Arteriole. (B) Venule. Arrow indicates cytoplasm of endothelial cell.
EC - endothelial cell; P - pericyte.
Magnification: (A) x5,000; (B) x3,000.

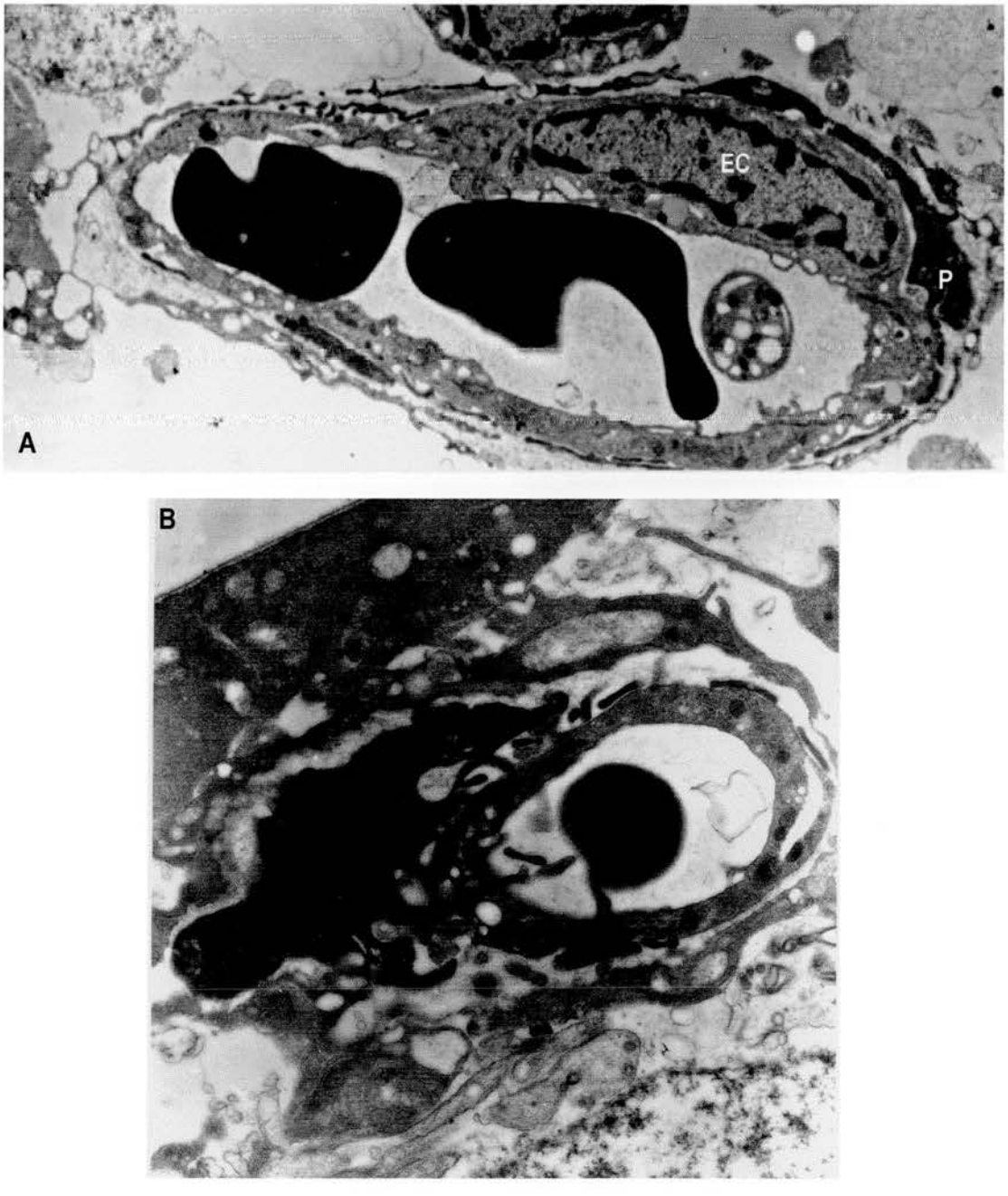

Figure 2.20: Electron micrographs of P14 retinal vessels of pups exposed to variable oxygen.
(A) Venule. The cells are relatively similar to those of a control vessel. (B) Capillary. Arrow indicates remains of basement membrane.
EC - endothelial cell; P - pericyte.
Magnification: (A) x3,800; (B) x8,000.

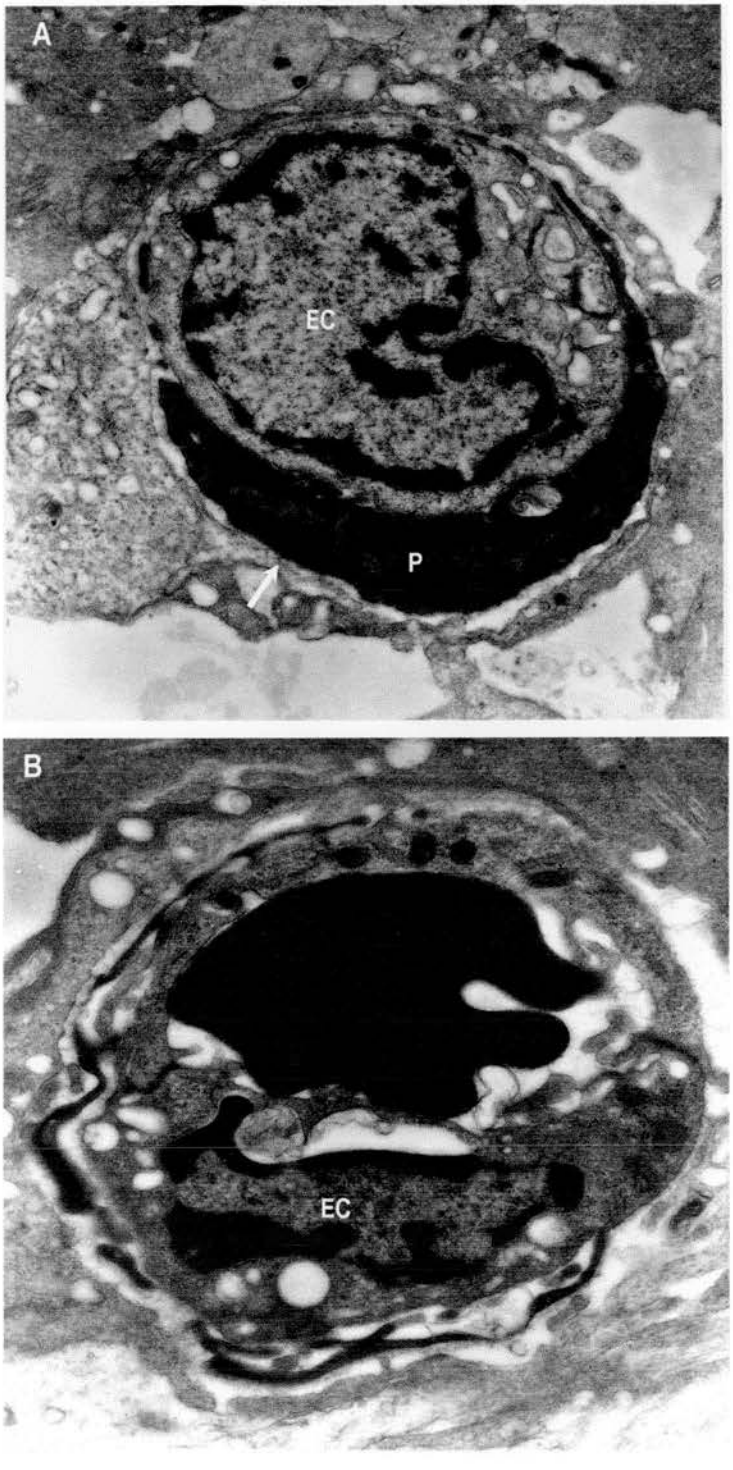

Figure 2.21: Electron micrographs of P14 oxygen exposed retinal capillaries.
Arrow indicates intact basement membrane
EC - endothelial cell; P - pericyte.
Magnification: (A) x8,000; (B) x3,000.

2.5 DISCUSSION

2.5.1 Mural Cells of the Retinal Vasculature

The retinal vasculature consists of the smallest sized arterioles and venules [Wise, Dollery and Henkind, 1971] that are connected by an intricate network of pre-, mid- and post-capillaries [Zimmermann, 1923[10]]. The entire retinal vasculature, like that of any tissue, is associated with a layer of mural cells, called smooth muscle cells and pericytes. Smooth muscle cells are elongated, spindle shaped cells with fine tapered ends and a large nucleus in the centre. These cells encapsulate arterioles and to a lesser extent the venules [Bloom and Fawcett, 1968; Leeson and Leeson, 1976]. Capillaries, on-the-other-hand, are invested by pericytes that are elongated cells with multiple, long processes [Zimmermann, 1923[11]]. Some cells are without a doubt identified as mural cells (by their location and orientation), however their morphology does not appear to be either of a true pericyte or a smooth muscle cell. As a result many researchers prefer to group the two cell types and refer to them as pericytes/smooth muscle cells [Antonelli-Orlidge et al., 1989; Benjamine, Hemo and Keshet, 1998; Darland and D'Amore, 2001a].

There is a great body of evidence supporting the theory that stabilisation of the vessel wall and maintenance of vascular integrity are important functions of the pericytes [Crocker, Murad and Geer, 1970; Tilton et al., 1985; Orlidge and D'Amore, 1987; Suri et al., 1996]. In proliferative retinal disorders, such as diabetic retinopathy, it is suggested that both the stabilisation and integrity of vessels may be compromised due to a loss of capillary pericytes [Kuwabara and Cogan, 1961; Speiser, Gittelsohn and Patz, 1968]. Similarly, it is suggested that the neovascularisation which develops as a complication of ROP arises from immature microvessels that have not yet established a pericyte coverage [Patz, 1968]. Perhaps for this reason pericyte coverage in animal models of ROP has never been studied.

---

[10] Reviewed in Darland and D'Amore, 2001b.
[11] Reviewed in Nehls and Drenkhahn, 1993 and in Darland and D'Amore, 2001b.

Therefore, retinal mural cell coverage was investigated in the Edinburgh model of ROP.

2.5.2 Selecting the Markers

Over the years, several protein markers including α-SMA, myosin, desmin and vimentin have been used for the labelling of mural cells. But, because published data on these markers is contradictory and markers specific for either smooth muscle cells or pericytes are currently unavailable, selecting a marker for the immunohistochemistry was difficult. α-SMA and desmin were selected for several reasons:

- labelling of the mural cells by α-SMA and desmin has been reported by several researchers [Skalli et al., 1989; Mitchell et al., 1990; Nehls, Denzer and Drenckhahn, 1992; Newcomb and Herman, 1993; Nicosia and Viallaschi., 1995]
- other markers are not strictly specific to mural cells; myosin [Joyce, Haire and Palade, 1985; Ehler et al., 1995], vimentin [Mitchell et al., 1990; Ehler et al., 1995] and NG-2 [Pagan-Mercado et al., 2002] are all reported to be expressed by endothelial cells.
- 3G5, which may be a good marker for pericytes, is not available commercially and literature on this marker is limited.

2.5.3 Labelling and Specificity of the Markers

α-SMA

In the fully formed vasculature, α-SMA labelled elongated, spindle-shaped cells; the cells had a large round central area, which presumably contained the nucleus, and had tapered processes. The cells had a tendency to be arranged perpendicular to the axis of the arterioles and pre-capillaries. Thus, α-SMA stained the smooth muscle cells. These results are in agreement with previous studies where α-SMA was detected on the arterioles and venules, but not on the capillaries of the bovine retina [Nehls and Drenkhahn, 1991]. In addition, vessels of the human brain, like the

retina, are mainly covered by pericytes and it was found that a very small number of the mural cells contained α-SMA [Verbeek et al., 1994]. Therefore, the use of this marker for the identification of pericytes is limited, instead it should be considered as a marker for smooth muscle cell differentiation.

Desmin

Desmin labelling was dependent upon the fixative used during tissue processing. The retinas did not stain when the eyes were fixed in 2% paraformaldehyde or 70-100% ethanol. Positive results were obtained using acetone at a 3:1 dilution with 1M PBS. The drawbacks to using acetone as the fixative were that the outer tissue of the eye became very rigid, making dissection difficult, and that despite piercing the eye prior to fixation, the retinal tissue remained fragile and damage to the surface occurred easily.

Unlike α-SMA, desmin expression was associated with all vessels of the retina and labelled long slender cells with numerous processes. The structure of the pericytes was different depending on their location; on the venular vessels the cells were highly branched and not arranged in any particular manner, but on the capillaries the cells were slightly less branched and lay across the axis of the capillaries. Their structure altered further on the arterioles where the cells were long and thin, and encircled the wall of the vessel.

The background labelling of the flatmounts stained with α-SMA and desmin was considerably high. Figure 2.22 A (page 84) shows that this high background was not a result of antibody labelling, but that of Texas red streptavidin, which stained the ganglion cells and the retinal pigmented epithelium. This problem may be overcome by using a different detection system, such as Alexa Fluor 568.

Lectin

Lectin has been widely used for staining vessels as it is suggested to be very specific for endothelial cells. Hence, *G. simplicifolia* (Bandeiraea) isolectin B4 was used in this study for visualising the vessels.

The negative control (Figure 2.22 B, page 84), where the retinal flatmounts were incubated in wash solution instead of lectin, showed that background labelling of the lectin antibody was minimal. However, in the lectin labelled tissues, a bed of large round cells beneath the vasculature were also stained; these cells were the ganglion cells. In addition, at earlier stages of development, lectin also stained small fine cells in the avascular areas of the retina. These cells were the microglia, which have previously been reported to stain with lectin [Hughes, Yang and Chan-Ling, 2000].

Although lectin has been used extensively in studies of the retinal vasculature [Benjamin, Hemo and Keshet, 1998; Hughes, Yang and Chan-Ling, 2000], none of these studies have evaluated its staining pattern at high magnification. During the initial analysis of the retinal vasculature, it seemed that lectin stained the endothelial cells, however doubts of lectin specificity arose after viewing the vessels at high magnification. Lectin did not label elongated cells that lay in the direction of the vessels, but fine fibres wrapped around the vessels (Figure 2.23, page 85). Some of the lectin positive cells were clearly on the external surface of the vessel.

Further examination was conducted by using TO-PRO-3 to stain the nuclei of the vascular cells. Figure 2.24 (page 85) shows that large round nuclei were protruding from the surface of the vessel wall, and that under this layer elongated nuclei were indeed running along the direction of the vessel; these nuclei belonged to the endothelial cells. Thus, lectin did not stain endothelial cells, but rather appeared to stain the membrane of the entire vessel. Perhaps lectin was staining the basement membrane that splits whilst it approaches the mural cell, and therefore provides a layer on both sides of the cell to enclose it completely.

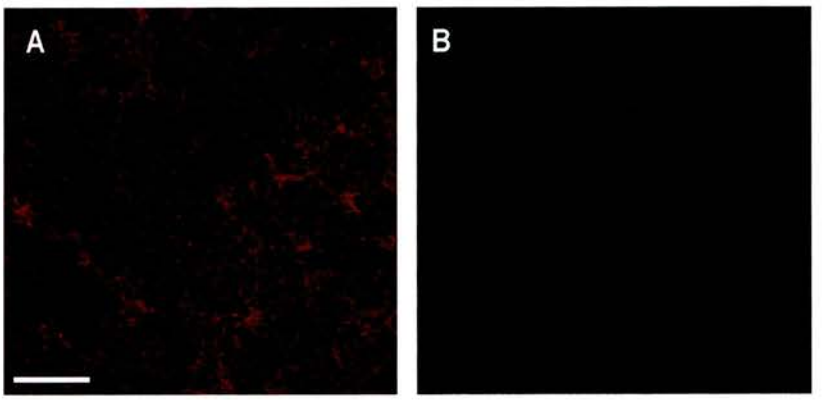

Figure 2.22: Negative controls.
(A) α-SMA and desmin labelling. (B) Lectin staining.
Scale bar: 100µm.

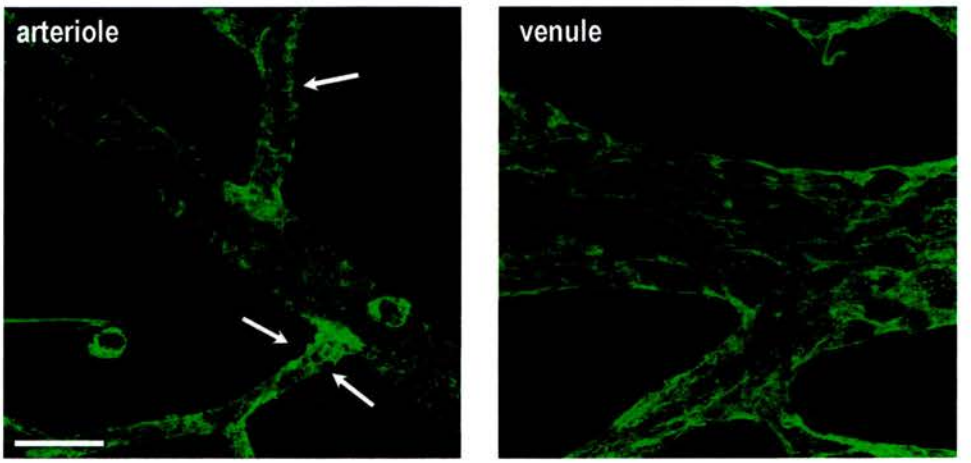

Figure 2.23: Flatmounted retina stained with lectin only.
On the arteriole lectin outlined cells that were protruding from the vessels (arrows). These cells may be mural cells.
Scale bar: 32μm.

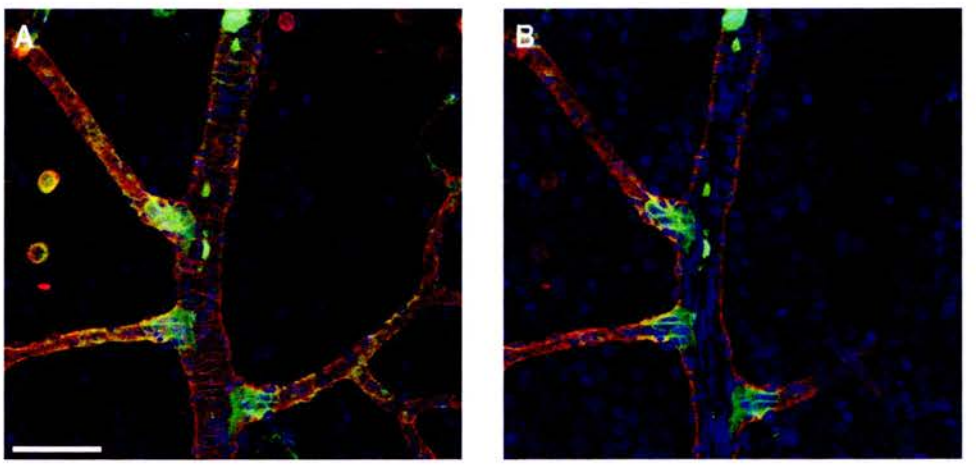

Figure 2.24: Retinal flatmount labelled with lectin, α-SMA and TO-PRO-3.
The nuclei were visualised using a nuclear marker, TO-PRO-3 Iodide.
(A) An arteriole labelled with lectin (green), α-SMA (red) and TOPRO-3 (blue); projected focus stack of 8 optical sections at 0.76μm. (B) Cross section of image A showing optical section number 3.
Scale bar: 32μm.

Other markers considered to be specific to endothelial cells are Von Willebrand factor and VE cadherin. However, Von Willebrand factor failed to stain the endothelial cells *in vitro* [Ehler et al., 1995] and the smallest capillaries of the vasculature *in vivo* [Hughes, Yang and Chan-Ling, 2000]. Although VE cadherin may be suitable for labelling endothelial cells in culture [Lampugnani et al., 1992; Breier et al., 1996], to date this marker has not been used for *in vivo* work.

2.5.4 Mural Cell Coverage of the Vessels in Normal Development

The frequency, distribution, orientation and structure of the mural cells varied depending on the type and location of the vessel. As mentioned above, it appeared that α-SMA stained smooth muscle cells and desmin stained the pericytes. There were however several cells, on the arteriole in particular, that stained positively for both markers.

α-SMA expression on the retinal vessels increased progressively from P2 to P21 and was limited to the vasculature that had undergone complete remodelling. On P2, the arteriole near the optic disc was labelled and by P21 the labelling was observed along the whole length of the arterioles, the pre-capillaries and the venules, but other retinal vessels (the mid-capillaries and the post-capillaries) remained negative for α-SMA. These results are very similar to those reported by Benjamin and colleagues who also stained rat retinal flatmounts with lectin and α-SMA [Benjamin, Hemo and Keshet, 1998]. They reported staining of the artery on P2 which, by P10, progressed onto the primary branches and by P18 on to the secondary and tertiary branches. They referred to these cells as pericytes. However, there is evidence to suggest that these cells were not pericytes; 1) the labelling was only observed on the arteriolar vessels and not across the capillary bed which has been previously reported to have pericyte coverage [Zimmermann, 1923[12]; Kuwabara and Cogan, 1963; Rhodin, 1968; Fujiwara & Uehara, 1984; 2) the cells positive for α-SMA were closely packed along the vessels, whereas it is well established that pericytes do not

[12] Reviewed by Sims, 1986.

form a continuous layer along vessels [Zimmermann, 1923[13]; Rhodin, 1968] nor do pericytes make contact with each other [Rhodin, 1968]; and 3) α-SMA is a poor marker for pericytes.

During early development, α-SMA positive cells were flat and lacked distinct structure. By P7, the labelled cells had a very different appearance; the cells were bulging from the vessels, and by P14 these cells had differentiated fully into smooth muscle cells. These findings suggest that α-SMA labelled the precursors of smooth muscle cells and that differentiation of these cells was a slow process. At P21, the peripheral arteriolar vessels and the venules also stained for α-SMA, but the cells were undifferentiated precursor cells. It is likely that these cells may also differentiate into smooth muscle cells at a later stage; this could be easily investigated by staining retinas of older rats.

In comparison to α-SMA, desmin staining was widely distributed and dispersed across the whole vasculature including the advancing peripheral edge. On P2, desmin labelled very fine and long strands on the surface of the retinal vessels; many vessels near the arterioles lacked these cells, probably because these were vessels that would eventually regress to form capillary free zones. By P7, the cells on the vessels of the central region had thick multiple processes, and had gained the structure of pericytes. Peripherally the cells were very similar to those observed on the vessels at P2. By P14, most of the pericytes of the vasculature were fully formed; those of the arteriole had few processes, whereas those of the venule had many processes (primary and secondary). The pericytes of the peripheral retinal area had also completely differentiated by P21.

The fine long unbranched cells observed in the central retina on P2 and the peripheral edge on P7 and P14 were most likely the pericyte precursor cells; thus desmin was expressed very early in the process of pericyte differentiation. This is in agreement with Nehls et al. who suggested that desmin antibody labelled fine

[13] Reviewed in Darland and D'Amore, 2001b.

processes belonging to the youngest pericytes [Nehls, Denzer and Drenckhahn, 1992]. However, these researchers also stated that true pericytes only existed on the mid-capillaries, but the post-capillaries and the venules of the retinas in my study were also covered by desmin stained cells that had the typical structure of pericytes.

The orientation of the pericytes differed on the vessels during development. On P2, the cells were wrapped around the arteriole near the optic disc, but towards the periphery, and on all arteriolar branches, they lay across the axis of the vessel. The cells of the venule, at this stage, were not arranged in any distinct pattern. By day 14, the cells were encircling the walls of the central arterioles and the pre-capillaries, but towards the periphery the cells did not appear to be positioned in any particular manner. The pericytes were arranged both parallel and perpendicular to the walls of the venules and the post-capillaries. The facts that the orientation of the cells differed during development and that some precursor cells appeared to be very loosely attached to the vasculature in early development suggest that, unlike smooth muscle cells, pericytes display a high degree of plasticity, agreeing with Clark and Clark who described pericytes as non-static structures [Clark and Clark, 1925]. Another difference between the two mural cells is that the pericytes appeared to differentiate rather rapidly in comparison to smooth muscle cells.

Figures 2.3 to 2.5 (pages 54 and 55) which contain images of retinal flatmounts double-labelled with α-SMA and desmin antibodies, show that some differentiated cells surrounding the arterioles expressed both markers. Some of these cells had the typical structure of smooth muscle cells with only two processes, whereas other cells had three or four processes. There are several possible explanations for this staining pattern. Firstly, smooth muscle cells expressed desmin along with α-SMA which has been previously suggested [Nicosia and Villachi, 1995]. This seems unlikely since only some, not all, of the smooth muscle cells stained for desmin. Secondly, desmin expression depended on the state of cell differentiation, i.e. as the smooth muscle cells matured their expression of desmin decreased. This could be easily determined by double-staining retinal flatmounts of younger and older animals with

α-SMA and desmin; if expression levels of desmin were lower in the older animals then perhaps desmin is expressed by immature smooth muscle cells. Thirdly, some pericytes had the potential to differentiate into smooth muscle cells on demand, which may be interpreted from the findings of previous studies: (1) Rouget[14] described pericytes as less differentiated smooth muscle cells; (2) Zimmerman[15] found that pericytes merged into smooth muscle cells on the arteriolar and venular sides; (3) transforming growth factor-β, which is reported to induce mesenchymal cell to pericyte differentiation [Hirschi, Rohovsky and D'Amore, 1998], was also found to increase α-SMA expression of cultured human brain pericytes, suggesting that the pericytes differentiated into smooth muscle cells [Verbeek et al., 1994]; and (4) pericytes have been suggested to be derived from nearby smooth muscle cells that 'dedifferentiate' [Nicosia and Villaschi, 1995; Lindahl et al., 1997; Hellström et al., 1999]. Earlier I suggested that α-SMA may be an early marker for smooth muscle cell differentiation, hence it may also be expressed at the earliest stages of pericyte to smooth muscle cell differentiation. Thus, two distinct types of pericytes may indeed exist; true pericytes that remain static once formed and transitional pericytes that have the potential to undergo further differentiation. But what induces the differentiation of a pericyte into a smooth muscle cell? Perhaps the formation of the surrounding precursor cells into smooth muscle cells is a signal for these pericytes to differentiate further and become smooth muscle cells.

In summary, α-SMA and desmin were very early markers for smooth muscle cells and pericytes, respectively. Transitional pericytes, however, expressed both proteins, although desmin expression may decrease as these cells differentiate into mature smooth muscle cells. Thus, further investigations on more suitable and specific markers for both types of mural cells are still required.

---

[14] Reviewed in Darland and D'Amore, 2001b.
[15] Reviewed in Kuwabara and Cogan, 1963.

2.5.5 Mural Cell Coverage of Vessels in the Edinburgh Model of ROP

As previously reported retinal vessel formation of pups exposed to variable oxygen was retarded and abnormal; the peripheral edge of the vasculature, which reached the ora serrata by P14, was still a significant distance from the ora serrata, and the central capillary network had not undergone extensive remodelling [McColm et al., 2004].

Immunohistochemically stained flatmounts showed that coverage of the vessels by both smooth muscle cells and pericytes was affected by the oxygen regime. α-SMA labelling on all days examined did not progress as far as it did on the control days; the extent of coverage along the length of the arteriole and its branches appeared slightly reduced. In addition, the differentiation of the precursor cells into smooth muscle cells seemed delayed; less fully formed smooth muscle cells were observed on the arterioles of the experimental retinas. Surprisingly, expression of the marker was increased on the venules; during normal development α-SMA expression was low on P14 and more intense on P21, but in the oxygen treated retinas, the venules stained as early as P7 and continued on P14. These cells surrounding the venules did not appear to be smooth muscle cells. Although difficult to interpret, two possible explanations are offered. First, in response to the variable oxygen regime the venules may have acquired coverage by a layer of smooth muscle cell precursors which may differentiate to provide a form of protection for the venule; these cells would probably differentiate on demand i.e. if the insult continued. Second, the pericytes of the venules may have differentiated into smooth muscle cells in response to the oxygen. In support of this is the report by Meyrick and Reid who found that under hypoxic stress pericytes of the lung microvasculature had the potential to develop into smooth muscle cells [Meyrick and Reid, 1978].

Western analysis confirmed that in comparison to control retinas, α-SMA expression was marginally reduced in the experimental retinas. As discussed above, α-SMA coverage was only seen on arteriolar vessels once the surrounding vasculature had

undergone complete remodelling, indicating maturation and stabilisation of the vessels. It is possible then that the reduction of α-SMA expression and coverage of smooth muscle cells in the oxygen exposed retinas was the result of the delayed/reduced remodelling of the vasculature.

Regarding pericytes, it has been suggested that there cannot be a loss of pericytes in ROP since the vessels are too immature for coverage [Patz, 1968], however, in my studies desmin positive pericytes were visualised at a very early stage of development. One condition in which retinal pericytes are preferentially lost is diabetes. This was first suggested by Cogan and colleagues who evaluated retinas of diabetic patients and observed that loss of pericytes appeared to be the initial stage in diabetic retinopathy and may underlie the pathogenesis of microaneurysms [Cogan, Toussaint and Kuwabara, 1961; Kuwabara and Cogan, 1961]. This was soon confirmed by Speiser et al. who compared the retinas of diabetic patients to retinas of healthy controls and reported that the endothelial cell:pericyte ratio was greater in the diseased retinas (this increase in ratio was due to a reduction in pericyte number and not an increase in endothelial cell number), and that the greatest loss took place in the central retina [Speiser, Gittlesohn and Patz, 1968].

In the retinal vasculature of the Edinburgh model, the extent of the pericyte coverage could not be commented on because unlike smooth muscle cells, pericytes did not form a continuous layer along the retinal vessels. However, it appeared that there was a decrease in the number of pericyte precursor cells in younger animals and a decrease in the number of differentiated pericytes in the older animals. Thus, pericytes were present on the vasculature, but were fewer in number. To confirm that there was a reduction in the number of pericytes, Western blotting was performed. However, no desmin expression was detected at any point during development, despite using different desmin antibodies at various concentrations. The only parameter that remained unchanged was the amount of protein loaded for separation, but more than 75µg of total protein could not be loaded as it would have exceeded the recommended loading volume. As an alternative, images of the central

and peripheral retina from five control and five oxygen exposed retinas were taken, and using computer thresholding techniques, the percentage of vasculature covered by pericytes was calculated. The results indicated that there was indeed a significant reduction in pericyte coverage of the oxygen treated retinas.

There are, however, several drawbacks of using this method of quantification. First, as mentioned above, Texas red streptavidin produced significant background labelling. It is possible that when setting the gain and off-set of the confocal microscope to eliminate all background staining some of the true labelling was also eliminated. This may be overcome by using other fluorescent molecular probes. Second, due to time constraints, a very small number of samples were evaluated, and although the results clearly showed that there were less pericytes in the model, increasing the sample numbers would be useful. Third, only retinas of P14 animals were used because retinas fixed in acetone were fragile, and the retinas of younger animals were more vulnerable to damage during dissection. Thus, finding a more suitable fixative would allow the investigation of younger animals. In addition, instead of threshold analysis an alternative method of analysis would be very valuable. A possibility would be to stain the cell nuclei using the trypsin digestion technique employed by Speiser and colleagues [Speiser, Gittlesohn and Patz, 1968]. This would allow me to measure and compare the endothelial cell:pericyte ratio of controls and experimental retinas.

The electron microscope results showed that pericyte structure was altered in some retinal blood vessels of the oxygen treated animals. The interactions between the endothelial cells and pericytes were also compromised; the cells were no longer within close proximity to each other. In addition, degradation of the basement membrane was observed and some vessels lacked a basement membrane completely. It is possible that the effect of variable oxygen on endothelial cell and pericyte structure was due to the degradation or absence of the basement membrane. Conversely, the abnormal pericyte and endothelial cell interactions may have caused the degradation of the basement membrane. The data, unfortunately, cannot

distinguish between the two possibilities. Only two control and two experimental retinas were analysed due to time and financial restraints. Although structural changes of the retinal vessels were observed in the oxygen treated rats, increasing the sample number would be beneficial.

In summary, the results presented in this chapter suggest that there is a reduction in the number of both smooth muscle cells and pericytes in a clinically relevant model of ROP. The decrease in smooth muscle cells is most likely a result of reduced remodelling of the vasculature, whereas the decrease in pericyte coverage may be the result of reduced recruitment of pericyte precursor cells or apoptosis of the pericytes in response to the oxygen regime. In addition, the differentiation of both cell types is delayed in this model of ROP.

CHAPTER THREE

EXPRESSION OF PLATELET-DERIVED GROWTH FACTOR IN THE EDINBURGH MODEL OF ROP

3.1 INTRODUCTION

In the mid-1970s a protein capable of inducing cell proliferation was identified in whole blood serum [Kohler and Lipton, 1974; Ross et al., 1974; Rutherford and Ross, 1976; Westermark and Wasteson, 1976; Scher, Stone and Stiles, 1979]. It was later purified from human platelets [Antoniades, Scher and Stiles, 1979; Heldin, Westermark and Wasteson, 1979; Deuel et al., 1981], where it was predominantly stored in the α-granules [Kaplan et al., 1979]. The protein was subsequently named platelet-derived growth factor (PDGF). Along with promoting cell proliferation [Kohler and Lipton, 1974; Ross et al., 1974; Rutherford and Ross, 1976; Westermark and Wasteson, 1976; Scher, Stone and Stiles, 1979], PDGF was also found to promote the migration of certain cell types [Bernstern, Antoniades and Zetter, 1982; Grotendorst et al., 1982; Hosang et al., 1989; Koyama et al., 1992; Shure et al., 1992].

3.1.1 Ligands

PDGF is a basic glycoprotein that consists of two polypeptide chains joined by disulfide bonds [Heldin, Westermark and Wasteson, 1979]. The polypeptides are denoted chain A and chain B and are estimated to have molecular weights of 11-18kDa and 15-16kDa, respectively [Johnsson et al., 1982; Waterfield, 1983; Hammacher et al., 1988a]. Thus, the molecular weight of PDGF ranges between 28 and 35kDa [Heldin et al., 1979; Antoniades, 1981; Deuel et al., 1981; Johnsson et al., 1982, 1984; Waterfield et al., 1983]. Both chains are synthesised as precursor molecules that undergo proteolytic processing prior to secretion; the A chain is cleaved at the N-terminal whereas the B chain is cleaved at both the N- and C-termini [Östman et al., 1991]. Due to incomplete purification and lack of overlapping sequences, the precise sequence of both precursors has not been fully established. The two mature polypeptide chains, which share around 60% homology [Johnsson et al., 1982], give rise to three possible dimeric isoforms; PDGF-AA, PDGF-AB and PDGF-BB [Hammacher et al., 1988a]. This dimeric structure of PDGF seems to be essential for biological activity [Hammacher et al., 1988a]. Recently, two additional PDGF molecules were identified and named PDGF-CC and PDGF-DD [Kazlauskas, 2000; Li et al., 2000; Bergsten et al., 2001]. The C and D chains are structurally related to each other, but rather distantly related to the A and B chains; hence, they do not form heterodimers with A or B. The receptor binding, signalling and biological functions of the C and D chains are still to be elucidated.

3.1.2 Receptors

The A and B chains of PDGF exert their effects by activating two cell surface receptors called PDGF receptor-α and PDGF receptor-β [Yarden et al., 1986; Claesson-Welsh et al., 1989a, 1989b; Matsui et al., 1989]. Both receptors are transmembrane glycoproteins with tyrosine kinase activity [Claesson-Welsh et al., 1988, 1989a, 1989b]. The α-receptor is synthesised as a 140kDa precursor that is processed to a mature size of 170kDa, whereas the β-receptor is synthesised as a

160kDa precursor that matures to around 180kDa [Keating and Williams, 1987; Hart et al., 1988; Claesson-Welsh et al., 1989a, 1989b]. Because PDGF isoforms are dimeric molecules, they simultaneously bind two receptors, and therefore dimerise receptors upon binding [Bishayee et al., 1989; Heldin et al., 1989]. The α-receptor binds both the A and B chains with equal affinity, whereas the β-receptor binds only the B chain. Thus, PDGF-AA induces $\alpha\alpha$-receptor homodimers, PDGF-AB induces both $\alpha\alpha$-receptor homodimers and $\alpha\beta$-receptor heterodimers, and PDGF-BB binds all three receptor combinations [Hammacher et al., 1988a; Kanakaraj et al., 1991].

3.1.3 Biological Effects of PDGF

PDGF was initially discovered as a factor that promoted the replication of cultured mouse fibroblasts [Kohler and Lipton, 1974] and monkey arterial smooth muscle cells [Ross et al., 1974]. Since then the proliferative effect of PDGF on both fibroblasts [Rutherford and Ross, 1976; Westermark and Wasteson, 1976; Scher, Stone and Stiles, 1979; Shure et al., 1992] and smooth muscle cells [Rutherford and Ross, 1976; Grosendorst et al., 1982] have been confirmed in several reports. Studies on retinal glial cells (astrocytes and Müller cells), however, have produced conflicting results; PDGF was mitogenic for the retinal glial cells of rats [De Juan, Dickson and Hjelmeland, 1988] and humans [Westermark and Wasteson, 1976; Uchihori and Puro, 1991], but did not stimulate the proliferation of those of the rabbit retina [Burke, 1982; Scherer and Schnitzer, 1994]. In most of these early studies PDGF was predominantly obtained from human platelet-rich plasma, 70% of which was found to consist of A and B chain heterodimers and 30% of B chain homodimers [Hammacher et al., 1988a]. Thus, both the α-receptor and β-receptor are capable of mediating cell proliferation.

To understand the mechanisms of PDGF-induced cell proliferation, Scher and colleagues exposed cultured fibroblasts to PDGF and suggested that the protein acts during the late stages of the cell cycle; it stimulates cells to enter the S phase, progress through G_0/G_1, synthesise DNA and then divide. In addition, PDGF

prevents any replicating cells from entering the G_0 (quiescent) phase [Scher, Stone and Stiles, 1979].

PDGF also induces the migration of several cell types, including fibroblasts [Hosang et al., 1989; Koyama et al., 1992] and smooth muscle cells [Bernstein, Antoniades and Zetter, 1982; Grotendorst et al., 1982]. The migratory role of PDGF is thought to be mediated by the B chain only; when PDGF-AA, -AB and -BB were added to cultures of rat aortic smooth muscle cells, the PDGF-AB and -BB isoforms induced migration of the cells, but PDGF-AA inhibited the migration induced by the other isoforms [Koyama et al., 1992]. PFGF-AA, however has been shown to induce the migration of other cell types, namely fibroblasts, monocytes and neutrophils [Shure et al., 1992]. In comparison to the proliferative effect of PDGF, the chemotactic response of the cells is more rapid and occurs at a lower concentration of ligand [Grotendorst et al., 1982].

Therefore, upon activation, both the α- and β-receptors of PDGF transduce potent mitogenic signals by promoting cells to enter the S phase of the cell cycle. Although it is firmly established that the β-receptor stimulates chemotaxis, the migratory response of the α-receptor is cell type dependent; it stimulates the chemotaxis of certain cell types whilst inhibiting that of others.

3.1.4 PDGF Transgenics

Most PDGF-A knockouts die within the first few days of birth, however some survive until around six weeks of age. The transgenic mice are only slightly smaller than normal mice at birth, but the difference in size increases with age and by three or four weeks, the mutants are half the weight of normal mice. The knockout mice develop a range of defects including reduction in the number of oligodendrocytes in the brain, lack of alveolar smooth muscle cells, and defects of the mesenchyme [Beström et al., 1996].

The phenotype of PDGF receptor-α knockouts is more severe (perhaps because none of the three PDGF isoforms are able to bind), and the mice die *in utero* [Soriano, 1997]. The mice have a cleft face, skeletal and vascular defects, and suffer from spina bifida, all resulting in death between embryonic days 8 and 16 (E8 and E16).

Mice carrying a null mutation in the gene encoding the B chain of PDGF, and therefore deficient with regards to PDGF-BB and PDGF-AB, were generated by Levéen and colleagues [Levéen et al., 1994]. Although some of the mutant mice die one or two days prior to birth (E17-E18.5), most survive to term and die soon after due to subcutaneous haemorrhaging. The mice also display enlarged and deformed hearts and abnormal kidney glomeruli. The larger arteries are also dilated, for example, the aorta is enlarged to twice the normal size, but there is no sign of hyperplasia since smooth muscle cells are present in normal numbers.

PDGF receptor-β null mice also die at birth, due to their inability to breathe [Soriano, 1994]. Like the PDGF-B null mice, these mice exhibit abnormalities in the kidneys; the capillary tufts of the glomeruli and the number of mesangial cells are reduced or even absent. In addition, some mice also suffer from oedema and anaemia. These defects are presumably caused by a lack of PDGF-B signalling to the β-receptor.

3.1.5 Roles in the Vasculature

Normal vessel formation

Early *in vitro* studies found that 1) PDGF is secreted by endothelial cells [Barette et al., 1984; Collins et al., 1985], 2) their receptors are expressed by both endothelial and smooth muscle cells [Smits et al., 1989; Beitz et al., 1991], and 3) it promotes the proliferation and migration of smooth muscle cells [Ross et al., 1974; Rutherford and Ross, 1976; Bernstein, Antoniades and Zetter, 1982; Grosendorst et al., 1982]. Despite these findings, the formation of blood vessels during the early stages of embryonic development is not affected in mice lacking the PDGF or the PDGF receptor genes [Levéen et al., 1994; Soriano, 1994, 1996; Beström et al., 1996].

However, some abnormalities in vessel formation are observed during the later stages of development.

Lindahl and colleagues investigated the effects of PDGF-B deficiency on pericyte formation [Lindahl et al., 1997]. The authors crossed heterozygous mice with mice lacking the Lac Z promoter gene, and found that in the wild types and heterozygotes the capillaries were straight and of a uniform diameter, but those of the homozygotes were tortuous, variable in diameter and had numerous microaneurysms. Their main finding was that the brains of E16.5 mice homozygous for the mutation lacked microvascular pericytes, which suggests that PDGF-B produced by the capillary endothelial cells signalled neighbouring vascular smooth muscle cell and pericyte progenitors (carrying the PDGF receptor-β) to promote their co-migration along the vessels. The researchers then investigated PDGF-B expression in the normal developing embryo [Hellström et al., 1999]. In the brain, PDGF-B was detected in the endothelial cells of the capillaries and the arterioles, but not in the endothelial cells of the venules. The developing pericytes and arterial smooth muscle cells were positive for both PDGF receptor-β and BrdU labelling. In comparison, PDGF-B and PDGF receptor-β knockout mice showed reduced BrdU labelling (indicative of reduced proliferation). Thus, the lack of pericyte coverage in both transgenic mice was a combined effect of reduced proliferation [Hellström et al., 1999] and migration of pericyte progenitor cells [Lindahl et al., 1997].

Further evidence for a role of PDGF in pericyte recruitment came from quantitative analysis of brains from PDGF-B and PDGF receptor-β knockout mice. When the number of endothelial cell nuclei were counted in wild type and transgenic brain sections, it was found that in both transgenics there was a marked increase in endothelial cell number (around 60%). This endothelial hyperplasia was most likely a secondary effect of reduced pericyte coverage along the vessels [Hellström et al., 2001]. This study is consistent with previous published studies which suggest that

one function of pericytes is to inhibit endothelial cell proliferation [Orlidge and D'Amore, 1987; Sato and Rifkin, 1988].

Regarding recent *in vitro* studies Hirschi and co-workers assessed the effects of PDGF on the migration of 10T1/2 cells (a multipotent cell line used as presumptive mural cell precursors) [Hirschi, Rohovsky and D'Amore, 1998]. When plated in the presence of PDGF, the 10T1/2 cells exhibited a random movement in response to all three dimers; PDGF-BB produced the greatest chemotactic affect, followed by PDGF-AB and then PDGF-AA. The authors also investigated the effects of 10T1/2 cell migration in the presence of endothelial cells. In these co-cultures, the 10T1/2 cells migrated towards the endothelial cells in a directional manner, suggesting that the endothelial cells secreted some kind of chemoattractant. When a neutralising antibody against PDGF-B was added to the culture, the endothelial cell-induced migration was completely inhibited. In contrast, cell migration was unaffected in the presence of a neutralising antibody to PDGF-A.

In summary, the above mentioned studies all demonstrate that PDGF-B has an important role in vessel formation; that of recruiting smooth muscle cells and pericytes to the vasculature.

Wound healing

It is suggested that PDGF-B released at the site of injury is involved in the process of wound healing. Firstly, PDGF-B causes the proliferation of fibroblasts and smooth muscle cells to proliferate adjacent to the wound site [Kaplan et al., 1979]. Secondly, fibroblast and smooth muscle cell expression of the β-receptor, which is normally low in resting tissue, is up-regulated in the skin from chronic wounds and lesions [Krane et al., 1991] and during inflammation [Terracio et al., 1988]. Thirdly, PDGF has been shown to stimulate neutrophil and macrophage migration [Shure et al., 1992], and the production of extracellular matrix proteins [Blatti et al., 1988; Canalis et al., 1993], all of which are involved in the process of wound repair.

Cancer

A large number of tumour cell types have been studied with regards to their expression of PDGF isoforms and receptors, and although both the A and the B chains are commonly expressed in such cell lines [Langerak et al., 1996a, 1996b], PDGF-AA is usually predominantly secreted [Hammacher et al., 1988b]. PDGF receptor-α positive cells are found in all grades of human gliomas, but the highest density of α-receptor is seen in the high grade tumours [Hermanson et al., 1988]. Expression of the A chain is also dramatically increased from undetectable levels in low grade to high levels in high grade tumours suggesting that the A chain is involved in tumour growth progression.

3.2 AIMS AND HYPOTHESIS

The aims of the work detailed in this chapter were:

- to establish the pattern of PDGF-B protein expression during normal development
- to determine the expression of PDGF-B protein in relation to the endothelial cells and mural cells by staining retinal flatmounts
- to investigate if the expression levels of PDGF-B were altered in the Edinburgh model of retinopathy of prematurity (ROP).

During normal retinal development, it is postulated that the protein expression levels of PDGF-B would increase during early retinal development, but decrease once the vasculature has established a complete mural cell coverage. Because PDGF-B is known to induce mural cell proliferation and migration, it is expected that PDGF-B expression would occur near the advancing peripheral edge of the vasculature where mural cell coverage is underway.

It is suggested that retinal vessels of infants with ROP lack coverage by pericytes [Patz, 1982], or at least have reduced pericytes coverage [Hirschi and D'Amore, 1997], thus it is hypothesised that the expression of PDGF-B would be reduced in the Edinburgh model of ROP.

3.3 METHODS

3.3.1 Experiments

The experiments were conducted as described in Chapter Two. Briefly, litters of 12 or more pups were exposed from birth to postnatal day 2 (P2), P7 and P14 to the 10kPa variable oxygen profile of the Edinburgh ROP model. The pups were killed immediately upon removal from the oxygen chamber. Some litters were raised in room air and sacrificed on P2, P7, P14 and P21. Both eyes from the pups were enucleated; the right eye was used for the immunohistochemical staining of pericytes and smooth muscle cells (Chapter Two) and the left was used for Western blot analysis. In addition, four control retinas at P7 and P14 were stained with PGDF-B antibody.

3.3.2 Western Blot Analysis

Protein extraction and assays

Retinas from each control and experimental litter were dissected fresh in 1M PBS (phosphate buffered saline), pooled and stored at -70°C. At a later stage, the retinal proteins were extracted by homogenising the retinas in extraction buffer containing a proteinase inhibitor (Sigma). The samples were then centrifuged at 14,000g for 10mins after which the supernatant was removed and spun for a further 30mins. The resulting supernatant was then transferred into eppendorf tubes and stored at -70°C.

The protein content of the samples was measured using the BCA protein assay method according to the manufacturer's instructions (Perbio). Briefly, 5µl of each sample was added to the extraction buffer, followed by 95µl of BCA protein assay reagent. All samples were incubated at 37°C for 30mins after which the OD_{562} of each sample was measured. Bovine serum albumin was used as standard.

Protein separation and transfer

A biotinylated molecular weight marker (Bio-Rad Laboratories) and 75μg of total retinal protein for each control and experimental timepoint were loaded onto a 12% acrylamide gel. 75μg of each sample was used since it allowed the greatest quantity of protein to be loaded without exceeding the recommended volume. The proteins were separated by SDS-PAGE electrophoresis for around 2 hours and then transferred onto PVDF membranes (Bio-Rad Laboratories) using a semi-dry transfer cell (Bio-Rad Laboratories).

Blotting

The membranes were washed twice (1M PBS/0.1% Tween) for 5mins with gentle shaking and blocked overnight at 4°C in 5% non-fat dry milk prepared in the wash solution. The next morning, the membranes were washed twice with gentle shaking for 5mins each, and incubated in PDGF-B primary antibody (Santa Cruz), diluted to 1:200 using the blocking solution, for 1 hour at room temperature with gentle shaking. The membranes were then washed three times for 5mins followed by two 15mins washes, and incubated in horseradish peroxidase conjugated anti-goat secondary antibody (1:5000, Dako) prepared in the blocking solution containing additional streptavidin horseradish peroxidase (Amersham Bioscience, 1:2000) for detection of the molecular weight marker. The membranes were then washed again and incubated in ECL-Plus Western blotting developer (Amersham Bioscience) for 5mins. Finally, the membranes were exposed to X-ray film for around 2mins.

To ensure that any difference in expression between control and experimental retinas was genuine and not due to loading variable quantities onto the gel, the membranes were stripped for 15mins at 37°C using Restore Western Blot Stripping Buffer (Pierce), and then reprobed for actin. Briefly, the membranes were blocked overnight in non-fat dry milk and then incubated in actin primary antibody (1:1000, Santa Cruz). The membranes were incubated in anti-goat secondary antibody

(1:5000, Dako). After the washing stage, developer solution was applied to the membranes which were then exposed to X-ray film.

Analysis

An image of the X-ray film was captured using the computer software, 'Quantity-One' (Bio-Rad Laboratories). The bands that had developed on the X-ray film were manually selected and the software calculated the amount of PDGF-B protein expressed by taking the area and the intensity of each band into consideration.

3.3.3 Immunofluorescent Labelling

PDGF-B single-staining

P7 and P14 retinas were dissected as described in Chapter Two and then stained for PDGF-B antibody as follows. The flattened retinas were first permeabilised in 1M PBS/1% Triton X-100 (wash solution) for 30mins and blocked using 5% goat serum for 20mins. The retinas were then incubated in PDGF-B antibody prepared in 5% serum (1:100, Santa Cruz) overnight at 4°C. The following morning, the retinas were first washed three times for 10mins each, and then incubated in biotinylated goat anti-rabbit secondary antibody (1:200, Dako) for 2 hours at room temperature, with gentle shaking. The retinas were washed again and Alexa Fluor 647 (1:200, Molecular Probes) was applied for 2 hours with gentle shaking at room temperature. The retinas were washed for the final time, mounted in PBS:glycerol (1:1) and the coverslip sealed with nail varnish.

PDGF-B, desmin/α-SMA and lectin triple-staining

The retinal flatmounts were first stained for PDGF-B labelling as described above. After the incubation in Alexa Fluor 647, the flatmounts were washed in 1M PBS/1% Triton X-100. The tissues were then blocked using avidin and biotin (Vector Laboratories) and then incubated in 5% rabbit serum (Diagnostic Scotland) diluted in 1M PBS/1% Triton X-100 for 20mins each. The retinas were incubated in either desmin (1:50, Dako) or α-SMA (1:400, Sigma) antibody overnight at 4°C to label the

pericytes or smooth muscle cells, respectively. The next day, the tissues were washed in 1M PBS/1% Triton X-100, and incubated in biotinylated rabbit anti-mouse secondary antibody (1:200, Dako) for 2 hours at room temperature (with gentle shaking). The retinas were washed and Texas red streptavidin (1:100, Vector Laboratories) applied for 2 hours at room temperature with gentle shaking. After washing, the flatmounts were blocked again using avidin and biotin for 20mins each before incubating with biotinylated *G. simplicifolia* (Bandeiraea) isolectin B4 (1:50, Vector Laboratories) overnight at 4°C to stain the endothelial cells. The following day the washes were repeated and the retinas incubated in fluorescein streptavidin (1:100, Vector Laboratories) for 2 hours with gentle shaking at room temperature. The wholemounts were washed one last time, mounted in PBS:glycerol (1:1) and sealed with nail varnish.

For the PDGF-B negative control, a retinal wholemount was incubated in 5% serum instead of the primary antibody solution. The above protocol was then continued; the secondary antibody was applied followed by Alexa Fluor 647.

Analysis

The retinal flatmounts were viewed using a Leica TCSNT confocal system with a mixed gas argon/krypton laser. Cells stained using fluorescein were labelled green and excited at 488nm (filter BP 525/50), cells stained with Texas red were labelled red and excited at 568nm (filter LP 590), and PDGD-B staining detected by Alexa Fluor 647 was labelled blue and excited at 647nm. Representative images were taken and digitally stored for later analysis.

3.4 RESULTS

3.4.1 Western Analysis

In the Western blot analysis, the polyclonal PDGF-B antibody recognised 4 peptides on all days examined (Figure 3.1). 5 (out of 9) molecular weight markers were identified; these were soya bean trypsin inhibitor at 21.5kDa, carbonic anhydrase at 31kDa, ovalbumin at 45kDa, bovine serum albumin at 66.2 kDa and phosphorylase 6 at 97.4kDa. The distance migrated by each marker was measured and a graph of molecular weight against distance migrated was plotted (Figure 3.2). The molecular weights of the bands detected by the PDGF-B antibody were then estimated: Band 1 at 52.5kDa; Band 2 at 46.0kDa; Band 3 at 30.5; and Band 4 at 27.5kDa.

The expression of the higher molecular weight proteins, Bands 1 and 2, followed a similar pattern of expression. During normal development, the expression levels of the proteins increased from P2 to P14, but there was no increase between P14 and P21. The expression of both peptides was reduced in the oxygen treated samples; although there was not much difference in expression on day 2, the reduction on days 7 and 14 was evident.

The expression of the lower molecular weight peptides (Bands 3 and 4) also increased progressively from P2 to P14, however, the effects of oxygen exposure on these peptides differed from Bands 1 and 2. The expression on P2 and P7 was around the same for both the control and oxygen treated groups; but on P14, the expression in the oxygen treated retinas was reduced in comparison to the P14 controls.

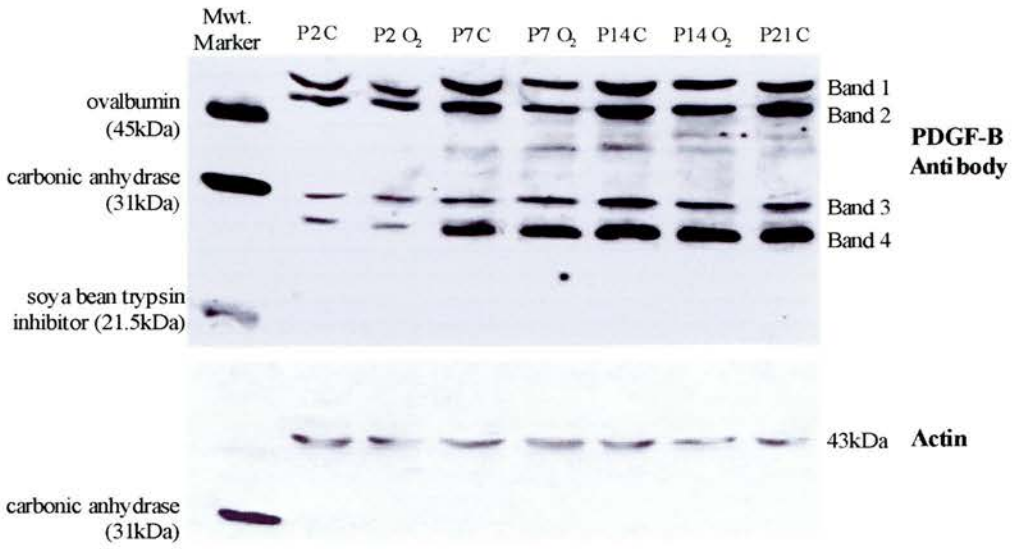

Figure 3.1: Western blot of retinal PDGF-B expression in control and oxygen treated rat pups.
The blot compares control litters to oxygen treated litters at P2, P7 and P14. The lower blot of actin shows that the same quantity of protein was loaded for all samples.
C - control litter; O_2 - litter exposed to the Edinburgh model; P - postnatal day.

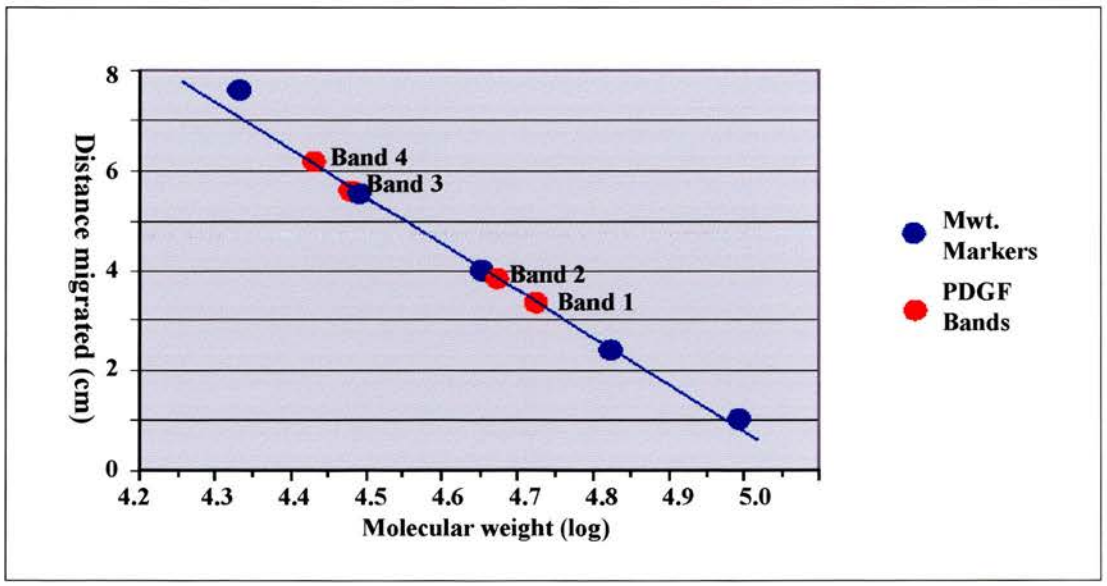

Figure 3.2: Graph of distance migrated by bands against molecular weight.
The molecular weight markers were plotted and the molecular weights of the bands detected by the PDGF antibody were estimated.

These results were confirmed by quantitative analysis using the computer software called 'Quantity-One':

	P2 C	P2 O_2	P7 C	P7 O_2	P14 C	P14 O_2	P21 C
Band 1	3621.88	3198.27	4462.47	3448.49	4625.64	3644.06	4632.44
Band 2	3703.06	3312.38	4308.46	3534.78	4561.14	3601.89	4234.14
Band 3	2880.67	2792.48	3464.18	3487.19	4230.89	3214.85	3835.87
Band 4	2651.97	2582.21	4261.42	4132.37	5084.29	4268.33	4992.95

Table 3.1: Retinal PDGF-B expression of control and oxygen treated rat pups.
Using the 'Quantity One' software the bands from the Western blot were highlighted and the total volume of each band was calculated by multiplying the area of the band by its intensity to give the densitometric values.
O_2 - oxygen treated litter; P - postnatal day.

3.4.2 Immunofluorescent Labelling

Retinal flatmounts were labelled with PDGF-B to determine if its expression was associated with the vasculature. Figure 3.3 shows the expression of the growth factor in relation to lectin (endothelial cells) and α-SMA (smooth muscle cells); the pattern of PDGF-B staining was almost identical to that for lectin.

Likewise, in Figure 3.4, in which the flatmounts were stained with desmin instead of α-SMA, the PDGF-B labelling was identical to lectin staining. This pattern of labelling was seen across the entire vasculature; from the arteriole to the venule and from the centre to the periphery. However, when the laser signal for lectin (488nm) and desmin (568nm) were set to 0, and the signal for PDGF-B (647nm) was increased to its maximum level, no staining was observed (Figure 3.4 C). Thus, the staining detected in the triple-labelled flatmounts was entirely a result of cross-talk.

The lack of PDGF-B labelling was confirmed by staining flatmounts with PDGF-B antibody alone (Figure 3.5, page 111). Thus, the PDGF-B antibody, although produced results in Western blotting, failed to produce any staining of the retinal flatmounts.

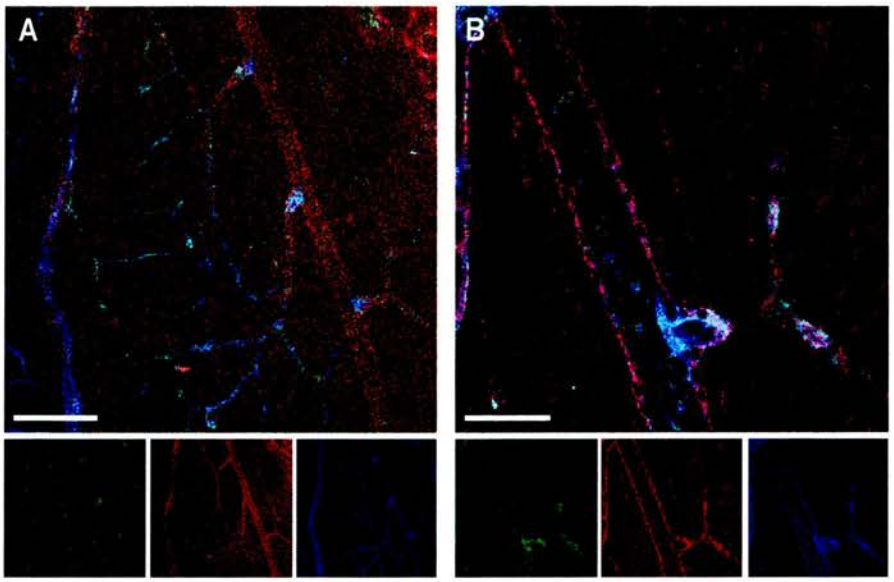

Figure 3.3: Triple-labelled retinal flatmount of a P14 room-air raised pup.
The flatmount was stained using lectin/endothelial cells (green) α-SMA/smooth muscle cells (red) and PDGF-B (blue). (A) Image of central retina. (B) Image of arteriole cross section.
Scale bar: (A) 100μm; (B) 32μm.

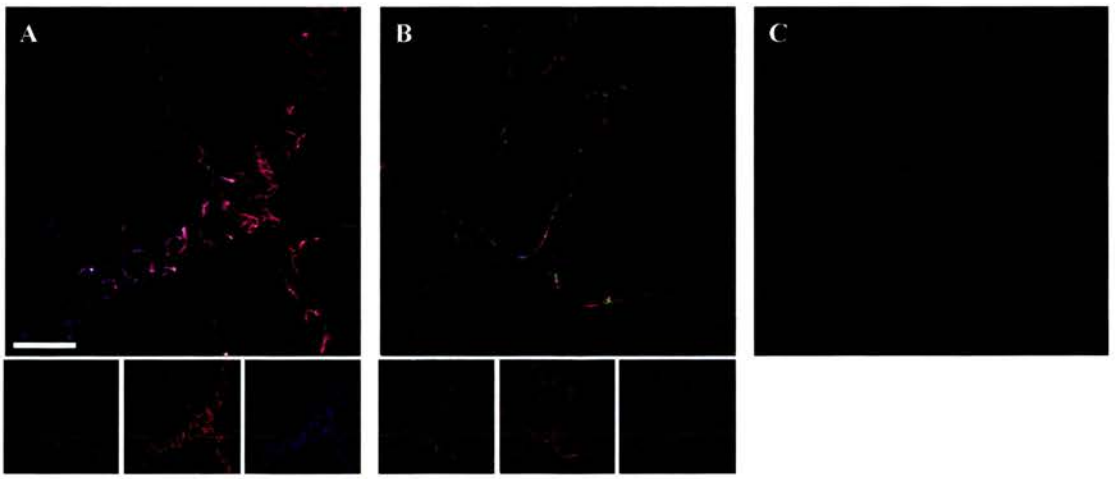

Figure 3.4: Triple-labelled retinal arteriole of P7 pup.
The flatmount was stained using lectin/endothelial cells (green), desmin/pericytes (red) and PDGF-B (blue). (A) Image of arteriole. (B) Image of advancing peripheral edge. (C) Image B with green (488nm) and red (568nm) lasers eliminated. This image shows that the PDGF-B staining observed in image B was due to crosstalk.
Scale bar: 32μm.

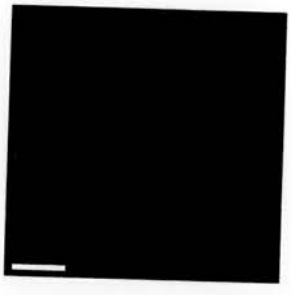

Figure 3.5: P7 retinal flatmount stained for PDGF-B only.
Scale bar: 100µm.

3.5 DISCUSSION

3.5.1 PDGF-B in the Vasculature

PDGF is a glycoprotein produced by platelets [Heldin, Westermark and Wasteson, 1979; Antoniades, 1981; Deuel et al., 1981], although cells such as endothelial cells have also been reported to express the protein [Barette et al., 1984; Collins et al., 1985]. The spatial and temporal expression patterns of PDGF-B and its receptor, PDGF-β, suggest that PDGF-B released from endothelial cells promotes the proliferation of adjacent pericyte or smooth muscle cell precursors [Levéen et al., 1994; Soriano, 1994, 1996; Beström et al., 1996]. This has been confirmed by analysis of mice lacking either the PDGF-B or PDGF-β gene where both transgenics showed a reduction in the proliferation and thus a reduction in the number of mural cells [Levéen et al., 1994; Soriano, 1994]. Therefore, the PDGF-B binding to its receptor signals the recruitment of pericytes to the endothelial tubules. Taking these studies into consideration the PDGF-B protein expression in the retina of rat pups was measured and compared to the expression in the retinas of pups raised in the fluctuating oxygen regime of the Edinburgh ROP model.

3.5.2 PDGF-B Protein Expression in the Retina

A polyclonal antibody raised against a recombinant protein corresponding to amino acids 136 to 190 at the carboxyl terminal of mature human PDGF-B was used for the Western analysis. This antibody recognised four proteins expressed in the rat retina. The molecular weights of these proteins were estimated at 52.5, 46.0, 30.5 and 27.5kDa. The expression of all four peptides increased from P2 to P14, when the vasculature was forming and remained elevated even once the vasculature was fully matured at P21. In response to the variable oxygen regime, the expression of Bands 1 and 2 (52.5 and 46.0kDa) decreased on all days examined, but the levels of Bands 3 and 4 (30.5 and 27.5kDa) were reduced only on P14.

The mature B chain of PDGF has a molecular weight of between 15 and 16kDa, making the homodimer around 30-32kDa [Johnsson et al., 1982; Waterfield, 1983; Hammacher et al., 1988a]. In the Western blots, Band 3 was calculated at approximately 30.5kDa, which suggests that this Band may correspond to the PDGF-BB isoform. The PDGF-B precursor expressed by endothelial cells has been reported to be 241 amino acids long and has a molecular weight of 27,281kDa [Collins et al., 1985]. Thus, the band detected at 27.5kDa (Band 4) may be the PDGF-B precursor peptide. The other possibility is that Band 4 was the AB heterodimer; however this is unlikely since it is unknown whether endothelial cell derived PDGF is a heterodimer or if endothelial cells even synthesize the A chain [Collins et al., 1985]. The other source of PDGF-AB would be the platelets [Hammacher et al., 1988a], but all control and experimental animals were perfused before killing.

Although there was no difference in expression of the presumed precursor and mature PDGF-B proteins between control and oxygen exposed retinas at P2 and P7, on P14 the levels of PDGF-B expression were reduced in the oxygen treated retinas compared to the controls. This would suggest that PDGF-B expression was altered only with a prolonged exposure to the variable oxygen regime, or that the greater variability in oxygen levels during the second week of the profile produced the decrease in PDGF-B expression (see Figure 1.2, page 25).

What caused the down-regulation of the presumed PDGF-B precursor and the mature B chain in the Edinburgh model? Currently there is limited literature available on the direct influence of oxygen concentration on the expression of PDGF, but the few studies that have been conducted have shown that *in vitro* PDGF-B levels rise in response to hypoxia. In one such study, human umbilical vein endothelial cells were exposed to hypoxic conditions and the transcription rate of the PDGF-B gene increased significantly [Kourembanas, Hannan and Faller, 1990]. This increase was inversely proportional to oxygen tension and was reversed upon reoxygenation at

room air. Consistent with this report, the pups exposed to the oxygen regime of the Edinburgh model used here spent very little time (8%) in hypoxic conditions (below 21% O_2) [McColm et al., 2004]. Thus, it is possible that the protein expression of both PDGF-BB and its precursor decreased as a result of the hyperoxic environment (above 21% O_2) experienced by the pups.

At first I thought that the higher molecular weight bands were the result of sample contamination. However, this explanation was rejected for several reasons. Firstly, the samples were obtained and processed at difference times, therefore it is unlikely that contamination of all samples would have occurred. Secondly, contaminants would have produced diffuse bands, not distinct bands as observed here. Thirdly, the expression pattern of both bands was rather specific, if the samples contained contaminants a greater variation in the levels of expression would have resulted. These bands were also not the result of non-specific binding because the membranes were blocked overnight and all antibodies were prepared in the blocker solution, neither was it due to non-specific binding of the secondary antibody because the same secondary antibody was used for transforming growth factor-β_1 protein detection (Chapter Four) and only one band was detected in the blots.

Because the two bands followed a very similar pattern of expression, it is likely that these two proteins are closely related. It is plausible that the antibody recognised another protein, where one band was the precursor molecule and the other the mature, secreted molecule. On-the-other-hand, the antibody may have recognised two different isoforms of the same protein. What can be said regarding these higher molecular weight proteins is that their expression increased as the retinal vasculature was developing and remained high once the vasculature had fully formed. In addition, the expression of the peptides was reduced in fluctuating oxygen conditions. It could simply be that a poor antibody was used; the polyclonal antibody was raised against a recombinant protein and it is possible that other proteins were indeed being detected. Perhaps using a different (monoclonal) PDGF-

B antibody would produce more acceptable results. I have been in touch with the suppliers of the antibody, Santa Cruz, regarding this problem, but as yet have not received a reply.

3.5.3 Immunofluorescent Labelling by PDGF-B

Unfortunately our immunohistochemical staining for the detection of PDGF-B in the retinal flatmounts was unsuccessful despite attempts at changing the fixative used (from paraformaldehyde to acetone) and increasing the concentrations of the antibody (from 1:200 to 1:50). It is possible that the expression of PDGF-B was too low for detection by this method, but if that was the case then only faint bands would have been detected in the Western blots.

Previously researchers who investigated the expression of PDGF-B and PDGF receptor-β found both to be associated with retinal blood vessels. One study looked at frozen sections of the rat retina and detected mRNA expression using *in situ* hybridisation techniques [Mudhar et al., 1993]. The other study preformed immunohistochemical staining on frozen and wax sections of the human retina using both polyclonal and monoclonal antibodies [Robbins et al., 1994]. In the wax sections, high non-specific binding was observed when using the monoclonal antibody whereas on frozen sections, PDGF-B staining was seen in the neural retina and the choroidal vessels. In comparison, the polyclonal antibody did not stain the wax or the frozen sections. A polyclonal antibody was used in my study, thus it is possible that the lack of staining here was due to a poor quality antibody. This could be simply determined by using a monoclonal antibody on frozen retinal flatmounts.

In summary, the PDGF-B antibody recognised four proteins expressed in the rat retina, two of which were identified as the PDGF-B chain precursor (27.5kDa) and the PDGF-B homodimer (30.5kDa). The retinal expression levels of these two proteins were reduced with 14 days of exposure to the variable oxygen regime of the Edinburgh ROP model.

CHAPTER FOUR

THE EFFECTS OF OXYGEN ON TRANSFORMING GROWTH FACTOR-β PROTEIN EXPRESSION

4.1 INTRODUCTION

Transforming growth factor-β (TGF-β) is a growth factor which is capable of playing different and often opposite roles on a number of cell types. Besides being multifunctional, TGF-β is part of a large superfamily of growth factors that includes the inhibins, activins and Mullerian inhibiting substance [reviewed in Massaguè, 1990].

TGF-β is synthesised as a large precursor protein of about 390 amino acids in size [Derynck et al., 1985], but undergoes intracellular modification where proteolytic digestion cleaves the precursor between amino acids 278 and 279 [Dubois et al., 1995; Blanchette et al., 1997] to yield two separate products prior to secretion. The peptide from the N-terminal region is called latency-associated peptide (LAP), whereas that from the C-terminal is called mature TGF-β [Brown et al., 1990; Gentry

and Nash, 1990; Blanchette et al., 1997]. The mature form of the protein has a molecular weight of 25kDa and is composed of two identical 12kDa chains held together by disulfide bonds [Assoian et al., 1983].

4.1.1 Ligands

Of the five TGF-β isoforms identified so far, three are mammalian and designated TGF-β_1, TGF-β_2 and TGF-β_3. TGF-β_1 was first isolated from human and porcine blood platelets, the richest source of TGF-β_1 [Assoian et al., 1983]. TGF-β_2 was identified as one of two naturally occurring peptides in bone tissue and was named CIF-B (cartilage-inducing factor-B) based on its cartilage-inducing activity [Seyedin et al., 1985]. CIF-A (the other peptide in bone tissue) was then realised to be identical to TGF-β_1, consequently CIF-B was renamed TGF-β_2 [Seyedin et al., 1987]. Later TGF-β_2 was also isolated from procine blood platelets [Cheifetz et al., 1987]. Human TGF-β_3 was identified at the cDNA level [ten Dijke et al., 1988], and expressed in the recombinant form [ten Dijke et al., 1990]. All three isoforms often display similar activities and share considerable sequence homology; around 70% of the amino acids of TGF-β_1 are identical to those of TGF-β_2 [Cheifetz et al., 1987; Seyedin et al., 1987], and both isoforms share around 80% homology with TGF-β_3 [ten Dijke et al., 1988].

4.1.2 Receptors

Three cell surface receptors for TGF-β have been identified using receptor affinity-labelling methods [Massagué, 1985]. Transforming growth factor-β receptor I is a glycoprotein with a molecular weight of 65kDa [Massagué, 1985], whereas transforming growth factor-β receptor II, also a glycoprotein, varies greatly in size from 70-85kDa in most mammalian cells to around 100kDa in the chick embryo [Massagué, 1985; Cheifetz, Like and Massagué, 1986]. Both receptor types are transmembrane serine-threonine kinases [Lin et al., 1992; Franzen et al., 1993] and display a higher affinity for TGF-β_1 than TGF-β_2 [Cheifetz et al., 1987]. The third,

and most widely expressed, TGF-β receptor type is betaglycan. Depending on the species, this receptor has a molecular weight of between 280 and 330kDa [Massagué, 1985]. Betaglycan differs from receptors I and II in that it is a membrane anchored proteoglycan with a large extracellular domain [López-Casillas et al., 1991] and is capable of binding all three TGF-β ligands with high affinity [Cheifetz et al., 1987]. It is suggested that rather than being directly involved in signal transduction, betaglycan might act to control the access of the ligand to the signalling receptor, TGF-β receptor I [López-Casillas et al., 1991].

4.1.3 Signalling

The most important regulation of TGF-β signalling is based on whether or not the ligand is biologically active or latent. As mentioned above, prior to its secretion from the cell, TGF-β is cleaved to produce mature TGF-β from the N-terminal region [Dubois et al., 1995; Blanchette et al., 1997]. Despite cleavage of the precursor, however, LAP often remains non-covalently associated with the mature ligand [Brown et al., 1990; Gentry and Nash, 1990; ten Dijke et al., 1990]. The presence of LAP facilitates the transit of the ligand from the cell, but makes it biologically inactive (called latent TGF-β), hence the ligand is unable to interact with its receptor and evoke a biological effect [Brown et al., 1990; Gentry and Nash, 1990]. For latent TGF-β to become biologically active and bind to the receptor it must be released from its association with LAP. The conversion of latent to active ligand can be accomplished by changes in the extracellular environment, by exposure to extreme pH levels, or by exposure to high temperatures [Brown et al., 1990; Gentry and Nash, 1990].

Although TGF-β receptors I and II bind TGF-β [Cheifetz et al., 1987], the ligand is not recognised by receptor I, it instead binds to receptor II which is highly phosphorylated by cellular kinases in the absence of TGF-β, and therefore readily binds free ligand [Wrana et al., 1994]. However, receptor II fails to elicit a response;

it is suggested that receptor I recognises the ligand bound to receptor II to form a very stable ternary complex, called the signal receptor complex, at which point receptor I is phosphorylated and propagates the signal to substrates within the cell [Wrana et al., 1994]. Only a small number of the TGF-β receptor II population binds the ligand with high affinity. This limitation is overcome by the action of betaglycan, since receptor II binds TGF-β tethered to betaglycan better then it binds free TGF-β [López-Casillas et al., 1991; López-Casillas, Wrana and Massagué, 1993]. Thus, it is proposed that all three receptor types are involved in efficient TGF-β signalling: first, betglycan binds and presents the ligand to receptor II, forming a high affinity stable ternary complex; second, receptor I recognises the ligand bound to receptor II, displaces betaglycan, and binds the ligand to form the signal receptor complex [López-Casillas, Wrana and Massagué, 1993]. Therefore, betaglycan increases binding of the ligand to the signalling receptor, an effect that is particularly evident with TGF-β_2, which has low affinity for both receptor types I and II.

4.1.4 TGF-β in the Developing Embryo

The first study on the functions of TGF-β in the embryo was conducted by Heine et al. They reported that in the embryonic day 11 (E11) mouse, blood cells of the liver were positive for TGF-β_1 protein, implicating this growth factor in the control of haematopoiesis [Heine et al., 1987]. Akhurst et al. detected TGF-β_1 mRNA in the extraembryonic blood islands of the yolk sac and in cardiac mesoderm cells [Akhurst et al., 1990]. Within the embryo proper, TGF-β_1 transcripts were observed in the endothelial cells of major blood vessels, suggesting that this growth factor is also involved in vasculogenesis.

To further elucidate the functions of TGF-β_1 in embryonic development, mice lacking the TGF-β_1 gene were generated by cross breeding mice heterozygous for the TGF-β_1 gene [Shull et al., 1992; Kulkarni et al., 1993; Dickson et al., 1995]. All mice generated from the mating appeared normal at birth. However, statistical

analysis of the genotype of the mice showed a wild type:heterozygous:homozygous ratio of 1:1.5:0.5 [Kulkarni et al., 1993; Dickson et al., 1995], deviating significantly from the expected Mendelian ratio of 1:2:1. This indicated that approximately 25% of the heterozygous and 50% of the homozygous null mice died *in utero* [Dickson et al., 1995]. Examination of the litters showed that between E9.5 and E10.5, the embryos suffered abnormalities in yolk sac development that ranged from a simple delay in vasculogenesis and the development of disorganised and delicate vessels to more severe abnormalities where regions of the yolk sac were completely devoid of vessels. In control pups the layers of the yolk sac were closely apposed, with blood cells within the endothelial tubes; however in the TGF-β_1 null mice the cellular adhesion between the two endothelial layers of the yolk sac was disrupted and in some cases, blood cells appeared to have leaked into the yolk sac cavity, indicating instability of the endothelial tubes, and inadequate endothelial cell differentiation [Dickson et al., 1995].

In support of these roles of TGFβ_1, Oshima and colleagues demonstrated that when mice heterozygous for the TGF-β receptor II gene were intercrossed, only wild type or heretozygous mice survived to birth [Oshima, Oshima and Taketo, 1996]. The TGF-β receptor II null mice displayed defects almost identical to mice lacking the gene for TGF-β_1. Their yolk sac at E9.0 showed severe anaemia and slight embryonic growth retardation that worsened by E10.5-E11.5. Defects in haematopoiesis and vascular development were also observed and the endothelial cells never formed capillary-like tubes, with tight junctions. It is most likely that these defects in the TGF-β receptor II null mice were due to defective TGF-β_1 signaling.

4.1.5 Cellular Responses to TGF-β

TGF-β affects many cellular processes, which are highly dependent on cell type, culture conditions, state of cell differentiation, extracellular matrix conditions and dosage of TGF-β. Thus, TGF-β can have either a stimulatory or inhibitory effect on

the same cell depending on the cellular environment. Most studies that have investigated the role of TGF-β have used the β_1 isoform probably because it was the first of the family to be discovered.

The concept that TGF-β is a dual factor emanated first from studies on cell proliferation. Under certain conditions the growth of mesenchymal cells, such as fibroblasts [Moses et al., 1981; Roberts et al., 1981; Tucker et al., 1984] and osteoblasts [Moses et al., 1985] is stimulated by TGF-β. However, in most cells TGF-β acts as a potent growth inhibitor. These cell types include normal as well as transformed epithelial cells [Tucker et al., 1984], endothelial cells [Fràter-Schröder et al., 1986; Heimark, Twardzik and Schwartz, 1986], haematopoietic cells [Ohta et al., 1987], preadipocytes [Ignotz and Massagué, 1986] and smooth muscle cells [Owens et al., 1989]. It is suggested that this anti-proliferative effect of TGF-β is the result of arrested progression of the cell cycle in the G_1 phase [Heimark, Twardzik and Schwartz, 1986]. The response of a cell to TGF-β is also affected by cell attachment (or lack thereof) to a solid substrate. For example, TGF-β inhibits anchorage-dependent growth of fibroblasts and tumour cell lines and anchorage-independent growth of many human tumour cells, however, it promotes anchorage-independent growth of transformed rat kidney fibroblasts [Roberts et al., 1985]. Once the ligand is removed from the culture medium, the cells continue to proliferate as normal [Tucker et al., 1984; Massagué et al., 1986]. Thus, the growth inhibitory effect of TGF-β is usually reversible and non-toxic to cells [Fràter-Schröder et al., 1986].

The effects of TGF-β on cell differentiation are also cell type dependant. Although, the growth factor favours chrondogenesis and osteogenesis [Seyedin et al., 1985] and promotes the differentiation of epithelial cells [Mausi et al., 1986] and smooth muscle cells [Shah, Groves and Anderson, 1996], it fails to elicit the differentiation of embryonic myoblasts (skeletal muscle) [Massagué et al., 1986].

TGF-β is also involved in extracellular matrix production; it stimulates the syntheisis of many extracellular matrix components including collagens and fibronectin [Seyedin et al., 1985; Massagué et al., 1986; Centralla, McCarthy and Canalis, 1987], and suppresses matrix degradation by down-regulating the expression of proteinase but inducing that of proteinase inhibitors [Edwards et al., 1987; Laiho, Saksels and Keski-Oja, 1987].

4.1.6 TGF-β as an Immunosuppressor

TGF-β_1 null mice that survive to birth appear normal and continue to gain weight as normal pups [Shull et al., 1992; Kulkarni et al., 1993]. About 3 weeks after birth, however, the animals begin to exhibit an acute wasting syndrome, resulting in death. The mice display a variable degree of mixed inflammatory cell infiltration and tissue necrosis in several organs, mainly the heart, stomach, liver and lungs [Shull et al., 1992; Kulkarni et al., 1993]. The infiltration contains lymphocytes and neutrophils, and cytokine mediators of inflammation, such as interferon-γ, tumour necrosis factor-α and macrophage inflammatory protein-1α, are increased in the liver and lungs of the mutants [Shull et al., 1992]. Thus, TGF-β_1 deficiency results in death associated with dysfunction of the immune and inflammatory systems. It is suggested that TGF-β_1 deficient animals that survive to birth are in fact rescued by their mother; *in utero* by placental transfer of the growth factor and postnatally by transmission in milk [Shull et al., 1992].

In vitro studies are consistent with an immunosuppressant action of TGF-β. First, B-lymphocytes and T-cells synthesise and secrete TGF-β, and express the three receptor types [Kehrl et al., 1986a, 1986b]. Second, the ligand inhibits the proliferation of B-lymphocytes [Kehrl et al., 1986a], and T-lymphocytes [Kehrl et al., 1986b]. Third, in cultures of resting monocytes, TGF-β activates inflammatory cytokine production such as interleukin-1, tumour necrosis factor-α, basic fibroblast growth factor and macrophage inflammatory protein-1α [Wahl et al., 1987]. Lastly, it is reported to act as a chemattractant for monocytes, T-lymphocytes and fibroblasts

to the site of tissue injury [Wahl et al., 1987]. Hence, TGF-β functions as a potent regulator of the immune and inflammatory system.

4.1.7 TGF-β in Cancer

Transgenic studies have provided evidence that one of the physiological roles of TGF-β signalling is to provide protection against malignant transformation. For example, transgenic mice that produce a constitutively active form of TGF-β_1 are resistant to mammary tumour formation [Pierce et al., 1995b]. Conversely, the absence of TGF-β_1 appears to promote tumour formation in skin keratinocytes isolated from TGF-β_1-/- embryos [Glick et al., 1994]. In some cases, loss of TGF-β expression may represent an early step in tumour progression [Wu et al., 1992]. However, many human carcinoma cell lines *in vitro* [Roberts et al., 1983] and human tumours *in vivo* [Kong et al., 1995; Tsushima et al., 1996; Perry, Anthony and Steiner, 1997] appear to express high levels of TGF-β than corresponding normal tissue. For example, TGF-β_1 and TGF-β_2 are both detected in a majority of primary breast cancers [MacCallum et al., 1994].

It is proposed then, that TGF-β acts predominantly as a potent tumour suppressor during the early stages of cancer. However, at some point during development and progression of malignant neoplasia, the cells escape from the growth arrest induced by TGF-β. Although the molecular mechanisms remain to be elucidated, tumour cells somehow switch from a TGF-β sensitive to TGF-β resistant state.

4.1.8 TGF-β in Vascular Development

Thus far, several roles of TGF-β have been discussed and much of the experimental work mentioned above is also supportive of a role for TGF-β in the development of the vasculature:

- the mesenchyme of the mouse embryo is strongly positive for TGF-β_1 when it interacts with the adjacent epithelium during remodelling [Heine et al., 1987]
- the yolk sac of TGF-β_1 and TGF-β receptor II knockout mice develop disorganised and delicate vessels; some areas are devoid of vessels [Shull et al., 1992; Kulkarni et al., 1993; Oshima, Oshima and Taketo, 1996]
- TGF-β inhibits the proliferation of smooth muscle cells [Owens et al., 1989], but induces their differentiation [Shah, Groves and Anderson, 1996]
- TGF-β up-regulates the expression of fibronectin and collagen to increase extracellular production and enhance both cell-matrix and cell-cell adhesion [Seyedin et al., 1985; Massagué et al., 1986; Centralla, McCarthy and Canalis, 1987].

In addition to the above studies, two research groups have investigated the role of TGF-β_1 on single and co-cultures of endothelial cells, smooth muscle cells and pericytes.

Sato and colleagues demonstrated that when a confluent endothelial cell monolayer is wounded by a razor blade, the endothelial cells move rapidly into the denuded space to repair the damage [Sato and Rifkin, 1988]. This movement is inhibited by the addition of neutralising antibodies to TGF-β_1 [Sato and Rifkin, 1989] and by growing endothelial cells in the presence of pericytes or smooth muscle cells [Sato et al., 1990]. They also found that depending on the length of time the two cell types are together, 1-10% of the latent TGF-β_1 species is rapidly converted into the active form, reaching a maximum by about 12 hours [Sato et al., 1990]. After the initial 12 hours, the conversion of latent to active TGF-β_1 decreases due to the stimulation of plasminogen activator inhibitor, which is synthesised by the ligand. The plasminogen activator inhibitor in turn inhibits the generation of plasmin that

activates latent TGF-β. Therefore, TGF-β in vascular development may be self-regulated.

The second group, lead by D'Amore, began by investigating the effects of pericytes and smooth muscle cells on endothelial cells, and showed that when endothelial cells are cultured alone they tripled in number over a 14 day period. However, when the cells are co-cultured with pericytes or smooth muscle cells, their growth is completely inhibited [Orlidge and D'Amore, 1987]. This inhibition requires that either the two cell types make direct contact with each other or that the two cell types lie in close proximity. Like others researchers [Fràter-Schröder et al., 1986; Heimark, Twardzik and Schwartz, 1986; Sato and Rifkin, 1988] Antonelli-Orlidge et al. also found that endothelial cell growth is inhibited by the addition of TGF-β_1 to the culture medium, and reported that the latent TGF-β_1 secreted by endothelial cells and pericytes is activated only when both cells come into contact [Antonelli-Orlidge et al., 1989]. Next, they found that the endothelial cells in three-dimensional co-cultures become tightly associated in cord like structures that resemble the early stages of capillary formation *in vivo*, and that the 10T1/2 cells (presumptive mesenchymal cells) become elongated and either stretch along or wrap around the endothelial cells [Darland and D'Amore, 2001a]. However, when soluble TGF-β receptor or TGF-β antibody is added to the culture, the cells do not elongate nor form cords, but instead form large aggregates of rounded cells. In addition, a decrease in the expression levels of NG-2 and α-smooth muscle actin (presumed markers for pericytes and smooth muscle cells, respectively) in the co-culture is detected, suggesting that TGF-β is required for smooth muscle differentiation during capillary formation [Darland and D'Amore, 2001a].

TGF-β, therefore, appears to play a critical role in vascular development by mediating differentiation of mesenchymal cells towards smooth muscle cells and/or pericytes, and in maintaining vascular quiescent by acting as a direct inhibitor of endothelial cell proliferation.

4.2 AIMS AND HYPOTHESIS

The aims of the work described in this chapter were:

- to determine the expression pattern of TGF-β_1 protein during normal development of the rat retina
- to study the distribution of TGF-β_1 protein within the retina
- to investigate the expression of TGF-β_1 in relation to the retinal vasculature
- to determine if the expression of TGF-β_1 protein was affected by the oxygen regime of the Edinburgh model of retinopathy of prematurity (ROP).

It is hypothesised that during normal development the expression of TGF-β_1 protein would increase progressively from birth to postnatal day 21 (P21). The reason for this is that as the endothelial tubules spread across the two layers of the retina, the vessels become encapsulated by pericytes and smooth muscle cells, thus from P0 to P21 the number of cells on which TGF-β_1 would exert an effect will increase.

Based on current knowledge, it is expected that rats raised in the Edinburgh model of ROP would have a decreased expression of retinal TGF-β_1 protein when compared to rats raised in room air because pups raised in the oxygen regime have a reduced retinal vascular area [Cunningham et al., 2000] and a reduced coverage of pericytes and smooth muscle cells [Chapter Two].

4.3 METHODS

4.3.1 Experiments

The experiments were conducted as described in Chapter Two. Briefly, litters of 12 pups or more were exposed to the 10kPa minute-by-minute variable oxygen profile from birth to P2, P7 and P14, and killed immediately. Control litters, raised in room air, were sacrificed on P2, P7, P14 and P21. Both eyes from each pup were enucleated; the right eye was used for immunohistochemistry (Chapter Two) and the left was dissected fresh for Western blot analysis. A few additional eyes from day 14 control pups were obtained to examine the distribution of TGF-β_1 protein in the retina.

4.3.2 Western Blot Analysis

Protein extraction and assays

Retinas from each control and experimental litter were dissected fresh in 1M phosphate buffered saline (PBS), pooled and stored at -70˚C. At a later stage, the samples were homogenised in extraction buffer containing proteinase inhibitor (Sigma). The samples were then centrifuged at 14,000g for 10mins, after which the supernatant was transferred into a new tube. The samples were spun for a further 30mins and the resulting supernatant, which contained the total retinal protein, was transferred into clean tubes and stored at -70˚C.

To determine the protein content of the samples, 5µl of each sample was added to 95µl of extraction buffer, followed by 2mls of BCA protein assay reagent (Perbio). All samples were incubated at 37˚C for 30mins, and the OD_{562} of each sample was measured. Bovine serum albumin was used as standard.

Protein separation and transfer

75μg of total retinal protein for each control and experimental timepoint was loaded onto a 12% acrylamide gel. A biotinylated molecular weight marker (Bio-Rad Laboratories) was also loaded. The proteins were then separated by SDS-PAGE electrophoresis and then transferred onto PVDF membranes (Bio-Rad Laboratories) using the semi-dry transfer cell (Bio-Rad Laboratories).

Blotting

The membranes were washed twice in 1M PBS/0.1% Tween for 5mins while shaking gently and then blocked overnight at 4˚C in 5% non-fat dry milk prepared in the wash solution. The next morning, the membranes were washed twice and incubated in TGF-β_1 primary antibody (1:200, Santa Cruz), prepared in the blocking solution, for 1 hour at room temperature with gentle shaking. The membranes were then washed; three times for 5mins each and twice for 15mins each. The membranes were incubated in horseradish peroxidase conjugated goat anti-rabbit secondary antibody (1:5000, Dako) which contained additional horseradish peroxidase (1:2000, Amersham Bioscience) for the detection of the molecular weight marker. The membranes were washed again and then developed by applying ECL-Plus, a chemiluminescent reagent (Amersham Bioscience) to the membrane for 5mins. The membranes were then exposed to X-ray film for around 90secs.

To ensure that any difference in expression between control and experimental retinas was genuine and not due to loading errors, each membrane was stripped and reprobed for actin. Briefly, the membranes were first stripped for 15mins at 37˚C using Restore Western Blot Stripping Buffer (Pierce), washed and blocked again in 5% non-fat dry milk overnight. The following morning, the membranes were incubated in actin primary antibody (1:100, Santa Cruz) and then in secondary antibody containing horseradish peroxidase. After the washing step, developer solution was applied and the membranes exposed to X-ray film.

Analysis

An image of the X-ray film was captured using 'Quantity-One' software designed by Bio-Rad Laboratories. Individual bands that had developed on the X-ray film were manually selected. The software then calculated the amount of TGF-β_1 protein expressed in each sample by taking the area and the intensity of each band into consideration.

4.3.3 Immunohistochemistry

Whole eye wax sections

Eyes from pups raised in room air until P2, P7, P14 and P21 were fixed in 10% formalin overnight and then transferred to 70% alcohol. The eyes were later dehydrated through a graded series of ethanol solutions (70%, 90%, 100%) followed by xylene, and then embedded in wax. 5μm serial sections were cut and mounted onto poly-L-lysine coated slides and left overnight to dry at 60°C.

The sections were deparaffinised and hydrated by first immersing the slides in xylene, then decreasing alcohol concentrations (100%, 90%, 70%) and finally tap water. To prevent the binding of endogenous peroxidase, the sections were treated with 0.3% hydrogen peroxide for 20mins followed by a 5min wash in 1M PBS. The sections were then incubated in 5% normal goat serum for 20mins to block non-specific binding. TGF-β_1 antibody (1:100, Santa Cruz) was applied for 30mins, after which the sections were washed. Goat anti-rabbit biotinylated secondary antibody (1:200, Dako) was applied for 30mins and then washed. The sections were then incubated in horseradish peroxidase (1:100, Vector Laboratories) for 30mins and washed again. Finally, the sections were incubated in DAB reagent (Vector Laboratories) until the staining developed. The sections were counterstained using thionine (blue stain) for 15secs, dehydrated and mounted. For the negative control the above protocol was followed, except that the primary antibody incubation was replaced with an incubation in 5% serum/1M PBS. The sections were viewed using

a conventional light microscope (Leica) with a colour video camera attached (JVC) and digital images were obtained.

Retinal wholemounts

Four eyes from 7 and 14 day old pups, raised in room air, were fixed in 75% acetone, dissected (as described in Chapter Two) and the retinas stained to determine the distribution TGF-β_1 protein expression in the vasculature. The protocols detailed below were used where, unless otherwise stated, each wash stage consisted of three 10mins incubations in 1M PBS/1%Triton X-100, and the antibodies/fluorescent markers were prepared in the wash solution and applied for 2 hours at room temperature with gentle shaking.

The flattened retinal wholemounts were first permeabilised in 1M PBS/1% Triton X-100 for 30mins and blocked using 5% rabbit serum (Diagnostic Scotland) diluted in 1M PBS/Triton X-100 for 20mins. The wholemounts were then incubated in TGF-β_1 antibody (1:100, Santa Cruz) overnight at 4°C. The next day, the wholemounts were washed and incubated in biotinylated goat anti-rabbit secondary antibody (1:200, Dako). The wholemounts were washed again and Alexa Fluor 647 (1:200, Molecular Probes) was applied. The wholemounts were given a final wash and then mounted in PBS:glycerol (1:1) and the coverslip sealed with nail varnish.

For the triple-labelling, the retinal wholemounts were incubated overnight at 4°C in either anti-α-smooth muscle actin (α-SMA) primary antibody (1:400, Sigma) or desmin primary antibody (1:50, Dako) prepared in 5% serum/1M PBS/1% Triton X-100 to stain the mural cells. The following day, the tissues were washed and then incubated in biotinylated rabbit anti-mouse secondary antibody (1:200, Dako), followed by Texas red streptavidin (1:100, Vector Laboratories). The retinas were then blocked using avidin and biotin for 20mins each (Vector Laboratories) before applying biotinylated *G. simplicifolia* (Bandeiraea) isolectin B4 (1:50, Vector Laboratories) overnight at 4°C to stain the endothelial cells. The next day, the retinas

were incubated in fluorescein streptavidin (1:100, Vector Laboratories), blocked using avidin, biotin and then 5% goat serum each for 20mins, and incubated overnight in TGF-β_1 antibody (1:100, Santa Cruz) at 4°C. On the fourth day, the retinas were washed and incubated in biotinylated secondary antibody, followed by Alexa Fluor 647. The retinas were washed for the final time and mounted.

For the negative control labelling, retinas were treated as above, however, each primary antibody incubation was replaced with an incubation of 5% serum/1M PBS/1% Triton X-100.

The retinal flatmounts were viewed using a Leica TCSNT confocal system with a mixed gas argon/krypton laser. The endothelial cells stained using fluorescein were labelled green and excited at 488nm (filter BP 525/50), mural cells stained with Texas red were labelled red and excited at 568nm (filter LP 590), and TGF-β_1 expression, detected by Alexa Fluor 647, was labelled blue and excited at 647nm. Representative images at x10, x20 and x63-oil magnification were taken and digitally stored.

4.4 RESULTS

4.4.1 Western Blots

The retinas from each litter of rat pups raised in room air or in variable oxygen were pooled, the proteins were extracted and then separated by SDS-PAGE electrophoresis. The membranes onto which the proteins were transferred were then probed using a polyclonal antibody for TGF-β_1. As shown in Figure 4.1, the antibody recognised a peptide with a molecular weight of around 25kDa.

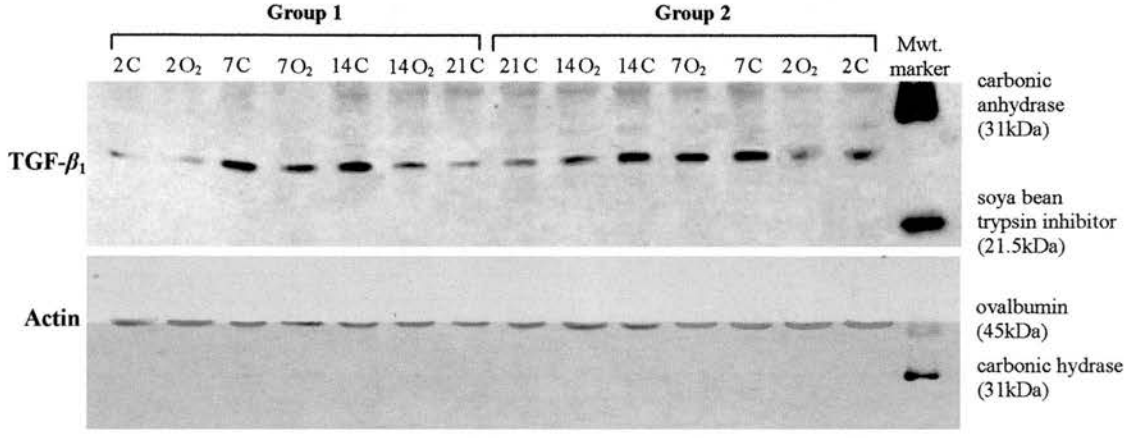

Figure 4.1: Western blot of retinal TGF-β_1 expression in control and oxygen treated rat pups.
The lower blot shows actin (43kDa) expression as a loading control.
C - control litter; O_2 - oxygen treated litter; numbers correspond to age of pups.

In normal development, very little TGF-β_1 was expressed in the retina at P2. There was a marked increase by P7, which remained high at P14. On P21, however, the expression of TGF-β_1 had decreased. In comparison to the controls, rats exposed to the variable oxygen regime of the Edinburgh ROP model had a reduced expression of the protein at each developmental timepoint; the greatest decrease occurred in the retinas exposed to oxygen for 14 days.

These results were confirmed by quantitative analysis (densitometric values):

		Mean Weight (g)	TGF-β_1 values	% decrease in O_2 group
Group 1	P2 Control	8.8	1245.81	
	P2 O_2	7.9 *	1044.16	16.2
	P7 Control	15.3	3317.53	
	P7 O_2	13.9 *	2726.30	17.8
	P14 Control	22.3	1836.08	
	P14 O_2	24.5 *	1257.91	31.5
	P21 Control	37.6	1428.05	
Group 2	P2 Control	9.1	749.25	
	P2 O_2	8.5 **	696.07	7.1
	P7 Control	15.7	2601.37	
	P7 O_2	16.3	2453.74	5.7
	P14 Control	24.1	2001.38	
	P14 O_2	26.9 *	1316.61	34.2
	P21 Control	35.7	847.56	

Table 4.1: The percentage decrease of retinal TGF-β_1 expression in oxygen treated rat pups.
Using the 'Quantity One' software, the bands from the Western blot were highlighted and the total volume of each band was calculated by multiplying the area of the band by its intensity.
O_2 - oxygen treated litter; P - postnatal day; * - $p < 0.005$ (t-test); ** - $p < 0.05$ (t-test)

The values obtained show that the highest expression of TGF-β_1 in normal development occurred at around day 7, falling slightly by day 14 and dramatically by day 21. From Table 4.1 it can also be seen that 14 days of the variable oxygen exposure resulted in a greater decrease in TGF-β_1 protein expression than 2 or 7 days of exposure; for example, in Group 1, on day 2 and day 7 the percentage decrease in the oxygen treated rats was around 17%, but on day 14 the reduction in expression was almost twice as much at 32%. These results suggest that TGF-β_1 expression was

regulated by oxygen and that the duration of the oxygen exposure was an important factor.

The membranes were stripped and reprobed using polyclonal goat actin which acted as a loading control. The expression levels of actin were similar for all samples (Figure 4.1), thus similar quantities of protein were loaded for each sample.

4.4.2 Immunohistochemistry

To determine if the observed decrease in TGF-β_1 expression was a direct effect of oxygen on the cells of the vasculature, and not other cells of the retina, TGF-β_1 immunohistochemistry was conducted.

Wax sections

The first stage involved determining the distribution of TGF-β_1 protein expression within the retina. 5μm paraffin wax sections of whole eyes from P2, P7, P14 and P21 control animals were stained using the same TGF-β_1 antibody used in the Western blots. Figure 4.2 (page 136) shows that both the vitreous and the choroid stained strongly for TGF-β_1 protein. On P2, no staining was detected within the neural retina. On P7, positive staining was present in the ganglion cell layer (GCL), but only around the optic nerve area. By P14, scattered cells stained positive for the protein; these cells were located in the GCL and the posterior edge of the inner nuclear layer (INL). This labelling pattern was also observed on P21. Upon further examination (Figure 4.3, page 137), it seemed that these scattered cells may be blood vessels, suggesting that the Western results were reflective of TGF-β_1 acting on the vascular cells, and not other retinal cells. In the negative controls, where only serum was applied to the sections instead of primary antibody, no staining was observed.

4.4.3 Immunofluorescent Labelling

Finally, the expression of TGF-β_1 in relation to the vascular cells was briefly investigated. Retinas of a few pups raised in room air until 14 days of life were triple-labelled for endothelial cells, mural cells and TGF-β_1. Previously, in Chapter Two, it was suggested that desmin and α-SMA were suitable markers for pericytes and smooth muscle cells, respectively. As illustrated in Figure 4.4 (page 137), positive TGF-β_1 labelling was observed around the vessels; all vessels were stained from the centre of the retina to the periphery.

It was expected that the positive labelling would be observed between the endothelial and mural cells, since TGF-β has been reported to act on both cells types [Fràter-Schröder et al., 1986; Heimark, Teardzik and Schwartz, 1986; Antonelli-Orlidge et al., 1989; Owens et al., 1989; Sato and Rifkin, 1989; 1990]. Figure 4.5 (page 138) shows arterioles triple-labelled for endothelial cells, smooth muscle cells or pericytes, and TGF-β_1. The positive staining for the growth factor was very close to that of the three cell types. This is illustrated best in Image D, where it can also be seen that TGF-β_1 staining occurred on the inner surface of the smooth muscle cells. The negative controls showed no positive staining, except those for desmin and α-SMA; which had high background labelling (Chapter Two). Whilst examining these images it was observed that the staining pattern of TGF-β_1 was almost identical to that of the endothelial cells (lectin). Indeed, this is seen in the images showing each individual stain for Figure 4.5 A and Figure 4.5 C.

Thus, flatmounted retinas were stained for TGF-β_1 protein expression alone. Positive TGF-β_1 labelling was detected on the arterioles and venules; as illustrated in Figure 4.6 A (page 138), staining of the venule was markedly weaker than that of the arteriole. In Figure 4.6 B, which shows an arteriole at a higher magnification, there was a little staining on either side of the arteriole; it is possible that this staining was of the primary capillary branches. These results suggest that TGF-β_1 predominantly exerts its effects on the vascular cells of the main retinal vessels.

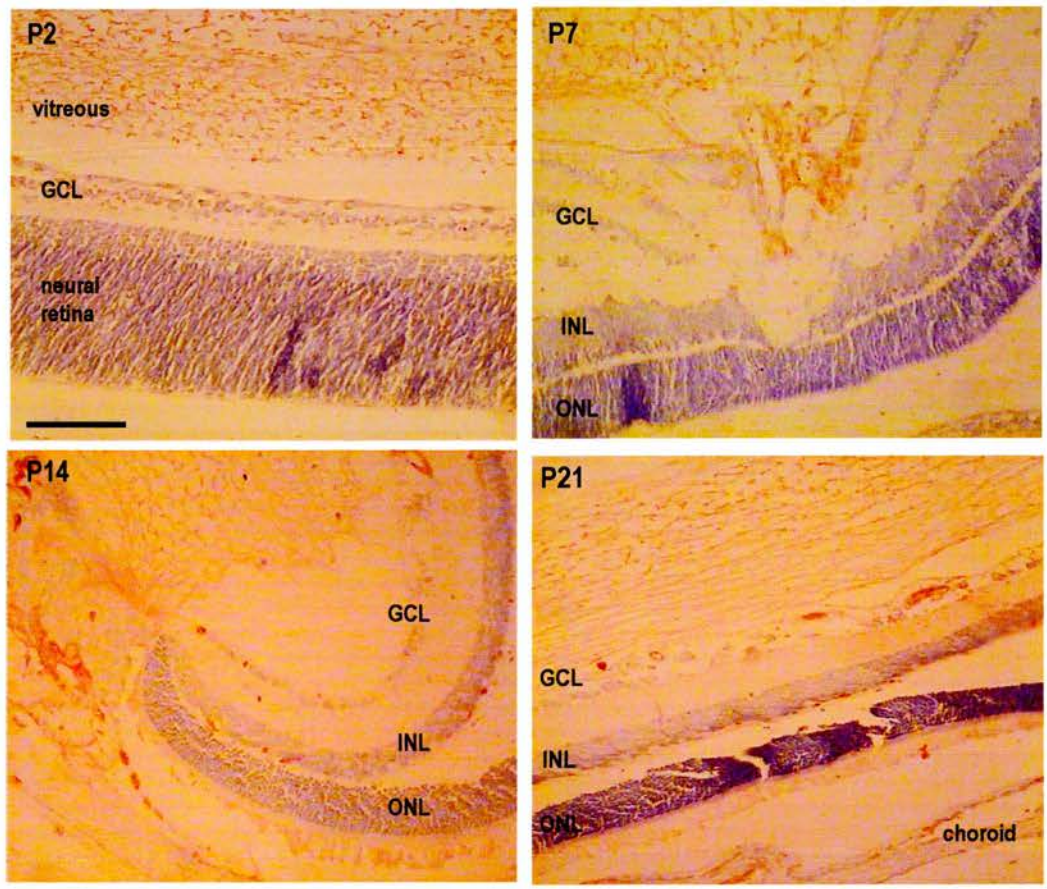

Figure 4.2: Immunohistochemical staining for TGF-β_1 expression in wax sections of normal rat eyes.
Positive labelling for the protein was detected using DAB (brown). The sections were then counterstained using thionine (blue).
GCL - ganglion cell layer; INL - inner nuclear layer; ONL - outer nuclear layer; P - postnatal day;
Scale bar: 100µm.

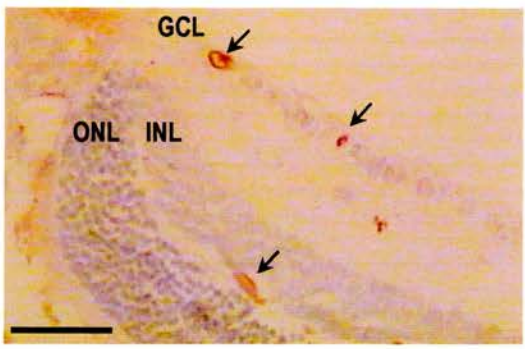

Figure 4.3: Enlarged image of P14 retinal section in Figure 4.2.
Arrows indicate positive labelling of what may be blood vessels.
GCL - ganglion cell layer; INL - inner nuclear layer; ONL - outer nuclear layer.
Scale bar: 50μm

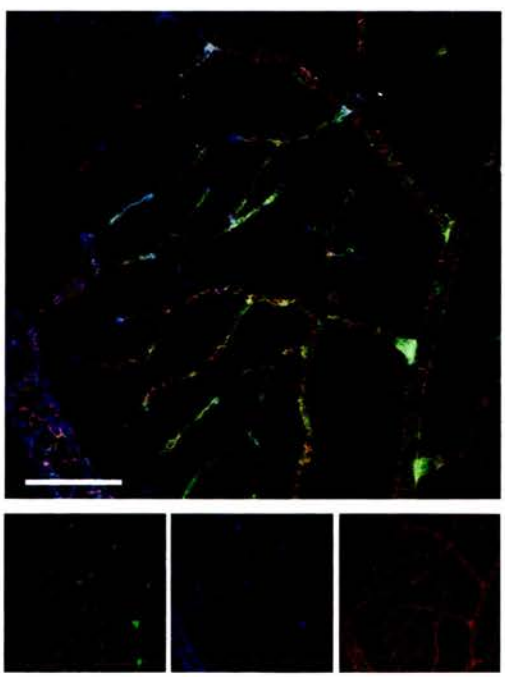

Figure 4.4: Fluorescent triple-labelling of the retinal vasculature at P14.
Image of the central retinal vasculature stained for lectin/endothelial cells (green), desmin/pericytes (red) and TGF-β_1 (blue).
Scale bar: 100μm.

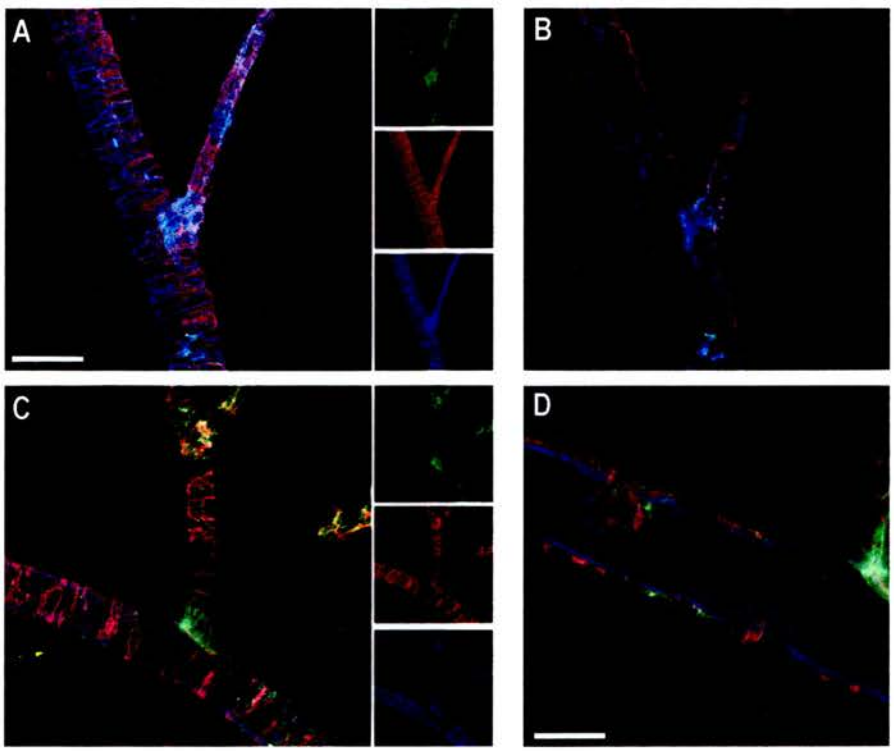

Figure 4.5: Fluorescent triple-labelling of the retinal arterioles at P14.
(A) Arertiole stained with lectin/endothelial cells (green), α-SMA/smooth muscle cells (red) and TGF-β_1 (blue); projected focus stack of 10 optical sections at 0.94μm. (B) Cross-section of image A. (C) Arteriole stained with lectin/endothelial cells (green), desmin/pericytes (red) and TGF-β_1 (blue); projected focus stack of 15 optical sections at 0.49μm. (D) Cross-section of image C.
Scale bar: (A) 32μm; (B) and (C) as A; (D) 15μm.

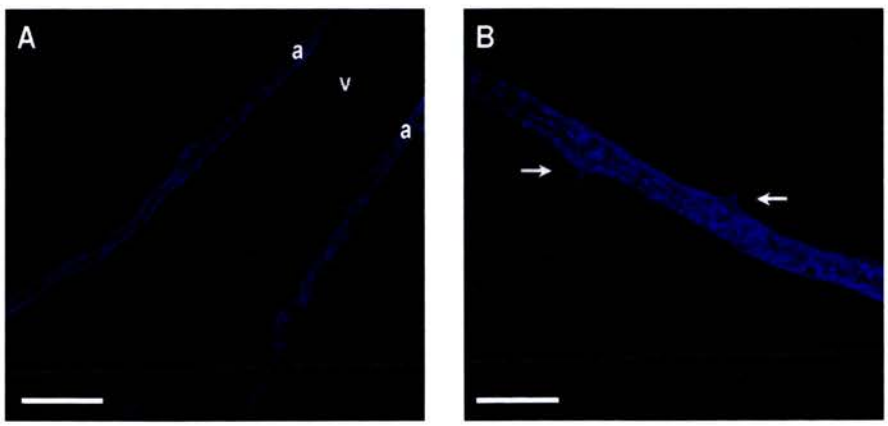

Figure 4.6: Fluorescent labelling for TGF-β_1 expression on P7.
(A) Labelling of the two arterioles (a) is strong in comparison to the venule (v). (B) Labelling of an arteriole at a higher magnification than A. Positive labelling appears to have begun on the primary branches (arrows).
Scale bar: (A) 200μm; (B) 100μm.

4.5 DISCUSSION

4.5.1 Evidence for a Role of TGF-β_1 in Vascular Development

Genetic studies on mice have revealed a role for TGF-β_1 in embryonic vascular assembly and in the establishment and maintenance of vessel wall integrity [Shull et al., 1992, Kulkarni et al., 1993; Dickson et al., 1995; Oshima, Oshima and Taketo, 1996]. In addition, immunohistochemical analysis of the mouse embryo showed that the endothelial cells of major blood vessels are positive for TGF-β mRNA [Akhurst et al., 1990], and that the mesenchyme per se or tissues derived from the mesenchyme are positive for protein expression [Heine et al., 1987].

Indeed, *in vitro* studies also support a role for TGF-β_1 in vessel formation. First, aortic endothelial cells cultured in media are growth inhibited in the presence of TGF-β [Fráter-Schröder et al., 1986; Heimark, Twardzik and Schwartz, 1986], as are endothelial cells of capillaries from bovine adrenal cortex [Antoneli-Orlidge et al., 1989]. Second, when smooth muscle cells, which express all three TGF-β receptors [Goodman and Majack, 1989], are plated at subconfluent densities their growth is inhibited by TGF-β_1 in a dose-dependent manner [Majack, 1987; Owens et al., 1989; Schor et al., 1995]. Third, neural crest stem cells in culture differentiate into smooth muscle cells in response to TGF-β_1 [Shah, Groves and Anderson, 1996]. Finally, the level of α-SMA and active TGF-β vary similarly along the length of arteries *in vivo* [Granger et al., 1998].

In comparison to endothelial cells and smooth muscle cells, studies on the effects of TGF-β_1 on pericytes are limited. One reason for this is that pericytes are difficult to positively identify and therefore to isolate and grow *in vitro*. Thus far, TGF-β_1 is reported not to have an effect on pericyte proliferation [Verbeek et al., 1994; Schor et al., 1995], but promote *in vitro* differentiation of human brain pericytes to smooth muscle cells [Verbeek et al., 1994] and differentiation of presumptive mesenchymal

cells to the pericytye/smooth muscle cell lineage [Hirschi, Rohovsky and D'Amore, 1998]. The differential potential of TGF-β_1, however, is disputed; Schor et al. found that TGF-β_1 did not affect α-SMA synthesis by bovine retinal pericytes [Schor et al., 1995], but α-SMA, as discussed in Chapter Two, is not a suitable marker for the identification of pericytes.

One of the main functions of TGF-β is to promote vessel stability by inhibiting the proliferation and migration of endothelial cells; it is suggested that pericytes express the active form of TGF-β once they come into contact with endothelial cells [Sato 1988, 1989; Antonelli-Orlidge et al., 1989]. Thus, I investigated if the expression of TGF-β_1 in the retina would differ between rats raised in room air and rats exposed to a minute-by-minute oxygen regime that induces features of ROP [Cunningham et al., 2000; McColm et al., 2004].

4.5.2 The TGF-β_1 Antibody

A polyclonal antibody raised against the carboxyl terminus of the TGF-β_1 precursor purified from human platelets was obtained from Santa Cruz. From the Western analysis it can be seen that this antibody recognised a component of around 25kDa that corresponds to the mature form of TGF-β_1 [Assoian et al., 1983]. This detected TGF-β_1 was biologically active; if the ligand was inert, the LAP protein would be bound to the mature ligand and a band at around 90-100kDa would have been detected instead [Brown et al., 1990; Gentry and Nash, 1990; Blanchette et al., 1997].

Physiologically activated TGF-β_1 within the retina would be readily recognised by the receptors, and once the ligand is bound to the receptor it would not be detected in the Western blots. In the wax sections, on-the-other-hand, activated ligand bound to any cell surface receptors would be readily detected. Extreme pH (less than 3 or above 10), high temperatures (above 100°C) and chaotophic agents can convert the latent form of the ligand to the activated state [Lawrence, Pircher and Jullien, 1985;

Wakefield et al., 1988; Brown et al., 1990]. Although the samples for the Western blots were never exposed to extreme pH conditions, the proteins were extracted in buffer containing SDS, a chaotrophic agent that coats the molecules and allows their migration during electrophoresis, and later the samples were heated at 90-100°C for 3 minutes to denature the proteins before electrophoresis. It is therefore possible that a high proportion of latent TGF-β could have been converted into the active form during the processing of the tissues.

4.5.3 Retinal TGF-β_1 Expression During Normal Development

On P2, TGF-β_1 was barely detected in the Western blots and none was detected in the immunohistochemically stained sections. At this point, the superficial vasculature was in the initial stages of development; the endothelial cells were forming into tubules and were still required to proliferate for further vessel formation, and there was very little mural cell coverage (Chapter Two). Thus, the low level of TGF-β_1 expression observed in the Western blots was probably due to secretion of the latent ligand by mural cells and endothelial cells; *in vivo*, none of the secreted protein was probably converted into the active form. Vessels of the superficial layer had progressed much further to the periphery by day 7, the central vasculature had undergone remodelling and extensive mural cell coverage was apparent. The Western blots showed a marked increase in TGF-β_1 expression compared to P2, however in the sections, positive staining was only observed around the optic nerve area. Although the activated ligand was acting on a few cells at this stage, the number of cells secreting the ligand had increased greatly. Thus, in the Westerns it may be assumed that the high TGF-β_1 levels detected was the result of an increase in the presence of both latent and active TGF-β_1. At day 14, the formation of the superficial vasculature came to an end, and the expression of TGF-β_1 in the Westerns although still high, was slightly reduced in comparison to day 7. In the wax sections, positive labelling was noted in the GCL and the INL from the centre to the periphery of the retina. TGF-β_1 was now acting on a greater number of cells to promote the differentiation of mural cells [Shah, Groves and Anderson, 1996;

Hirschi, Rohovsky and D'Amore, 1998] and inhibit the proliferation of endothelial cells [Fráter-Schröder et al., 1986; Heimark, Twardzik and Schwartz, 1986; Sato and Rifkin, 1988, 1989; Antonelli-Orlidge et al., 1989]. Since many TGF-β receptors on the cells of the vasculature were occupied by the ligand, there may have been a slight decrease in the level of ligand secreted and consequently a decrease in the amount detected in the Western blot. The formation of the whole retinal vascular network was completed by day 21; both layers had undergone remodelling and maturation with sufficient mural cell coverage. Although there was a decrease in the level of expression detected in the Western blot, in the wax sections positive staining was still observed as on P14. Perhaps, basal levels of TGF-β_1 were expressed to maintain vascular integrity by promoting the contact between endothelial cells and between endothelial cells and pericytes/smooth muscle cells.

The purpose of the immunohistochemical staining of wax sections was to identify which retinal cells expressed the mature activated ligand and therefore which cells were affected by oxygen exposure. Positive TGF-β_1 labelling in the retina was mainly noted on postnatal days 14 and 21 in some cells of the GCL and INL; cells which appeared to be blood vessels of the superficial and deep vascular layers. These results differ from previous studies which have shown TGF-β_1 immunoreactivity within the photoreceptors. Firstly, Pfeffer et al. detected positive staining around the outer segments of photoreceptors of monkeys. However, the antibody used was raised against the TGF-β_1 precursor molecule [Pfeffer et al., 1994]. Secondly, Anderson and colleagues detected labelling in the choroid, the photoreceptors, the outer plexiform layer (OPL) and GCL in human and monkey retinas using an antibody raised against the mature form of TGF-β_1 [Anderson et al., 1995]. Immunohistochemical results should be interpreted cautiously, since labelling patterns vary significantly from species to species and under different conditions of fixation and tissue processing. For example, Heine et al. found that the distribution of TGF-β was dependant on the fixative used; paraformaldehyde (neutral pH) stained only the cartilage whereas Bouin's solution (pH2) stained cartilage and strongly

stained the mesenchymal cells in many areas of the mouse embryo [Heine et al., 1987]. It is possible that in that study the acidic pH of the Bouin's solution altered the latent:active ratio of TGF-β. Although Anderson et al. claimed that the retinas fixed in Bouin's solution produced the same extent of immunohistochemical staining as retinas fixed in paraformaldehyde, their results only contained images of stained tissues that were fixed using Bouin's solution. Thus, their tissue processing techniques may have induced the conversion of TGF-β from the latent to the active state.

In support of the findings reported here, that TGF-β_1 was only acting on retinal vascular cells, is a study by Yamada and colleagues. This group investigated the expression of the type I and type II TGF-β receptors in the rat retina and found that receptor II was expressed in the GCL, INL, ONL, and within the photoreceptors and retinal pigmented epithelium from late embryonic stages to adulthood, whereas type I was observed in the GCL and single nuclear layer at E17, but not in the adult photoreceptor layer [Yamada et al., 1999]. The type II receptor is incapable of producing a response when occupied by the ligand, however it presents the ligand to the type I receptor which then propagates a cellular response [Wrana et al., 1994]. Hence, active TGF-β_1 labelling would be observed where it could induce a response; in the GCL and INL.

In addition to staining the retinal cells, the antibody also stained the vitreous and choroid. However the expression of TGF-β_1 by these tissues had no effect on the results of the Western blots; the vitreous although difficult to remove in fixed tissue lifts off the surface of the retina easily in fresh tissue, and the choroid comes away when separating the retina from the sclera. Thus, TGF-β_1 detected in the Western was that expressed by scattered cells of the GCL and INL.

In the triple-labelled flatmounted retinas, positive labelling occurred across the whole of the superficial vasculature, however when the tissues were labelled with TGF-β_1

alone, positive labelling was only noted on the main vessels. The extensive labelling of TGF-β_1 in the triple-labelled retinas may have resulted if insufficient blocking solution was applied after lectin staining. Due to time constraints the triple-labelling could not be repeated, but would be worth further investigation. In Chapter Two, it was shown that smooth muscle cells encapsulated the arterioles, its branches and possibly venules, while pericytes were observed to line the endothelial tubules of the entire vasculature. Looking at the single stained flatmounts, it would appear that TGF-β_1 acted only on the smooth muscle cells, which contradicts the findings of other researchers that differentiated pericytes also express TGF-β_1 [Antonelli-Orlidge et al., 1989], and that TGF-β_1 induces the differentiation of pericytes into smooth muscle cells [Verbeek et al., 1994]. It also contradicts the findings of the immunohistochemical staining of the wax sections; positive labelling was detected in the deeper layer where smooth muscle cells were not present. A possible explanation is that the quantity of TGF-β_1 secreted by the pericytes was too low for detection by the fluorescent immunohistochemical technique employed here.

4.5.4 The Effects of Oxygen Fluctuations on Retinal TGF-β_1 Expression

Raising pups in the Edinburgh model of ROP caused a decrease in the expression of TGF-β_1 protein at all timepoints examined, although the greatest reduction was observed with 14 days of oxygen exposure. In Chapter Two, it was found that the variable oxygen regime resulted in a significant decrease in pericyte coverage and a slight reduction in α-SMA expression which stained smooth muscle cells, thus the reduction in TGF-β_1 could be a reflection of the decrease in the number of mural cells. Another explanation is that because the retinal vasculature spreads at a slower rate when pups are exposed to oxygen, the number of endothelial and mural cells is further reduced, thus in comparison to the retinas of room air raised pups, less active TGF-β_1 is required. This though seems unlikely because in the Edinburgh model when pups were exposed to the 10kPa oxygen regime, the percentage of the retinal area that remained avascular was only 4.6% (average) [McColm et al., 2004]. If the reduction was only due to less endothelial and mural cells as a result of decreased

spread of the vasculature, then a similar decrease in TGF-β_1 at P14 would have been expected, but here a much greater difference was observed, of around 30%.

The next step would be to establish whether the decrease in TGF-β_1 protein was the result of the hypoxic or hyperoxic periods, or if it was in response to the constant switching between the two (where the genes may be switching 'on' and 'off' repeatedly). This could be investigated by exposing pups to each of the following oxygen regimes: room-air (as control); constant hyperoxia (70-80% oxygen) [Ashton, Ward and Serpell, 1954; Ashton and Blach, 1961; Smith et al., 1994]; the conventional hyperoxic/hypoxic cycle [Penn, Tolman and Lowery, 1993; Penn, Henry and Tolman, 1994; Penn et al., 1995], and constant hypoxia (around 15% oxygen). The expression of retinal TGF-β_1 protein could then be compared by various methods for each group. This may give an indication of how oxygen regulates TGF-β_1 *in vivo*.

The percentage reduction in the experimental samples on P2 and P7 was greater in Group 1 than in Group 2. This may have been due to a difference in the weights of the pups since weight directly effects development. In Group 1 the p-value for weights of control and experimental was less than 0.005 (t-test) for both P2 and P7. However, in Group 2 the p-value on P2 was reduced to less than 0.05 and the difference in the weights of the P7 controls compared to the experimental pups was not significant. In comparison, the p-value obtained for P14 in both groups was less than 0.005.

From all timepoints examined, the greatest decrease in the level of TGF-β_1 expression occurred with 14 days of fluctuating oxygen exposure. This decrease may have been due to a longer duration of oxygen exposure. If that was the case, then in comparison to P2, a further decrease in protein levels should have been observed on P7. It is possible that instead of the duration of exposure, the variability of oxygen was more important. As illustrated in Figure 4.7, the oxygen profile in the

second week is more variable than the first week making the extent of relative hypoxia/hyperoxia greater in week two than week one:

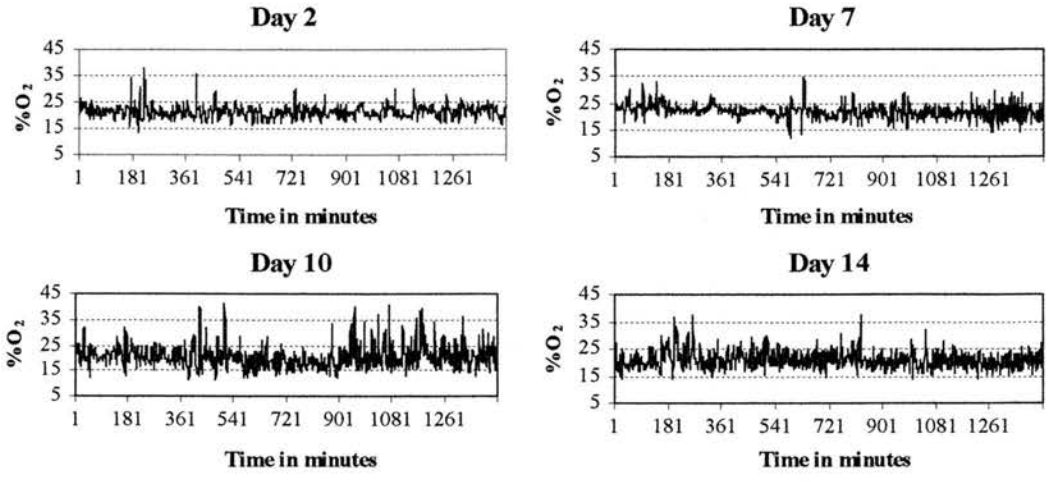

Figure 4.7: The change in oxygen variability on days 2, 7, 10 and 14.

Two studies have investigated the effects of oxygen on TGF-β_1 expression. Khaliq and colleagues grew solo cultures of endothelial cells and pericytes, reduced the pO_2 from 135mmHg (18kPa) to 18mmHg (2.4kPa), and found that total TGF-β, in particular TGF-β_2, was decreased in both cultures, although endothelial cells were more effected [Khaliq et al., 1995]. However, this contrasts with previous work by Falanga et al., where TGF-β_1 secretion and synthesis were shown to be elevated in response to hypoxia and TGF-β_2 to be unaffected [Falanga et al., 1991]. This study was conducted on human dermal fibroblasts and as discussed earlier, TGF-β_1 response differs with cell types.

The Western blot data reported here does not ascertain whether the observed decrease in TGF-β_1 expression in the retinas of experimental pups was the result of its decreased secretion by the cell or a reduction in its synthesis (either decreased mRNA expression or rate of transcription). This could be answered very simply by measuring (by Western or ELISA analysis) the amount of TGF-β_1 precursor protein

in control and experimental retinas using an antibody that recognised only the precursor molecule. If less precursor protein was detected in the experimental samples, then the reduction in TGF-β_1 levels would have been due to a reduction in its synthesis. If no change was observed in the experimental retinas, then the oxygen may have caused a reduction in the secretion of the protein. It is possible that oxygen had a direct effect on the conversion of latent to active TGF-β_1. This could be deduced by investigating the occupancy of the TGF-β receptors using a technique called immunoprecipitation. The samples are first homogenised in protein extraction solution containing TGF-β_1 antibody and Protein-A/G Sepharose (which would bring all structures forming a complex with TGF-β_1 to the bottom of the tube when centrifuging); the proteins are then separated by electrophoresis, and transferred onto a membrane which is blotted using an antibody for the TGF-β_1 receptor.

A major drawback of the Western analysis is that the retinas of each litter were pooled, thus TGF-β_1 protein expression was studied in only two control and two experimental groups which does not allow for statistical analysis. The retinas were grouped and then the proteins extracted since sufficient protein for loading onto the acrylamide gel would not be obtained from individual retinas. Using the 'Quantity-One' software which calculated the amount of protein expressed by multiplying the intensity of the band with the area it occupied, was not the most reliable method for determining the level of expression between the control and experimental groups since errors can easily occur when selecting the band areas. Therefore, in order to quote any difference in expression with confidence, all retinas should not be pooled, but stored in groups of two or three and then the proteins extracted. This would allow up to as many as six samples (compared to only one) from each litter. The protein expression would then be measured in all samples and the statistical significance determined.

To further understand the roles of TGF-β_1 in retinal vessel development, investigating the retinas of the TGF-β null mice that survived postnatally to 3 weeks

of age may prove valuable; would the endothelial cells migrate normally and would the tubules gain a smooth muscle cell or pericyte coverage? For this, double-labelled immunohistochemistry would be conducted as in Chapter Two. Granger et al. investigated the aorta of mice heretozygous for the TGF-β_1 gene and found that active TGF-β in these mice was lower compared to wild type mice, and that α-SMA levels were also depressed in the heterzygotes [Granger et al., 1998]. Hence, smooth muscle cell differentiation was reduced as a consequence of the reduction in TGF-β_1 levels.

Thus, during normal development, the retinal expression of TGF-β_1 increased from P2 to P14. The levels of expression, however, were reduced in the Edinburgh ROP model. It is possible that the oxygen environment of the model directly modulated the production of TGF-β_1 and in turn affected mural cell coverage of the vessels.

CHAPTER FIVE

THE ANGIOPOIETINS IN THE DEVELOPING RAT RETINA

5.1 INTRODUCTION

Recently another family of growth factors specific for the vascular endothelium was identified. To date, this family consists of two receptors, called Tie-1 and Tie-2 (tyrosine kinase with immunoglobulin and epidermal growth factor homology domains) [Sato et al., 1993], and four ligands, named angiopoietin-1 [Davis et al., 1996], angiopoietin-2 [Maisonpierre et al., 1997], angiopoietin-3 and angiopoietin-4 [Valenzuela et al., 1999]. The angiopoietins are structurally divided into three domains; an N-terminal region, an α-helical rich coiled-coil segment and a fibrinogen-like domain [Davis et al., 1996; Maisonpierre et al., 1997; Valenzuela et al., 1999]. All four ligands bind to the Tie-2 receptor, but it is unclear as to whether or not they utilise the Tie-1 receptor. It is possible that other proteins for this receptor will be identified at a later date.

5.1.1 The Angiopoietins

The first member of the angiopoietins was discovered using a novel cloning technique called 'secretion-trap expression cloning' [Davis et al., 1996]. Angiopoietin-1 (Ang-1) is a 70kDa protein consisting of 498 amino acids. Unlike other vascular growth factors that induce proliferation of endothelial cells, Ang-1 binds and phosphorylates the Tie-2 receptor, but it is incapable of inducing a mitogenic response [Davis et al., 1996].

Angiopoietin-2 (Ang-2) was identified by homology screening in the mouse and in human [Maisonpierre et al., 1997]; the proteins of these two species share around 85% homology. Ang-2 is reported to be slightly smaller than Ang-1, consisting of 496 amino acids, and both ligands share around 60% identity [Maisonpierre et al., 1997]. Like Ang-1, Ang-2 also binds to the Tie-2 receptor; however, unlike Ang-1, it fails to induce receptor phosphorylation. In fact, Ang-1 induced phosphorylation of cultured endothelial cell lines is completely inhibited by Ang-2 [Maisonpierre et al., 1997]. Thus, Ang-2 is the naturally occurring antagonist for Ang-1/Tie-2 binding.

Valenzuela and co-workers identified mouse angiopoietin-3 (Ang-3) and human angiopoietin-4 (Ang-4) using homology based cloning techniques. Whereas Ang-3 appears to be an antagonist, Ang-4 is an agonist [Valenzuela et al., 1999]. Currently, literature on both of these angiopoietin isoforms is very limited, thus the biological roles of Ang-1 and Ang-2 only will be discussed in this chapter.

5.1.2 Biological Functions of the Ang/Tie-2 System

In vivo studies

Many of the functions of the Tie receptors and the angiopoietins were elucidated by investigating their embryonic expression patterns and by in depth analysis of mice with targeted gene mutations. The following is an overview of the findings from such studies.

In mice, expression of both receptor types is relatively abundant during the early stages of embryogenesis, when it is detected only in cells associated with the vascular system such as the aorta and endocardium [Sato et al., 1993]. Homozygous mice deficient for Tie-1 die between embryonic day 13.5 (E13.5) and birth due to haemorrhaging and oedema [Sato et al., 1995]. The mice have smaller hearts compared to normal mice and the alveoli of the lungs fail to expand. Ultrastructural analysis of the blood vessels indicated that the mice have poor endothelial integrity causing the leakage of interstitial fluid (oedema) and blood (haemorrhaging) through the vessels. In contrast, Tie-2 homozygous mutants die earlier, at E10.5 when the mice are severely growth retarded in comparison to the controls [Sato et al., 1995]. The mice also display abnormalities of the vascular network; although endothelial cells are present in normal number and assemble into tubules, the vasculature fails to organise into large and small vessels and lacks encapsulation by mural cells.

Embryonic Ang-1 expression is predominantly found in the heart myocardium surrounding the endocardium [Suri et al., 1996]. However, later in development its expression becomes much more widely distributed, most often in the mesenchyme surrounding developing vessels in close association with Tie-2 expressing endothelial cells. Lack of the Ang-1 gene results in death at around E12 [Suri et al., 1996], a day or two after Tie-2 knockouts [Sato et al., 1995]. The primary capillary plexus, which is normally a highly branched and intricate vascular network, appears relatively immature in the knockout mice. Endothelial cells are present in normal number, but the organisation of the vasculature is compromised in that the vasculature does not consist of large and small vessels, instead most of the vessels are of a similar size and diameter. Ultrastructural analysis showed that the endothelial cells are poorly associated with the underlying matrix and fail to recruit and associate with mural cells. Thus, lack of the Ang-1 gene results in defects reminiscent of, but slightly less severe, than mice lacking the Tie-2 receptor gene.

Transgenic mice overexpressing Ang-1 generally appear normal, however their skin is markedly different from normal mice; the skin appears very red and has more

larger blood vessels than normal [Suri et al., 1998]. Transmission electron microscopy confirmed that the vessels of these mice exhibit normal cell-to-cell contact between endothelial cells and adjacent pericytes, but the number, size and branching pattern of the blood vessels is increased dramatically, suggesting that Ang-1 promotes sprouting and branching *in vivo*.

Ang-2 expression is not readily detected in the heart of the mouse embryo, but it is abundant in the smooth muscle layer beneath the vessel endothelium [Maisonpierre et al., 1997]. The distinct but overlapping expression patterns of Ang-1 and Ang-2 suggests that Ang-2 might regulate Ang-1 function at particular sites and stages of vascular development. Although mice lacking the Ang-2 gene have not been generated, transgenic mice overexpressing Ang-2 have been studied [Maisonpierre et al., 1997]. The vascular defects of these mice are very similar, but more severe, than mice homozygous for Ang-1 [Suri et al., 1996] or Tie-2 gene mutation [Sato et al., 1995], consistent with the concept that Ang-2 is an antagonist for Ang-1/Tie-2 binding.

In vitro studies

When added to cultured endothelial cells, Ang-1 fails to elicit a significant growth response of the cells [Davis et al., 1996; Koblizek et al., 1998; Witzenbichler et al., 1998], nor does it induce tubule formation [Davis et al., 1996]. Ang-1, however, is capable of promoting a dose-dependent migration of endothelial cells, but not smooth muscle cells [Witzenbichler et al., 1998], indicating that it may also function in angiogenesis, as previously suggested by *in vivo* studies. Indeed, when Ang-1 is added to a confluent monolayer of endothelial cells, the cells migrate and form long capillary sprouts [Koblizek et al., 1998]. When Ang-1 and VEGF (vascular endothelial growth factor, a potent endothelial cell mitogen and chemoattractant) [Ferrara and Henzel, 1989; Millauer et al., 1993] are added to the culture together, there is a further increase in the number of sprouts. This suggests that VEGF and Ang-1 can act synergistically to induce sprout formation [Koblizek et al., 1998]. Consistent with this, in the mouse cornea micropocket assay neither Ang-1 nor

Ang-2 are seen to induce neovascularisation, but when administered with VEGF, Ang-1 enhances the capillary density and the luminal diameter of the vessels while Ang-2 produces longer vessels. Thus, Ang-1 promotes the maturation of the vasculature but Ang-2 initiates a neovascular response [Ashara et al., 1998].

It is reported that the Tie-2 receptor is associated with the p85 subunit of phosphatidlyinositol 3-kinase (PI3-kinase), a second messenger that is activated upon Tie-2 receptor phosphorylation. Further downstream in the signalling pathway, Tie-2 and PI3-kinase activation also causes phosphorylation of Akt, a critical survival messenger [Kontos et al., 1998]. This finding triggered several studies on the effects of the Tie-2 system on endothelial cell survival. When endothelial cells are cultured they became organised into a network consisting of tubules and cords, however some of the tubules regress in the later stages of the culture. In the presence of Ang-1, the endothelial networks survive for a longer period of time [Papapetropoulos et al., 1999]. Similarly, when endothelial cells are cultured in the absence of serum, many of the cells undergo apoptosis, but this cell death is reduced significantly in the presence of Ang-1 [Papapetropoulos et al., 1999; Kwak et al., 1999]. The involvement of the Tie-2/PI3-kinase/Akt pathway in cell survival has also been investigated; when endothelial cells are stimulated with Ang-1, an up-regulation in both Akt and PI3-kinase phosphorylation is observed [Papapetropoulos et al., 2000; Kim et al., 2000a]. This effect is antagonised by the addition of Ang-2 antibody, Tie-2 soluble receptor [Papapetropoulos et al., 2000], and completely blocked by wortmannin, a PI3-kinase inhibitor [Kim et al., 2000a]. In addition to causing activation of Akt, Ang-1 also induces a rapid increase in the mRNA levels of survivin, an antiapoptotic agent [Papapetropoulos et al., 2000]. Recently, Kim et al. also reported that Ang-2 can promote cell survival by utilising the same pathway as Ang-1, but in order to produce this response a concentration four times that for Ang-1 is required [Kim et al., 2000b].

In summary, the above mentioned studies have established that the Ang-1/Tie-2 system functions in the later stages of vasculogenesis, namely vessel maturation and

stabilisation by mainly promoting the associations between endothelial cells and mural cells. The angiopoietins also have some function during angiogenic growth since Ang-2 antagonises the effects of Ang-1 by competitively binding to the Tie-2 receptor. However, the exact roles and mechanisms of the angiopoitein/Tie-2 system in vessel formation have yet to be elucidated.

5.1.3 The Ang/Tie-2 System in Postnatal Life

Basal levels of Ang-1 and Tie-2 continue to be expressed once the vasculature is established and quiescent [Wong et al., 1997]. Ang-2 levels though are quite restricted in the adult, but increase dramatically (along with Tie-2) in organs of the female reproductive system [Maisonpierre et al., 1997], and during the processes of wound repair [Wong et al., 1997] and tumour formation [Stratman, Risau and Plate, 1998; Holash et al., 1999; Tanaka et al., 1999].

In early follicle development within the ovary, the vasculature is quiescent, thus Ang-1, but little Ang-2, is expressed. In the late pre-ovulatory follicle and the post-ovulatory corpus luteum, angiogenesis is quite active and the Ang-2 gene appears to be up-regulated while Ang-1 expression remains unchanged [Maisonpierre et al., 1997]. In the non-productive follicles, which regress, Ang-2 expression is strong [Maisonpierre et al., 1997], as it is in the endometrium during the proliferative and secretory phases of the menstrual cycle [Krikun et al., 2000].

To establish if there is a role of the Ang/Tie-2 system in the process of wound repair, Wong and colleagues studied biopsy punch wounds on the dorsal skin of the rat [Wong et al., 1997]. In the initial stages of tissue repair following injury, Tie-2 mRNA and protein expression are increased in the dilated ecstatic vessels surrounding the wound. Newly formed vessels then invade the injured tissue and Tie-2 expression is further increased. Towards the later stages of the healing process, when the wound edges are contracted and many microvessels have regressed, Tie-2 is limited to the blood vessels of the wound edge. Thus, Tie-2

mRNA levels are rapidly increased after injury, but down-regulated as the repair process is completed.

Because the angiopoietin/Tie-2 system is essential for angiogenesis, several studies have investigated the roles of the angiopoietins in tumour formation, but they have produced conflicting results. For example, in Kaposi sarcoma the expression of Ang-2, Tie-1 and Tie-2 is reported to be strong, but that of Ang-1 is low [Brown et al., 2000]. Likewise, in breast cancer cell lines, high levels of Ang-2 are detected, but Ang-1 is rarely expressed [Stratmann et al., 2001]. In contrast, samples of human glioblastoma have increased levels of Ang-1 as well as Ang-2 and Tie-2 mRNA expression [Startmann, Risau and Palate, 1998]. Consistent with a role for Ang-2 in cancer, is the finding that when rat lung and mammary carcinoma cells are injected with Ang-2, the formation of metastatic tumours is inhibited and survival of the rats is prolonged [Yu and Stamenkovic, 2001]. In contrast, administration of Ang-1 has no effect on tumour growth and animal survival. Also, the administration of Tie-2 soluble receptor into rat mammary tumours results in a marked reduction in the growth and the vascular density of the tumour [Lin et al., 1997]. Hence, both Ang-2 and Tie-2 are believed to be up-regulated in cancerous cells, but the expression of Ang-1 in tumours is debated. It may be that the expression of Ang-1 is dependent on the developmental stage of the tumour.

Although the above mentioned studies are somewhat difficult to interpret, Holash et al. have put forward the following theory on how the angiopoietins are involved in tumour formation. Although most natural tumours begin as small avascular masses, many start as well-vascularised tumours and grow by co-opting existing host vessels [Holash, Weigand and Yancopoulos, 1999; Holash et al., 1999]. Soon after tumour co-option, host vessels express high levels of Ang-2 (which is now considered the earliest marker of tumour development [Holash et al., 1999]) and respond by regressing [Holash, Weigand and Yancopoulos, 1999; Holash et al., 1999]. As a result, the tumour becomes hypoxic, which in turn stimulates a rapid increase in VEGF expression. The high VEGF and Ang-2 expression induce new sprouting

from pre-existing vessels [Maisonpierre et al., 1997; Asahara et al., 1998] and allow survival and further growth of the tumour [Holash et al., 1999].

To summarise, in the adult vasculature VEGF, Ang-1 and Ang-2 collaborate to elicit angiogenesis. When Ang-2 expression is up-regulated (for example during menstruation or in tumour formation) the interaction of Tie-2 and Ang-1 is disrupted and vessels are destabilised. Once the endothelial cells separate from the perivascular cells and the endothelial cell matrix, vessels appear particularly vulnerable. In the presence of VEGF, Ang-2 promotes angiogenesis, but in its absence, Ang-2 causes the regression of the destabilised vessels.

5.2 AIMS AND HYPOTHESIS

The primary objective of this study was to investigate the mRNA expression of both Ang-1 and Ang-2 during normal development of the rat retina. Because Ang-2 antagonises the effects of Ang-1, the balance of Ang-1 and Ang-2 expression is considered critical for establishing a mature and stable vasculature. Therefore, the successful measurement of the mRNA of both angiopoietins would allow the ratio of Ang-1:Ang-2 in normal development to be determined. The second objective was to investigate if this ratio was affected by the fluctuating oxygen regime of the Edinburgh model of retinopathy of prematurity (ROP).

Ang-1 is a stabilising factor for the endothelium, whereas Ang-2 induces vessel instability, thus initiating angiogenesis. Therefore, it is expected that basal levels of Ang-1 mRNA will be detected throughout the period of retinal formation. In contrast, the expression of Ang-2 mRNA is predicted to be high during the development of the lower retinal vasculature, which forms as an extension of the superficial vasculature. Hence, Ang-2 expression is expected to be high during mid-vascular development (around days five to 12).

In the ROP model, it is postulated that the Ang-1:Ang-2 ratio would be altered as lower levels of Ang-1 mRNA and higher levels of Ang-2 mRNA may be expressed either as a direct result of the oxygen regime or as a result of the reduced association of endothelial cells and pericytes.

5.3 METHODS

5.3.1 Animals & Tissue Preparation

Litters of Sprague-Dawley rat pups were raised in room air and sacrificed, without perfusion, on all days from 0 to 14. The eyes were enucleated and processed for either frozen or wax sections.

Frozen sections

The eyeballs were pierced by a needle and fixed for 2 hours in 4% paraformaldehyde prepared in 1M phosphate buffered saline (PBS). The eyes were then embedded in 1.5% agarose prepared in 1M PBS and supplemented with 5% sucrose. Once set, the solid agarose blocks were trimmed and left in 30% sucrose at 4˚C until the blocks sank. Using dry-ice, the blocks were slowly frozen and stored at -70˚C.

The frozen agarose blocks were sectioned using a freezing microtome set between -26˚C and -30°C. Thick sections of the eye were cut until close to the centre (just prior to reaching the optic nerve where all retinal layers are visible). 10µm serial sections were then obtained and mounted onto superfrost glass slides. The sections were stored at -70˚C until the *in situ* hybridisation was performed.

Wax sections

The eyes were fixed in 10% formalin overnight and transferred to 70% alcohol. The eyes were later dehydrated through a graded series of ethanol solutions (70%, 90% and 100%) followed by xylene and then embedded in wax.

The wax blocks were sectioned using a bench-top microtome (Heidelberg). 5µm serial sections near the optic disc region were cut and mounted onto superfrost glass slides. The sections were then left to dry overnight at 60˚C.

5.3.2 Probe Preparation

The complementary DNA for mouse Ang-1 and Ang-2 were the generous gift of Dr. G. D. Yancopoulos, Regeneron Pharmaceuticals (NY, USA). These DNA constructs were transformed into *E.coli* and stored as glycerol stocks at -70˚C.

A minute quantity of the *E-coli* was smeared onto an agar plate containing 100μg/ml ampicillin and grown overnight at 37˚C. A single colony was selected and added to 50ml Luria Broth base containing 100μg/ml ampicillin and cultured overnight at 37°C with vigorous shaking. The culture medium was then centrifuged at 6,000g for 15mins, the supernatant discarded and the pellet containing the DNA plasmid frozen at -20˚C.

The plasmid was purified using the HiSpeed Plasmid Midi Kit and protocol supplied by Qiagen, LTD. Briefly, the pellet was resuspended in buffer containing RNase A, lysed and then precipitated in acetate buffer (pH 5.5). After centrifugation, the supernatant was transferred to a QIAGEN-tip which caused the DNA to bind to its column. The DNA was then eluted and stored at -20˚C.

Using restriction enzymes (Roche Molecular Biochemicals) the DNA plasmid was linearised; 2.5units of enzyme was added per μg of DNA and incubated for an hour at 37˚C. The linearised plasmid was then purified using Elutip columns (Schleicher & Schuell). Briefly, the column was loaded with the DNA and all the nucleic acids bound to the column. The column was then washed in buffer, and the sample was eluted and stored at -20˚C.

Finally, using the DIG RNA Labeling Kit (Roche), the DNA was labelled with digoxigenin-UTP by *in vitro* transcription with T3 and T7 RNA polymerase. Both sense and antisense probes were prepared. Briefly, the following reagents were added to 1μg of purified DNA template and then incubated at 37˚C for 2 hours: NTP labelling mixture, transcription buffer, RNase inhibitor and RNA polymerase. The probe was now fully prepared and stored at -70˚C.

5.3.3 *In situ* Hybridisation

Solutions

All solutions were prepared using autoclaved double distilled water:

- SSC x20 was prepared using sodium chloride and sodium citrate dihydrate. The solution was pH adjusted to 7.0.
- 10x Salts was prepared using sodium chloride, tris sodium chloride, tris base, disodium hydrogen orthophosphate monohydrate, sodium hydrogen phosphate and ethylenediaminetetraacetic acid.
- Hybridisation buffer consisted of 1x salts, 50% deionised formamide, 10% dextran sulphate (at 50%), 1mg/ml yeast RNA and 1x Denhardts.
- Solution A consisted of 1x SCC, 50% deionised formamide and 0.1% Triton X-100.
- TBST contained 0.14M sodium chloride, 0.003M potassium chloride, 0.025M tris hydrogen chloride (pH 7.5) and 0.1% Triton X-100.
- NTMT solution was prepared using 0.1M sodium chloride, 0.1M tris-hydrogen chloride at (pH 9.5), 0.05M magnesium chloride hextrahydrate and 0.1% Triton X-100.
- Colour development solution consisted of TBST solution containing 0.34mg/ml NBT (4-nitro blue tetrazolium chloride, Roche Molecular Biochemical) and 0.18mg/ml BCIP (5-bromo-4-chloro-3-indolyl-phosphate, Roche Molecular Biochemical).

Digoxigenin-labelled hybridisation

15 slides (one for each developmental day) were defrosted at room temperature for at least an hour and stained together under the same conditions to determine the expression pattern of Ang-2.

The probe was prepared in the hybridisation buffer at a concentration of 100ng/ml or 150ng/ml. The probe mix was then denatured by heating it at 70°C for 5 to 10mins. 100µl of this probe mix was applied to each slide and a thin plastic coverslip placed on top. The slides were hybridised in a humidified chamber overnight at 45°C.

The following morning, the slides were transferred into a slide rack and washed three times in Solution A at 45˚C; the first wash was for 15mins, followed by two 30min washes. The slides were then washed in TBST solution at room temperature for 1 hour with a change of solution after 30mins. The slides were blocked using 10% heat inactivated sheep serum prepared in TBST for at least 1 hour at room temperature. The slides were dried around the edges and 100µl of anti-digoxigenin coupled alkaline phosphatase-Fab was added to each slide. The slides were again covered with thin plastic coverslips and incubated in a humidified chamber overnight at 4˚C.

The coverslips were removed again and the slides washed at room temperature in TBST solution five times for 20mins each, followed by a 20min wash in NTMT solution. The slides were then stained overnight at 4˚C in the dark using the colour development solution. The next morning, the reaction was stopped by washing the slides in distilled water. The sections were then fixed in 4% paraformaldehyde/0.1% gluteraldehyde for 20mins and counterstained: 5mins in tap water; 5mins in 10% nuclear fast red; 5mins in tap water. Finally, the sections were dehydrated through a graded alcohol series (30%, 50%, 70%, 95% and 100% for 30secs each) followed by xylene (10mins) before they were mounted using Vectamount (Vector Laboratories).

Radiolabelled hybridisation

Radiolabelled *in situ* hybridisation was performed by Helen Wilson working with Dr. Hamish Fraser in the Medical Research Council, Human Reproductive Sciences Unit (Edinburgh). The following is a brief outline of the method used in their laboratory (a more detailed methodology can be found in Wulff et al., 2000):

The complementary DNA for Ang-1 and Ang-2 were provided by Dr. G. D. Yancopoulos (Regeneron Pharmaceuticals, USA) and that for VEGF was provided by Dr. S. Charnock-James (University of Cambridge, UK). Sense and antisense probes were prepared using an RNA transcription kit and were labelled with [^{35}S]-UTP and then purified from free bases using Chroma Spin columns.

Paraffin wax sections of eyes from 7 and 14 day-old pups were deparaffinised in xylene and hydrated through an alcohol series. The sections were then incubated in hydrogen chloride solution followed by digestion in proteinase K. The sections were washed in SCC and then incubated in prehybridisation buffer at 55°C for 2 hours. Hybridisation was preformed overnight at 55°C with either the sense or antisense probe. After hybridisation, the slides were rinsed in SCC and treated with RNase A to remove excess probe. The slides were then dehydrated through another alcohol series, dried and dipped in liquid emulsion and exposed for either 4 weeks (VEGF) or 9 weeks (Ang-1 and Ang-2). The slides were developed and counterstained with haematoxylin and eosin, dehydrated and mounted.

Analysis

The digoxigenin-labelled slides were viewed under lightfield conditions and the radio-labelled slides under both lightfield and darkfield conditions. Digital images were obtained using a Leica microscope with an attached colour video camera (JVC).

5.4 RESULTS

5.4.1 Formation of the Retinal Layers

In the rat, the retinal layers were not completely differentiated until P14 as previously described [Stone et al., 1995; Yamada et al., 1999]. Briefly, as illustrated in Figure 5.1 (page 165), on day 0 the retina was comprised of only two layers called the ganglion cell layer (GCL) and the neuroblast layer (NBL). By postnatal day 6 (P6), the NBL began to differentiate, and by P10 the central NBL had developed into the inner nuclear layer (INL), the inner plexiform layer (IPL), the outer nuclear layer (ONL) and the outer plexiform layer (OPL). This differentiation of the NBL progressed towards the periphery until P14 at which point the entire retina had differentiated into several layers.

5.4.2 Digoxigenin-Labelled *in situ* Hybridisation

From P0 to P5, very faint labelling for Ang-2 mRNA expression was observed in the GCL and the anterior edge of the NBL which later differentiated into the INL (Figure 5.1, page 165). This labelling increased slightly on P6 to P9. On P10 to P14, the signal within the GCL and the INL was stronger in comparison to the earlier days, with maximum expression observed on P14. Hence, Ang-2 mRNA levels increased steadily from P0 to P14.

5.4.3 Radio-Labelled *in situ* Hybridisation

In comparison to digoxigenin-labelled probes, radio-labelled probes are more sensitive for the detection of mRNA. Thus, to confirm the results obtained with the digoxigenin-labelled probe *in situ* hybridisation was performed on wax sections of day 7 and day 14 retinas using a [^{35}S]-labelled probe. First radio-labelled VEGF probe was used as a positive control (Figure 5.2, page 166). VEGF expression was high in both the GCL and the INL on P7, when the vasculature of both the superficial

and deep layer was forming. On day 14, VEGF expression was very low because retinal vessel formation of both layers was complete.

Ang-1 mRNA expression, as shown in Figure 5.3 (page 167), was low on day 7 but high on day 14, suggesting that Ang-1 exerted an effect during the later stages of retinal development. However, the sections stained with the sense probe (as a negative control) also showed high Ang-1 expression on day 14, indicating that the expression seen with the antisense probe was a result of high background or non-specific staining. The low signal observed on day 7 may simply be due to insufficient probe applied to the slide.

Ang-2 labelling was similar on day 7 and day 14 (Figure 5.4, page 168). Again the sense probe showed high staining, therefore, the signal observed was mostly, if not entirely, non-specific.

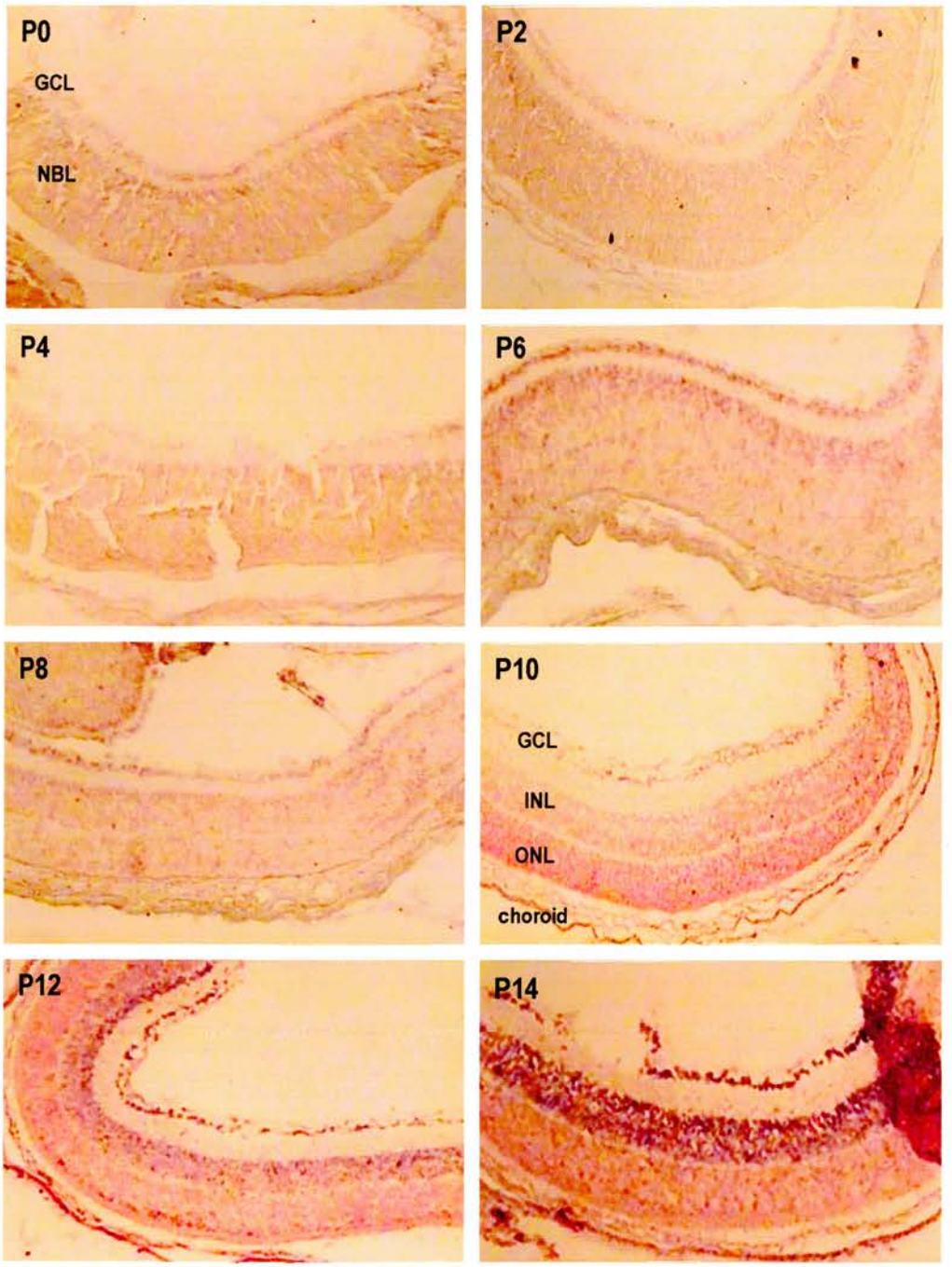

Figure 5.1 Expression of Ang-2 mRNA during formation of the rat retina.
10μm frozen sections stained with digoxigenin-labelled Ang-2 probe (purple) and counterstained with nuclear fast red (pink).
GCL - ganglion cell layer; INL - inner nuclear layer; NBL - neuroblast layer; ONL - outer nuclear layer; P - postnatal day.
Magnification: x20.

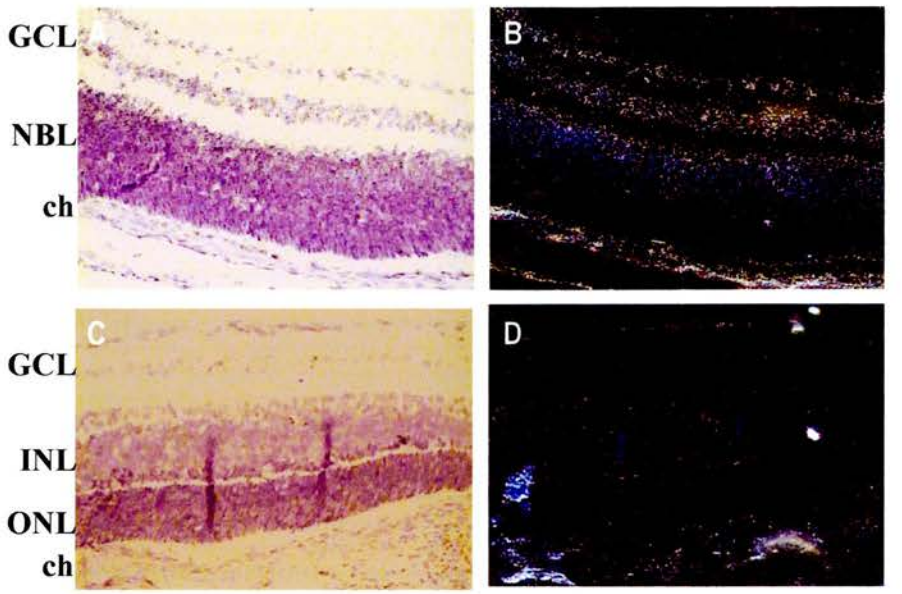

Figure 5.2 Expression of VEGF mRNA in the rat retina.
5μm wax sections of the rat retina stained with [^{35}S]-labelled VEGF probe and counterstained with hematoxylin and eosin. (A) P7 retina viewed under light-field conditions to show retinal morphology. (B) Image A viewed under dark-field conditions to show labelling with VEGF probe. (C) P14 retina viewed under light-field conditions. (D) Image C viewed under dark-field conditions.
ch - choroid; GCL - ganglion cell layer; INL - inner nuclear layer; NBL - neuroblast layer; ONL - outer nuclear layer.
Magnification: x20.

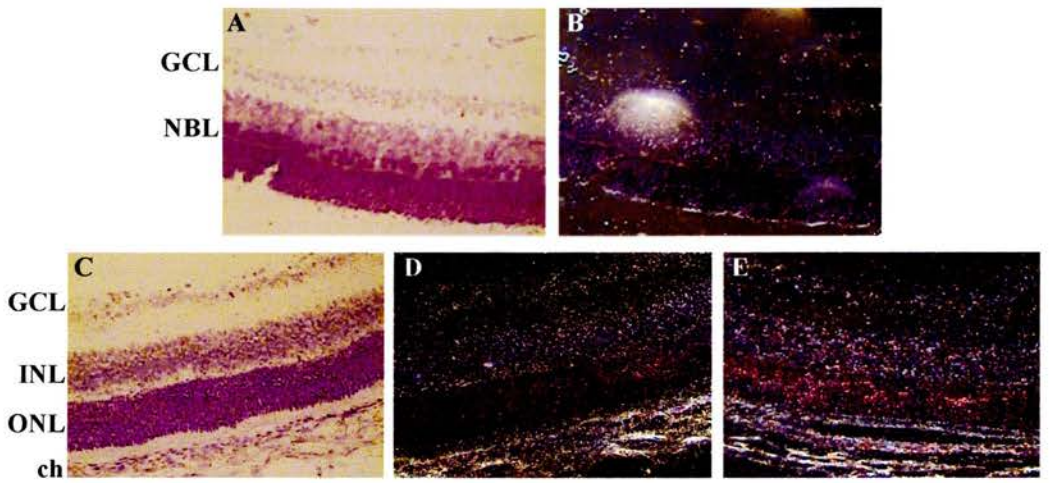

Figure 5.3 Expression of Ang-1 mRNA in the rat retina.
5μm wax sections of the rat retina stained with [^{35}S]-labelled Ang-1 probe and counterstained with hematoxylin and eosin. (A) P7 retinal section viewed under light-field conditions to show retinal morphology. (B) Image A viewed under dark-field conditions to show labelling with Ang-1 probe. (C) P14 retinal section viewed under light-field conditions. (D) Image C viewed under dark-field conditions. (E) Negative control. P14 retinal section labelled with Ang-1 sense probe and viewed under dark field conditions.
ch - choroid; GCL - ganglion cell layer; INL - inner nuclear layer; NBL - neuroblast layer; ONL - outer nuclear layer.
Magnification: x20.

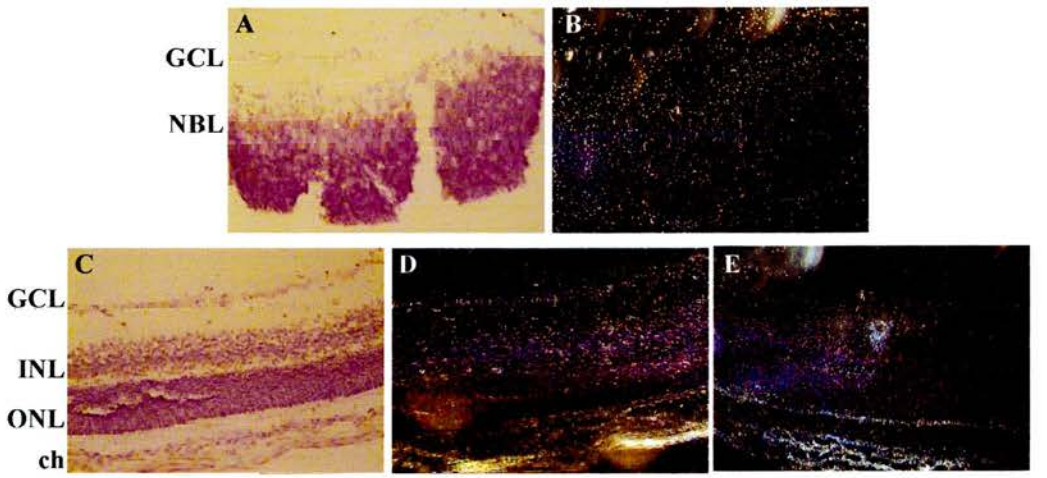

Figure 5.4 Expression of Ang-2 mRNA in the rat retina.
5µm wax sections of the rat retina stained with [^{35}S]-labelled Ang-2 probe and counterstained with hematoxylin and eosin. (A) P7 retina viewed under light-field conditions to show retinal morphology. (B) Image A viewed under dark-field conditions to show labelling with Ang-2 probe. (C) P14 retina viewed under light-field conditions. (D) Image C viewed under dark-field conditions. (E) Negative control. P14 retinal section labelled with Ang-2 sense probe and viewed under dark field conditions.
ch - choroid; GCL - ganglion cell layer; INL - inner nuclear layer; NBL - neuroblast layer; ONL - outer nuclear layer.
Magnification: x20.

5.5 DISCUSSION

5.5.1 The Ang/Tie-2 System

In vessel formation

Targeted disruption of the Ang-1 and Tie-2 gene in the mouse revealed that this ligand-receptor system is not required for the early stages of vasculogenesis (which involves endothelial cell differentiation and proliferation), but is essential for correct vascular assembly, maintaining endothelial cell and matrix associations and for the recruitment of mural cells [Sato et al., 1995; Suri et al., 1996]. In comparison, Ang-2 is a naturally occurring antagonist for Ang-1 [Maisonpierre et al., 1997], and therefore, may counteract Ang-1 mediated blood vessel stability and maintain the endothelium in a more plastic state to promote angiogenesis.

The effects of oxygen

In vitro studies have reported that the angiopoietins and the Tie-2 receptor are regulated by oxygen concentration. Exposure of cultured endothelial cells to hypoxic conditions resulted in a time-dependent increase in Ang-2 mRNA expression [Mandriota and Pepper, 1998; Oh et al., 1999] and Tie-2 expression [William et al., 2000]. The up-regulation of Tie-2 was reversible upon reoxygenation of the cells. Although Ang-1 mRNA expression was also investigated, the effects of oxygen tension on Ang-1 expression could not be commented on since Ang-1 was neither detected in the control nor in the treated cultures [Mandriota and Pepper, 1998].

Further support for the regulation of the angiopoietins by oxygen came from *in vivo* studies that used the Smith model of oxygen-induced retinopathy [Oh et al., 1999; Hackett et al., 2000]. In this model mice were exposed to 75% oxygen from P7 to P12 and then transferred to room air to induce neovascularisation [Smith et al., 1994]. During the ischemic period, the retinal Ang-2 mRNA levels were increased [Oh et al., 1999; Hackett et al., 2000]. In contrast, Ang-1 was down-regulated on the

first day of the hypoxic period, up-regulated for the following two days and then down-regulated again [Oh et al., 1999]. In another study adult rats were exposed to 10% oxygen for 12 or 48 hours [Abdulmalek et al., 2001] and it was found that the expression levels of Ang-1 mRNA in the cerebellum had decreased, and Ang-2 mRNA had risen in the hypoxic compared to the control group.

The data from the above mentioned studies suggest that the ratio of Ang-1:Ang-2 may be critical for establishing vascular integrity and that this ratio may be altered in response to oxygen changes. It is proposed that in ROP the vessels either have a reduced pericyte coverage (Chapter Two) or completely lack a pericyte coverage [Patz, 1982]. To establish if the Ang-1:Ang-2 ratio is altered in ROP I decided to investigate the retinal mRNA expression of both ligands in normal rats and rats raised in the Edinburgh ROP model.

5.5.2 Ang-2 mRNA Expression in Retinal Development

Using a digoxigenin-labelled Ang-2 probe, *in situ* hybridisation was performed on whole eye sections of the rat. When the probe was prepared at a concentration of 100ng/ml, no staining was detected, except in the choroidal vessels. The concentration of the probe was then increased to 150ng/ml and the results illustrated in Figure 5.1 were obtained (page 165). Ang-2 expression was noted on all days; the signal was low during the early stages of development and increased as retinal formation progressed.

These results differ from those reported previously. Oh et al. looked at the expression of Ang-2 mRNA on P12, P17 and P21 in the mouse. Using a digoxigenin-labelled probe at a concentration of 50ng/ml, a low signal was observed in the GCL and INL on all three days [Oh et al., 1999]. In another study, Hackett and co-workers generated mice with targeted disruption of the Ang-2 gene where the gene expressed β-galactosidase under control of the Ang-2 promoter. In these mice, Ang-2 mRNA labelling was low during the early stages of vascular development, but

intense in the INL on day 8 (when the deep capillary bed was forming). This expression decreased again by day 12 and further still by day 14 [Hackett et al., 2000].

The conflicting results may simply be the result of species difference, however this is unlikely because retinal formation is very similar in rats and mice. The next possibility is that my *in situ* hybridisation technique was flawed. Therefore, the methodology used here was compared to that in the literature, but no obvious discrepancies were noted. In addition, the digoxigenin-labelled *in situ* hybridisation method used in this study had been performed in this laboratory on several occasions; primarily for detection of VEGF, which is abundantly expressed in the retina. Figure 5.5 (page 172) shows that on P14 VEGF was detected only in the INL towards the periphery where the formation of the deep plexus is almost complete. In comparison, VEGF levels in the retina of the P14 pups exposed to the 8kPa regime of the Edinburgh Model were markedly increased.

Finally, it is possible that the staining which developed was the result of applying a very high probe concentration. Other researchers have found that the use of digoxigenin-labelled probes in conjunction with alkaline phosphatase coupled anti-digoxigenin antibodies is a relatively insensitive *in situ* hybridisation method (personal communication, Stan Weigand, Regeneron Pharmaceuticals, NY, USA). While it is quite suitable for detection of precise localisation of abundantly expressed mRNAs, it is less useful for *in situ* localisation of mRNAs which are expressed at low to moderate levels. This method is prone to produce artefact when it is 'pushed'.

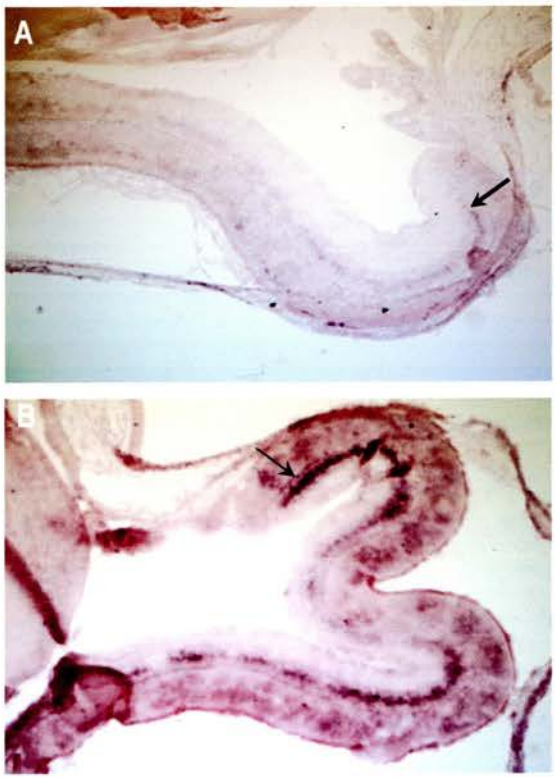

Figure 5.5[1] Expression of VEGF mRNA on P14.
10μm frozen sections of the rat retina stained with digoxigenin-labelled VEGF probe (purple) and counterstained with nuclear fast red (pink). (A) P14 retina of a control pup. (B) P14 retina of a pup exposed to the 8kPa oxygen regime of the Edinburgh ROP model. Arrows indicate staining in inner nuclear layer.
Magnification: x20.

[1] Taken, with permission, from Jean Wade.

Thus, *in situ* hybridisation was performed using Ang-1 and Ang-2 probes labelled with [^{35}S]-UTP [2], a more sensitive technique for the detection of mRNA. Positive Ang-2 expression was not observed on either P7 nor on P14, which showed that the digoxigenin-labelling (which was most intense on P14) may indeed be incorrect. Additionally, the expression of Ang-1 was looked into with the hope that its expression levels may be detected instead. Unfortunately, any staining that resulted was non-specific. These findings suggest that retinal expression of the angiopoietins is too low for detection using *in situ* hybridisation methods.

5.5.3 Alternative Detection Methods for the Angiopoietins

Studies in the literature that investigated the mRNA expression of the angiopoietins have used either reverse transcriptase-polymerase chain reaction (RT-PCR) or Northern blotting, presumably due to the relatively low abundance of these transcripts in retinal tissue. In an attempt to investigate the Ang-1:Ang-2 ratio in normal development, Northern blot analysis was first considered. In a study conducted by Hackett and colleagues, Ang-2 expression was detected using 10μg of total RNA, but Ang-1 expression remained undetected. Thus, I decided to use 20μg of total retinal RNA with the hope that Ang-1 expression may also be detected. The total retinal RNA of a few rat pups was extracted using an RNA extraction kit (Qiagen, LTD) according to the manufacturer's instructions. Less than 10μg of total RNA was obtained from a single retina. Therefore, because too many animals would be required, this method of mRNA extraction was abandoned. One technique which would overcome this problem of animal numbers is RT-PCR. In brief, this involves using a reverse transcriptase enzyme that catalyses the conversion of RNA to DNA. Next using a PCR thermocycler the DNA sequence is amplified by repeatedly 'running off' copies of the sequence using a Tag DNA polymerase. Thus, from a small quantity of tissue, adequate amounts may be easily obtained. Unfortunately, the laboratory was not equipped with the appropriate apparatus for this technique. In addition to these difficulties, Northern blotting is a very complicated technique to

[2] As mentioned in the Methods, this was conducted by Helen Wilson because our laboratory was not equipped for use of radioactive isotopes.

establish and would, therefore, be very time consuming. Finally, this technique involves high costs. Thus, detection of the levels of Ang-1 and Ang-2 expression by Northern blot analysis was not considered any further.

The remaining possibility was the investigation of the protein expression of Ang-1 and Ang-2 which has an advantage over mRNA detection in that contamination of samples is not a problem. When this study was conducted (in 2000) the availability of antibodies for the angiopoietins was limited. For example, Santa Cruz offered an antibody for Ang-1 that was reactive with human, rat and mouse tissue, but also detected the expression of the other angiopoietin isoforms. An Ang-2 specific antibody was also available, but it was only weakly reactive with tissues of rat origin. However, recently this company has produced type-specific antibodies that are reactive with rat material and can be used in many procedures including Western blotting and ELISA analysis. Therefore, this study could have been conducted now, but due to time limitations it was not possible.

Thus, because attempts to detect the mRNA expression by *in situ* hybridisation were unsuccessful and alternative techniques had the above-mentioned drawbacks, this study was abandoned.

CHAPTER SIX

TESTING THE EDINBURGH ROP MODEL

6.1 INTRODUCTION

6.1.1 Retinopathy of Prematurity and the Clinical Situation

In the 1950s, extreme prematurity together with high concentrations of supplemental oxygen during the first few weeks of life were firmly established as risk factors for retinopathy of prematurity (ROP) [Campbell, 1951; Patz, Hoeck and Cruz, 1952]. In an attempt to reduce the incidence of this disease, the use of oxygen therapy on neonates was restricted. Although this resulted in a reduction in the number of infants developing the retinal disorder [Cross and Evans, 1952; Ryan, 1952; Guy, Lanman and Dancis, 1956], the limited use of supplemental oxygen led to an increase in infant mortality [Avery and Oppenhiemer, 1960]. Thus, in the 1970s the use of oxygen was reintroduced with a reoccurrence of ROP [reviewed in Weakley and Spencer, 1992; and in Ziavras and Javitt, 1995].

Today, in high income countries because more immature babies are surviving due to advanced neonatal care, the incidence of ROP has remained high. This is despite the ability of neonatal intensive care units to control more carefully the levels of oxygen at which the infants are maintained [Cunningham et al., 1995; The STOP-ROP Multicenter Study Group, 2000]. Fortunately, in most cases the disease spontaneously regresses without scarring or causing visual impairment. In America around 85% of premature survivors born at less than 28 weeks gestation develop the disorder. Around 20% of these infants develop loss of vision [Palmer et al., 1991; Cryotherapy for Retinopathy of Prematurity Cooperative Group, 1994]. Using the Oxford Register of Early Childhood Impairment, Crofts and colleagues gathered information on all babies with severe visual impairment born between 1984 and 1988. This sample was considered representative of the United Kingdom. Of the 166 children with severe vision loss diagnosed by the age of 5 years (1.25 per 1000 births), 5.4% suffered from blindness due to ROP [Crofts, King and Johnson, 1998]. Others have reported a slightly higher incidence of the disorder in the UK [Rogers, 1996; Dezateux and Rahi, 1998].

In comparison to high income countries, the incidence of severe ROP and blindness due to retinal detachment is markedly higher in middle income countries, such as Latin America [Sirtautiené, 1997] and Eastern Europe [Gilbert et al., 1997]. In these countries, although advanced neonatal care permits the increased survival of preterm babies, the health resources are relatively limited and neonatal care is less than ideal. As a result, around 40% of infants with severe ROP develop some degree of visual impairment.

In low income countries, no cases of blindness due to ROP were reported by Gilbert et al. [1997]. Unfortunately, such countries have a low health care provision and lack the facilities to support the survival of babies born prematurely. Hence, few preterm babies survive to develop the disease.

6.1.2 Conventional Animal Models of Oxygen-Induced Retinopathy

Preterm infants with severe ROP, which is characterised by retinal neovascularisation, develop the disorder whilst still receiving supplemental oxygen therapy. As discussed earlier, upon transfer to room air the disease usually regresses and the retinal vasculature appears normal, but in some cases the neovascularisation can progress further to cause retinal detachment and blindness.

In animal models of oxygen-induced retinopathy, hyperoxia alone does not result in retinal neovascularisation, rather a short room air recovery period (relative hypoxia), after the hyperoxic exposure is essential for inducing the profuse growth of the retinal vessels into the vitreous. This was first demonstrated by Ashton and colleagues [Ashton, Serpell and Ward, 1954; Ashton, 1966; Ashton, Garner and Knight, 1971]. Their studies found that animals subjected to extreme concentrations of oxygen developed complete vaso-obliteration of the retinal vessels. When the animals were returned to room air, the obliteration was irreversible in a majority of the vessels and a profuse outgrowth of vessels took place. This outgrowth comprised of numerous corkscrew (endothelial cell) proliferations extending from the retinal surface into the vitreous, mimicking the human disease.

Several animal models of oxygen-induced retinopathy have since been developed [Flower and Blake, 1981; Chan-Ling et al., 1992; Penn, Tolman and Lowery, 1993; Penn, Henry and Tolman, 1994; Penn, Tolman and Henry, 1994; Smith et al., 1994]. As discussed in detail in Chapter One, each of these models use a different oxygen regime to halt the normal process of retinal vascularisation, and depend on a relative hypoxic period (room air recovery) to induce neovascularisation. The duration of this relative hypoxic period is crucial as shown by Smith and by Penn. The Smith model involves placing mice at postnatal day 5 (P5) in constant 75% oxygen until P12 to induce sufficient vaso-obliteration. The animals are then returned to room air where maximum neovascularisation occurs between P17 and P21 (five to nine days of hypoxia). With a longer period in room air, the neovascularisation eventually regresses and the vasculature essentially appears normal [Smith et al., 1994]. In one

of Penn's model of oxygen-induced retinopathy, newborn rat pups are switched between 80% and 40% oxygen every 12 hours until P14. When the animals are killed immediately on removal from oxygen, no neovascularisation is observed. With two days of room air recovery, some neovascularisation is noted, but the greatest incidence occurs with a period of four days in room air. By the seventh day, the neovascularisation decreases possibly due to spontaneous resolution of the pathology [Penn, Tolman and Lowery, 1993].

6.1.3 Neovascularisation in the Edinburgh Model?

The Edinburgh model of ROP was developed since the typical models of oxygen-induced retinopathy did not represent the oxygen environment experienced by a premature ventilated infant. Infants are no longer maintained in high oxygen (70-80%) nor does their oxygen environment switch between high and low levels on a regular basis. Instead the arterial oxygen levels of the babies are constantly fluctuating between clinically 'safe' limits [Cunningham et al., 1995]. Thus, the first 14 days of the transcutaneous oxygen profile of a preterm infant who developed severe ROP was selected and translated into percentage inspired oxygen to produce equivalent arterial oxygen levels in the rat. Rat pups exposed to this clinically relevant profile, which had a mean oxygen concentration of 21.3%, developed features of ROP [Cunningham et al., 2000].

The drawback of the Edinburgh model is that, unlike the conventional oxygen-induced retinopathy models, the retinas of this model do not develop neovascularisation. Instead lectin-positive tufts, called abnormal terminal vessels, form at the vascular/avascular junctions (Figure 6.1, page 180).

When the profile is set to fluctuate around a mean of 8kPa, only 21% of the retinas are identified as having abnormal terminal vessels, but when the oxygen fluctuated around a mean of 10kPa, 42.5% of the retinas are affected [McColm et al., 2004]. Thus, a higher mean oxygen level results in an increase in the number of retinas with

abnormal terminal vessels. It is suggested that these tufts represent the initial stages of neovascularisation (precursors) or that they are simply the proliferating endothelial cells at the leading edge of the retinal vasculature. The origin and role of these tufts may be better understood by either exposing pups to the oxygen profile for a longer period of time, or by placing the pups into room air after oxygen treatment.

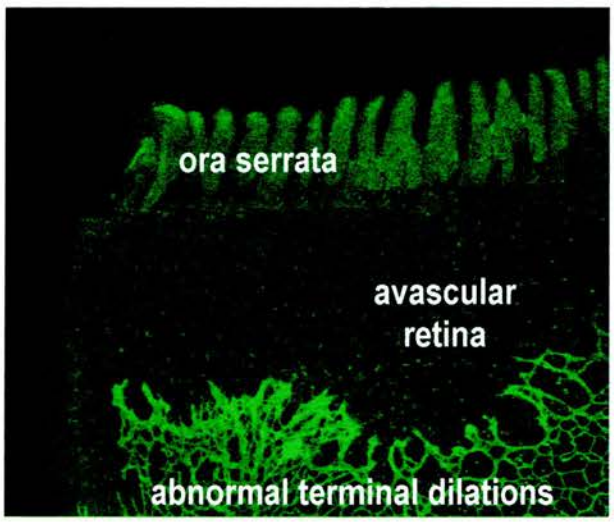

Figure 6.1 Abnormal terminal vessels.
P14 retina exposed to the 8kPa minute variable oxygen profile.

6.2 AIMS AND HYPOTHESIS

The lack of neovascularisation in the Edinburgh model may be seen as indicating a poor model of ROP. Therefore, the aim of the work discussed in this chapter was to establish whether the Edinburgh model simply delays retinal vascularisation, or if the model is capable of inducing retinal neovascularisation. In order to determine this, two additional regimens were used; newborn pups were either exposed to the variable oxygen for a longer period of time (until P18) or returned to room air after 14 days of oxygen exposure.

Since the oxygen regimen of the Edinburgh model consists of frequent small fluctuations in inspired oxygen levels, it does not produce severe retinopathy as in the traditional models. Thus, it is proposed that with 18 days of variable oxygen exposure retinal vascular changes of the Edinburgh model would still be observed, namely altered capillary density, increased peripheral avascularity and the formation of abnormal terminal vessels; however, the extent of these vascular changes may be reduced in comparison to the pups exposed to the variable oxygen profile for 14 days alone. With a period of room air recovery, retinal neovascularisation may be observed. On-the-other-hand, this period in room air may result in the resolution of the disease.

6.3 METHODS

6.3.1 Experiments

Five animal groups were analysed, two of which were reared in room air and three raised in the minute-to-minute variable oxygen profile set at 8kPa [described in Chapter One and in Cunningham et al., 2000]:

- P14 control[1] - pups were raised in room air until postnatal day 14
- P18 control - pups were raised in room air until postnatal day 18
- P14 8kPa[1] - pups were exposed to the variable oxygen regime from birth to postnatal day 14
- P18 8kPa - pups were exposed to the variable oxygen regime which had been extended to run until postnatal day 18. This was accomplished by running the profile from day 0 to day 10 without interruption, and then running the oxygen profile form day 11 to day 14 twice
- P14 8kPa + 4d RA - pups were raised in the variable oxygen regime from birth until postnatal day 14 and then transferred to room air for four days.

A minimum of 12 Sprague-Dawley pups was required per litter and three litters were analysed per group. The rat pups were first weighed and then anaesthetised, perfused and killed as described in Chapter Two. Both eyes were enucleated; the right was fixed in 2% paraformaldehyde for 2 hours, the retinas dissected and stained for endothelial cells, whilst the left was dissected fresh and stored at -70°C for any possible future studies.

6.3.2 Lectin Staining

Endothelial cells were visualised by incubation with *G. simplicifolia* (Bandeiraea) isolectin B4 as follows. The flattened wholemounted retinas were fixed in 70%

[1] These experiments had been conducted earlier by the ROP research group at the Department of Child Life and Health.

ethanol for 20mins (-20°C), and then permeabilised in 1M PBS/1% Triton X-100 for 30mins. Biotinylated *G. simplicifolia* (Bandeiraea) isolectin B4 (Vector Laboratories) was prepared in 1M PBS/1% Triton X-100 at a 1:50 dilution, and applied to the wholemounts overnight at 4°C. The following day, the retinas were washed three times in 1M PBS/1% Triton X-100 for 10mins each. The tissues were then incubated at room temperature in streptavidin-conjugated flourescein (Vector Laboratories) at a dilution of 1:100 prepared in 1M PBS/1% Triton X-100 for 2 hours. The tissues were again washed three times in 1M PBS/1% Triton X-100 for 10mins each. Finally, the wholemounts were mounted in PBS:glycerol (1:1) and the coverslip sealed with nail varnish.

6.3.3 Analysis

Confocal microscopy

The stained, flatmounted retinas were viewed using an argon krypton laser confocal microscope (Leica Microsystems, Germany) excited at 488nm (filter BP 525/50). Images of each retinal quadrant were taken at x2.5 and x10 magnification and digitally stored for later analysis.

Capillary density

Capillary bed areas were chosen within the mid-periphery of the retina, and where possible major vessels (arterioles and venules) were not included in the field of view. Because each retina was divided into four quadrants, an image of each quadrant was scanned at x10 magnification. Using the Image Tool Software (designed by the University of Texas, Health Sciences Center, San Antonio), the retinal capillary branches of each quadrant were marked and counted. An average was then calculated for each retina which represented the capillary density. Some retinas were recounted to validate the results.

Avascular area

Images of the whole retinal quadrant (at 2.5x magnification) were saved and the total retinal area and peripheral avascular area were measured using Scion Image Software (Scion Corporation, USA). The avascular area of each retina was then expressed as a percentage of the total retinal area.

Abnormal terminal vessels

Each retina was carefully examined for abnormal terminal blood vessels at the vascular/avascular junction and simply graded 0 or 1 for the absence or presence of these vessels, respectively[2]. The number of retinas with abnormal terminal vessels within each experimental group was then expressed as a percentage.

Statistics

Summary statistics are presented as median (interquartile range). Comparisons between the groups were made by Mann Whitney U correlation using the SPSS statistics package (SPSS, Inc., Chicago, USA).

[2] This analysis was conducted by Dr. Brian Fleck, an ophthalmologist and a member of the ROP research group.

6.4 RESULTS

The results for all five groups are given in Table 6.1. Two methods of assessing the changes in the vasculature are described; capillary density (branches/mm^2) and peripheral avascularity expressed as a percentage of the total retinal area. In addition, the retinal wholemounts were examined for the presence of abnormal terminal vessels.

	P14 Control	P18 Control	P14 8kPa	P18 8kPa	P14 8kPa + 4d RA
Sample number	27	32	28	28	32
Median capillary density (branches/mm^2)	194.6 (180.4 - 206.1)	175.4 (169.9 - 187.2)	183.1 (162.7 - 196.4)	169.9 (155.2 - 183.8)	181.5 (174.4 - 194.1)
Median retinal avascularity (%)	0.0 (0.0 - 0.0)	0.0 (0.0 - 0.0)	1.7 (0.0 - 7.6)	0.0 (0.0 - 0.7)	0.0 (0.0 - 0.0)
% of retinas with abnormal terminal vessels	0	0	21.4	10.7	0

Table 6.1 Results of the retinal analysis.
The interquartile range is given in parenthesis.

6.4.1 Capillary Density

The retinal capillary density of pups raised in room air until P14 was greater than those raised in room air until P18. The difference between these two groups was statistically significant ($p<0.001$). Although the number of capillary branches per mm^2 in the retinas of the P14 8kPa group was less than that of the P14 control group, the difference was not statistically significant. This was also the case when the capillary density of the P18 8kPa group was compared to that for the P18 control group.

Representative images of the retinal capillary beds from each group are shown in Figure 6.2 (page 188). The retinas of the P14 8kPa + 4d RA pups had a median capillary density less than the P14 control (significant at $P<0.05$), but greater than the P18 control (not significant). The capillary density value calculated for this group was very close to that for the P14 8kPa group.

6.4.2 Peripheral Avascularity

As expected, retinas of the P18 control pups were fully vascularised (Figure 6.3, page 188). However, a small proportion of the P14 control group had a slight peripheral avascular area (average 0.22%, median 0%). In comparison, most retinas (20 out of 28) of the P14 8kPa group had some extent of peripheral avascularity. On average 4.6% of the total retinal area was non-vascularised (median 1.7%). Fewer retinas of the P18 8kPa group had an avascular area, with an average of 0.3% and a median of 0%. Thus, the peripheral avascularity of both the P14 8kPa and P18 8kPa retinas were significantly greater than the 14 controls and P18 control retinas, respectively. In the P14 8kPa + 4d RA group only 7 of the 32 retinas examined had peripheral avascularity. The average of this group was 0.2% and the median was 0%, values very similar to the P14 controls, but significantly greater than the P18 controls ($p<0.005$).

6.4.3 Abnormal Terminal Vessels

As in the original Edinburgh model study [Cunningham et al., 2000], no neovascularisation was noted in any of the groups investigated here. However, abnormal terminal vessels were observed in both the P14 8kPa (21%) and P18 8kPa (11%) groups. Abnormal terminal vessels were not present in any of the control and P14 8kPa + 4d RA retinas.

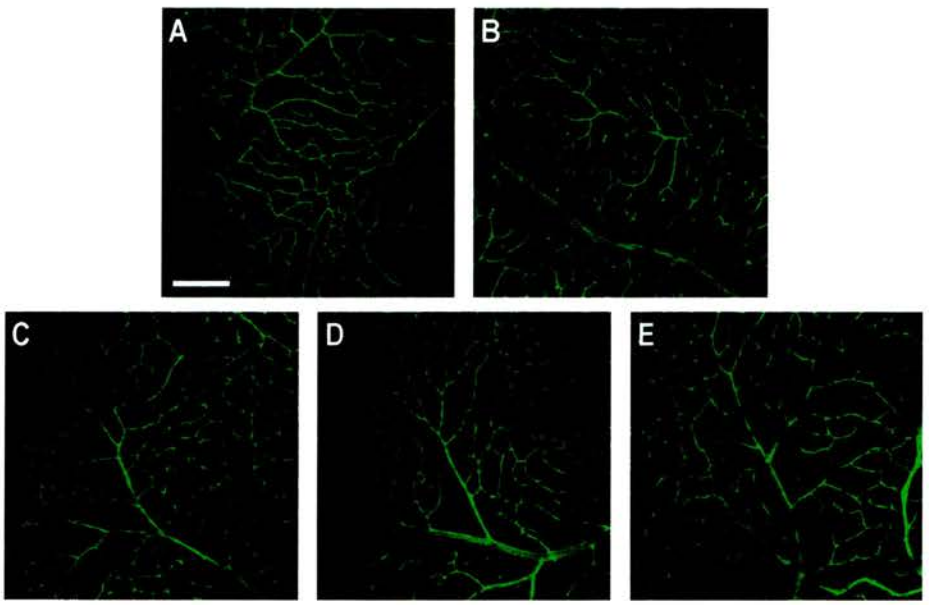

Figure 6.2 The retinal capillary bed of all groups.
(A) P14 Control. (B) P14 8kPa. (C) P18 Control. (D) P18 8kPa. (E) P14 8kPa + 4d RA. Scale bar: 200μm.

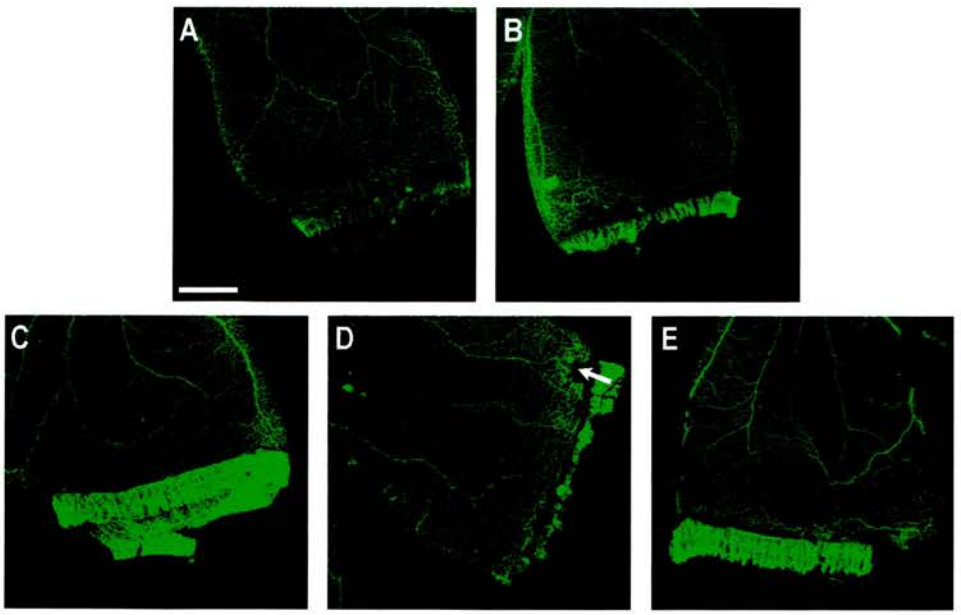

Figure 6.3 Extent of peripheral avascularity of all groups.
(A) P14 Control. (B) P14 8kPa. (C) P18 Control. (D) P18 8kPa. Abnormal terminal vessels were also observed in this retina (arrow). (E) P14 8kPa + 4d RA. Scale bar: 800μm.

6.5 DISCUSSION

6.5.1 Normal Retinal Vessel Development

Under normal conditions retinal vascular development of the rat is usually complete by day 14 [Penn, Tolman and Lowery, 1993; Holmes, Duffner and Kappil, 1994], however, the results of this study suggest that some further vascular development occurs between P14 and P18. Firstly, all of the retinas of the P18 control group were fully vascularised, whereas a few of the P14 controls still had a small peripheral avascular area. Secondly, there was a significant reduction in the capillary density of the P18 controls compared to the P14 controls suggesting that the capillary network underwent some further remodelling.

6.5.2 Neovascularisation in the Model

It is suggested that the abnormal terminal vessels in the P14 8kPa group may either be proliferating endothelial cells at the advancing edge of the vasculature or may represent precursors of pathologic neovascularisation [Cunningham et al., 2000]. If the former is true, then the small tufts would be observed at the vascular/avascular junction at all stages of retinal development. However, in the P2 and P7 retinas that were double stained for endothelial cells and mural cells (Chapter Two), no such structures were observed. There is, however, some support for the suggestion that the tufts may be precursors of neovascularisation. Firstly, the tufts occurred at the vascular/avascular junction where neovascularisation develops in other rat models [Penn, Henry and Tolman, 1994; Penn, Tolman and Henry, 1994]. Secondly, the proportion of retinas with abnormal terminal vessels increased as the insult increased (21% in 8kPa and 42% in 10kPa [McColm et al., 2004]). Thirdly, in a model where the oxygen concentration cycled between 80% and 20% every 12 hours (oxygen-induced retinopathy), 73% of the retinas were affected with abnormal terminal vessels [Cunningham et al., 2000]. This value is very similar to that quoted by Penn for the 80/40% model where neovascularisation developed in 72% of the retinas [Penn, Henry and Tolman, 1994].

If the small tufts are neovascular precursors, then this model would have greater clinical relevance since infants develop neovascularisation whilst still ventilated. Therefore, the aim of the experiments described in this chapter was to establish if these tufts developed into neovascular vessels with a prolonged oxygen treatment or with post-exposure room air maintenance (relative hypoxia).

6.5.3 Effects of Prolonged Oxygen Treatment

The 14 day profile of the model was extended to run for 18 days. This was accomplished by repeating the oxygen data of days 11 to 14. Thus, from birth to P10, the pups were exposed to the 24 hour data corresponding to the equivalent days, i.e. days 0 to day 10. But from P11 to P18, the oxygen profile of days 11 to 14 ran for 48 hours each, i.e. on P11 and P12 the pups were exposed to the data of day 11, on P13 and P14 the pups were exposed to that of day 12, and so on.

Raising pups in this regime resulted in a slight reduction in the capillary density in comparison to P18 controls. Some of the retinas also had a peripheral avascular area, although markedly less than the P14 8kPa group. There was also a fall in the proportion of retinas with abnormal terminal vessels; only 11% of the retinas had abnormal vessels. If the abnormal terminal vessels are precursors of neovascularisation, then the pathology spontaneously regressed in 89% of the retinas, a proportion similar to that of infants in developing countries who develop ROP but is naturally corrected. Hence, the extended variable oxygen profile still produced features of ROP, suggesting that the Edinburgh model is not simply a model of delayed retinal vessel development.

6.5.4 Effects of Transfer to Room Air

In the original experiments of the Edinburgh model, the pups were not transferred to room air after oxygen exposure [Cunningham et al., 2000]. Ventilated infants are not abruptly switched from a high oxygen environment to normoxia, instead they are

gradually reintroduced to room air by withdrawing them from oxygen. Thus, it was felt that post-exposure room air maintenance would not reflect the clinical set up.

Animal studies investigating 'oxygen weaning' have produced conflicting results. Phelps and Rosenbaum induced retinopathy in kittens and then gradually lowered the oxygen concentration within the chamber to room air over a period of a few weeks. They reported that the retinas of the kittens raised in this regimen were not appreciably different to those exposed to high oxygen and then transferred to room air [Phelps and Rosenbaum, 1987]. Chan-Ling and colleagues also exposed kittens to high oxygen for several days and then gradually lowered the oxygen concentration until the kittens were four weeks of age. Some of the regimes tested by the researchers actually offered some degree of protection in the long term and the formation of the pre-retinal vessels was effectively prevented by supplemental oxygen therapy [Chan-Ling, Gock and Stone, 1995].

In the experiments described here, it was felt that 'oxygen weaning' was not necessary since the profile fluctuated at a mean of 21% and the minute-to-minute changes between day 12 and day 14 were very small in comparison to the changes during the earlier days. Thus, animals were transferred directly into room air on P14 to investigate if the retinal vasculature 'normalised' or developed neovascularisation. The animals were given four days of recovery after 14 days of oxygen exposure in keeping with other animal models [Penn, Tolman and Lowery, 1993; Penn, Henry and Tolman, 1994; Penn, Tolman and Henry, 1994; Chan-Ling et al., 1992].

The retinal vasculature of the pups exposed to this regimen appeared no different to P14 control retinas; the capillary density and extent of avascularity were very similar in both groups and no abnormal terminal vessels were observed. Thus, four days of room air exposure may have resulted in 'normalisation' of the retinal vasculature.

In conclusion, the Edinburgh model of ROP does not produce the same extent of avascularity as the conventional models nor does it induce neovascularisation with a longer exposure to the oxygen regime or with a period of relative hypoxia. It is possible that neovascularisation did occur in both of the groups analysed in this study, but an extended period of four days of oxygen or room air was too long and the retinal vasculature normalised. A shorter duration of 12 or 24 hours may instead result in neovascularisation. Thus, the Edinburgh model would benefit from further manipulation of the data in order to induce neovascularisation, but still keeping the oxygen environment within clinical levels.

CHAPTER SEVEN

DISCUSSION

7.1 VESSEL STABILITY IN THE EDINBURGH MODEL OF ROP

During the early stages of vasculogenesis, angioblasts differentiate into endothelial cells that proliferate to form a primary vascular network [reviewed in Risau, 1997]. During the later stages, this network matures by rapidly remodelling into large and small vessels [reviewed in Risau, 1997], and develops a coverage by mural cells [Rhodin, 1968]. Mural cell coverage has been suggested to signal the stability of blood vessels [Kuwabara and Cogan, 1963; Speiser, Gittelsohn and Patz, 1968; Crocker, Murad and Geer, 1970; Tilton et al., 1985; Orlidge and D'Amore, 1987]. Several growth factors, including platelet-derived growth factor (PDGF) [Lindahl et al., 1997], transforming growth factor-β (TGF-β) [Antonelli-Orlidge et al., 1989a], and the angiopoietins [Suri et al., 1996], are implicated in regulating vessel stabilisation. In retinopathy of prematurity (ROP), the retinal vessels either lack support cells or have a limited coverage of support cells. Consequently, the retinal capillaries are susceptible to injury by hyperoxia and prone to leakage [Patz, 1968].

The first purpose of the work detailed in this thesis was to investigate blood vessel stability during the normal development of the rat retina by studying the interaction between endothelial cells and mural cells, and the retinal expression of the above-mentioned growth factors. The second aim of this project was to determine if mural cell coverage and the expression of PDGF-B, TGF-β and the angiopoietins were affected by the fluctuating oxygen regime of the Edinburgh model of ROP.

7.1.1 Mural Cell Coverage

Pericytes and smooth muscle cells have been reported to express a number of proteins [Joyce, Haire and Palade, 1985; Nayak et al., 1988; Skalli et al., 1989; Mitchell et al., 1990; Schlingemann et al., 1990; Nehls, Denzer and Drenckhahn, 1992; Newcomb and Herman, 1993; Ehler et al., 1995]. However, the expression of only two mural cell markers, α-smooth muscle actin (α-SMA) and desmin, were investigated in the work reported here.

α-SMA expression increased progressively from P2 to P21 in the control retinas, but was seen only on the arterial vessels that had undergone remodelling. On P2, α-SMA positive cells were flat and lacked distinct structure, but by P14, the cells were elongated and spindle-shaped, and arranged perpendicular to the axis of the vessels. Thus, α-SMA stained the smooth muscle cells of the retinal vasculature. In contrast, desmin expression was observed on all vessels of the retina. On P2, desmin labelled very fine and long strands on the surface of the retinal vessels (which may be immature pericytes or undifferentiated precursor cells). However, by P7 the cells had gained the typical structure of pericytes; they were long and slender with numerous processes. Unlike the smooth muscle cells, the structure and orientation of the pericytes altered depending on their location. On the arterioles, the cells were long, thin, and encircled the wall of the vessel, whereas on the venules the cells had several processes (primary and secondary) and were arranged both perpendicular and parallel to the axis of the vessels. Occasional cells of the arterioles expressed both protein markers; some had the typical structure of smooth muscle cells whilst others

appeared more like pericytes. These cells were presumably the transitional pericytes, which may have the potential to differentiate into smooth muscle cells on demand.

In the Edinburgh model of ROP, there was a slight reduction in the expression of α-SMA. This reduction was most likely a result of the limited remodelling of the vasculature in response to the oxygen exposure. Desmin expression, however, was significantly reduced in the retinas of the oxygen treated pups. This reduction may be the result of reduced recruitment of pericyte precursor cells or apoptosis of some pericytes. Electron microscopic analysis showed that in some retinal vessels of the oxygen treated pups the structure of the pericytes was altered. The basement membrane was degraded and the pericytes were no longer within close proximity to the endothelial cells.

7.1.2 Platelet-Derived Growth Factor-B

PDGF-B released from endothelial cells promotes the proliferation of adjacent pericyte or smooth muscle cell precursors [Levéen et al., 1994; Soriano 1994, 1996; Beström et al., 1996]. Thus, PDGF-B, by binding to its receptor, signals the recruitment of pericytes to the endothelial tubules.

When Western immunoblotting of the retinal proteins was performed using a polyclonal antibody to PDGF-B, four proteins were detected. Although the two higher molecular weight proteins were not clearly identified, the lower molecular weight proteins were suggested to be the PDGF-B chain precursor and the PDGF-BB isoform. During normal development the expression of both proteins increased from P2 to P14 and remained high at P21. The expression on P2 and P7 was unaffected by the variable oxygen regime, however, with 14 days of exposure, the expression of both the PDGF-B chain precursor and PDGF-BB were reduced in comparison to the P14 control retinas.

7.1.3 Transforming Growth Factor-β_1

TGF-β_1 is suggested to play a role in vessel stabilisation as it inhibits the proliferation of both endothelial cells [Fràter-Schröder et al., 1986; Heimark, Twardzik and Schwartz, 1986] and mural cells [Majack, 1987; Owens et al., 1989; Verbeek et al., 1994; Schor et al., 1995], but promotes the differentiation of the mural cells [Shah, Groves and Anderson, 1996; Hirschi, Rohovsky and D'Amore, 1998].

In retinal vessel development, TGF-β_1 protein levels increased markedly from P2 to P7, but fell slightly on P14 and further on P21. Much of this detected protein was believed to be the latent form that converted into the active form during the preparation of the tissue samples. With immunohistochemical analysis, which only detected the active form of TGF-β_1, the expression of the protein increased from P2 to P14.

When compared to the controls, retinas of the pups raised in the variable oxygen regime had decreased expression of the protein at all timepoints examined, suggesting that either the secretion or the synthesis of the protein was reduced in response to fluctuating oxygen.

7.1.4 The Angiopoietins

The angiopoietins are critical for the maintenance of endothelial cell-matrix and endothelial cell-mural cell interactions [Sato et al., 1995; Suri et al., 1996; Maisonpierre et al., 1997]. Thus, the angiopoietins function during both the later stages of vasculogenesis and during angiogenesis.

Using both digoxigenin-labelled and radio-labelled probes I was unable to detect any expression of Ang-2. Thus, further investigation of the angiopoietins was abandoned, however, it had been previously reported that Ang-2 mRNA is low during the early and late stages of retinal vessel formation [Oh et al., 1999; Hackett

et al., 2000], but high during the middle period of retinal development (around P8) [Hackett et al., 2000].

7.1.5 Clinical Implications

The results of these studies suggest that blood vessel stability may be compromised by fluctuating oxygen levels. This compromised stability may cause the retinal vessels to become fragile and vulnerable to rupture and leakage. It may also underlie the process of neovascularisation since the vessels which burst into the vitreous probably sprout from vessels that have a reduced (or a lack of) pericyte coverage.

Therefore, using the Edinburgh model a potential targeting point for ROP would be to promote stability of the vessels by (1) increasing the recruitment of the pericyte precursors, (2) promoting their differentiation into mature pericytes or (3) preventing their apoptosis. Of course, further studies are required to determine which of these mechanisms are responsible for the reduced stability of the retinal vessels in the Edinburgh model.

As far as potential therapeutic agents are concerned, although PDGF-B and TGF-β induce pericyte recruitment and differentiation, respectively, the use of these may be limited in the treatment of ROP: firstly, administration of PDGF-B has been found to disrupt the association between endothelial cells and pericytes by causing the detachment of the pericytes from newly coated retinal vessels [Benjamin, Hemo and Keshet, 1998]; secondly, to date the effects of TGF-β administration on blood vessels has not been investigated. Recent studies have found that the acute administration of Ang-1 can protect the vasculature against leakage [Thurston et al., 2000; Xu, Zhang and Adelman, 2003] and reduce retinal neovascularisation [Nambu et al., 2003]. Although the mechanisms by which Ang-1 protects the vasculature is unknown, administration of Ang-1 may prove a potential strategy for the treatment of ROP in the future.

7.2 THE MODEL

Early studies found that persistent hyperoxia along with retinal immaturity are risk factors for ROP [Campbell, 1951; Patz, Hoeck and Cruz, 1952]. However, infants are no longer exposed to continued high oxygen concentrations; instead their transcutaneous oxygen levels fluctuate from minute-to-minute, but kept between clinically defined limits [Cunningham et al., 1992]. It has been reported that infants experiencing a greater variability of oxygen during the first two weeks of life are at an increased risk of developing the condition [Cunningham et al., 1995]. The Edinburgh model of ROP was designed to mimic this clinical situation [Cunningham et al., 2000].

7.2.1 The Profiles

The purpose of this project was to determine if vessel stability was compromised in the Edinburgh ROP model. For these studies, pups were exposed to the 10kPa oxygen profile since, in comparison to the other profiles, it induced a higher incidence and greater severity of disease [Cunningham et al., 2000]. Thus, it was predicted that if vessel integrity was indeed compromised in the model, then it would be more readily detected in the 10kPa model.

When the model was being tested for neovascularisation, two regimens were studied; an extended duration of oxygen exposure (18 days) and a period of room air recovery (14 days of oxygen exposure followed by four days in room air). For both of these regimens, the 8kPa profile was used since the original study used an oxygen profile with a mean of 8kPa [Cunningham et al., 2000]. As in the original study, neither of these two regimens induced neovascularisation. However, abnormal terminal vessels were observed at the vascular/avascular junction in the retinas killed immediately after oxygen exposure. In contrast, pups transferred to room air after oxygen exposure did not appear appreciably different to the P14 controls.

7.2.2 Improvements to the Model

Although the Edinburgh model of ROP represents more realistically the oxygen environment experienced by preterm infants receiving supplemental oxygen therapy, the lack of neovascularisation in the retinas may be a weakness of this model. The model could benefit from manipulation to induce the proliferation of vessels into the vitreous.

Animal models have shown that hypercarbia can induce retinopathy [Flower, 1988; Holmes, Duffner and Kappil, 1994; Holmes et al., 1997, 1998]. In the Edinburgh model, when pups were exposed to the 8kPa profile with a constant carbon dioxide level of 5%[1], the retinal vasculature appeared very immature in comparison to that of pups raised in room air or variable oxygen alone. The retinal vasculature consisted of numerous smaller vessels and lacked capillary-free zones around the arterioles, suggesting that the vasculature had not undergone sufficient remodelling. In addition, the retinas had increased peripheral avascularity, and a greater number of retinas contained abnormal terminal vessels. If these abnormal terminal vessels are indeed neovascular precursors, then these results are in agreement with other studies that carbon dioxide is a risk factor for ROP [Flower, 1988; Holmes, Duffner and Kappil, 1994; Holmes et al., 1997, 1998].

Clinical studies investigating the effects of carbon dioxide on the retina have however produced conflicting results; whilst some consider carbon dioxide to be a risk factor [Shoat et al., 1983; Brown et al., 1987], others have failed to show any relationship between carbon dioxide and ROP [Bauer, 1982; Gellen et al., 2001]. Thus, although in the animal model carbon dioxide along with variable oxygen exposure induced a more severe disease, because the clinical relevance of carbon dioxide is not fully understood the use of carbon dioxide to induce retinopathy may be inappropriate.

[1] Unpublished results of the ROP research team in the Department of Child Life and Health.

The lungs of preterm infants are poorly developed, thus the babies have great breathing difficulties. During resuscitation, preterm infants commonly experience a very short period of hypoxia, followed by a short exposure to 100% oxygen before they are maintained in clinically 'safe' oxygen levels. It is possible that this early insult may play a crucial role in the induction and outcome of ROP. Therefore, exposing rat pups to 10% oxygen for 10 minutes followed by 100% oxygen for 10 minutes prior to starting the variable oxygen regime may produce more severe retinopathy than the variable oxygen regime alone, and perhaps even induce neovascularisation. This regime would further mimic the oxygen environment experienced by a preterm ventilated infant. These experiments are currently underway in the laboratory.

In the current model, a minimum of 12 pups per litter are required to induce the early features of ROP [Cunningham et al., 2000]. Using a rat model of oxygen-induced retinopathy, Holmes and Duffner induced more frequent and more severe abnormal retinal neovasculatisation in larger litters (25 pups) than smaller litters (10 pups) [Holmes and Duffner, 1996]. Hence, litter size can determine retinal outcome possibly due to competition within the litter leading to malnourishment and postnatal growth retardation. Therefore, in addition to manipulation of the oxygen regime, using larger litter sizes may also result in increased severity of retinal changes in the Edinburgh model.

7.3 FUTURE STUDIES

Along with the further studies and improvements suggested in the individual chapters, there is scope for a number of future studies on retinal vessel stability. In addition, the Edinburgh model may prove very useful in establishing the effects, if any, of variable oxygen in other tissues and systems.

7.3.1 The Angiopoietins

At the time of conducting the initial experiments on the angiopoietins, antibodies for use in immunohistochemistry and Western analysis were not available. However, suitable angiopoietin antibodies are now available. Thus, in order to complete this project, the first experiments carried out would investigate the expression of the angiopoietins during retinal development in control and oxygen treated rat pups.

Since pericyte coverage and the expression of PDGF-B and TGF-β_1 were affected by the variable oxygen regime, it would be expected that retinal expression of Ang-1 and Ang-2 would also be altered.

7.3.2 Blood Vessel Leakiness

The work discussed in Chapter Two found that mural cell coverage was reduced in the Edinburgh model and that the basement membrane, which forms a continuous layer around pericytes and endothelial cells, was disrupted in the retinas of the variable oxygen group. These factors can result in vessel destabilisation and leakage of fluids.

Thurston and colleagues measured vascular leakage of the ear skin of VEGF (vascular endothelial growth factor) and Ang-1 transgenic mice by injecting Evans blue dye into the femoral vein [Thurston et al., 1999, 2000]. This technique has been adapted to measure vessel leakage of the rat retina [Xu, Quam and Adamis, 2001] and may be easily applied to the Edinburgh model. Because leakage sites expose the

basement membrane to the vessel lumen, Thurston et al. also investigated the leakage sites in the ear skin of the transgenics [Thurston et al., 1999]. The exposed basement membrane was visualised by staining the vasculature with biotinylated *Ricinus comminis I* lectin. This technique can also be used to establish any retinal vascular leakiness of the oxygen treated pups and has an advantage over the Evans blue dye methodology in that UK Home Office approval would not be required.

7.3.3 The Effects of Oxygen on the Retina

It would be interesting to establish if the reduced expression of PDGF-B and TGF-β_1 was due to hypoxic episodes alone, or to hyperoxic periods, or was a result of the variability which may have caused the relevant genes to be switched 'on' and 'off' repeatedly.

In the Edinburgh model of ROP, the oxygen concentration does not exceed 50%. Thus, to investigate the effect of hyperoxia alone, the pups could be maintained in 50% oxygen until 14 days of life. In order to determine if the effects were the result of hypoxia, the pups could be exposed to 50% for seven days followed by room air maintenance (relative hypoxia) until P14. Alternatively, pups could be raised from birth to postnatal day 14 in a slightly hypoxic environment (15% oxygen). Following exposure, the pups would be sacrificed, the tissues collected and Western analysis performed.

7.3.4 Differentiation of Pericytes into Smooth Muscle Cells

Zimmermann[2] identified three types of mural cells: smooth muscle cells around larger vessels; transitional pericytes found around the pre- and post-capillaries; and true pericytes around the mid-capillaries. Transitional pericytes have been described as undifferentiated smooth muscle cells [Rouget, 1873[3]; Nicosia and Villaschi, 1995;

[2] The original paper was written in German and a translation was not available. This is taken from the review by Darland and D'Amore, 2001b.

[3] The original paper was written in French and a translation was not available. This is taken from the review by Darland and D'Amore, 2001b.

Lindahl et al., 1997; Hellström et al., 1999]. Since 10T1/2 cells (mesenchymal cell precursors) have been shown to differentiate into pericytes or smooth muscle cells in the presence of TGF-β [Hirschi, Rohovsky and D'Amore, 1998], the theory that pericytes are undifferentiated smooth muscle cells could be investigated by maintaining cultures of retinal capillaries *in vitro* and testing the effects of TGF-β addition to the cultures.

It may also be worthwhile to adapt cell culture incubators so that the direct effects of oxygen variability could be investigated in various cell types and systems. For example, on the formation of capillary structure in three-dimensional co-cultures of endothelial cells and 10T1/2 cells [Darland and D'Amore, 2001a].

7.3.5 Effects of Variable Oxygen on the Developing Brain

More extremely premature infants are surviving today as a result of improvements in neonatal care. However, a large proportion (around 50%) of these babies is found to have neurodevelopmental abnormalities later in life [Volpe, 1995]. Because most extremely premature babies are ventilated for a period of time, many of them experience fluctuations in their blood oxygen levels similar to those used in the Edinburgh model. Since the retina is an extension of the brain, the question has been asked whether the brain could be affected by oxygen variability too. If oxygen variability is indeed found to be harmful to the brain, it may account for some of the brain injuries in preterm infants which cause neurodevelopmental disorders. Such studies are currently underway in the laboratory by Dr. Sedowofia.

7.4 CONCLUSIONS

In summary, with 14 days of variable oxygen exposure, there was a reduction in the mural cell coverage of the retinal blood vessels. The small decrease observed in smooth muscle cell coverage was due to limited remodelling of the vasculature, whereas the marked decrease in pericyte coverage was most likely the result of a reduction in the number of precursors cells migrating onto the vasculature. This reduction in mural cell coverage was confirmed by the reduced expression of PDGF-B and TGF-β_1 proteins which function in the recruitment and differentiation of the mural cells, respectively.

These findings suggest that the stability of the retinal vasculature is indeed compromised in the Edinburgh model of ROP and merits further analysis.

REFERENCES

Abdulmalek et al., 2001

Abdulmalek K, Ashur F, Ezer N, Ye F, Magder S, Hussain SNA.
Differential expression of Tie-2 receptors and angiopoietins in response to *in vivo* hypoxia in rats.
American Journal of Physiology - Lung Cellular & Molecular Physiology 2001; **284**: L582-L590.

Aiello et al., 1995

Aiello LP, Northrup JM, Keyt BA, Takagi H, Iwamoto MA.
Hypoxic regulation of vascular endothelial growth factor in retinal cells.
Archives of Ophthalmology 1995; **113**: 1538-1544.

Akhurst et al., 1990

Akhurst RJ, Lehnert SA, Faissner A, Duffie E.
TGF-β in murine morphogenetic processes: The early embryo and cardiogenesis.
Development 1990; **108**: 645-656.

Anderson et al., 1995

Anderson DH, Guerin CJ, Hageman GS, Pfeffer BA, Falanders KC.
Distribution of transforming growth factor-β isoforms in the mammalian retina.
Journal of Neuroscience Research 1995; **42**: 63-79.

Antonelli-Orlidge, Smith and D'Amore, 1989

Antonelli-Orlidge A, Smith SR, D'Amore PA.
Influence of pericytes on capillary endothelial cell growth.
American Review of Respiratory Disease 1989; **140**: 1129-1131.

Antonelli-Orlidge et al., 1989

Antonelli-Orlidge A, Saunders KB, Smith LR, D'Amore PA.
An activated form of transforming growth factor-β is produced by cocultures of endothelial cells and pericytes.
Proceedings of the National Academy of Sciences of the United States of America 1989; **86**: 4544-4548.

Antoniades, 1981

Antoniades HN.
Human platelet-derived growth factor (PDGF): Purification of PDGF-I and PDGF-II and separation of their reduced subunits.
Proceedings of the National Academy of Sciences of the United States of America 1981; **78**: 7314-7317.

Antoniades, Scher and Stiles, 1979

Antoniades HN, Scher CD, Stiles CD.
Purification of human platelet-derived growth factor.
Proceedings of the National Academy of Sciences of the United States of America 1979; **76**: 1809-1813.

Arruti and Courtois, 1978

Arruti C, Courtois Y.
Morphological changes and growth stimulation of bovine epithelial lens cells by a retinal extract *in vitro*.
Experimental Cell Research 1978; **117**: 283-292.

Asahara et al., 1998

Asahara T, Chen D, Takahashi T, Fujikawa K, Kearney M, Magner M, Yancopoulos GD, Isner JM.
Tie-2 receptor ligands, angiopoietin-1 and angiopoietin-2, modulate VEGF-induced postnatal neovascularization.
Circulation Research 1998; **83**: 233-240.

Ashton, 1966

Ashton N.
Oxygen and the growth and development of retinal vessels.
American Journal of Ophthalmology 1966; **62**: 412-435.

Ashton, 1970

Ashton N.
Retinal angiogenesis in the human embryo.
British Medical Bulletin 1970; **26**: 103-106.

Ashton, 1968

Ashton N.
Donders lecture 1967. Some aspects of the comparative pathology of oxygen toxicity in the retina.
British Journal of Ophthalmology 1968; **52**: 505-531.

Ashton and Blach, 1961

Ashton N, Blach R.
Studies on developing retinal vessels: VIII. Effects of oxygen on the retinal vessels of the ratling.
British Journal of Ophthalmology 1961; **45**: 321-340.

Ashton and de Oliveria, 1966

Ashton N, de Oliveria F.
Nomenclature of pericytes. Intramural and extramural.
British Journal of Ophthalmology 1965; **50**: 119-123.

Ashton, Garner and Knight, 1971

Ashton N, Garner A, Knight G.
Intermittent oxygen in retrolental fibroplasia.
American Journal of Ophthalmology 1971; **71**: 153-160.

Ashton, Ward and Serpell, 1954

Ashton N, Ward B, Serpell G.
Effect of oxygen on developing retinal vessels with particular reference to the problem of retrolental fibroplasia.
British Journal of Ophthalmology 1954; **38**: 397-430.

Assoian et al., 1983

Assoian R, Komoriya A, Meyers C, Miller D.
Transforming growth factor-β in human platelets.
Journal of Biological Chemistry 1983; **258**: 7155-7160.

Avery and Glass, 1998

Avery GB, Glass P.
Retinopathy of permaturity: What causes it?
Clinical Perinatology 1998; **15**: 917-928.

Avery and Oppenheimer, 1990

Avery ME, Oppenheimer EH.
Recent increase in mortality from hyaline membrane disease.
Journal of Pediatrics 1990; **57**: 553-559.

Barette et al., 1984

Barette TB, Gajdusek CM, Schwartz SM, McDougall JK, Benditt EP.
Expression of the sis gene by endothelial cells in culture *in vivo*.
Proceeding of the National Academy of Sciences of the United States of Amierica 1984; **81**: 6772-6774.

Barinaga, 1995

Barinaga M.
Shedding light on blindness.
Science 1995; **267**: 452-453.

Barleon et al., 1994

Barleon B, Hauser S, Schollmann C, Weindel K, Marme D, Yayon A, Weich HA.
Differential expression of the two VEGF receptors flt and KDR in placenta and vascular endothelial cells.
Journal of Cellular Biochemistry 1994; **54**: 56-66.

Battig and Low, 1961

Battig CG, Low FN.
The ultrastructure of human cardiac muscle and its associated tissue space.
American Journal of Anatomy 1961; **108**: 199-230.

Bauer, 1982

Bauer CR.
Does carbon dioxide play a role in retrolental fibroplasia?
Pediatrics 1982; **70**: 663.

Beck and D'Amore, 1997

Beck L, D'Amore PA.
Vascular development: Cellular and molecular regulation.
FASEB Journal 1997; **11**: 365-373.

Beitz et al., 1991

Beitz JG, Kim IS, Calabresi P, Frackelton AR.
Human microvascular endothelial cells express receptors for platelet-derived growth factor.
Proceedings of the National Academy of Sciences of the United States of America 1991; **88**: 2021-2025.

Benjamin, Hemo and Keshet, 1998

Benjamin LE, Hemo I, Keshet E.
A plasticity window for blood vessel remodelling is defined by pericyte coverage of the preformed endothelial network and is regulated by PDGF-B and VEGF.
Development 1998; **125**: 1591-1598.

Bergsten et al., 2001

Bergstein E, Uutela M, Li X, Pietras K, Heldin C-H, Östman A, Alitalo K, Eriksson U.
PDGF-D is a specific and protease activated ligand for the PDGF-β receptor.
Nature Cell Biology 2001; **3**: 512-516.

Bernstein, Antoniades and Zetter, 1982

Bernstein LR, Antoniades H, Zetter BR.
Migration of cultured vascular cells in response to plasma and platelet-derived factors.
Journal of Cell Science 1982; **56**: 71-82.

Beström et al., 1996

Beström H, Willetts K, Pekny M, Levéen P, Lindahl P, Pekna M, Hellström M, Kurland S, Törnell J, Heath JK, Betsholtz C.
PDGF-A signalling is a critical event in lung alveolar myofibroblast development and alveogenesis.
Cell 1996; **85**: 863-873.

Betsholtz, Karlsson and Lindahl, 2001

Betsholtz C, Karlsson L, Lindahl P.
Developmental roles of platelet-derived growth factors.
Bioessays 2001; **23**: 494-507.

Bishayee et al., 1989

Bishayee S, Majumdar S, Khire J, Das M.
Ligand-induced dimerization of the platelet-derived growth factor receptor. Monomer-dimer interconversion occurs independent of receptor phosphorylation.
Journal of Biological Chemistry 1989; **264**: 11699-11705.

Blanchette et al., 1997

Blanchette F, Day R, Dong W, Laprise MH, Dubois CM.
TGF-β_1 regulates gene expression of its own converting enzyme.
Journal of Clinical Investigation 1997; **99**: 1974-1983.

Blatti et al., 1988

Blatti SP, Foster DN, Ranganathan G, Moses HL, Getz MJ.
Induction of fibronectin gene transcription and mRNA is a primary response to growth-factor stimulation of ARK-2B cells.
Proceedings of the National Academy of Sciences of the United States of Ameria 1988; **85**: 1119-1123.

Bloom and Fawcett, 1968

Bloom W, Fawcett DW.
A Textbook of Histology, Ch11 & Ch13.
Philadelphia, Saunders; 9th edition, 1968.

Bossi and Koerner, 1995

Bossi E, Koerner F.
Retinopathy of prematurity.
Intensive Care Medicine 1995; **21**: 241-246.

Breier et al., 1996

Breier G, Breviario F, Caveda L, Berthier R, Schnurch H, Gotsch U, Vestweber D, Risau W, Dejana E.
Molecular cloning and expression of murine vascular endothelial-cadherin in early stage development of cardiovascular system.
Blood 1996; **87**: 630-41.

Brogi et al., 1993

Brogi E, Wu T, Namiki A, Isner JM.
Indirect angiogenic cytokines up-regulate VEGF and bFGF gene expression in vascular smooth muscle cells, whereas hypoxia up-regulates VEGF expression only.
Circulation 1993; **90**: 649-652.

Brown et al., 1987

Brown DR, Milley JR, Ripepi UJ, Biglan AW.
Retinopathy of prematurity: Risk factors in a five-year cohort of critically ill premature neonates.
American Journal of Disease in Childhood 1987; **141**: 154-160.

Brown et al., 2000

Brown LF, Dezube BJ, Tognazzi K, Dvorak HF, Yancopoulos GD.
Expression of Tie-1, Tie-2, and angiopoietin 1, 2, and 4 in Kaposi's sarcoma and cutaneous angiosarcoma.
American Journal of Pathology 2000; **156**: 2179-2183.

Brown et al., 1990

Brown PD, Wakefield L, Levinson AD, Sporn M.
Physiochemical activation of recombinant latent transforming growth factor-β's 1, 2, and 3.
Growth Factors 1990; **3**: 35-43.

Browning, Wylie and Gole, 1997

Browning J, Wylie CK, Gole G.
Quantification of oxygen-induced retinopathy in the mouse.
Investigative Ophthalmology & Visual Science 1997; **38**: 1168-1174.

Burg et al., 1999

Burg MA, Pasqualini R, Arap W, Ruoslahti E, Stallcup WB.
NG-2 proteoglycan-binding peptide targets tumor neovascularisation.
Cancer Research 1999; **59**: 2869-2874.

Burke, 1982

Burke JM.
Cultured retinal glial cells are insensitive to platelet-derived growth factor.
Experimental Eye Research 1982; **35**: 663-669.

Campbell, 1951

Campbell K.
Intensive oxygen therapy as a possible cause of retrolental fibroplasia: A clinical approach.
The Medical Journal of Australia 1951; **2**: 48-50.

Canalis et al., 1992

Canalis E, Varghese S, McCarthy TL, Centrella M.
Role of platelet-derived growth factor in bone cell function.
Growth Regulation 1992; **2**: 151-155.

Carlson, 1999

Carlson BM.
Human Embryology & Developmental Biology, pp262-276.
London, Mosby; 2nd edition, 1999.

Carmeliet and Collen, 1998

Carmeliet P, Collen D.
Vascular development and disorders: Molecular analysis and pathological insights.
Kidney International 1998; **53**: 1519-1549.

Carmeliet et al., 1996

Carmeliet P, Ferreira V, Breier G, Pollefeyt S, Kiechens L, Gertsenstein M, Fahrig M, Vandenhoeck A, Harpal K, Eberhardt C, Declercq C, Pawling J, Moons L, Collen D, Risau W, Nagy A,
Abnormal blood vessel development and lethality in embryos lacking a single VEGF allele.
Nature 1996; **380**: 435-439.

Centralla, McCarthy and Canalis, 1987

Centralla M, McCarthy TL, Canalis E.
Transforming growth factor-β is a bifunctional regulator of replication and collagen synthesis in osteoblast-enriched cell cultures from fetal rat bone.
Journal of Biological Chemistry 1987; **62**: 2869-2874.

Chan-Ling and Stone, 1993

Chan-Ling T, Stone J.
Retinopathy of prematurity: Origins in the architecture of the retina.
Progress in Retinal Research 1993; **12**: 155-178.

Chan-Ling, Gock and Stone, 1995a

Chan-Ling T, Gock B, Stone J.
The effect of oxygen on vasoformative cell division: Evidence that 'physiological hypoxia' is the stimulus for normal retinal vasculogenesis.
Investigative Ophthalmology & Visual Science 1995; **36**: 1201-1214.

Chan-Ling, Gock and Stone, 1995b

Chan-Ling T, Gock B, Stone J.
Supplemental oxygen therapy: Basis for noninvasive treatment of retinopathy of prematurity.
Investigative Ophthalmology & Visual Science 1995; **36**: 1215-1230.

Chan-Ling, Halasz and Stone, 1990

Chan-Ling TL, Halasz P, Stone J.
Development of retinal vasculature in the cat: Processes and mechanisms.
Current Eye Research 1990; **9**: 459-478.

Chan-Ling et al., 1992

Chan-Ling T, Tour S, Hollander H, Stone J.
Vascular changes and their mechanisms in the feline model of retinopathy of prematurity.
Investigative Ophthalmology & Visual Science. 1992; **33**: 2128-2147.

Cheifetz, Like and Massagué, 1986

Cheifetz S, Like B, Massagué J.
Cellular distribution of type I and type II receptors for transforming growth factor-β.
Journal of Biological Chemistry 1986; **261**: 9972-9978.

Cheifetz et al., 1987

Cheifetz S, Weatherbee J, Tsang M-S, Anderson J, Mole J, Lucas R, Massagué J.
The transforming growth factor-β system, a complex pattern of cross-reactive ligands and receptors.
Cell 1987; **48**: 409-415.

Claesson-Welsh, 1996

Claesson-Welsh L.
Mechanism of action of platelet-derived growth factor.
International Journal of Biochemical & Cellular Biology 1996; **28**: 373-385.

Claesson-Welsh et al., 1988

Claesson-Welsh L, Eriksson A, Moren A, Severinsson L, Ek B, Östman A, Betsholtz C, Heldin CH.
cDNA cloning and expression of a human platelet-derived growth factor (PDGF) receptor specific for B-chain-containing PDGF molecules.
Molecular & Cellular Biology 1988; **8**: 3476-3486.

Claesson-Welsh et al., 1989a

Claesson-Welsh L, Eriksson A, Westermark B, Heldin CH.
cDNA cloning and expression of the human A-type platelet-derived growth factor (PDGF) receptor establishes structural similarity to the B-type PDGF receptor.
Proceeding of the National Acedemy of Sciences of the United States of America 1989; **86**: 4917-4921.

Claesson-Welsh et al., 1989b

Claesson-Welsh L, Hammacher A, Westermark B, Heldin CH, Nister M.
Identification and structural analysis of the A type receptor for platelet-derived growth factor. Similarities with the B type receptor.
Journal of Biological Chemistry 1989; **264**: 1742-1747.

Clark and Clark, 1925

Clark ER, Clark EL.
Development of adventitial (Rouget) cells on the blood capillaries of amphibian larvae.
The American Journal of Anatomy 1925; **35**: 239-264.

Cogan, Toussaint and Kuwabara, 1961

Cogan DG, Toussaint D, Kuwabara T.
Retinal vascular patterns. Part IV: Diabetic retinopathy.
Archives of Opthalmology 1961; **66**: 366-378.

Collins et al., 1985

Collins T, Ginsburg D, Boss JM, Orkin SH, Pober JS.
Cultured human endothelial cells express platelet-derived growth factor B chain: cDNA cloning and structural analysis.
Nature 1985; **316**: 748-750.

The Committee for the Classification of Retinopathy of Prematurity, 1984

The Committee for the Classification of Retinopathy of Prematurity.
An international classification of retinopathy of prematurity.
Archives of Ophthalmology 1984; **102**: 1130-1134.

Crocker, Murad and Geer, 1970

Crocker DJ, Murad TM, Geer JC.
Role of the pericyte in wound healing: An ultrastructural study.
Experimental & Molecular Pathology 1970; **13**: 51-65.

Crofts, King and Johnson, 1998

Crofts BJ, King R, Johnson A.
The contribution of low birthweight to severe vision loss in geographically defined populations.
British Journal of Ophthalmology 1998; **82**: 9-13.

Crosse and Evans, 1952

Crosse VM, Evans PJ.
Prevention of retrolental fibroplasia.
Archives of Ophthalmology 1952; **48**: 83-87.

Cryotherapy for Retinopathy Cooperative Group, 1990
Cryotherapy for Retinopathy Cooperative Group.
Multicenter trial of cryotherapy for retinopathy of prematurity – 3 month outcome.
Archives of Ophthalmology 1990; **108**: 1195-1204.

Cryotherapy for Retinopathy of Prematurity Cooperative Group, 1994
Cryotherapy for Retinopathy of Prematurity Cooperative Group.
The natural ocular outcome of premature birth and retinopathy: Status at 1 year.
Archives of Ophthalmology 1994; **112**: 903-912.

Cunningham et al., 1992
Cunningham S, Deere S, Elton RA, McIntosh N.
Neonatal physiological trend monitoring by computer.
International Journal of Clinical Monitoring & Computing 1992; **9**: 221-227.

Cunningham et al., 1995
Cunningham S, Fleck BW, Elton RA, Mclntosh N.
Transcutaneous oxygen levels in retinopathy of prematurity.
The Lancet 1995; **346**: 1464-1465.

Cunningham et al., 2000
Cunningham S, McColm J, Wade J, Sedowofia K, McIntosh N, Fleck B.
Novel model of retinopathy of prematurity simulating preterm oxygen variability in the rat.
Investigative Ophthalmology & Visual Science 2000; **41**: 4275-4280.

D'Amore and Smith, 1993
D'Amore PA, Smith SR.
Growth factor effects on cells of the vascular wall: A survey.
Growth Factors 1993; **8**: 61-75.

Darland and D'Amore, 1999
Darland DC, D'Amore PA.
Blood vessel maturation: Vascular development comes to age.
Journal of Clinical Investigation 1999; **103**: 157-158.

Darland and D'Amore 2001a
Darland DC, D'Amore PA.
TGF-β is required for the formation of capillary-like structures in three-dimentional cocultures of 10T1/2 and endothelial cells.
Angiogenesis 2001; **4**: 11-20.

Darland and D'Amore, 2001b

Darland DC, D'Amore PA.
Cell-cell interaction in vascular development.
Current Topics in Developmental Biology 2001; **52**: 107-149.

Davis et al., 1996

Davis S, Aldrich TH, Jones P, Acheson A, Compton D, Jain V, Ryan TE, Bruno J, Radziejewski C, Maisonpierre PC, Yancopoulos GD.
Isolation of angiopoietin-1, a ligand for the Tie-2 receptor, by secretion-trap expression cloning.
Cell 1996; **87**: 1161-1169.

Debus, Weber and Osborn, 1983

Debus E, Weber K, Osborn M.
Monoclonal antibodies to desmin, the muscle-specific intermediate filament protein.
EMBO Journal 1983; **2**: 2305-2312.

De Juan, Dickson and Hjelmeland, 1988

De Juan E, Dickson JS, Hjelmeland L.
Serum is chemotactic for retinal-derived glial cells.
Archives of Ophthalmology 1988; **106**: 986-990.

de Oliveria, 1966

de Oliveria F.
Pericytes in diabetic retinopathy.
British Journal of Ophthalmology 1966; **50**: 134.

Derynck et al., 1985

Derynck R, Jarett JA, Chen EY, Eaton DH, Bell JR, Assoian K, Roberts AB, Sporn MB.
Human transforming growth factor-β complementary DNA sequence and expression in normal and transformed cells.
Nature 1985; **316**: 701-705.

Deuel et al., 1981

Deuel TF, Huang JS, Proffitt RT, Baenziger, JU, Chang D, Kennedy BB.
Human platelet-derived growth factor: Purification and resolution into two active protein fractions.
Journal of Biological Chemistry 1981; **256**: 8896-8899.

Dezateux and Rahi, 1998

Dezateux C, Rahi J.
Epidemiology of visual impairment in Britain.
Archives of Disease in Childhood 1998; **78**: 381-386.

Diaz-Flores, Gutiérrez and Varela, 1994

Diaz-Flores L, Gutiérrez R, Varela H.
Angiogenesis: An update.
Histology & Histopathology 1994; **9**: 807-843.

Diaz-Flores et al., 1991

Diaz-Flores L, Gutiérrez R, Varela H, Rancel N, Valladares F.
Microvascular pericytes: A review of their morphology and functional characteristics.
Histology & Histopathology 1991; **6**: 269-286.

Dickson et al., 1995

Dickson MC, Martin JS, Cousins FM, Kulkarni AB, Karlsson S, Akhurst RJ.
Defective haematopoiesis and vasculogenesis in transforming growth factor-β1 knockout mice.
Development 1995; **121**: 1854-1854.

Dubois et al., 1995

Dubois CM, Laprise MH, Blanchette F, Gentry LE, Leduc R.
Processing transforming growth factor-β_1 precursor by human convertase.
Journal of Biological Chemistry 1995; **270**: 10618-10624.

Dumont et al., 1992

Dumont DJ, Yamaguchi TP, Conlon RA, Rossant J, Breitman ML.
Tek, a novel tyrosine kinase gene located on mouse chromosome 4, is expressed in endothelial cells and their presumptive precursors.
Oncogene 1992; **7**: 1471-1480.

Edwards et al., 1987

Edwards DR, Murphy G, Reynolds JJ, Whitham SE, Docherty AJP, Angel P, and Heath JK.
Transforming growth factor-β modulates the expression of collagenase and metalloproteinase inhibitor.
EMBO Journal 1987; **6**: 1899-1904.

Ehler et al., 1995

Ehler E, Karlhuber G, Bauer H-C, Draeger A.
Heterogeneity of smooth muscle-associated proteins in mammalian brain microvasculature.
Cell & Tissue Research 1995; **279**: 393-403.

Ernest and Goldstick, 1984

Ernest JT, Goldstick TK.
Retinal oxygen tension and oxygen reactivity in retinopathy of prematurity in kittens.
Investigative Ophthalmology & Visual Science 1984; **25**: 1129-1134.

Falanga et al., 1991

Falanga V, Qian SW, Danielpour D, Katz MH, Roberts A, Sporn M.
Hypoxia upregulates the synthesis of TGF-β_1 by human dermal fibroblasts.
Journal of Investigative Dermatology 1991; **97**: 634-637.

Ferrara and Henzel, 1989

Ferrara N, Henzel WJ.
Pituitary follicular cells secrete a novel heparin-binding growth factor specific for vascular endothelial cells.
Biochemical & Biophysical Research Communications 1989; **161**: 851-858.

Fielder and Reynolds, 2001

Fielder AR, Reynolds JD.
Retinopathy of prematurity: Clinical aspects.
Seminars in Neonatology 2001; **6**: 461-475.

Flamme and Risau, 1992

Flamme I, Risau W.
Induction of vasculogenesis and hematopoiesis *in vitro*.
Development 1992; **116**: 435-439.

Flower, 1988

Flower RW.
Physiology of the ocular vasculature.
Birth Defects 1988; **24**: 129-146.

Flower and Blake, 1981

Flower RW, Blake DA.
Retrolental fibroplasia: Evidence for a role of the prostaglandin cascade in the pathogenesis of oxygen-induced retinopathy in the newborn beagle.
Pediatric Research 1981; **15**; 1293-1302.

Flower et al, 1985

Flower RW, McLeod DS, Lutty GA, Goldberg B, Wajer SD.
Postnatal retinal vascular development of the puppy.
Investigative Ophthalmology & Visual Science 1985; **26**: 957-968.

Flynn, 1987

Flynn JT.
Retinopathy of prematurity
Pediatric Clinics of North America 1974; **34**: 1487-1516.

Folkman, 1971

Folkman J.
Tumor angiogenesis: Therapeutic implications.
New England Journal of Medicine 1971; **285**: 1182-1186.

Folkman and D'Amore, 1996

Folkman J, D'Amore PA.
Blood vessel formation: What is its molecular basis?
Cell 1996; **87**: 1153-1156.

Fong et al., 1995

Fong GH, Rossant J, Gertsenstein M, Breitman ML.
Role of the Flt-1 receptor kinase in regulating the assembly of vascular endothelium.
Nature 1995; **376**: 66-70.

Frank, Dutta and Mancini, 1987

Frank RN, Dutta S, Mancini MA.
Pericyte coverage is greater in the retinal than in the cerebral capillaries of the rat.
Investigative Ophthalmolology & Visual Sciences 1987; **28**: 1086-1091.

Franzen et al., 1993

Franzen P, ten Deijke P, Ichijo H, Yamashita H, Schulz P, Heldin CH, Miyazono K.
Cloning of TGF-β type I receptor that forms a heteromeric complex with the TGF-β II receptor.
Cell 1993; **75**: 681-692.

Fràter-Schröder et al., 1986

Fràter-Schröder M, Müller G, Birchmeiser W, Böhlen P.
Transforming growth factor-β inhibits endothelial cell proliferation.
Biochemical & Biophysical Research Communications 1986; **137**: 295-302.

Friedman et al., 1949

Friedman E, Smith T, Kuwabara T.
Retinal microcirculation *in vivo*.
Investigative Ophthalmology 1949; **3**: 217.

Fujiwara and Uhara, 1984

Fujiwara T, Uehara Y.
The cytoarchitecture of the wall and the innervation pattern of the microvessels in the rat mammary gland: A scanning electron microscopic observation.
American Journal of Pathology 1984; **170**: 39-54.

Gellen et al., 2001

Gellen B, McIntosh N, McColm J, Fleck B.
Is the partial pressure of carbon dioxide in the blood related to the development of retinopathy of prematurity?
British Journal of Ophthalmology 2001; **85**: 1044-1045.

Gentry and Nash, 1990

Gentry LE. Nash BW.
The pro domain of pre-pro-transforming growth factor-β_1 when independently expressed is a functional binding protein for the mature growth factor.
Biochemistry 1990; **29**: 6851-6857.

Gilbert et al., 1997

Gilbert C, Rahi J, Eckstein M, O'Sullivan J, Foster A.
Retinopathy of prematurity in middle-income countries.
Lancet 1997; **349**: 12-14.

Glick et al., 1994

Glick AB, Lee MM, Darwiche N, Kulkarni AB, Karlsson.
Targeted deletion of the TGF-β_1 gene causes rapid progression to squamous cell carcinoma.
Genes Development 1994; **8**: 2429-2440.

Goodman and Majack, 1989

Goodman L, Majack R.
Vascular smooth muscle cells express distinct transforming growth factor-β receptor phenotypes as a function of cell density in culture.
Journal of Biological Chemistry 1989; **264**: 5241-5244.

Grako and Stallcup, 1995

Grako KA, Stallcup WB.
Participation of the NG-2 proteoglycan in rat aortic smooth muscle cell responses to platelet-derived growth factor.
Experimental Cell Research 1995; **221**: 231-240.

Granger et al., 1998

Granger DJ, Metcalfe JC, Grace AA, Mosedale DE.
Transforming growth factor-β dynamically regulates vascular smooth muscle differentiation *in vivo*.
Journal of Cell Science 1998; **111**: 2977-2988.

Grosendorst et al., 1982

Grotendorst G, Chang T, Seppä H, Kleinman H, Martin G.
Platelet-derived growth factor is a chemoattractant for vascular smooth muscle cells.
Journal of Cell Biology 1982; **113**: 261-266.

Guy, Lanman and Dancis, 1956

Guy LP, Lanman JT, Dancis J.
The possibility of total elimination of retrolental fibroplasia by oxygen restriction.
Pediatrics 1956; **17**: 247-249.

Hack and Fanaroff, 1989

Hack M, Fanaroff AA.
Outcomes of extremely-low birthweight infants between 1982 and 1988.
New England Journal of Medicine 1989; **321**: 1642-1647.

Hackett et al., 2000

Hackett SF, Ozaki H, Strauss RW, Wahlin K, Suri C, Maisonpierre PC, Yanopoulos G, Campochario PA.
Angiopoietin-2 expression in the retina: Upregulation during physiologic and pathologic neovascularisation.
Journal of Cell Physiology 2000; **184**: 275-284.

Hammacher et al., 1988a

Hammacher A, Hellman U, Johnsson A, Östman A, Gunnarsson K, Westermark B, Wasteson A, Heldin CH.
A major part of platelet-derived growth factor purified from human platelets is a heterodimer of one A and one B chain.
Journal of Biological Chemistry 1988; **263**: 16493-16498.

Hammacher et al., 1988b

Hammacher A, Nister M, Westermark B, Heldin CH.
A human glioma cell line secretes three structurally and functionally different dimeric forms of platelet-derived growth factor.
European Journal of Biochemistry 1988; **176**: 179-186.

Hart et al., 1988

Hart CE, Forstrom JW, Kelly JD, Seifert RA, Smith RA, Ross R, Murray MJ, Bowen-Pope, DF.
Two classes of PDGF receptor recognise different isoforms of PDGF.
Science 1988; **240**: 1529-1531.

Heimark, Twardzik and Schwartz, 1986

Heimark RL, Twardzik DR, Schwartz SM.
Inhibition of endothelial regeneration by type-β transforming growth factor from platelets.
Science 1986; **233**: 1078-1080.

Heine et al., 1987

Heine U, Munoz E, Flanders K, Ellingsworth L, Lam HP, Thompson N, Roberts AB, Sporn MB.
Role of transforming growth factor-β in the development of the mouse embryo.
Journal of Cell Biology 1987; **105**: 2861-2876.

Heldin, 1992

Heldin CH.
Structural and functional studies in platelet-derived growth factor.
The EMBO Journal 1992; **11**: 4251-4259.

Heldin and Westermark, 1999

Heldin C-H, Westermark B.
Mechanism of action and *in vivo* role of platelet-derived growth factor.
Physiological Reviews 1999; **79**: 1283-1316.

Heldin, Östman and Rönnstrand, 1998

Heldin C-H, Östman A, Rönnstrand L.
Signal transduction via platelet-derived growth factor receptors.
Biochimica et Biophysica Acta 1998; **1378**: F79-F113.

Heldin, Westermark and Wasteson, 1979

Heldin C-H, Westmark B, Wasteson Å.
Platelet-derived growth factor: Purification and partial characterisation.
Proceedings of the National Academy of Sciences of the United States of America 1979; **76**: 3722-3726.

Heldin et al., 1989

Heldin C-H, Ernlund A, Rorsman C, Rönnstrand L.
Dimerisation of B-type platelet-derived growth factor receptors occurs after ligand binding and is closely associated with receptor kinase activation.
Journal of Biological Chemistry 1989; **264**: 8905-8912.

Hellstrõm et al., 1999

Hellstrõm M, Kalén M, Lindahl P, Abramsson A, Betsholtz C.
Role of PDGF-B and PDGF-β in recruitment of vascular smooth muscle cells and pericytes during embryonic blood vessel formation in the mouse.
Development 1999; **126**: 3047-3055.

Hellström et al., 2001

Hellstrõm M, Gerhardt H, Kalén M, Li X, Eriksson U, Wolburg H, Betzholtz C.
Lack of pericytes leads to endothelial hyperplasia and abnormal vascular morphogenesis.
Journal of Cell Biology 2001; **153**: 543-553.

Henkind and de Oliveira, 1967

Henkind P, de Oliveira LF.
Development of retinal vessels in the rat.
Investigative Ophthalmology & Visual Science 1967; **6**: 520-530.

Herman and D'Amore, 1985

Herman IM, D'Amore PA.
Microvascular pericytes contain muscle and non-muscle actins.
Journal of Cell Biology 1985; **101**: 43-52.

Herman and Jacobson, 1988

Herman IM, Jacobson S.
In situ analysis of microvascular pericytes in hypertensive rat brains.
Tissue & Cell 1988; **20**: 1-12.

Herman et al., 1987

Herman IM, Newcomb PM, Coughlin JE, Jacobson S.
Characterization of microvascular cell cultures from normotensive and hypertensive rat brains: Pericyte-endothelial cell interactions *in vitro*.
Tissue & Cell 1987; **19**: 197-206.

Hermansson et al., 1988

Hermansson M, Nister M, Betsholtz C, Heldin CH, Westermark B, Funa K.
Endothelial cell hyperplasia in human glioblastoma: Coexpression of mRNA for platelet derived growth factor (PDGF) B chain and PDGF receptor suggests autocrine growth stimulation.
Proceedings of the National Academy of Sciences of United States of America 1988; **85**: 7748-7752.

Hirschi and.D'Amore, 1996

Hirschi KK, D'Amore PA.
Pericytes in the microvasculature.
Cardiovascular Research 1996; **32**: 687-698.

Hirschi and D'Amore, 1997

Hirschi KK, D'Amore PA.
Control of angiogenesis by the pericyte: Molecular mechanisms and significance.
EXS 1997; **79**: 419-428.

Hirschi, Rohovsky, D'Amore, 1998

Hirschi KK, Rohovsky SA, D'Amore PA.
PDGF, TGF-β, and heterotypic cell-cell interactions mediate endothelial cell-induced recruitment of 10T1/2 cells & their differentiation to a smooth muscle fate.
Journal of Cell Biology 1998; **141**: 805-814.

Holash, Weigand and Yancopoulos, 1999

Holash J, Wiegand SJ, Yancopoulos GD.
New model of tumor angiogenesis: Dynamic balance between vessel regression and growth mediated by angiopoietins and VEGF.
Oncogene 1999; **18**: 5356-5362.

Holash et al., 1999

Holash J, Maisonpierre PC, Compton D, Boland P, Alexander CR, Zagzag D, Yancopoulos GD, Weigand SJ.
Vessel cooption, regression and growth in tumors mediated by angiopoietins and VEGF.
Science 1999; **284**: 1994-1998.

Holmes and Duffner, 1996

Holmes JM, Duffner LA.
The effect of growth retardation on abnormal neovascularisation in the oxygen-exposed neonatal rat.
Current Eye Research 1996; **15**: 403-409.

Holmes, Duffner and Kappil, 1994

Holmes JM, Duffner LA, Kappil JC.
The effect of raised inspired carbon dioxide on developing rat retinal vasculature exposed to elevated oxygen.
Current Eye Research 1994; **13**: 779-782.

Holmes et al., 1997

Holmes JM, Zhang S, Leske DA, Lanier WL.
The effect of carbon dioxide on oxygen-induced retinopathy in the neonatal rat.
Current Eye Research 1997; **16**: 725-732.

Holmes et al., 1998

Holmes JM, Zhang S, Leske DA, Lanier WL.
Carbon dioxide-induced retinopathy in the neonatal rat.
Current Eye Research 1998; **17**: 608-16.

Hosang et al., 1989

Hosang M, Rouge M, Wipf B, Eggimann B, Kaufmann F, Hunziker W.
Both homodimeric isoforms of PDGF (AA and BB) have mitogenic and chemotactic activity and stimulate phosphoinositol turnover.
Journal of Cell Physiology 1989; **140**: 558-564.

Hughes et al., 1996

Hughes AD, Clunn GF, Refson J, Demoliou-Mason C.
Platelet-derived growth factor (PDGF): Actions and mechanisms in vascular smooth muscle.
General Pharmacology 1996; **27**: 1079-1089.

Hughes, Yang and Chan-Ling, 2000

Hughes S, Yang H, Chan-Ling T.
Vascularisation of the human fetal retina: Roles of vasculogenesis and angiogenesis.
Investigative Ophthalmology & Visual Science 2000; **41**: 1217-1228.

Hungerford and Little, 1999

Hungerford JE, Little CD.
Developmental biology of the vascular smooth muscle cell: Building a multilayered vessel wall.
Journal of Vascular Research 1999; **36**: 2-27.

Ignotz and Massagué, 1986

Ignotz RA, Massagué J.
Transforming growth factor-β stimulates the expression of fibronectin and collagen and their incorporation into the extracellular matrix.
The Journal of Biological Chemistry 1986; **261**: 4337-4345.

Johnsson et al., 1982

Johnsson A, Heldin CH, Westermark B, Wasteson Å.
Platelet-derived growth factor: Identification of constituent polypeptide chains.
Biochemical & Biophysical Research Communications 1982; **104**: 66-74.

Johnsson et al., 1984

Johnsson A, Heldin C-H, Wasteson Å, Westermark B, Deuel T, Huang J, Seeburg PH, Gray A, Illrich A, Scrace G.
The c-sis gene encodes a precursor of the B chain of platelet-derived growth factor.
EMBO Journal 1984; **3**: 921-928.

Joyce, Haire and Palade, 1985

Joyce NC, Haire MF, Palade GE.
Contractile proteins in pericytes: 2. Immunocytochemical evidence for the presence of two isomyosins in graded concentrations.
The Journal of Cell Biology 1985; **100**: 1387-1395.

Kanakaraj et al., 1991

Kanakaraj P, Raj S, Khan SA, Bishayee S.
Ligand-induced interaction between α- and β-type platelet derived growth factor (PDGF) receptors: Role of receptor heterodimers in kinase activation.
Biochemistry 1991; **30**: 1761-1767.

Kaplan et al., 1979

Kaplan D, Chao F, Stiles CD, Antoniades H, Scher C.
Platelet α granules contain a growth factor for fibroblasts.
Blood 1979; **53**: 1043-1052.

Kazlauskas, 2000

Kazlauskas A.
A new member of an old family.
Nature Cell Biology 2000; **2**: E78-E79.

Keating and Williams, 1987

Keating MT, Williams LT.
Processing of the platelet-derived growth factor receptor. Biosynthetic and degradation studies using antireceptor antibodies.
Journal of Biological Chemistry 1987; **262**: 7932-7937.

Kehrl et al., 1986a

Kehrl J, Roberts A, Wakefield L, Jakowlew S, Sporn M, Fauci A.
Transforming growth factor-β is an important immunomodulatory protein for human B lymphcytes.
Journal of Immunology 1986; **137**: 3855-3860.

Kehrl et al., 1986b

Kehrl J, Wakefield L, Roberts A, Jakowlew S, Alvarez-Mon M, Derynck R, Sporn MB, Fauci AS.
Production of transforming growth factor-β by human T lymphocytes and its potential role in the regulation of T cell growth.
Journal of Experimental Medicine 1986; **163**: 1037-1050.

Khaliq et al., 1995

Khaliq A, Patel B, Jarvis-Evans J, Moriarty P, McLeod D, Boulton M.
Oxygen modulates production of bFGF and TGF-β by retinal cells *in vitro*.
Experimental Eye Research 1995; **60**: 415-424.

Kim et al., 2000a

Kim I, Kim H-G, So J-N, Kim J-H, Kwak HJ, Koh GY.
Angiopoietin-1 regulates endothelial cell survival through the phosphatidylinositol 3'-kinase/Akt signal transduction pathway.
Circulation Research 2000; **86**: 24-29.

Kim et al., 2000b

Kim I, Kim J-H, Moon S, Kwak HJ, Kim NG, Koh GY.
Angiopoietin-2 at high concentration can enhance endothelial cell survival through the phosphatidylinositol 3'-kinase/Akt signal transduction pathway.
Oncogene 2000; **17**: 4549-4552.

Kinsey, 1956

Kinsey VE.
Retrolental fibroplasia: Cooperative study of retrolental fibroplasia and the use of oxygen.
Archives of Ophthalmology 1956; **56**: 481-543.

Koblizek et al., 1998

Koblizek TI, Weiss C, Yancopoulos GD, Deutsch U, Risau W.
Angiopoietin-1 induces sprouting angiogenesis *in vitro*.
Current Biology 1998; **8**: 529-532.

Kohler and Lipton, 1974

Kohler N, Lipton A.
Platelets as a source of fibroblast growth-promoting activity.
Experimental Cell Research 1974; **87**: 297-301.

Kong et al., 1995

Kong F, Anscher M, Murase T, Abbott BD, Iglehart J, Jirtle RL.
Elevated plasma transforming growth factor-β_1 levels on breast cancer patients decrease after surgical removal of the tumor.
Annals of Surgery 1995; **222**:115-162.

Kontos et al., 1998

Kontos CD, Stauffer TP, Yang W-P, York JD, Huang L, Blanar MA, Meyer T, Peters KG.
Tyrosine 1101 of Tie-2 is the major site of association of p85 and is required for activation of phosphatiylinositol 3'-kinase and Akt.
Molecular & Cellular Biology 1998; **18**: 4131-4140.

Kourembanas, Hannan and Faller, 1990

Kourembanas S, Hannan RL, Faller DV.
Oxygen tension regulates the expression of the platelet-derived growth factor-B chain gene in human endothelial cells.
Journals of Clinical Investigation 1990; **86**: 670-674.

Koyama et al., 1992

Koyama N, Morisaki N, Saito Y, Yoshida S.
Regulatory effects of platelet-derived growth factor-AA homodimer on migration of vascular smooth muscle cells.
Journal of Biological Chemistry 1992; **267**: 22806-22812.

Krane et al., 1991

Krane JF, Murphy DP, Gottlier AB, Carter DM, Hart CE, Krueger JG.
Increased dermal expression of platelet-derived growth factor receptors in growth-activated skin wounds and psoriasis.
Journal of Investigative Dermatology 1991; **96**: 983-986.

Krikun et al, 2000

Krikun G, Schatz F, Finlay T, Kadner S, Mesia A, Gerrets R, Lockwood CJ.
Expression of angiopoietin-2 by human endometrial endothelial cells: Regulation by hypoxia and inflammation.
Biochemical & Biophysical Research Communication 2000; **275**: 159-163.

Kulkarni et al., 1993

Kulkarni A, Huh C-G, Becker D, Geiser A, Lyght M, Flanders K, Roberts AB, Sporn MB, Ward JM, Karlsson S.
Transforming growth factor-β_1 null mutation on mice causes excessive inflammatory response and early death.
Proceedings of the National Academy of Science of the United States of America 1993; **90**: 770-774.

Kuwabara and Cogan, 1960

Kuwabara T, Cogan DG.
Studies of retinal vascular patterns. Part I: Normal architecture.
Archives of Ophthalmology 1960; **64**: 904-911.

Kuwabara and Cogan, 1963

Kuwabara T, Cogan DG.
Retinal vascular Pattern. Part VI: Mural cells of the retinal capillaries.
Archives of Ophthalmology 1963; **69**: 492-502.

Kwak et al., 1999

Kwak HJ, So J-N, Lee SJ, Kim I, Koh GY.
Angiopoietin-1 is an apoptosis survival factor for endothelial cells.
FEBS Letters 1999; **448**: 249-253.

Laiho, Saksels and Keski-Oja, 1987

Laiho M, Saksela O, Keski-Oja J.
Transforming growth factor-β induction of type-I plasminogen activator inhibitor. Pericellular deposition and sensitiviy to exogenous urokinase
Journal of Biological Chemistry 1987; **262**: 17467-17474.

Lampugnani et al., 1992

Lampugnani MG, Resnati M, Raiteri M, Pigott R, Pisacane A, Houen G, Ruco LP, Dejana E.
A novel endothelial-specific membrane protein is a marker of cell-cell contacts.
Journal of Cell Biology 1992; **118**: 1511-1522.

Langerak et al., 1996a

Langerak AW, De Laat P, Van der Linden-van Beurden CAJ, Delahaye M, Van der Kwast TH, Hoogsteden HC, Benner R.
Expression of platelet-derived growth factor (PDGF) and PDGF receptors in human malignant mesothelioma *in vitro* and *in vivo*.
Journal of Pathology 1996; **178**: 151-160.

Langerak et al., 1996b

Langerak AW, Van der Linden-van Beurden CAJ, Versnel MA.
Regulation of differential expression of platelet-derived growth factor α- and β-receptor mRNA in normal and malignant human mesothelial cell lines.
Biochemica et Biophysica Acta 1996; **1305**: 63-70.

Larsen, 1997

Larsen WJ.
Human Embryology, pp375-384.
Edinburgh, Churchill Livingstone; 2nd edition, 1997.

Lawrence et al., 1981

Lawrence DA, Pircher R, Kryceve-Martinerie C, Jullien P.
Normal embryo fibroblasts release transforming growth factors in a latent form.
Journal of Cell Physiology 1981; **121**: 184-188.

Lawrence, Pircher and Jullien, 1985

Lawrence D, Pircher R, Jullien P.
Conversion of a high molecular weight latent β-TGF from chicken embryo fibroblasts into a low molecular weight active β-TGF under acidic conditions.
Biochemical & Biophysical Research Communication 1985; **133**: 1026-1034.

Leeson and Leeson, 1976

Leeson CR, Leeson TS.
Histology, Ch9 & Ch11.
Philadelphia, WB Saunders; 3rd edition, 1976.

Levéen et al., 1994

Levéen P, Pekny M, Gebre-Medhin S, Swolin B, Larsson E, Betsholtz C.
Mice deficient for PDGF-B show renal, cardiovascular, and hematological abnormalities.
Genes & Development 1994; **8**: 1875-1887.

Li et al., 2000

Li X, Pontén A, Aase K, Karlsson L, Abramsson A, Uutela M, Backström G, Hellström M, Beström H, Li H, Soriano P, Betsholtz C, Heldin C-H, Alitalo K, Östman A, Eriksson U.
PDGF-C is a new protease-activated ligand for the PDGF alpha receptor.
Nature of Cell Biology 2000; **2**: 302-309.

Lin et al., 1992

Lin HY, Wang XF, Ng-Eaton E, Weinberg RZ, Lodish HF.
Expression cloning of the TGF-β type II receptor, a functional trasmembrane serine/threonine kinase.
Cell 1992; **68**: 775-785.

Lin et al., 1997

Lin P, Polverini P, Dewhirst M, Shan S, Rao PS, Peters K.
Inhibition of tumor angiogenesis using a soluble receptor establishes a role for Tie-2 in pathologic vascular growth.
Journal of Clinical Investigation 1997; **100**: 2172-2178.

Lindahl et al, 1997

Lindahl P, Johansson BR, Levéen P, Betsholtz C.
Pericyte loss and microaneurysm formation in PDGF-B deficient mice.
Science 1997; **227**: 242-245.

Ling and Stone, 1988

Ling TL, Stone J.
The development of astrocytes in the cat retina: Evidence of migration from the optic nerve.
Developmental Brain Research 1988; **44**: 73-85.

López-Casillas, Wrana and Massagué, 1993

López-Casillas F, Wrana J, Massagué J.
Betaglycan presents ligand to TGF-β signaling receptor.
Cell 1993; **73**: 1435-1444.

López-Casillas et al., 1991

López-Casillas F, Cheifetz S, Doody J, Andres J, Lane W, Massagué J.
Structure and expression of membrane proteoglycan betaglycan, a component of TGF-β receptor system.
Cell 1991; **67**: 785-795.

MacCallum et al., 1994

MacCallum J, Bartlett JM, Thompson AM, Keen JC, Dixon JM, Miller WR.
Expression of transforming growth factor-β mRNA isoforms in human breast cancer.
British Journal of Cancer 1994; **69**: 1006-1009.

Maisonpierre et al., 1997

Maisonpierre PC, Suri C, Jones P, Bartunkova S, Wiegand SJ, Radziejewski C, Compton D, McClain J, Aldrich TH, Papadopoulos N, Daly TJ, Davis S, Sato TN, Yancopulos GD.
Angiopoietin-2, a natural antagonist for Tie-2 that disrupts *in vivo* angiogenesis.
Science 1997; **277**: 55-60.

Majack, 1987

Majack R.
β-type transforming growth factor specifies organizational behavior in vascular smooth muscle cell cultures.
Journal of Cell Biology 1987; **105**: 465-467.

Majno and Palade, 1961

Majno G, Palade GE.
Studies on inflammation. I: The effects of histamine and serotonin on vascular permeability: An electron microscopic study.
Journal of Biophysical & Biochemical Cytology 1961; **11**: 571-605.

Mandriota and Pepper, 1998

Mandriota SJ, Pepper MS.
Regulation of angiopoietin-2 mRNA levels in bovine microvascular endothelial cells by cytokines and hypoxia.
Circulation Research 1998; **83**: 852-859.

Martin et al., 1995

Martin JS, Dickson MC, Cousins FM, Kulkarni AB, Karlsson S, Akhurst RJ.
Analysis of homozygous TGF-β_1 null mouse embryos demonstates defects in yolk sac vasculogenesis and Hematopoiesis.
Annals of the New York Academy of Sciences 1995; **752**: 300-308.

Massagué, 1985

Massagué J.
Subunit structure of a high-affinity receptor for type β-transforming growth factor: Evidence for a disulfide-linked glycosylated receptor complex.
Journal of Biological Chemistry 1985; **260**: 7059-7066.

Massaguè, 1990

Massagué J.
The transforming growth factor-β family.
Annual Review of Cell Biology 1990; **6**: 597-641.

Massagué et al., 1986

Massagué J, Cheifetz S, Endo T, Hadal-Ginard B.
Type-β transforming growth factor is an inhibitor of mitogenic differentiation.
Proceedings of the National Academy of Sciences of the United States of America 1986; **83**: 8206-8210.

Matsui et al., 1989

Matsui T, Heidaran M, Miki T, Popescu N, La Rochelle W, Kraus M, Pierce J, Aaronson S.
Isolation of a novel receptor cDNA establishes the existence of two PDGF receptor genes.
Science 1989; **243**: 800-804.

Mausi et al., 1986

Mausi T, Wakefield LM, Lechner JF, LaVeck MA, Sporn MB, Harris CC.
Type-β transforming growth factor is the primary differentiation inducing serum factor for normal human bronchial epithelial cells.
Proceedings of the National Academy of Sciences of the United States of America 1986; **83**: 2438-2442.

McColm and Cunningham, 2000

McColm J, Cunningham S.
The development of a computer controlled system to simulate in rats, the rapid, frequent changes in oxygen experienced by preterm infants developing retinopathy of prematurity.
Journal of Medical Engineering & Technology 2000; **24**: 45-52.

McColm and Fleck, 2001

McColm JR, Fleck BW.
Retinopathy of prematurity: Causation.
Seminars in Neonatology 2001; **6**: 453-460.

McColm et al., 2004

McColm JR, Cunningham S, Wade J, Sedowofia K, Gellen B, Sharma T, McIntosh N, Fleck BW.
Hypoxic oxygen fluctuations produce less severe retinopathy than hyperoxic fluctuations in a rat model of retinopathy of prematurity.
Pediatric Research 2004; **1**: 107-113.

McDonnel, 1994

McDonnel JM.
Ocular embryology and anatomy.
In Ogden TE, ed. *Retina*, pp5-17.
St. Louis, Mosby; 1994.

McLeod, Brownstein and Lutty, 1996

McLeod DS, Brownstein R, Lutty GA.
Vaso-obliteration in the canine model of oxygen-induced retinopathy.
Investigative Ophthalmology & Visual Science 1996; **37**: 300-311.

McLeod, Crone and Lutty, 1996

McLeod DS, Crone SN, Lutty G.
Vasoproliferation in the neonatal dog model of oxygen-induced retinopathy.
Investigative Ophthalmology & Visual Science 1996; **37**: 1322-1333.

McLeod, D'Anna and Lutty, 1998

McLeod DS, D'Anna SA, Lutty GA.
Clinical and histopathologic features of canine oxygen-induced proliferative retinopathy.
Investigative Ophthalmology & Visual Science 1998; **39**: 1918-1932.

Meyrick and Reid, 1978

Meyrick B, Reid L.
The effect of continued hypoxia on rat pulomary arterial circulation. An ultrastructural study.
Laboratory Investigation 1978; **38**: 188-200.

Michaelson, 1948

Michaelson IC.
The mode of development of the vascular system of the retina, with some observations on its significance for certain retinal diseases.
Transactions of the Ophthalmogical Society, UK 1948; **68**: 137 180.

Millauer et al., 1993

Millauer B, Wizigmann-Voos S, Schnurch H, Martinez R, Meller NPH, Risau W, Ullrich A.
High affinity VEGF binding and developmental expression suggest Flk-1 as a major regulator of vasculogenesis and angiogenesis.
Cell 1993; **72**: 835-846.

Mitchell et al., 1990

Mitchell JJ, Reynolds SE, Leslie KO, Low RB, Woodcock-Mitchell J.
Smooth muscle cell markers in developing rat lung.
American Journal of Respiratory Cell & Molecular Biology. 1990; **3**: 515-523.

Moses et al., 1981

Moses HL, Branum EL, Proper JA, Robinson RA.
Transforming growth factor production by chemically transformed cells.
Cancer Research 1981; **41**: 2842-2848.

Moses et al., 1985

Moses H, Tucker R, Leod E, Coffey R, Halper J, Shipley G.
Type-β transforming growth factor is a growth stimulator and a growth inhibitor.
In Feramisco J, Ozanne B, Stiles C, ed. *Cancer Cells*, pp 65-71. New York, Cold Springer Harbor Press; 1985.

Mudhar et al., 1993

Mudhar HS, Pollock RA, Wang C, Stiles CD, Richardson WD.
PDGF and its receptors in the developing rodent retina and optic nerve.
Development 1993; **118**: 539-552.

Nambu et al., 2003

Nambu H, Nambu R, Oshima Y, Duh E, Hackett SF, Zack DJ, Campochiaro PA.
Angiopoietin 1 decreases ocular neovascularisation and VEGF-induced breakdown of the blood-retinal barrier
Investigative Ophthalmology & Visual Science 2003; **44**: E-Abstract 2901.

Nayak et al., 1988

Nayak RC, Berman AB, George KL, Eisenbarth GS, King GL.
A monoclonal antibody (3G5)-defined ganglioside antigen is expressed on the cell surface of microvascular pericytes.
Journal of Experimental Medicine 1988; **167**: 1003-1015.

Nehls and Drenckhahn, 1991

Nehls V, Drenckhahn D.
Heterogeneity of microvascular pericytes for smooth muscle type alpha-actin.
Journal of Cell Biology 1991; **113**: 147-154.

Nehls and Drenckhahn, 1993

Nehls V, Drenckhahn D.
The versatility of microvascular pericytes: From mesenchyme to smooth muscle?
Histochemistry 1993; **99**: 1-12.

Nehls, Denzer and Drenckhahn, 1992

Nehls V, Denzer K, Drenckhahn D.
Pericyte involvement in capillary sprouting during angiogenesis *in situ*.
Cell & Tissue Research 1992; **270**: 469-474.

Newcomb and Herman, 1993

Newcomb PM, Herman IM.
Pericyte growth and contractile phenotype: Modulation by endothelial-synthesized matrix and comparison with aortic smooth muscle.
Journal of Cellular Physiology 1993; **155**: 385-393.

Nicosia and Villaschi, 1995

Nicosia RF, Villaschi S.
Rat aortic smooth muscle cells become pericytes during angiogenesis *in vitro*.
Laboratory Investigation 1995; **73**: 658-666.

Oh et al., 1999

Oh H, Tagaki H, Suzuma K, Otani A, Matsumura M, Honda Y.
Hypoxia and vascular endothelial growth factor selectively up-regulate angiopoietin-2 in bovine microvascular cells.
Journal of Biological Chemistry 1999; **274**: 15732-15739.

Ohta et al., 1987

Ohta M, Greenberger JS, Anklesaria P, Bassols A, Massague J.
Two forms of transforming growth factor-β distinguished by multipotential haematopoietic progenitor cells.
Nature 1987; **329**: 539-541.

Orlidge and D'Amore, 1987

Orlidge A, D'Amore PA.
Inhibition of capillary endothelial cell growth by pericytes and smooth muscle cells.
Journal of Cell Biology 1987; **105**: 1455-1462.

Oshima, Oshima and Taketo, 1996

Oshima M, Oshima H, Taketo MM.
TGF-β receptor type II deficiency results in defects of yolk sac hematopoiesis and vasculogenesis.
Developmental Biology 1996; **179**: 297-302.

Östman et al., 1991

Östman A, Andersson M, Hellman U, Heldin C-H.
Identification of three amino acids in the platelet-derived growth factor (PDGF) B-chain that are important for binding to the PDGF β-receptor.
Journal of Biological Chemistry 1991; **266**: 10073-10077.

Owens and Thompson, 1986

Owens GK, Thompson MM.
Developmental changes in isoactin expression in rat aortic smooth muscle cells *in vivo*. Relationship between growth and cytodifferentiation.
Journal of Biological Chemistry 1986; **261**: 13373-13380.

Owens et al., 1989

Owens G, Geisterfer A, Yang Y-H, Komoriya A.
Transforming growth factor-β-induced growth inhibition and cellular hypertrophy in cultured vascular smooth muscle cells.
Journal of Cell Biology 1989; **107**: 771-780.

Owens, 1995

Owens GK.
Regulation of differentiation of vascular smooth muscle cells.
Physiological Reviews 1995; **75**: 487-517.

Pagan-Mercado et al., 2002

Pagan-Mercado G, Yamamoto T, Hickman FI, Fariss RN, Tsai JY.
Analysis of NG-2 as a marker for retinal pericytes.
Investigative Ophthalmology & Visual Science 2002; **43**: E-Abstract 3700.

Palmer et al., 1991

Palmer EA, Flynn JT, Hardy RJ, Phelps DL, Phillips CL, Schaffer DB, Tung B.
The cryotherapy for retinopathy of prematurity cooperative group. Incidence and early course of retinopathy of prematurity.
Ophthalmology 1991; **98**: 1628-1640.

Papapetropoulos et al., 1999

Papapetropoulos A, Maisonpierre PC, Yancopoulos GD, Sessa WC.
Direct action of Angiopoietin-1 on human endothelium: Evidence for network stabilisation, cell survival, and interaction with other angiogenic growth factors.
Laboratory Investigation 1999; **79**: 213-223.

Papapetropoulos et al., 2000

Papapetropoulos A, Fulton D, Mahboubi K, Kalb RG, O'Connor DS, Li F, Altieri DC, Sessa WC.
Angiopoietin-1 inhibits endothelial cell apoptosis via the Akt/survivin pathway.
The Journal of Biological Chemistry 2000; **275**: 9102-9105.

Patz, 1968

Patz A.
The role of oxygen in retrolental fibroplasia.
Transactions of the American Ophthalmological Society 1968; **66**: 940-985.

Patz, 1980a

Patz A.
Studies on retinal neovascularisation.
Investigative Ophthalmology & Visual Sciences 1980; **19**: 1133-1138.

Patz, 1980b

Patz A.
Retrolental fibroplasia (retinopathy of prematurity).
Transactions of the Ophthalmological Society of New Zealand 1980; **32**: 49-54.

Patz, 1982

Patz A.
Clinical and experimental studies in retinal neovascularisation.
XXXIX Edward Jackson Memorial Lecture.
American Journal of Ophthalmology 1982; **94**: 715-743.

Patz, Hoeck and DelaCruz, 1952

Patz A, Hoeck LE, DelaCruz E.
Studies on the effect of high oxygen administration in retrolental fibroplasia: Nursery observations.
American Journal of Ophthalmology 1952; **35**: 1248-1253.

Patz et al., 1953

Patz A, Eastham A, Higgenbotham DH, Kleh T.
Oxygen studies in retrolental fibroplasia: Production of the microscopic changes of retrolental fibroplasia in experimental animals.
Americal Journal of Ophthalmology 1953; **36**: 1151-11.

Penn, Henry and Tolman, 1994

Penn JS, Henry MM, Tolman BL.
Exposure to alternating hypoxia and hyperoxia causes severe proliferative retinopathy in the newborn rat.
Pediatric Research 1994; **36**: 724-731.

Penn, Tolman and Henry, 1994

Penn JS, Tolman BL, Henry MM.
Oxygen-induced retinopathy in the rat: Relationship of retinal nonperfusion to subsequent neovascularization.
Investigative Ophthalmology & Visual Science 1994; **35**: 3429-3435.

Penn, Tolman and Lowery, 1993

Penn JS, Tolman BL, Lowery LA.
Variable oxygen exposure causes preretinal neovascularisation in the newborn rat.
Investigative Ophthalmology & Visual Science 1993; **34**: 576-585.

Penn et al., 1995

Penn JS, Henry MM, Wall PT, Tolman BL.
The range of PaO_2 variation determines the severity of oxygen induced retinopathy in newborn rats.
Investigative Ophthalmology & Visual Science 1995; **36**: 2063-2070.

Perry, Anthony and Steiner, 1997

Perry KT, Anthony CT, Steiner MS.
Immunohistochemical localisation of TGF-β_1, TGF-β_2, and TGF-β_3 in normal and malignant human prostate.
Prostate 1997; **33**: 133-140.

Pfeffer et al., 1994

Pfeffer BA, Flanders KC, Danielpour D, Anderson DH.
Transforming growth factor-β_2 is the predominant isoform in the neural retina, retinal pigment epithelium-choriod and vitreous of the monkey eye.
Experimental Eye Research 1994; **59**: 323-333.

Phelps, 1992

Phelps DL.
Retinopathy of prematurity.
The New England Journal of Medicine 1992; **326**; 1078-1080.

Phelps, 1993

Phelps DL.
Retinopathy of prematurity.
The Pediatric Clinics of North America 1993; **40**: 705-714.

Phelps and Rosenbaum, 1987

Phelps DL, Rosenbaum AL.
Effects of variable oxygenation and gradual withdrawal of oxygen during the recovery phase of oxygen-induced retinopathy: Kitten model.
Pediatric Research. 1987; **22**: 297-301.

Pierce et al., 1995a

Pierce EA, Avery RL, Foley ED, Aiello LP, Smith LEH.
Vascular endothelial growth factor/vascular permeability factor expression in a mouse model of retinal neovascularization.
Proceedings of the National Academy of Sciences of the United States of America 1995; **92**: 905-909.

Pierce et al., 1995b

Pierce DF, Gorska AE, Chytil AA, Meise KS, Page DL, Coffey RJ, Moses HL.
Mammary tumor suppression by transforming growth factor-β_1 transgene expression.
Proceeding in the National Academy Sciences of the United States of America 1995; **92**: 4254-4258.

Provis et al., 1995

Provis JM, Penfold PL, Edwards AJ, van Driel D.
Human retinal microglial: Expression of immune markers and relationship to the glia limitans.
Glia 1995; **14**: 243-256.

Provis, 2001

Provis JM.
Development of the primate retinal vasculature.
Progress in Retinal & Eye Research 2001; **20**: 799-821.

Reynolds, Killilea and Redmer, 1992

Reynolds LP, Killilea SD, Redmer DA.
Angiogenesis in the female reproductive system.
FASEB Journal 1992; **6**: 886-892.

Rhodin, 1968

Rhodin JAG.
Ultrastructural of mammalian venous capillaries, venules and small collecting veins.
Journal of Ultrastructure Research 1968; **25**: 452-500.

Risau, 1997

Risau W.
Mechanisms of angiogenesis.
Nature 1997; **386**: 671-674.

Robbins et al., 1994

Robbins SG, Mixon RN, Wilson DJ, Hart CE, Robertson JE, Westra I, Planck SR, Rosenbaum JT.
Platelet-derived growth factor ligands and receptors immunolocalized in proliferative retinal diseases.
Investigative Ophthlamology & Visual Science 1994; **35**: 3649-3663.

Roberts et al., 1981

Roberts AB, Anzano MA, Lamb LC, Smith JM, Sporn MB.
New class of transforming growth factors potentiated by epidermal growth factor.
Proceedings of the National Academy of Sciences of the United States of America 1981; **78**: 5339-5343.

Roberts et al., 1983

Roberts AB, Frolik CA, Anzano MA, Sporn MB,
Transforming growth factors from neoplastic and non neoplastic tissues.
Federation Proceedings 1983; **42**: 2621-2626.

Roberts et al., 1985

Roberts A, Anzano M, Wakefield L, Roche N, Stern D, Sporn M.
Type-β transforming growth factor: A bifunctional regulator of cellular growth.
Proceedings of the National Academy of Sciences of the United States of America 1985; **82**: 119-123.

Rogers, 1996

Rogers W.
Vision impairment in Liverpool: prevalence and morbidity.
Archives of Disease in Childhood 1996; **74**: 299-303.

Ross et al., 1974

Ross R, Glomset J, Kariya B, Harker L.
A platelet-dependent serum factor that stimulates the proliferation of arterial smooth muscle cells *in vitro*.
Proceedings of the National Academy of Sciences of the United States of America 1974; **71**: 1207-1210.

Rouget, 1873

Rouget C.
Memoire sur le developpement, la structure et les propietes des capillaries sanguins and lymphatiques.
Archives de Physiologie Normale et Pathologique 1873; **5**: 603-661.

Rutherford and Ross, 1976

Rutherford R, Ross R.
Platelet factors stimulate fibroblasts and smooth muscle cells quiescent in plasma serum to proliferate.
Journal of Cell Biology 1976; **69**: 196-203.

Ryan, 1952

Ryan H.
Retrolental fibroplasia: A clinical study.
American Journal of Ophthalmology 1952; **35**: 329-342.

Sato and Rifkin, 1988

Sato Y, Rifkin DB.
Autocrine activities of basic fibroblast growth factor: Regulation of endothelial cell movement, plasminogen activator synthesis, and DNA synthesis.
Journal of Cell Biology 1988; **107**: 1199-1205.

Sato and Rifkin, 1989

Sato Y, Rifkin D.
Inhibition of endothelial cell movement by pericytes and smooth muscle cells: Activation of a latent transforming growth factor-β_1-like molecule by plasmin during co-culture.
Journal of Cell Biology 1989; **109**: 309-315.

Sato et al., 1990

Sato Y, Tsuboi R, Lyons R, Moses H, Rifkin DB.
Characterisation of the activation of latent TGF-β by co-cultures of endothelial cells and pericytes or smooth muscle cells: A self regulating system.
Journal of Cell Biology 1990; **111**: 757-763.

Sato et al., 1993

Sato TN, Qin Y, Kozak CA, and Audus KL.
Tie-1 and Tie-2 define another class of putative receptor tyrosine kinase genes expressed in early embryonic vascular system.
Proceedings of the National Academy of Sciences of the United States of America 1993; **90**: 9355-9358.

Sato et al., 1995

Sato TN, Tozawa Y, Deutsch, Wolburg-Buccholz K, Fujiwara Y, Gendron-Maguire M, Gridley T, Wolburg H, Risau W, Qin Y.
Distinct roles of the receptor tyrosine kinases Tie-1 and Tie-2 in blood vessel formation.
Nature 1995; **376**: 70-74.

Scher, Stone and Stiles, 1979

Scher C, Stone ME, Stiles CD.
Platelet-derived growth factor prevents G_0 growth arrest.
Nature 1979;**281** :390-392.

Scherer and Schnitzer, 1994

Scherer J, Schnitzer J.
Growth factor effects on the proliferation of different retinal glial cells *in vitro*.
Developmental Brain Research 1994; **80**: 209-221.

Schlingemann et al., 1990

Schlingemann RO, Rietveld FJR, de Waal RMW, Ferrone S, Ruiter DJ.
Expression of the high molecular weight melanoma-associated antigen by pericytes during angiogenesis in tumors and in healing wounds.
American Journal of Pathology 1990; **136**: 1393-1405.

Schor et al., 1995

Schor AM, Canfield AE, Sutton AB, Arciniegas E, Allen TD.
Pericyte differentiation.
Clinical Orthopaedics & Related Research 1995; **313**: 81-91.

Seyedin et al., 1985

Seyedin S, Thomas T, Thompson A, Rosen D, Piez K.
Purification and characterisation of two cartilage inducing factors from bovine demineralised bone.
Proceedings of the National Academy of Sciences of the United States of America 1985; **82**: 2267-2270.

Seyedin et al., 1987

Seyedin SM, Segarini PR, Rosen DM, Thompson, AY, Bentz H, Graycar J.
Cartilage-inducing factor-B is a unique protein structurally and functionally related to transforming growth factor-β.
Journal of Biological Chemistry 1987; **262**: 1946-1949.

Shah, Groves and Anderson, 1996

Shah N, Groves A, Anderson D.
Alternative neural crest cell fates are instructively promoted by TGF-β superfamily members.
Cell 1996; **85**: 331-343.

Shakib and de Oliveria, 1966

Shakib M, de Oliveria F.
Studies on developing retinal vessels. X. Formation of the basement membrane and differentiation of intramural pericytes.
British Journal of Ophthalmology 1966; **50**: 124-133.

Shalaby et al., 1995

Shalaby F, Rossant J, Yamaguchi TP, Gertenstein M, Wu XF, Breitman ML, Schch AC.
Failure of blood-island formation and vasculogenesis in Flk-1-deficient mice.
Nature 1995; **376**: 62-66.

Shepro and Morel, 1993

Shepro D, Morel NML.
Pericyte physiology.
FASEB Journal 1993; **7**: 1031-1038.

Shoat et al., 1983

Shoat M, Reisner SH, Krikler R, Nissenkorn I, Ben-Sir I.
Retinopathy of prematurity: Incidence and risk factors.
Pediatrics 1983; **72**: 159-163.

Shull et al., 1992

Shull M, Ormsby I, Kier A, Pawlowski S, Diebold R, Yin M, Allen R, Sidman C, Proetzel G, Calvin D.
Targeted disruption of the mouse transforming growth factor-β_1 gene results in multifocal inflammatory disease.
Nature 1992; **359**: 693-699.

Shure et al., 1992

Shure D, Senior R, Griffin G, Deuel T.
PDGF AA homodimers are potent chemoattractants for fibroblasts and neutrophils, and for monocytes activated by lymphocytes or cytokines.
Biochemical & Biophysical Research Communication 1992; **186**: 1510-1514.

Shweiki et al., 1992

Shweiki D, Itin A, Soffer D, Keshet E.
Vascular endothelial growth factor induced by hypoxia may mediate hypoxia-initiated angiogenesis.
Nature 1992; **359**: 843-845.

Sims, 1986

Sims DE.
The pericyte - A review.
Tissue & Cell 1986; **18**: 153-174.

Sirtautiené, 1997

Sirtautiené BR.
Threshold ROP in Lithuania: Tendencies during 3 years.
In Reibadi A, Di Pietro M, Scuteri A, Malerbi E, ed. *Progress in Retinopathy of Prematurity,* pp31-36.
Amsterdam, Kluger; 1997.

Skalli et al., 1989

Skalli O, Pelte M-F, Peclet M-C, Gabbiani G, Gugliotta P, Bussolati G, Ravazzola M, Orci L.
α-smooth muscle actin, a differential marker of smooth muscle cells, is present in microfilamentous bundles of pericytes.
The Journal of Histochemistry & Cytochemistry 1989; **37**: 315-321.

Smith et al., 1994

Smith LH, Wesolowski E, McLellan A, Kostyk SK, D'Amato R, Sullivan R, D'Amore PA.
Oxygen-induced retinopathy in the mouse.
Investigative Ophthalmology & Visual Science 1994; **35**: 101-111.

Smits et al., 1989

Smits A, Hermansson M, Nister M, Karnushina I, Heldin CH, Westermark B, Funa K.
Rat brain capillary endothelial cells express functional PDGF B-type receptors.
Growth Factors 1989; **2**: 1-8.

Soriano, 1994

Soriano P.
Abnormal kidney development and hematological disorders in PDGF β-receptor mutant mice.
Genes & Development 1994; **8**: 1888-1896.

Soriano, 1997

Soriano P.
The PDGFα receptor is required for neural crest cell development and for normal patterning of the somites.
Development 1997; **124**: 2691-2700.

Speiser, Gittelsohn and Patz, 1968

Speiser P, Gittelsohn AM, Patz A.
Studies on diabetic retinopathy. 3. Influence of diabetes on intramural pericytes.
Archives of Opthalmology 1968; **80**: 332-3337.

Stein et al., 1995

Stein I, Neeman M, Shweiki D, Itin A, Keshet E.
Stabilisation of vascular endothelial growth factor mRNA by hypoxia and hypoglycaemia and coregulation with other ischaemia-induced genes.
Molecular & Cellular Biology 1995; **15**: 5636-5368.

Steinberg, 1963

Steinberg MS.
ECM: Its nature, origin and function in cell aggregation.
Experimental Cell Research 1963; **30**: 257-279.

Stone and Maslim, 1997

Stone J, Maslim J.
Mechanisms of retinal angiogenesis.
Progress in Retinal & Eye Research 1997; **16**: 157-181.

Stone et al., 1995

Stone J, Itin A, Alon T, Peer J, Gnessin H, Chan Ling T, Pe'er Y, Keshet E.
Development of retinal vasculature is mediated by hypoxia-induced vascular endothelial growth factor (VEGF) expression by neuroglia.
Journal of Neuroscience 1995; **15**: 4738-4747.

Stone et al., 1996

Stone J, Chan-Ling T, Pe'er J, Itin A, Gnessin H, Keshet E.
Roles of vascular endothelial growth factor and astrocyte degeneration in the genesis of retinopathy of prematurity.
Investigative Ophthalmology & Visual Science 1996; **37**: 290-299.

The STOP-ROP Multicenter Study Group, 2000

The STOP-ROP Multicentre Study Group.
Supplemental therapeutic oxygen for prethreshold retinopathy of prematurity (STOP-ROP), a randomised, controlled trial. I. Primary outcomes.
Pediatrics 2000; **105**: 295-309.

Stratman, Risau and Plate, 1998

Stratmann A, Risau W, Plate KH.
Cell type-specific expression of angiopoietin-1 and angiopoietin-2 suggests a role in glioblastoma angiogenesis.
American Journal of Pathology 1998; **153**: 1459-1466.

Stratmann et al., 2001

Stratmann A, Acker T, Burger AM, Amann K, Risau W, Plate KH.
Differential inhibition of tumor angiogenesis by Tie-2 and vascular endothelial growth factor receptor-2 dominant-negative receptor mutants.
International Journal of Cancer 2001; **92**: 273-282.

Suri et al., 1996

Suri C, Jones P, Patan S, Bartunkova S, Maisonpierre PC, Davis S, Sato TN, Yancopoulos D.
Requisite role of angiopoietin-1, a ligand for the Tie-2 receptor, during embryonic angiogenesis.
Cell 1996; **87**: 1171-1180.

Suri et al., 1998

Suri C, McClain J, Thurston G, McDonald DM, Zhou Z, Oldmixon EH, Sato TN, Yancopoulos GD.
Increased vascularisation in mice overexpressing angiopoietin-1.
Science 1998; **282**: 468-471.

Tanaka et al., 1999

Tanaka S, Mori M, Sakamoto Y, Makuuchi M, Sugimachi K, Wands JR.
Biologic significance of angiopoietin-2 expression in human hepatocellular carcinoma.
Journal of Clinical Investigation 1999; **103**: 341-345.

ten Dijke et al., 1988

ten Dijke P, Hansen P, Iwata K, Pieler C, Foulkes J.
Identification of another member of the transforming growth factor type-β gene family.
Proceedings of the National Academy of Sciences of the United States of America 1988; **85**: 4715-4719.

ten Dijke et al., 1990

ten Dijke P, Iwata KK, Thorikay M, Schwedes J, Stewart A, Pieler C.
Molecular characterization of transforming growth factor type-β_3.
Annals of the New York Academy of Sciences 1990; **593**: 26-42.

Terracio et al., 1988

Terracio L, Rönnstrand L, Tingström A, Rubin K, Claesson-Welsh L, Funa K, Heldin CH.
Induction of platelet-derived growth factor receptor expression in smooth muscle cells and fibroblasts upon tissue culturing.
Journal of Cell Biology 1988; **107**: 1947-1957.

Terry, 1942

Terry TL.
Extreme prematurity and fibroblastic overgrowth of persistent vascular sheath behind each crystalline lens.
American Journal of Ophthalmology 1942; **25**: 203-204.

Thurston et al., 1999

Thurston G, Suri C, Smith K, McClain J, Sato TN, Yancopoulos GD, McDonald DM.
Leakage-resistant blood vessels in mice transgenically overexpressing angiopoietin-1.
Science 1999; **286**: 2511-2514.

Thurston et al., 2000

Thurston G, Rudge JS, Ioffe E, Zhou H, Ross L, Croll SD, Glazer N, Holash J, McDonald DM, Yancopoulos GD.
Angiopoietin-1 protects the adult vasculature against plasma leakage.
Nature Medicine 2000; **6**: 460-463.

Tilton et al., 1985

Tilton RG, Miller EJ, Kilo C, Williamson JR.
Pericyte form and distribution in rat retinal and uveal capillaries.
Investigative Ophthalmology & Visual Science 1985; **26**: 68-73.

Tsushima et al., 1996

Tsushima H, Kawata S, Tamura S, Ito N, Shirai Y, Kiso S, Imai Y, Shimomukai H, Nomura Y, Matsuzawa Y.
High levels of transforming growth factor-β_1 in patients with colorectal cancer association with disease progression.
Gastroenterology 1996; **110**: 375-382

Tucker et al., 1984

Tucker R, Shipley G, Moses H, Holley R.
Growth inhibition from BSC-1 cells closely related to platelet type-β transforming growth factor.
Science 1984; **226**: 705-707.

Uchihori and Puro, 1991

Uchihori Y, Puro DG.
Mitogenic and chemotactic effects of platelet-derived growth factor on human retinal glial cells.
Investigative Ophthlamology & Visual Sciencce 1991; **32**: 2689-2695.

Valenzuela et al., 1999

Valenzuela DM, Griffiths JA, Rojas J, Aldrich TH, Jones PF, Zhou H, McCalin J, Copeland NG, Gilbery DJ, Jenkins NA, Huang T, Papadopoulos N, Maisonpierre PC, Davis S, Yancopoulos GD.
Angiopoietins 3 and 4: Diverging gene counterparts in mice and humans.
Proceedings of the National Academy of Sciences of the United States of America 1999; **96**: 1904-1909.

Volpe, 1995

Volpe JJ.
Neurology of the Newborn.
Philadelphia, Saunders; 3rd edition, 1995.

Verbeek et al., 1994

Verbeek MM, Otte-Holler I, Wesseling P, Ruiter DJ, de Waal RM.
Induction of α-smooth muscle actin expression in cultured human brain pericytes by transforming growth factor-β_1.
Americal Journal of Pathology 1994; **144**: 372-382.

Wahl et al., 1987

Wahl S, Hunt D, Wakefield L, McCartney-Francis N, Wahl L, Roberts AB, Sporn MB.
Transforming growth factor type-β induces monocyte chemotaxis and growth factor production.
Proceedings of the National Academy of Sciences of the United States of America 1987; **84**: 5788-5792.

Wakefield et al., 1987

Wakefield LM, Smith DM, Matsui T, Harris CC, Sporn MB.
Distribution and modulation of the cellular receptor for transforming growth factor-β.
Journal of Cell Biology 1987; **105**: 965-975.

Wakefield et al., 1988

Wakefield LM, Smith DM, Masui T, Harris CC, Sporn MB.
Latent transforming growth factor-β.
Journal of Cell Biology 1988; **105**: 965-975.

Watanabe and Raff, 1998

Watanabe T, Raff MC.
Retinal astrocytes are immigrants from the optic nerve.
Nature 1998; **332**: 834-837.

Waterfield et al., 1983

Waterfield MD, Scrace GT, Whittle N, Stroobant P, Johnsson A, Wasteson Å, Westermark B, Heldin CH, Huang JS, Deuel TF.
Platelet derived growth factor is structurally related to the putative transforming p28sis of simian sarcoma virus.
Nature 1983; **304**: 35-39.

Weakley and Spencer, 1992

Weakley DR, Spencer R.
Current concepts in retinopathy of prematurity.
Early Human Development 1992; **30**: 121-138.

Weiss, 1988

Weiss L.
Cell and Tissue Biology: A Textbook of Histology, Ch8.
Baltimore, Urban & Schwarzenberg Inc; 1988.

Weiter, Zuckerman and Schepens, 1982

Weiter JJ, Zuckerman R, Schepens CL.
A model for the pathogenesis of retrolental fibroplasias based on the metabolic control of blood vessel development.
Ophthalmic Surgery 1982; **13**: 1013-1017.

Westermark and Wasteson, 1976

Westermark B,.Wasteson Å.
A platelet factor stimulating human normal glial cells.
Experimental Cell Research 1976; **98**: 170-174.

William et al., 2000

Willam C, Koehne P, Jërgensen JS, Gräfe M, Wagner KD, Bachmann S, Frei U, Eckardt KU.
Tie-2 receptor expression is stimulated by hypoxia and proinflammatory cytokines in human endothelial cells.
Circulation Research 2000; **87**: 370-377.

Wise, Dollery and Henkind, 1971

Wise GN, Dollery CT, Henkind P.
The Retinal Circulation, pp34-48.
New York, Harper and Row; 1971.

Witzenbichler et al., 1998

Witzenbichler B, Maisonpierre PC, Jones P, Yancopoulos GD, Isner JM.
Chemotactic properties of angiopoietin-1 and -2, ligands for the endothelial-specific receptor tyrosine kinase Tie-2.
Journal of Biological Chemistry 1998; **273**: 18514-18521.

Wong et al., 1997

Wong AL, Haroon ZA, Werner S, Dewhirst M, Greenberg CS, Peters KG.
Tie-2 expression and phosphorylation in angiogenic and quiescent adult tissue.
Circulation Research 1997; **81**:567-574.

Wrana et al., 1994

Wrana J, Attisano L, Weiser R, Vntura F, Massagué J.
Mechanism of activation of the TGF-β receptor.
Nature 1994; **370**: 341-347.

Wu et al., 1992

Wu SP, Theodorescu D, Kerbel RS, Willson JK, Mulder KM, Humphrey LE, Brattain MG.
TGF-β_1 is an autocrine-negative growth regulator of human colon carcinoma FET cells in vivo as revealed by transfection of an antisense expression vector.
Journal of Cell Biology 1992; **116**: 187-196.

Wulff et al., 2000

Wulff C, Wilson H, Largue P, Duncan WC, Armstrong DG, Fraser HM.
Angiogenesis in the human corpus luteum: Localisation and changes in angiopoietins, Tie-2, and vascular endothelial growth factor messenger ribonucleic acid.
Journal of Clinical Endocrinology & Metabolism 2000; **85**: 4302-4309.

Xu, Quam and Adamis, 2001

Xu Q, Quam T, Adamis AP.
Sensitive blood-retinal barrier breakdown quantitation using Evans blue.
Investigative Ophthalmology & Visual Science 2001; **42**: 789-794.

Xu, Zhang and Adelman, 2003

Xu Z, Zhang J, Adelman RA.
Angiopoietin-1 gene transfer and its effects on the leakage of an experimental model of retinal neovascularisation.
Investigative Ophthalmology & Visual Science 2003; **44**: E-Abstract 568.

Yamada et al., 1999

Yamada H, Obata H, Kaji Y, Yamashita H.
Expression of transforming growth factor-β superfamily receptors in developing rat eyes.
Japanese Journal of Ophthalmology 1999; **43**: 290-294.

Yarden et al., 1986

Yarden Y, Escobedo J, Kuang W-J, Yang-Feng T, Daniel T, Tremble P, Chen EY, Ando ME, Harkins RN, Francke U.
Structure of the receptor for platelet-derived growth factor helps define a family of closely related growth factor receptors.
Nature 1986; **323**: 226-232.

Yu and Stamenkovic, 2001

Yu Q, Stamenkovic I.
Angiopoietin-2 is implicated in the regulation of tumor angiogenesis.
American Journal of Pathology 2001; **158**: 563-570.

Zhang and Stone, 1997

Zhang Y, Stone J.
Role of astrocytes in the control of developing retinal vessels.
Investigative Ophthalmology & Visual Science 1997; **38**: 1653-1666.

Ziavras and Javitt, 1995

Ziavras E, Javitt JJ.
Retinopathy of prematurity.
In David TJ, ed. *Recent Advances in Paediatrics*, pp177-91.
Edinburgh, Churchill Livingston; 1995.

Zimmermann, 1923

Zimmermann KW.
Der feinere bau der blutcapillaren.
Z Anat Entwicklungsgesch 1923; **68**: 29-109.

PUBLICATIONS

The Summer meeting of The Neonatal Society
7th March 2002, The Royal Society of Medicine, London

A comparison of the retinal vascular changes following a short or prolonged exposure to carbon dioxide in a variable oxygen model of retinopathy of prematurity. *Yaqoob, Z., McColm, J. R., Wade, J., Gellen, B., Fleck, B., Sharma, T., Gilmour, D., Cunningham, S., Sedowofia, K., McIntosh, N.*

Aims: To determine the effects of short versus long duration hypercarbia and fluctuating oxygen on the developing rat retinal vasculature.

Methods: Newborn rats were exposed to oxygen and carbon dioxide in one of three groups: (1) Variable oxygen exposure (VO_2) (2) VO_2 with 2 days 5% carbon dioxide ($2CO_2 + VO_2$) (3) VO_2 with 14 days 5% carbon dioxide ($14CO_2 + VO_2$). Following sacrifice at day 14, the eyes were enucleated, fixed in 2% PFA and retinal wholemounts prepared. Blood vessels were visualised by staining the endothelial cells using *G. simplicifolia* (Bandeiraea) isolectin B4 and the median number of branches and the peripheral avascular area were assessed by confocal microscopy.

Results:

	Control	**VO_2**	**$2CO_2 + VO_2$**	**$14CO_2 + VO_2$**
n	27	28	30	28
Median no. of branches/mm^2 (IQR)	702 (652 - 740)	645 * (646 - 702)	772 # (722 - 880)	785 # (742 - 896)
Median peripheral avascularity (IQR)	0% (0 - 0)	1.7% ** (0 - 7.6)	4.29% ** (3.03 - 5.54)	4.18% ** (3.12 - 4.92)
Median weights (g) (IQR)	29.8 (28.6 - 30.6)	22.9 ** (21.9 - 25.0)	25.8 # (24.8 - 27.7)	25.9 # (24.6 - 26.7)

* $p<0.05$ compared to control.
** $p<0.001$ compared to control.
\# $p<0.001$ compared to control and variable oxygen.

Conclusion: All experimental protocols induced features of retinopathy in rat pups. However, pups exposed to carbon dioxide had increased capillary branching and a greater peripheral avascular area when compared with controls. A prolonged exposure to carbon dioxide produced no greater retinopathy than a short, early exposure.

ARVO Meeting
5th-10th May, 2002, Fort Lauderdale, Florida
Published in Investigative Ophthalmology & Visual Science
2002; 43: E-abstract 1244

Retinal vascular changes in a variable oxygen model of retinopathy of prematurity comparing short and prolonged exposure to hypercarbia.

Yaqoob, Z., McColm, J. R., Wade, J., Gellen, B., Fleck, B., Sharma, T., Gilmour, D., Cunningham, S., Sedowofia, K., McIntosh, N.

Aims: To determine the effects of short versus long duration hypercarbia and fluctuating oxygen on the developing rat retinal vasculature.

Methods: Newborn rats were exposed to oxygen and carbon dioxide in one of three groups: (1) Variable oxygen exposure (VO_2) (2) VO_2 with 2 days 5% carbon dioxide ($2CO_2 + VO_2$) (3) VO_2 with 14 days 5% carbon dioxide ($14CO_2 + VO_2$). Following sacrifice at day 14, the eyes were enucleated, fixed in 2% PFA and retinal wholemounts prepared. Blood vessels were visualised by staining the endothelial cells using *G.simplicifolia* (Bandeiraea) isolectin B4 and the median number of branches and the peripheral avascular area were assessed by confocal microscopy.

Results:

	Control	VO_2	$2CO_2 + VO_2$	$14CO_2 + VO_2$
n	27	28	30	28
Median no. of branches/mm^2 (IQR)	702 (652 - 740)	645 * (646 - 702)	772 # (722 - 880)	785 # (742 - 896)
Median peripheral avascularity (IQR)	0% (0 - 0)	1.7% ** (0 - 7.6)	4.29% ** (3.03 - 5.54)	4.18% ** (3.12 - 4.92)
Median weights (g) (IQR)	29.8 (28.6 - 30.6)	22.9 ** (21.9 - 25.0)	25.8 # (24.8 - 27.7)	25.9 # (24.6 - 26.7)

* $p<0.05$ compared to control.
** $p<0.001$ compared to control.
\# $p<0.001$ compared to control and variable oxygen.

Conclusion: All experimental protocols induced features of retinopathy in rat pups. However, pups exposed to carbon dioxide had increased capillary branching and a greater peripheral avascular area when compared with controls. A prolonged exposure to carbon dioxide produced no greater retinopathy than a short, early exposure.

Retinal Vascular Changes in a Variable Oxygen Model of Retinopathy of Prematurity Comparing Short and Prolonged Exposure to Hypercarbia.

No. 1244

Z Yaqoob[1], JR McColm[2], J Wade[1], B. Gellen[1], BW Fleck[3], T Sharma[3], D Gilmour[3], S Cunningham[1], K Sedowofia[1], N McIntosh[1]

[1]Child life & Health, University of Edinburgh, Scotland, UK; [2]Dept of Ophthalmology, Louisiana State University, New Orleans, LA; [3]Princess Alexandra Eye Pavilion, Edinburgh, Scotland, UK

Introduction

Prolonged treatment of preterm infants with high oxygen levels has consistently been associated with the development of retinopathy of prematurity (ROP). Several studies have also investigated the effects of carbon dioxide on the development of the retinal vasculature. Although clinical studies have produced contradictory data[1,2], animal studies suggest that carbon dioxide is indeed a risk factor[3,4].

Most oxygen-induced retinopathy models involve the exposure of newborn animals to large swings of oxygen over long periods of time. These models do not represent the clinical situation of premature humans, hence, we developed an oxygen delivery system that mimics the clinical environment[5].

The aim of this project was to investigate the combination of oxygen variability with either an early, short or a prolonged exposure to hypercarbia on the developing retinal vasculature using our rat model.

Animal Model

The neonatal intensive care unit in Edinburgh continuously monitors the arterial oxygen of admitted infants by a computerised monitoring system. The first 14 days of the transcutaneous oxygen profile of an infant who developed ROP was selected and converted into percentage inspired oxygen levels to produce the equivalent arterial oxygen in a rat:

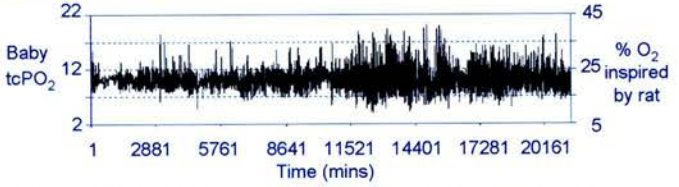

Rats exposed to this clinically relevant minute variable oxygen environment developed features of ROP[5].

Methods

3 groups of experimental rats were exposed to the unique Edinburgh oxygen variability model from birth to P14 (vO_2). In addition to the fluctuating oxygen, 2 of the groups were exposed to 5% CO_2 for either the first 48 hours of life (2d CO_2) or for the whole 14 day period (14d CO_2). A control group consisted of animals raised in room air.

Following sacrifice at day 14, the eyes were enucleated, fixed and retinal wholemounts prepared. Endothelial cells were visualised by overnight incubation with G. simplicifolia (Bandeiraea) isolectin B4 and images of sample retinal areas were captured using a confocal microscope. These images were used to visually assess the maturity of the vasculature and quantitatively assess the vascular changes in 2 ways: the capillary density and the extent of avascularity.

Results

Below are graphs illustrating the results from the analysis of the lectin stained retinal wholemounts. The median and interquartile range were determined and comparisons were made using the Mann-Whitney U test. Images of the representative retinal areas are adjacent to the appropriate graphs.

Median no. branches/mm^2 (IQR)

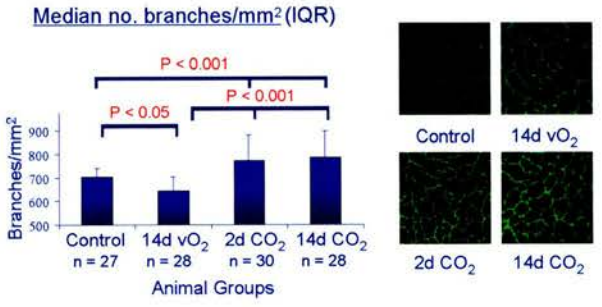

Median peripheral avascularity (IQR)

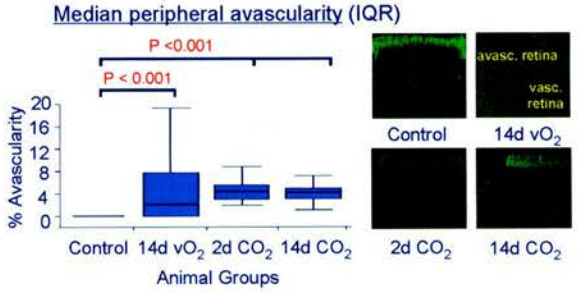

Abnormal terminal vessels

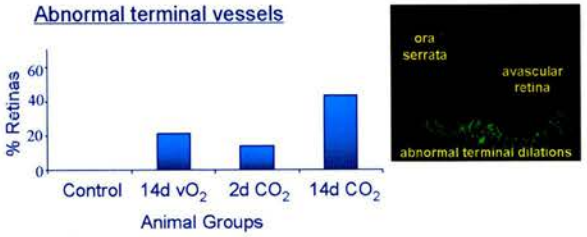

The retinas of the control group were fully vascularised with remodelled capillary beds and avascular areas around arteries. The capillary beds of the vO_2 group looked similar to the controls, but in fact had a decreased number of branches per mm^2 and a median avascular area of 1.8%. The vasculature of both CO_2 groups consisted of many smaller vessels with the absence of capillary free zones, hence groups 2d CO_2 and 14d CO_2 had a significantly greater capillary density than both the control and vO_2 groups. Although the median peripheral avascular area was greater in comparison to the vO_2 group, it was not statistically significant.

Discussion

Although we noted no neovascularisation, two masked observers did note abnormal terminal dilations present at the vascular/avascular interface of all experimental groups. Since these terminal vessels were stained with lectin, they may represent endothelial cell proliferation. The retinas of the 2d CO_2 group were not affected to the same extent as the retinas of the 14d CO_2 group, however, the 2d CO_2 retinas did have a distinct morphology; the terminal vessels were enlarged and the vessels ran along the circumference of the vascular/avascular junction.

Pups exposed to prolonged carbon dioxide had more abnormal terminal vessels than pups exposed to an early short period of carbon dioxide, however the extent of avascularity and the capillary density were similar in both CO_2 groups.

The exact mechanism of the induction of vascular changes by hypercarbia is unclear. Raised carbon dioxide acts as a vasodilator, causing increased retinal blood flow. This could result in increased tissue oxygen or oxygen variability causing a greater insult to the developing vasculature.

Conclusion

This study supports the view that carbon dioxide in addition to fluctuating oxygen produces more severe retinopathy than fluctuating oxygen alone. An early short exposure of carbon dioxide may be as clinically important as a prolonged exposure.

Acknowledgements

The oxygen delivery system was designed and built to our specification by BioSpherix (Reyfield, NY, USA).

This work has been supported by grants from Action Research and the Royal College of Surgeons, Edinburgh, U.K.

References

1. Brown DR, Milley JR, Ripepi UJ, et al. *Am J Dis Child* 1987;141:154-60.
2. Bauer CR. *Pediatrics* 1982;70:663.
3. Flower RW. *Birth Defects* 1988;24:129-46.
4. Holmes JM, Zhang S, Leske DA, et al. *Curr Eye Res* 1998;17:608-16.
5. Cunningham S, McColm JR, Wade J, et al. *Invest Ophthalmol Vis Sci* 2000;41:4275.

ARVO Meeting
4th-8th May, 2003, Fort Lauderdale, Florida
Published in Investigative Ophthalmology & Visual Science
2003; 44: E-abstract 585

Retinal pericyte/smooth muscle cell coverage in rats exposed to a variable oxygen model of retinopathy of prematurity (Edinburgh Model).

Yaqoob, Z., Sharp, L., Sedowofia, K., McColm, J. R., Wade, J. C., Giles, D. R., Fleck, B. W., Cunningham, S., McIntosh, N.

Purpose: To investigate pericyte/smooth muscle cell coverage during development of the normal rat retinal vasculature and determine how it is affected by fluctuating oxygen.

Methods: Litters of newborn rats were either reared in room air or exposed to a minute-by-minute variable oxygen profile, which induces features of retinopathy (including peripheral avascularity, vascular immaturity and abnormal terminal vessels) for 2, 7 and 14 days. Following sacrifice, the eyes were enucleated. The right eyes were fixed and retinal wholemounts prepared. The endothelial cells were visualised using *G.simplicifolia* (Bandeiraea) isolectin B4 and the pericytes/smooth muscle cells with α-smooth muscle actin (α-SMA) or desmin. The vasculature was examined using a confocal microscope. The left retinas of each litter were pooled, the protein extracted and blotted for α-SMA.

Results: In the normal rat retina, at day 2 α-SMA positive cells were found only on the arterioles. By day 7, coverage had begun on the arterial capillaries, and progressed further by day 14. Desmin positive cells, however, were present across the whole retinal vasculature, including the developing peripheral edge on all timepoints examined. Occasionally, cells were identified positive for both α-SMA and desmin. This pattern of labelling was also observed in retinas of rats exposed to variable oxygen. However, the retinal development in these rats was delayed and the longitudinal coverage of the arterioles with α-SMA positive cells does not progress as far as in controls. Desmin staining, although seen at the leading edge of the developing vasculature, was also reduced, particularly on the arterioles. Western blot analysis confirmed the decrease in α-SMA expression on days 7 and 14.

Conclusion: α-SMA stains smooth muscle cells; desmin stains pericytes. In normal development pericyte coverage is very rapid, but smooth muscle cell coverage lags significantly behind vessel formation. Smooth muscle cell coverage of the retinal vessels is decreased in rats exposed to variable oxygen in the Edinburgh model of retinopathy of prematurity.

RETINAL PERICYTE/SMOOTH MUSCLE CELL COVERAGE IN RATS EXPOSED TO A VARIABLE OXYGEN (EDINBURGH) MODEL OF RETINOPATHY OF PREMATURITY

No. 585

Z. Yaqoob[1], L. Sharp[2], K. Sedowofia[1], J. Wade[1], D.R. Giles[1], B.W. Fleck[3], J.R. McColm[4], S. Cunningham[1], N. McIntosh[1]

[1]Child Life & Health and [2]Department of Biomedical Sciences, University of Edinburgh, Scotland, UK; [3]Princess Alexandra Eye Pavilion, Edinburgh, Scotland, UK; [4]Dept of Ophthalmology, University of North Carolina, Chapel Hill, NC, USA.

INTRODUCTION

Mature retinal blood vessels are surrounded by a single layer of pericytes or smooth muscle cells, collectively called mural cells. This encapsulation by mural cells has been suggested to signal vessel stability. Smooth muscle cells are elongated, spindle shaped cells with fine tapered ends that encapsulate larger vessels[1], whereas pericytes are often elongated with multiple, long and slender cytoplasmic process that lie parallel to the axis of capillaries or encircle the capillary wall[2]. It is suggested that in retinopathy of prematurity (ROP), a potentially blinding eye disease affecting preterm infants, the vessels of the retina lack coverage by mural cells[3].

The aim of this study was to investigate the coverage of retinal vessels with pericytes/smooth muscle cells during development in rats and determine if it was affected by the fluctuating oxygen regime of the Edinburgh Model of ROP[4].

ANIMAL MODEL

The neonatal intensive care unit in Edinburgh continuously monitors the arterial oxygen of admitted infants by a computerised monitoring system. The first 14 days of the transcutaneous oxygen profile of an infant who developed severe ROP was selected and converted into percentage inspired oxygen levels to produce the equivalent arterial oxygen in a rat:

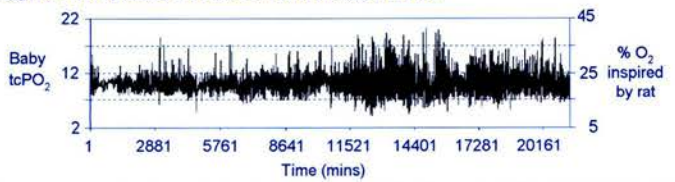

Rat pups exposed to this clinically relevant minute-variable oxygen environment developed features of ROP which included increased capillary density, peripheral avascularity and the formation of abnormal vessels[4].

METHODS

Litters of newborn rats were either reared in room air or exposed to the unique Edinburgh Model of fluctuating oxygen from birth to postnatal days 2, 7 or 14. Following sacrifice, the eyes were enucleated.

Retinal wholemounts were prepared for immunohistochemical staining; the endothelial cells were visualised with G. simplicifolia (Bandeiraea) isolectin B4 (Vector Laboratories), and the mural cells were stained using α-smooth muscle actin (α-SMA, Sigma) or desmin (Dako). The staining was then viewed using a confocal microscope.

For Western blotting, proteins were extracted from freshly dissected retinas, separated by SDS-electrophoresis and transferred onto a membrane which was probed using α-SMA antibody. The membrane was then stripped and blotted with actin as a loading control.

To determine the extent of desmin coverage, images at x20 magnification were taken of the central and peripheral areas of the retinas. Lectin and desmin staining were quantified using computer-threshold analysis (Image Tool software). Desmin staining was then expressed as a percentage of lectin staining.

References

1. Cell and Tissue Biology. In Weiss, L., ed. Baltimore, USA: Urban and Schwarzenberg, Inc.
2. Zimmermann, K. *Z. Anat. Entwickl.* 1923; 68: 29.
3. Patz, A. *Am J Ophthalmol* 1982; 94: 715.
4. Cunningham, S. et al. *Invest Ophthalmol Vis Sci* 2000;41:4275.

RESULTS

α-SMA expression was only seen on the arterial vessels, and increased progressively from P2 to P14 in both groups (Fig. 1). On P2, α-SMA positive cells were very simple, flat cells lacking distinct structure. The labelling was limited to the arterioles that had undergone complete remodelling (where capillary-free zones had formed, arrows). By P14, α-SMA labelled elongated, spindle-shaped cells that were arranged perpendicular to the axis of the vessels. Thus, α-SMA stained smooth muscle cells and their precursor cells.

Desmin expression was observed on all vessels of the retina (Fig. 2). On P2, desmin labelled very fine and long strands on the surface of the retinal vessels (these may be immature pericytes or undifferentiated precursor cells, arrow a). However, by P7 the cells had gained the structure of typical pericytes; they were long and slender with numerous processes. The structure of the pericytes altered depending on their location. On the arterioles, the cells were long, thin, and encircled the wall of the vessel (arrow b). On the venular vessels the cells had several processes (primary and secondary) and were not arranged in any particular manner (arrow c).

Fig. 1: Expression of α-SMA

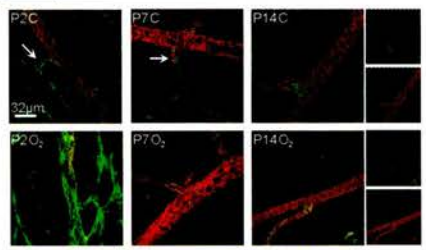

Double labelling: lectin (green) and α-SMA (red)

Fig. 2: Expression of desmin

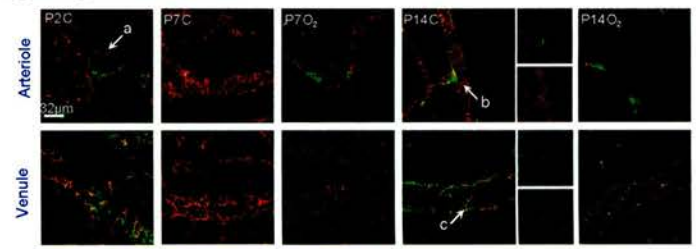

Double labelling: lectin (green) and desmin (red)

To ensure that the entire depth of the vessels were imaged, projected focus stacks of several optical sections from the upper to the lower surface of the vessels were obtained.

Occasional cells of the arterioles expressed both markers (Fig. 3); some had the typical structure of smooth muscle cells (arrow a) whilst others appeared more like pericytes (arrow b). It is possibly that along with α-SMA, differentiating smooth muscle cells also express desmin or that these cells are transitional pericytes and may have the potential to differentiate into smooth muscle cells on demand.

Fig. 3: α-SMA (green) and desmin (red) comparison

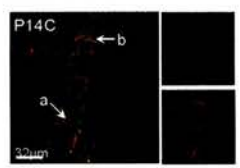

Fig. 4: Western blot analysis of α-SMA expression

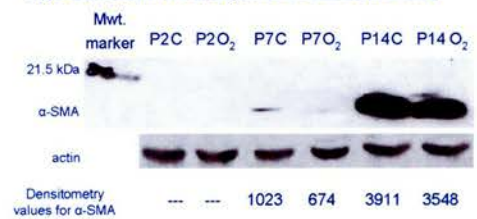

Fig. 5: Desmin coverage of endothelial tubules

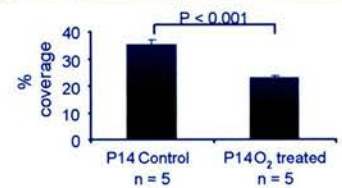

To determine if there was a difference in smooth muscle and pericyte coverage between control pups and those raised in the Edinburgh ROP Model, Western blotting for α-SMA staining (Fig 4) and computer thresholding for desmin staining (Fig 5) was conducted. It was found that a decrease in the expression of both markers occurred in the retinas of pups exposed to the Edinburgh Model of ROP; α-SMA expression was only slightly reduced in the oxygen treated pups, whereas the reduction in desmin staining was marked and significant.

CONCLUSION

α-SMA and desmin were very early markers for smooth muscle cell and pericytes, respectively. Transitional pericytes, however, expressed both proteins. In the Edinburgh Model of ROP, there was a small reduction in the expression of α-SMA. This reduction was most likely a result of the limited remodelling of the vasculature in response to the oxygen exposure[4]. Desmin expression was also reduced in the retina of oxygen treated pups. This reduction may be the result of (1) reduced recruitment of pericyte precursor cells, (2) inhibition or delay of pericyte differentiation, or (3) apoptosis of the pericytes in response to the oxygen regime.

In conclusion, mural cell coverage is reduced in a clinically relevant model of ROP.